What are the major susceptibility factors for glaucoma progression?

by

Gerasimos Laskaratos

MBBS, MSc(Oxon), MRCSEd(Ophth)

A thesis submitted for the degree of Doctor of Philosophy

Institute of Ophthalmology

University College London

2014

Declaration

I, Gerasimos Laskaratos confirm that the work presented in this thesis is my own. The help and contribution of others to this thesis is specified in the Acknowledgements section. Where information has been derived from other sources, I confirm that this has been indicated in the thesis.

More specifically, in the UKGTS I was responsible for the clinical examination of trial participants during their exit visit, and for the collection, analysis and presentation of data arising from this large study, particularly in relation to the study methodology, baseline characteristics, primary outcome and risk factor analysis. In the mitochondrial study, I was responsible for the preparation and submission of funding applications to support this project, the writing up of the research protocol, the coordination of the necessary ethics and R&D approvals, the recruitment and clinical phenotyping of the study participants, the experimental work (ATP, TMRM, DHE, aconitase, mTOR, 8OHdG), the preparation of annual progress reports, and the analysis and presentation of the data.

Dedications

To the two women that 'control' my life:

my mother Poly and my wife Eleftheria

Words would certainly fail to express my feelings for either of them

Abstract

Elevated intraocular pressure (IOP) is a major risk factor for open angle glaucoma (OAG) and medical IOP reduction is the standard treatment, yet no randomised placebo-controlled study of medical IOP reduction has been undertaken previously. In the present thesis, the methodology, baseline characteristics and results from the United Kingdom Glaucoma Treatment Study (UKGTS), the first randomised, double-masked, placebo-controlled, multicentre treatment trial for OAG, are presented. Survival analysis shows a statistically significant difference in the time from baseline to the event of confirmed visual field progression in the medical treatment (latanoprost) group, as compared to placebo, over 24 months. The role of average IOP during follow-up, as a risk factor for progression, is evaluated. Median IOP, as measured by Goldmann Applanation Tonometry (GAT), Dynamic Contour Tonometry and the Ocular Response Analyzer, is significantly, but weakly, correlated with visual field progression. Corneal compensated IOP (IOPcc) is the best predictor of progression across all the UKGTS sites. While the addition of central corneal thickness (CCT) slightly improves the GAT IOP prediction model, CCT on its own is not a significant predictor of progression in the UKGTS.

The role of mitochondrial dysfunction and oxidative stress as risk factors for glaucoma progression is investigated within an exploratory study. Experiments conducted on the lymphocytes of healthy subjects and patients, contrast individuals at the extremes of IOP susceptibility: rapidly progressing patients with Normal Tension Glaucoma (NTG) and non-progressing patients with Ocular Hypertension (OHT). The experimental data presented show, for the first time, that OHT patients may have more efficient mitochondria at a

systemic level, when compared to age-similar NTG subjects and non-glaucomatous controls. Overall, OHT lymphocytes produce higher levels of ATP (Complex I and Complexes II/III), have higher mitochondrial membrane potential, enhanced capacity to deal with exogenous oxidative stress insults, higher serum levels of urate, a potent antioxidant, and are more capable of taking up and buffering cytosolic calcium, as compared to NTG and control lymphocytes. Lymphocytes from NTG patients, when compared to the OHT and control groups, show lower ATP synthesis from Complex IV, lower aconitase activity, lower serum levels of vitamin C, and enhanced antioxidant defence (SOD2). In conclusion, this study implicates the role of a) systemic oxidative damage and complex IV-linked mitochondrial defects in the pathogenesis of NTG and b) efficient systemic mitochondria in resistance to glaucomatous optic neuropathy development and progression, particularly in the context of OHT.

Acknowledgements

It is difficult to overstate my gratitude to my PhD supervisor, Professor Ted Garway-Heath, who has been for me a great mentor and a true inspiration. I have always admired his enthusiasm for translational research, his intelligent and fair way of thinking, his thoughtful and always constructive comments, and mostly his ability to 'juggle' multiple tasks and projects, while maintaining a caring and friendly approach to his team. I could not have imagined having a better PhD supervisor (!) and I would like to express my sincere thanks and deep appreciation for his continuous guidance and support.

I must also offer my profoundest gratitude to my secondary supervisor Professor Anthony Schapira for giving me the opportunity to work at the Clinical Neurosciences Department on a stimulating project and in such a pleasant environment. Many thanks for your continuous encouragement, helpful comments and suggestions and sound advice.

I wish to express my sincere thanks and appreciation to Dr David Chau for his dedication to my lab work and career progression, for the time, patience, effort, ideas and concerns throughout the last three years. Thank you for teaching me how to think as a clinician scientist!

I would also like to express my gratitude to Dr Tuan Ho for appreciating and supporting my work at every step, and for playing a major role in the organisation of numerous successful meetings and training activities that encouraged me to develop my presentation and other skills.

I am especially grateful to Dr Catey Bunce, Miss Wen Xing, Dr Haogang Zhu and Dr Richard Russell for their invaluable statistical support and ideas which helped move this work forward.

Francesca Amalfitano, the UKGTS study coordinator, and Ed White, the UKGTS chief technician, are greatly thanked for their assistance and rapid response to all demands and queries relating to the trial. I also wish to thank all the members of the UKGTS steering committee for devoting their time and effort into this great study: Professor T Zeyen (Chair), Mr R Wormald (Moorfields Eye Hospital), Professor DF Garway-Heath (Chief Investigator, Moorfields Eye Hospital), Professor DP Crabb (Professor of Statistics and Measurements in Vision, City University London), Dr C Bunce (Senior Medical Statistician, Moorfields Eye Hospital), Mr N Anand (PI Huddersfield Royal Infirmary), Mr A Azuara-Blanco (PI Aberdeen Royal Infirmary), Professor R Bourne (PI Hinchingbrooke Hospital), Mr D Broadway (PI Norfolk and Norwich University Hospital), Mr I Cunliffe (PI 2006-08 Birmingham Heartlands and Solihull Hospitals), Mr J Diamond (PI Bristol Eye Hospital), Mr SG Fraser (PI Sunderland Eye Infirmary), Professor K Martin (PI Addenbrookes Hospital), Professor A McNaught (PI Cheltenham General Hospital), Mr A Negi (PI 2008-11 Birmingham Heartlands and Solihull Hospitals) and Dr P Spry (co-PI Bristol Eye Hospital).

Thank you to all my colleagues at the Moorfields Eye Hospital and the Royal Free Hospital, in particular Ameet Shah, Cornelia Hirn, Julia Lamparter, Katsu Suzuki, Hiroki Nomoto, Alisdair McNeil, Chien-Tai Hong, Michael Cleeter, Lydia Alvarez and Matthew Gegg, for providing a stimulating and fun environment in which to learn and grow, and for ‘volunteering’ to offer me a sample of their precious blood…

A special thank you to the Moorfields Eye Hospital patients, who kindly agreed to take part in the mitochondrial study, and to Miss Debbie Kamal for identifying suitable NTG patients from her clinic. I am also indebted to the

Friends of Moorfields and Liz Fisher for her invaluable help with the recruitment of controls. Thank you to Dr David Chau for his help with the mTOR, 8OHdG, CS and WB experiments. Thank you to Professor Ivan Gout for his kind input and advice on the mTOR project. Thank you to Mr Colin Willoughby for his useful comments on a recently published review paper from our group. Thank you to Dr Korsa Khan for her help with the flow cytometry.

My grateful thanks are also extended to the Moorfields Special Trustees, Fight for Sight and Allergan Europe, who funded the mitochondrial work, and to Pfizer Inc for funding the UKGTS. Also, a special acknowledgement goes to the NIHR Biomedical Research Centre at Moorfields Eye Hospital NHS Foundation Trust and UCL Institute of Ophthalmology for its financial support and for providing an excellent research environment.

Lastly, and most importantly, I wish to thank my family, on whose constant encouragement, patience and love I have relied throughout my PhD work. An immense thank you to my mother Professor Poly Lascaratou, who has raised and loved me, guided, encouraged and supported me at every stage of my life! My sincere thanks and apologies to my wife Dr Eleftheria Panteliou, whose unwavering love, patience and support have guided me over the last thirteen years of my life. I can think of no better person to walk this life with! A special thank you to Dr Faidon Lascaratos, who has always been a wonderful brother. Finally, this thesis would not have been possible without my father Professor John Lascaratos, whom I miss very much.

Contents

List of Tables

List of Figures

Abbreviations

Adenosine diphosphate	ADP
Adenosine triphosphate	ATP
Advanced Glaucoma Intervention Study	AGIS
Ambulatory blood pressure	ABP
α-amino-3-hydroxyl-5-methyl-4-isoxazole-propionate	AMPA
Anterior chamber depth	ACD
Apoptosis-inducing factor	AIF
Apoptosome activating factor-1	APAF-1
Association for Research in Vision and Ophthalmology	ARVO
Autosomal dominant optic atrophy	ADOA
Axial length	AL
Barbados Incidence Study of Eye Diseases	BISED
Basic-fibroblast growth factor	b-FGF
Bicinchoninic acid	BCA
4E-binding protein 1	4EBP1
Blood pressure	BP
Bovine serum albumin	BSA
Body mass index	BMI
Brain-derived neurotrophic factor	BDNF
Calcium	Ca^{2+}
Carbon Dioxide	CO_2
carbonyl cyanide 4-trifluoromethoxyphenyl hydrazone	FCCP
Caspase-3	Cas-3
Catalase	CAT
Central corneal thickness	CCT
Central retinal artery	CRA
Central retinal vein	CRV
Citrate synthase	CS
Collaborative Normal Tension Glaucoma Study	CNTGS
Collaborative Initial Glaucoma Treatment Study	CIGTS
Confidence interval	CI
Corneal-compensated IOP	IOPcc
Corneal hysteresis	CH
Corneal resistance factor	CRF
Cyclic guanosine monophosphate	cGMP
Cyclic nucleotide gated	CNG
Cytochrome c oxidase	COX
Decibel	dB
8-OH-deoxy-guanosine	8OHdG
Deoxyribonucleic acid	DNA
Diastolic blood pressure	DBP
Diastolic perfusion pressure	DPP
Diet restriction	DR
2', 7'-dihydroethidium	DHE

Dimethyl sulfoxide	DMSO
Dioptres	D
5, 5'-dithiobis-2-nitrobenzoic acid	DTNB
Dynamic Contour Tonometry	DCT
Early Manifest Glaucoma Trial	EMGT
Edinger-Westphal nucleus	EW
Electron transport chain	ETC
Endoplasmic reticulum	ER
Enzyme linked immunosorbent assay	ELISA
Ethylenediamine tetra-acetic acid	EDTA
Foetal bovine serum	FBS
Foetal calf serum	FCS
Gamma-amino-butyric acid	GABA
Ganglion cell layer	GCL
Glaucoma progression analysis	GPA
Glial fibrillary acidic acid	GFAP
Glutamine synthase	GS
Glutathione peroxidase	GPO
Glutathione-S-transferase	GST
Goldmann Applanation Tonometry	GAT
Guanosine monophosphate	GMP
Guanosine triphosphate	GTP
Guanylate cyclase	GC
Guanylate-cyclase-activating protein	GCAP
Hank's Balanced Salt Solution	HBSS
Hazard ratio	HR
Heat shock protein	HSP
Heidelberg Retina Tomography	HRT
High Performance Liquid Chromatography	HPLC
High tension glaucoma	HTG
Homocysteine	Hcy
Horseradish peroxidase	HRP
Hydrogen	H^+
Hydrogen peroxide	H_2O_2
Hydroxyl radical	HO•
Hypoxia inducible factor 1α	HIF1α
Immunoelectroblotting	IEB
Immunoreactive	IR
Inner limiting membrane	ILM
Inner nuclear layer	INL
Inner plexiform layer	IPL
Interquartile range	IQR
Intraocular lens	IOL
Intraocular pressure	IOP
Iron	Fe^{+2}
Kainate	KA
Koniocellular	K

Lamina cribrosa	LC
Lateral Geniculate Nucleus	LGN
Leber's Hereditary Optic Neuropathy	LHON
Lens Opacities Classification System	LOCS
L-Glutamate/L-aspartate transporter	GLAST
Los Angeles Latino Eye Study	LALES
Low-Pressure Glaucoma Treatment Study	LoGTS
Magnesium	Mg^{+2}
Magnocellular	M
Mammalian target of rapamycin	mTOR
Manganese	Mn
Mean deviation	MD
Mean arterial pressure	MAP
Mean ocular perfusion pressure	MOPP
Micrometres	µm
Millimetres	mm
Minimal Essential Medium	MEM
Mitochondrial calcium uniport	MCU
Mitochondrial calcium uptake 1	MICU1
Mitochondrial DNA	mtDNA
Mitochondrial membrane potential	ΔΨm
Mitochondrial permeability transition pore	mPTP
Mitochondrial superoxide dismutase	MnSOD
Molecular weight	MW
Nanometres	nm
National Institute of Clinical Excellence	NICE
Nerve fibre layer	NFL
Nicotinamide adenine dinucleotide phosphate (reduced)	NADPH
Nitric oxide	NO
Nitric oxide synthase	NOS
N-methyl-D-aspartate	NMDA
Normal tension glaucoma	NTG
Ocular hypertension	OHT
Ocular Response Analyzer	ORA
Open angle glaucoma	OAG
Optic nerve	ON
Optic nerve head	ONH
Optical Coherence Tomography	OCT
Outer limiting membrane	OLM
Outer nuclear layer	ONL
Outer plexiform layer	OPL
Oxidative phosphorylation	OXPHOS
Oxygen	O_2
Paraquat	PQ
Parvocellular	P
Peroxisome-proliferator-activated receptor coactivator 1α	PGC1α
Peripheral blood mononuclear cell	PBMC

Phosphatase and tensin homologue deleted on chromosome ten	PTEN
Phosphate buffered saline	PBS
Phosphodiesterase	PDE
Phosphoinositide 3	PI3
Photoreceptor(s)	PR(s)
Pituitary adenylate cyclase activating polypeptide	PACAP
Polyacrylamide gel electrophoresis	PAGE
Polymerase gamma gene	POLG
Polyphosphates	PolyPs
Polyvinylidene difluoride	PVDF
Posterior ciliary artery	PCA
Potassium	K^+
Prelaminar region	PLR
Primary angle closure glaucoma	PACG
Primary open angle glaucoma	POAG
Protein kinase B	PKB
Protein kinase C	PKC
Pseudoexfoliation	PXF
Pseudoexfoliation glaucoma	PXG
Reactive oxygen species	ROS
Research and Development	R&D
Retina	R
Retinal artery	RA
Retinal ganglion cell(s)	RGC(s)
Retinal nerve fibre layer	RNFL
Retinal pigment epithelium	RPE
Retinohypothalamic tract	RHT
p70 ribosomal S6 protein kinase	p70S6K
Roswell Park Memorial Institute	RPMI
Rotenone	Rot
Rotterdam Eye Study	RES
Serum separator tube	SST
Sodium	Na^+
Sodium dodecyl sulphate	SDS
Spherical equivalent	SE
Standard deviation	SD
Standard error of the mean	SEM
Subarachnoid space	SAS
Sulfur	S
Superoxide dismutase	SOD
Suprachiasmatic nucleus	SCN
Systolic blood pressure	SBP
Systolic perfusion pressure	SPP
3, 3', 5, 5'-tetramethylbenzidine	TMB
N, N, N', N'-tetramethyl-p-phenylenediamine	TMPD
Tetramethylrhodamine methyl ester	TMRM

Total antioxidant status	TAS
Total reactive antioxidant potential	TRAP
Trabecular meshwork	TM
Translocase of the Outer Membrane 20	TOM20
Triethylamine	TEA
Tumour necrosis factor-alpha	TNF-α
Tyrosine kinase receptor	TKR
Ultraviolet	UV
United Kingdom Glaucoma Treatment Study	UKGTS
Vascular endothelial growth factor	VEGF
Visual field	VF
Visual Impairment Project	VIP
Voltage-dependent anion-selective channel protein 1	VDAC1
Zinc	Zn

Chapter 1

General Introduction

Chapter 1: General Introduction

1.1 Anatomy of the eye and physiology of the retina

1.1.1 Gross anatomy of the eye

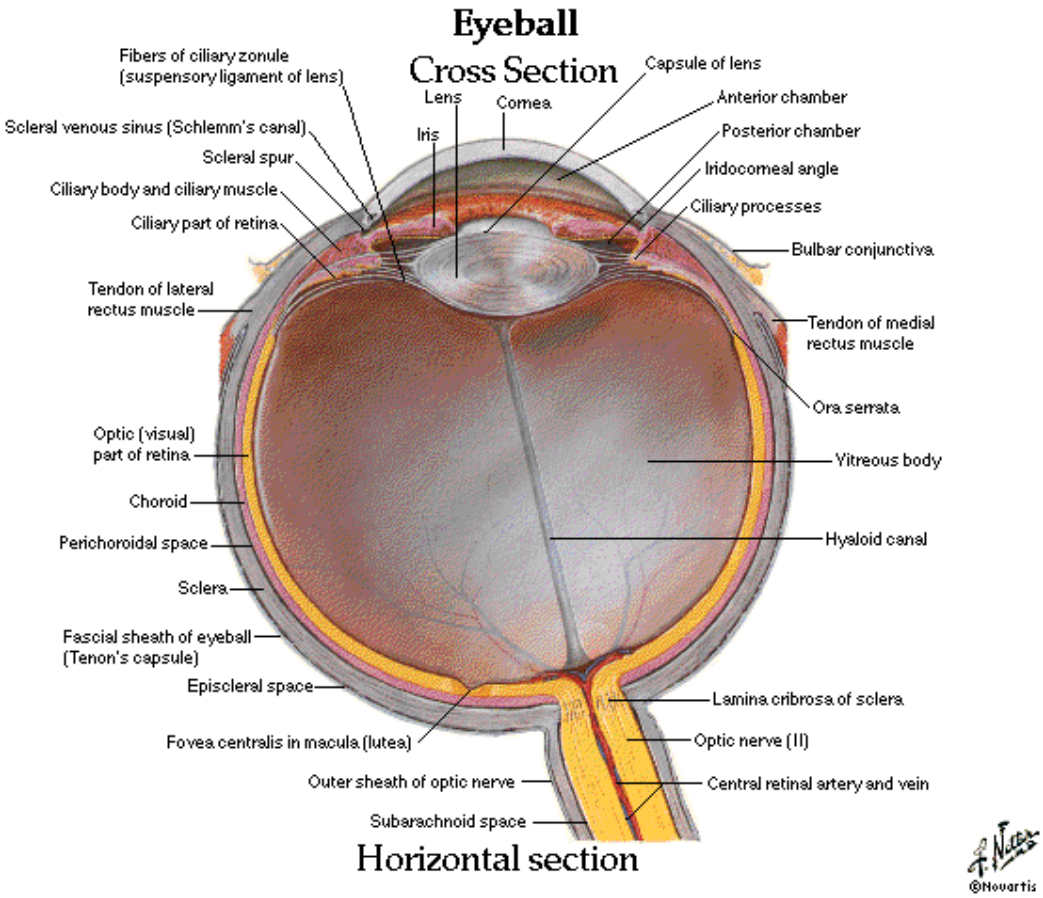

Fig 1.1: Sagittal section of the adult human eye (Netter's Anatomy Charts, Anatomy of the Eye, Third Edition, Saunders, 2003).

The human eye is an asymmetric sphere with a sagittal diameter of approximately 23-25 mm and a transverse diameter of 24 mm. A cross-sectional view of the eye (Fig 1.1) shows three layers:

- The external layer, formed by the sclera and cornea
- The intermediate layer, divided into two parts: anterior (iris and ciliary body) and posterior (choroid)
- The internal layer, or the sensory part of the eye, the retina

Moreover, three chambers of fluid can be identified:

- Anterior chamber (between cornea and iris)
- Posterior chamber (between iris, zonule fibres and lens)
- The vitreous chamber (between the lens and the retina)

The first two chambers are filled with aqueous humour, whereas the vitreous chamber is filled with a more viscous fluid, the vitreous humour.

The sagittal section of the eye also reveals the lens, which is a transparent body located behind the iris. The lens is suspended by ligaments, the zonule fibers, attached to the anterior portion of the ciliary body. The tension or relaxation of these ligaments, as a consequence of ciliary muscle actions, changes the shape of the lens, a process called accommodation that allows the formation of a sharp image on the retina.

The arterial input to the eye is provided by several branches from the ophthalmic artery, which is derived from the internal carotid artery (Fig 1.2). These branches include the central retinal artery, the short and long posterior ciliary arteries, and the anterior ciliary arteries. Venous outflow from the eye is primarily via the vortex veins and the central retinal vein, which merge with the superior and inferior ophthalmic veins that drain into the cavernous sinus, the pterygoid venous plexus and the facial vein (Fig 1.2).

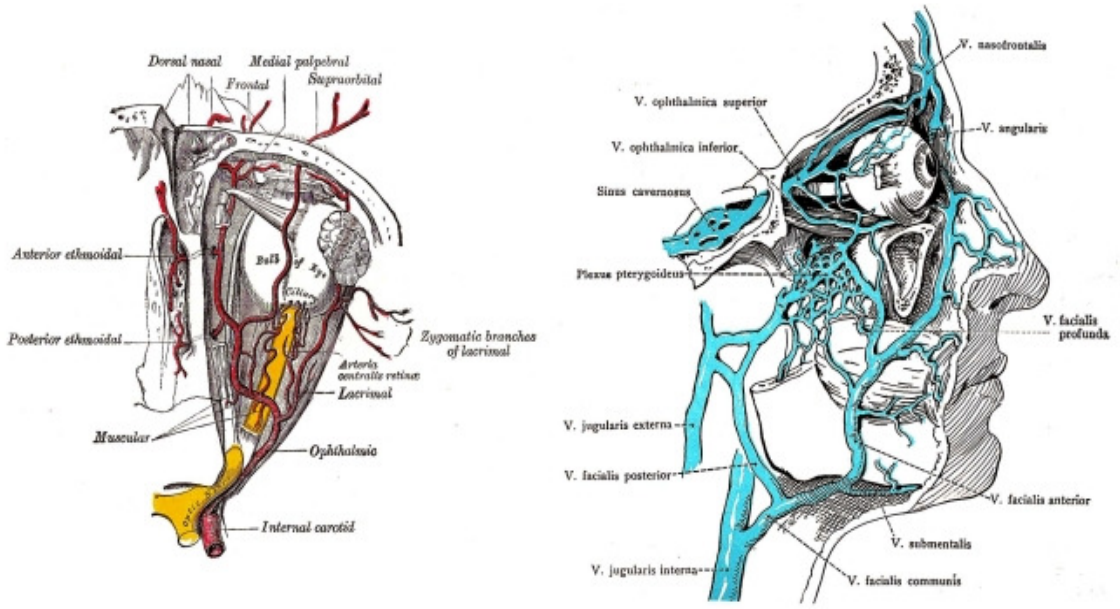

Fig 1.2: Arterial (left) and venous (right) connections to the systemic circulation (Anatomy of the Human Body, Gray H, 2th Edition, Lea & Febiger, Philadelphia, 1954).

1.1.2 Anatomy of the retina and optic nerve

All vertebrate retinas are composed of three layers of nerve cell bodies and two layers of synapses (Fig 1.3). The outer nuclear layer (ONL) contains the cell bodies of the photoreceptors (PRs), the inner nuclear layer (INL) contains the cell bodies of the bipolar, horizontal and amacrine cells and the ganglion cell layer (GCL) contains the cell bodies of the retinal ganglion cells (RGCs) and displaced amacrine cells (Anderson et al 1992). These nerve cell layers are divided by two neuropils, where synaptic contacts occur. The first area of neuropil is the outer plexiform layer (OPL) where connections between the rods and cones, as well as between the vertically running bipolar cells and horizontally oriented horizontal cells, occur. The second neuropil of the retina is the inner plexiform layer (IPL), which functions as a relay station for the

vertical-information-carrying bipolar cells to connect to RGCs. In addition, different varieties of horizontally- and vertically-directed amacrine cells interact in further networks to influence and integrate the ganglion cell signals. In other words, a direct three-neuron chain – from photoreceptor to bipolar and then to RGC – is the major route of information flow from the light source to the optic nerve, while the horizontal and amacrine cells are primarily responsible for lateral interactions. It is at the culmination of all this neural processing in the IPL that the message concerning the visual image is transmitted to the brain along the optic nerve (Kolb 1991).

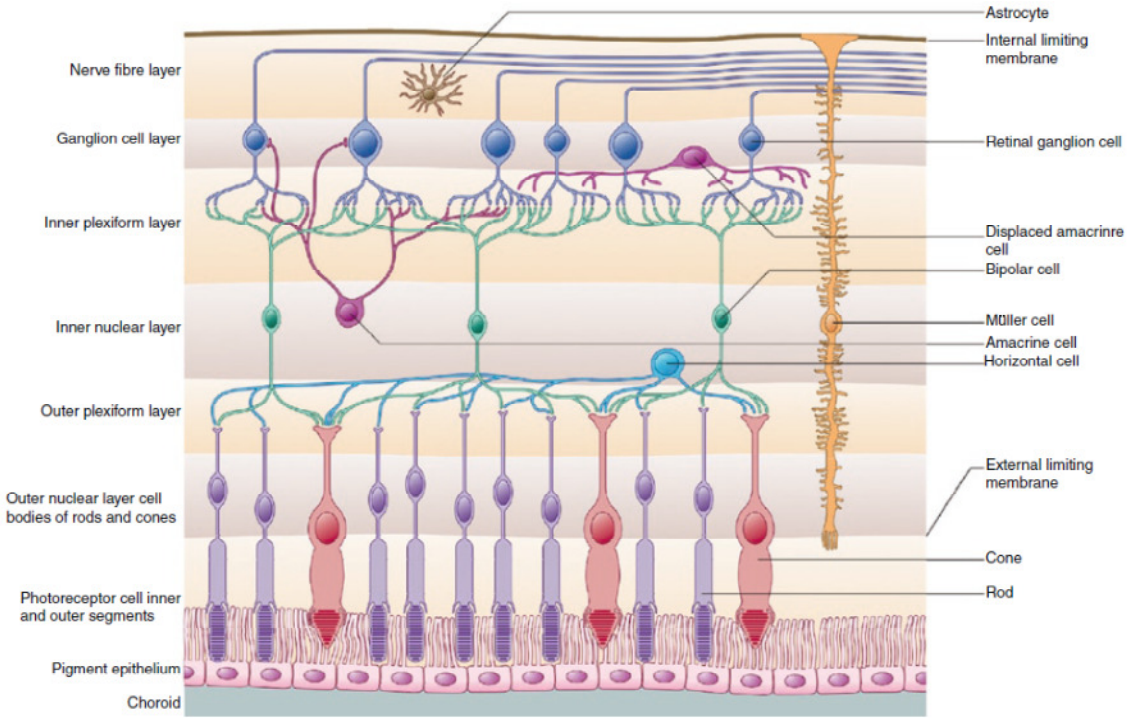

Fig 1.3: Schematic diagram of a vertical section through the human retina (Anatomy of the Human Body, Gray H, 2th Edition, Lea & Febiger, Philadelphia, 1954).

The retina is supplied by the central retinal artery and the short posterior ciliary arteries (PCAs). The central retinal artery travels in or beside the optic

nerve as it pierces the sclera then branches to supply the layers of the inner retina, while the photoreceptors and the greater portion of the OPL are nourished indirectly from the choriocapillaris, a richly anastomotic vascular layer that corresponds to the pia-arachnoid vessels in the rest of the brain. The main retinal vessels form two capillary plexuses: the superficial capillary network lying in the nerve fibre layer (NFL), and the deep capillary network lying in the boundary plane between the INL and the OPL. These two layers anastomose, but the main retinal arteries are end-arteries without inter-anastomoses; hence, occlusion of a retinal artery affects its entire distribution, causing complete inner retinal ischaemia (Osborne et al 2004). There are marked species differences in the inner retinal vascularisation, with primates having a complex 4-zone arrangement and an avascular zone at the fovea, lagomorphs having a rather simple narrow band of superficial vessels, rodents having a wagon-wheel spoke-like arrangement and guinea pigs having no inner retinal vessels (Fig 1.4). Retinal venules and veins coalesce into the central retinal vein, which exits the eye with the optic nerve parallel and counter-current to the central retinal artery.

Fig 1.4: Fundus photographs of the human (left), rabbit (middle) and rat (right) retina (The Ocular Circulation, Kiel JW, San Rafael (CA), Morgan & Claypool Life Sciences, 2010).

The RGC axon fibres travel within the NFL to converge on the optic disc while obeying strict retinotopic organisation. The adult optic nerve head (ONH) is

typically elliptical in shape, having a slightly greater mean vertical (1.9 mm) than mean horizontal (1.7–1.8 mm) diameter (Levin 2003). The retinal axons leave the retinal plane to enter the optic nerve head at an angle of about 90° taking up position in a specific order: central RCG axons are located in the inner part of the optic nerve rim whilst peripheral RCG axons are found in the outer layers of the optic disc rim, while some studies have shown that RGC axons from most points in the retina are scattered throughout the thickness of the RNFL (Fitzgibbon et al 1996). All RGC axons pass through the optic nerve head, which consists of three parts: the prelaminar portion (between the lamina cribrosa and the vitreous), the lamina cribrosa (the connective tissue extension of the sclera through which the optic nerve axons and the central retinal artery and vein pass), and the postlaminar portion. The RGC axons are surrounded by astrocytes in the prelaminar portion and then stream through the foramina of the lamina cribrosa to enter the postlaminar portion where oligodendrocytes and connective tissue become part of the glial structure. Here, the axon fibers become myelinated and the optic nerve ensheathed by the meninges. After passing through the optic disc, the RGC axons travel in the intraorbital (about 30 mm), the intracanalicular (5–12 mm), and the intracranial portions of the optic nerve (8–19 mm). At the optic chiasma, the nasal fibres decussate to join the temporal fibres of the contralateral optic nerve to form the optic tract, which projects to the lateral geniculate nucleus, the pretectal nuclei, the superior colliculus, the hypothalamus and possibly other brain structures (Levin 2003, Kanski 1999).

It is interesting to note that an excess number of RGCs is produced early during prenatal development. Up to 70% of axons in the human fetal optic nerve die between 16 weeks (3.7 million) and 29 weeks of gestation (1.1 million) (Taylor 2005). This excess production is thought to be required to achieve the

subsequent selection of axons that make correct contact with the above brain targets. After this rapid elimination of more than 2 million RGCs early in human embryonic development, axonal cell decline is gradual by an estimated 5,000 axons per year of life (Levin 2003).

The vascular supply of the optic nerve is complex (Fig 1.5). The optic nerve has three zones referenced to the lamina cribosa: the prelaminar optic nerve supplied by collaterals from the choroidal and retinal circulations, the laminar zone supplied by branches from the short posterior ciliary and pial arteries, and the post laminar zone supplied by the pial arteries. Venous drainage is via the central retinal vein and pial veins.

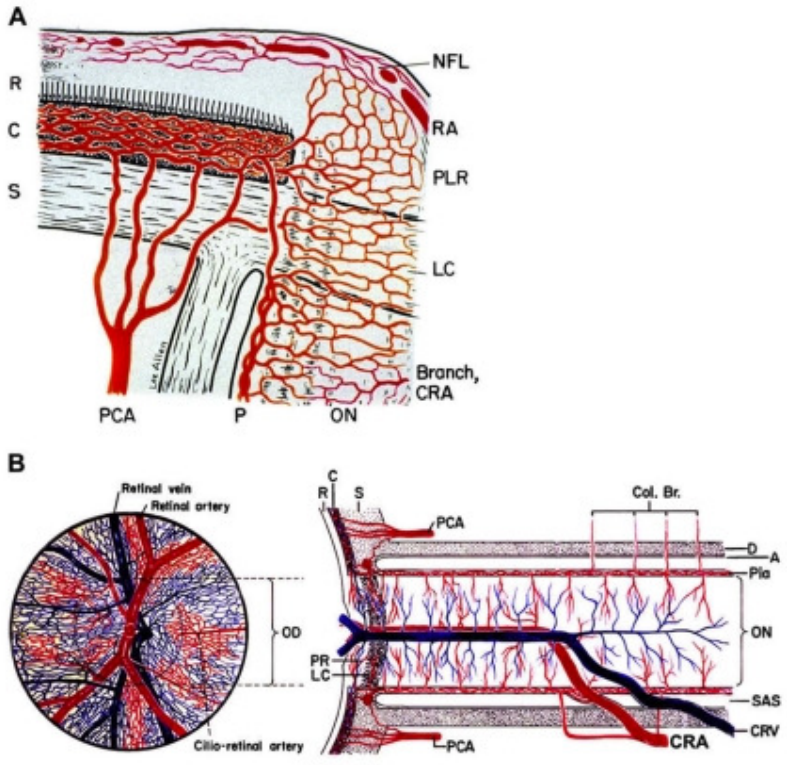

Fig 1.5: Vascular supply of the optic nerve. The following structures are shown: PCA, posterior ciliary artery; NFL, nerve fibre layer; LC, lamina cribrosa; ON, optic nerve; CRA, central retinal artery; CRV, central retinal vein; OD, optic disc; R, retina; C, choroid; S, sclera; P, pia; A, arachnoid; D, dura; PLR, prelaminar

region; RA, retinal artery; Col. Br., collateral branches; SAS, subarachnoid space (The Ocular Circulation, Kiel JW, San Rafael (CA), Morgan & Claypool Life Sciences, 2010)

It is, however, important to note that the central retinal artery circulation makes significant contributions only to the superficial optic nerve fibres (not the remaining prelaminar portion of the ONH) and the posterior portion of the ONH. Thus, the PCA circulation supplies both the outer retina via the choriocapillaris and most of the ONH. Also, PCAs and their branches in the choroid and ONH behave as end arteries *in vivo*, which helps to explain the localised nature of choroidal and ONH lesions (Hayreh 2004). Unlike the fenestrated capillaries of the choriocapillaris, the capillaries of the ONH are non-fenestrated with tight junctions. In addition, the ONH vessels are capable of autoregulation, unlike the choriocapillaris. Thus, even though the ONH circulation is derived from the posterior ciliary circulation, its blood-retina barrier function and capability to autoregulate resemble more the retinal than the choroidal circulation (Hayreh 1995). For the optic nerve vessels, the laminar zone marks the transition from exposure to the intraocular pressure (IOP) to exposure to the cerebral fluid pressure within the optic nerve sheath.

1.1.3 Anatomy and physiology of the retinal ganglion cells

There are approximately 1.2 to 1.5 million RGCs in the human retina. They consist of cell bodies, multiple dendrites and large diameter axons capable of passing the electrical signal to the retinal recipient areas of the brain many centimeters distant from the retina. Based on their projections and functions, there are at least five main classes of RGCs:

- Parvocellular (P)
- Magnocellular (M)
- Koniocellular (K)
- Photosensitive ganglion cells
- Other ganglion cells projecting to the lateral geniculate nucleus (LGN) for control of the pupillary light reflex

Parvocellular (P) retinal ganglion cells project to the parvocellular layers of the LGN. These cells are also known as midget RGCs, based on the small sizes of their dendritic trees and cell bodies. About 80% of RGCs are parvocellular cells. They receive inputs from relatively few PRs (rods and cones). They have slow conduction velocity and respond to changes in colour, but respond only weakly to changes in contrast unless the change is great (Kandel et al 2000). They have simple ON/OFF centre-surround receptive fields.

Magnocellular (M) retinal ganglion cells project to the magnocellular layers of the LGN. These cells are also known as parasol RGCs, based on the large sizes of their dendritic trees and cell bodies. About 10% of RGCs are magnocellular cells. They receive inputs from relatively many rods and cones. They have fast conduction velocity and can respond to low-contrast stimuli, but are not very sensitive to changes in colour. They have much larger receptive fields, which are nonetheless also centre-surround (Shapley et al 1986).

Koniocellular (K) retinal ganglion cells project to the koniocellular layers of the LGN. The name koniocellular comes from the Greek word “konis” which means “dust” and therefore koniocellular means “cells as small as dust”. The koniocellular retinal ganglion cells have been identified only relatively recently, as their small size makes them hard to find (Yucel et al 2003). About 10% of RGCs are koniocellular cells. They receive inputs from intermediate numbers of

rods and cones. They have moderate spatial resolution, moderate conduction velocity, can respond to moderate-contrast stimuli and may be involved in colour vision. They have very large receptive fields that only have centres (no surrounds) and are always ON to the blue cone and OFF to both the red and green cones.

Photosensitive ganglion cells contain their own photopigment, melanopsin, which makes them respond directly to light even in the absence of rods and cones. They project to the suprachiasmatic nucleus (SCN) via the retinohypothalamic tract (RHT) (Newman et al 2003, Hannibal et al 2004). In humans, melanopsin is expressed only in the eye and its expression is restricted to cells within the ganglion and amacrine cell layers of the primate and murine retinas. Notably, expression is not observed in retinal PR cells. The unique inner retinal localisation of melanopsin suggests that it is not involved in image formation, but rather may mediate nonvisual photoreceptive tasks, such as the regulation of circadian rhythms and the acute suppression of pineal melatonin (Provencio et al 2000). Typically, RGCs communicate information to central visual structures by receiving input from retinal PRs via bipolar and amacrine cells. As melanopsin ganglion cells do not require synaptic input to generate light-induced signals, these cells need not receive synapses from other neurones in the retina. Instead, the melanopsin ganglion cells are intrinsically sensitive to light, perhaps responding via a melanopsin-based signaling pathway (Peirson et al 2006). However, Belenky et al (2003) have shown that melanopsin-immunoreactive (IR) dendrites in the inner region of the IPL do receive bipolar and amacrine terminals, suggesting that PR signals may be capable of modifying the intrinsic light response in melanopsin-expressing RGCs.

Other retinal ganglion cells projecting to the LGN include cells making connections with the Edinger-Westphal nucleus (EW) for the control of the pupillary light reflex and giant retinal ganglion cells.

Of particular relevance to this thesis is the fact that RGC axons within the globe are laden with mitochondria (Fig 1.6). Wang et al (2003) have demonstrated that unmyelinated intraretinal ganglion cell axons in the primate eye (human and nonhuman) contain numerous bulb-shaped varicosities at all retinal eccentricities. Moreover, the fact that the unmyelinated part of the ganglion cell stains for cytochrome c oxidase (COX), whereas the myelinated part does not, supports the morphological studies regarding the distribution of mitochondria along the ganglion cell axon (Barron 2004). The varicosities associated with ganglion cell axons within the globe have been observed in human specimens ranging from 1 to 85 years old. The diameters of the varicosities are approximately four times larger, on average, than the interbulb regions of the axons. These bulb regions have no vesicle-containing chemical synaptic structures, but are rich in mitochondria, suggesting a possible zone of metabolic demand (Wang 2003). Previous studies have also described bulb-shaped structures on intraretinal ganglion cell axons in other mammalian species, such as rats (Hildebrand 1985, Black 1984), rabbits (Reichenbach 1988) and cats (Hollander 1991).

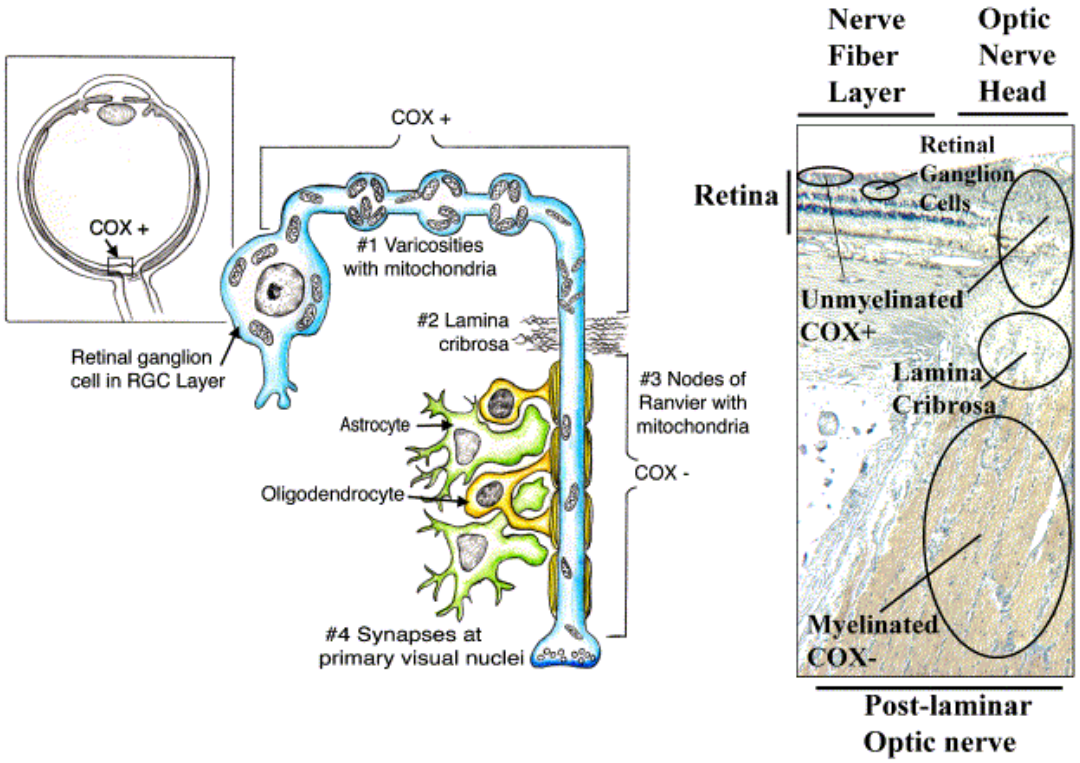

Fig 1.6: Diagrammatic view of pattern for staining of COX in the RGC system. On the left side is a sagittal view of the human eye. The boxed part is enlarged and schematically illustrated with emphasis on the RGC cellular system. Mitochondrial distribution is shown from the RGC somata through the unmyelinated (COX+) portion of the axon in the NFL and penetrating the lamina cribrosa at the optic nerve head. Mitochondrial accumulations are represented in the varicosities within the NFL and in the prelaminar region. There is a drastic decrease in mitochondrial numbers within the retrolaminar portion (COX−). Mitochondria in this part of the RGC axon are mostly located under the unmyelinated nodes of Ranvier. On the right side, a histological sagittal section of a normal human eye is illustrated showing a parallel transition from the retina to the optic nerve head, the lamina cribrosa and a portion of the myelinated retrolaminar optic nerve. The ocular tissue was stained by a method using immunoperoxidase for myelin basic protein (Carelli V et al 2004).

1.1.4 Other retinal neurones

In addition to RGCs, the retina has five other basic types of retinal neurones: PRs, horizontal, bipolar, inter-plexiform and amacrine cells (Masland 2012). The cell bodies of the PRs form the ONL, while horizontal cells lie along the outer margin of the INL and bipolar cell perikarya are located mainly in the middle of the INL. Amacrine and inter-plexiform cell perikarya are arranged along the proximal border of the INL (Fig 1.3).

The two types of photoreceptors are the rods and the cones. There are 120 to 130 million rods in each eye, while there are only 6.5 to 7 million cones. The outer segments of rods (Fig 1.7) contain the visual pigment rhodopsin within disks (up to 1000 per cell) enclosed by a single plasma membrane (Hargrave et al 1992). The disks are produced at the base of the outer segment and gradually travel to the distal end of the outer segment, where they are phagocytosed by the retinal pigment epithelium (RPE). Cones are typically shorter than rods and the photopigment is not stored in membranous disks, but rather invaginations of the cytoplasmic membrane. The cell bodies of rods and cones are connected by an inner fibre to specialised synaptic terminals, known as spherules and pedicles, respectively. The outer segments are separated by an extracellular ground substance containing inter-photoreceptor binding protein within a sialic acid and proteoglycan-binding matrix. The myoid represents the inner part of the inner segment and contains numerous organelles, including Golgi apparatus, smooth endoplasmic reticulum, microtubules and glycogen, indicating a metabolically and synthetically active cell. The ellipsoid represents the outer part of the inner segment and is connected to the outer segment by a modified cilium. The ellipsoid itself is rich

in mitochondria indicative of the high-energy requirements of these cells (Curcio et al 1991).

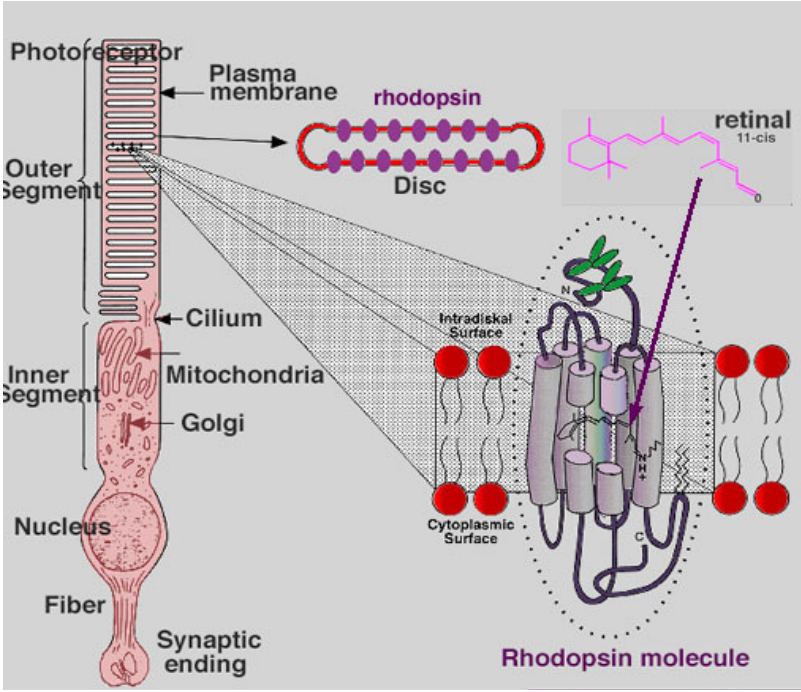

Fig 1.7: Schematic diagram of a photoreceptor (Hargrave PA, McDowell JH. Rhodopsin and phototransduction: a model system for G protein-linked receptors. FASEB J 1992; 6: 2323-31).

The rods and cones are unevenly distributed. The density of the rods exceeds that of the cones, except in the fovea, the central point for image focus in the human retina, where the cone density is the highest. The central region of the fovea (foveola) is rod-free. The rods and cones differ in the degree of convergence onto RGCs. The rods are more sensitive, slower in response, and have maximum sensitivity at wavelengths of light around 498 nm (green-blue). The cones are less sensitive, faster in response, and come in three different

varieties, with greatest sensitivity at three different wavelengths: short (S), medium (M), and long (L) wavelengths. Each of the 3 types of cone pigment is most sensitive to a certain wavelength of light: short (430-440 nm), medium (535-540 nm) and long (560-565 nm). Cones mediate colour vision, because they allow for different portions of the electromagnetic spectrum to be differentiated. Moreover, while inputs from many rods converge to a single ganglion cell, the latter receive inputs from a single cone or from very few. Convergence makes the rod system a better light detector, but reduces its spatial resolution. It is, therefore, the one-to-one mapping within the cone system that maximises the discrimination of fine detail, namely visual acuity. In the fovea a maximally focused image initiates resolution of the finest detail and direct transmission of that detail to the brain is needed for perception (Rodieck 1973). Light must travel through the thickness of the retina before striking and activating the rods and cones. Subsequently the absorption of photons by the visual pigment of the photoreceptors is translated into a biochemical message and then an electrical message that can stimulate all the succeeding neurones of the retina (Polyak 1941). The name of this biochemical process that takes place in the photoreceptors is phototransduction (Fig 1.8) and constitutes an essential component of light perception (Fain et al 2001).

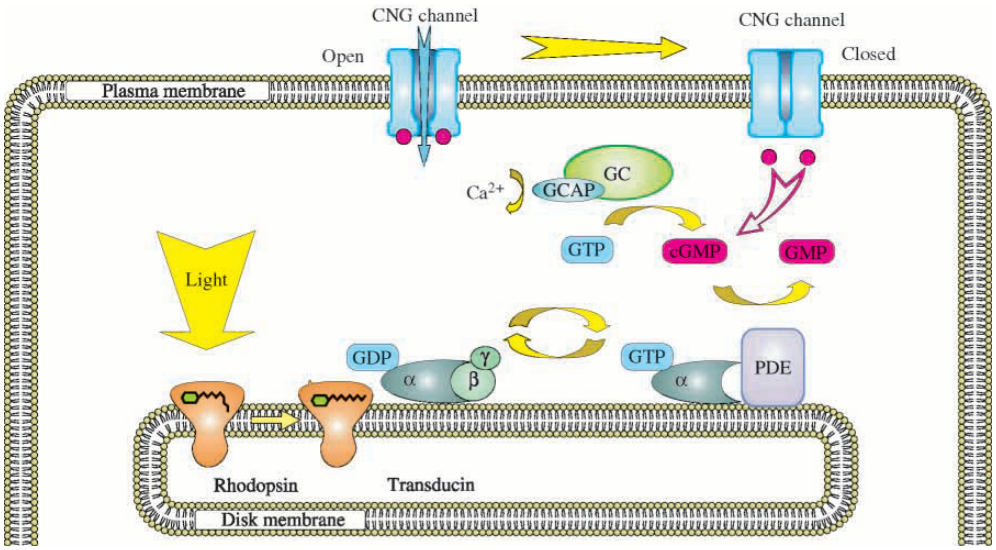

Fig 1.8: The phototransduction cascade. Light causes photoisomerisation of rhodopsin, activating the heterotrimeric G-protein transducin. The GTP-bound a-subunit activates phosphodiesterase (PDE), which degrades cGMP to GMP. The decrease in cGMP concentration leads to closure of cyclic-nucleotide-gated (CNG) channels, resulting in two effects, a decrease in Ca^{2+} influx and hyperpolarisation of the membrane potential. The resulting decrease in intracellular Ca^{2+} concentration is important for adaptation. Lowered intracellular Ca^{2+} concentration disinhibits guanylate-cyclase-activating protein (GCAP), leading to activation of guanylate cyclase (GC) and resynthesis of cGMP (Kramer et al 2001).

Horizontal cells derive their name from the extensive horizontal extensions of their cell processes. These processes extend widely in the OPL and mediate lateral interactions in this first synaptic zone (Thoreson 2012). There are two subtypes of horizontal cell: type A is an axonless cell with dendrites that synapse only with cones; type B has dendrites that make contact with cones, in addition to which it has an axon that synapses with multiple rod spherules. The horizontal cells have an integrative role in retinal processing and release inhibitory neurotransmitters, mainly gamma-amino-butyric acid (GABA).

The bipolar cells can be divided into ON and OFF bipolar cells, which respond differently to the PR signal, because they express different receptors (metabotropic and ionotropic glutamate receptors, respectively). The bipolar cells are the output neurones that carry visual information from outer to inner plexiform layers, while the inter-plexiform cells carry information from the inner to the outer plexiform layers. Inter-plexiform cells are either GABAergic

or dopaminergic and send their processes to both outer and inner plexiform layers.

The amacrine cells, while predominantly located in the proximal aspect of the INL, are also found in the IPL where they are known as interstitial cells and their main function is to mediate interactions within this layer. Amacrine cells display great morphologic diversity and contain a broad range of neurotransmitters (Kolb et al 1992).

1.1.5 Non-neuronal retinal cells

Three basic types of glial cell are found in the human retina: Müller cells, astroglia and microglia.

The predominant glial cell type in the retina is the Müller cell. These cells extend vertically through the retina, from the distal margin of the ONL to the inner margin of the retina. The distal border of Müller cells is marked by the OLM, which consists of junctional complexes made between the processes of different Müller cells or between the processes of Müller cells and photoreceptors. Müller cells extend beyond the OLM into the subretinal space, forming microvilli. The proximal border is marked by the ILM, consisting of an expansion of the cell membrane of the Müller cell, called the endfoot, and a basement membrane. The nuclei of the Müller cells are typically located in the middle of the INL. The Müller cells contain glycogen, mitochondria and intermediate filaments and have a range of functions all of which are vital to the health of the retinal neurons (Reichenbach et al 1995). They protect neurons from exposure to excess neurotransmitters, such as glutamate, using well developed uptake mechanisms to recycle this transmitter. They also

protect neurons from deleterious changes in their ionic environment by taking up extracellular K^+ and redistributing it. Moreover, they are thought to synthesise retinoic acid from retinol, which is known to be important in the development of the eye and the nervous system (Edwards et al 1994). Finally, Müller cells may be involved in phagocytosis of neuronal debris.

Astrocytes are sparsely distributed in the GCL and IPL. However, they are the major glial cell type in the ONH and are vital for RGC survival (Schnitzer 1988). Astrocytes not only provide mechanical support to nearby neurons (Stone et al 1987), but also aid in maintaining the extracellular levels of glutamate through the Na^+ dependent L-glutamate transporters (GLAST and GLT-1) and regulate the extracellular levels of K^+ and H^+ ions (Trivino et al 1996).

Microglial cells are present in three separate retinal layers: GCL, including the NFL, IPL and OPL. They may be of two types. One form is thought to enter the retina at earlier stages of development from the optic nerve mesenchyme and lie dormant in the retinal layers for much of the life of the retina. The other form of microglia appears to be blood borne cells, possibly originating from vessel pericytes (Boycott et al 1981). Both types can be stimulated into a macrophagic function on trauma to the retina and may engage in phagocytosis of degenerating retinal neurons (Gallego et al 1986).

1.2 Glaucoma: an overview

1.2.1 Introduction

Glaucoma is an irreversible progressive optic neuropathy in which RGC axons are damaged and degenerate, giving rise to a characteristic appearance of the ONH and pattern of visual field (VF) loss (Fig 1.9). The definition, relevant to

epidemiological studies, suggested by an international consensus panel in 2002 specifies that glaucoma is present when three or more locations of the field test, in a particular pattern, are notably outside the limits of normal between-subject variability and when, in the same eye, the cup-to-disc ratio is greater than that seen in 97.5% of the general population (Foster et al 2002). These criteria assure that the structural finding is unlikely to be simply a typical variation in healthy individuals and that both structural and functional injury has occurred.

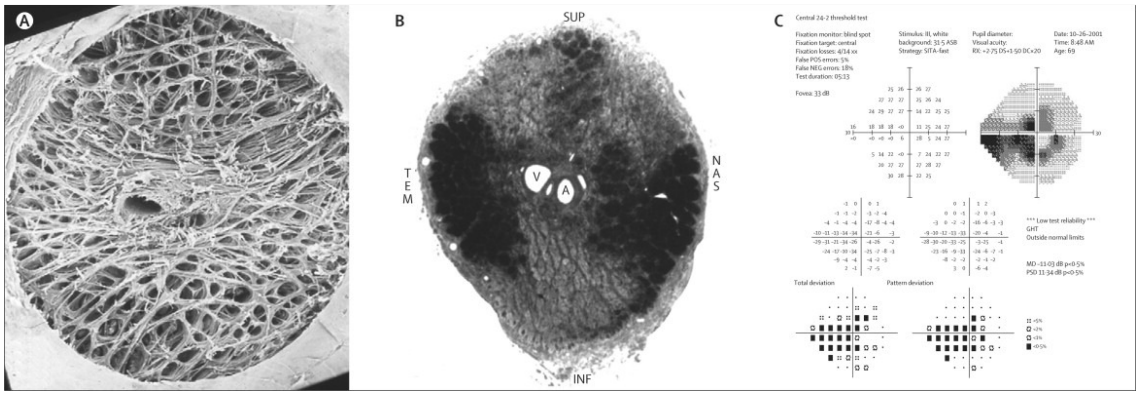

Fig 1.9: Histological basis for loss of ganglion cells in glaucoma. Loss of RGCs and their axons may occur preferentially, with upper and lower axons and their RGCs being more affected than nasal and temporal axons, which is evident as an hour-glass shaped pattern in the optic nerve just behind the eye (A). Atrophic areas are lighter in colour than non-atrophic areas (B). The preferential polar axon loss may be related to the lower density of connective tissue in the upper and lower quadrants of the optic nerve head (B). The visual field result shows the corresponding upper and lower mid-peripheral loss of function from polar area axons at a moderate stage of glaucoma (C). V=vein; A=artery; SUP=superior; TEM=temporal; INF=inferior; NAS=nasal (Quigley 2011).

1.2.2 Epidemiology

Worldwide, glaucoma is responsible for more blindness than any other eye condition, except cataract. Data from population-based surveys indicate that 1 in 40 adults older than 40 years has glaucoma with loss of visual function, which equates to 60 million people worldwide being affected; 8.4 million are bilaterally blind from glaucoma (Quigley 2011). In the United Kingdom, glaucoma remains the second leading cause of blind registrations (Bunce et al 2010). While glaucoma affects more than 2% of those older than 49 years of age, its prevalence rises to at least 4% in white and 13% in some black populations by the age of 80. Glaucoma can occur in all age groups, including in infants, but it is most common in elderly people. Although there are several conditions with the same end result of VF loss and ONH damage that are included under the umbrella term 'glaucoma', the most common types of glaucoma are primary open-angle glaucoma (POAG) and primary angle-closure glaucoma (PACG). Asia accounts for a disproportionate number of PACG cases, whereas the prevalence of POAG is more evenly distributed throughout the world (Quigley 1996). Clinical research reports still commonly refer to patients with open-angle glaucoma and untreated IOP of less than 21 mmHg as having normal tension glaucoma (NTG); however, there is little evidence that such dichotomous subdivision has a scientific basis, and investigators are now urged to treat IOP as a continuous variable in studies of open-angle glaucoma (OAG). For the purpose of this thesis, we shall focus mainly on OAG, as the most common form of glaucoma.

1.2.3 Clinical manifestations of glaucoma

In open angle glaucoma, RGC death may be accompanied by pathological ONH cupping (Fig 1.10 A-B), glaucomatous optic atrophy (Shields 1997), changes in the structure of the retinal nerve fibre layer (RNFL) (Read et al 1974) and a characteristic VF loss (Quigley 2011). This optic nerve excavation consists of both loss of RGC axons and deformation of connective tissues supporting the optic disc (Fig 1.10 C-F).

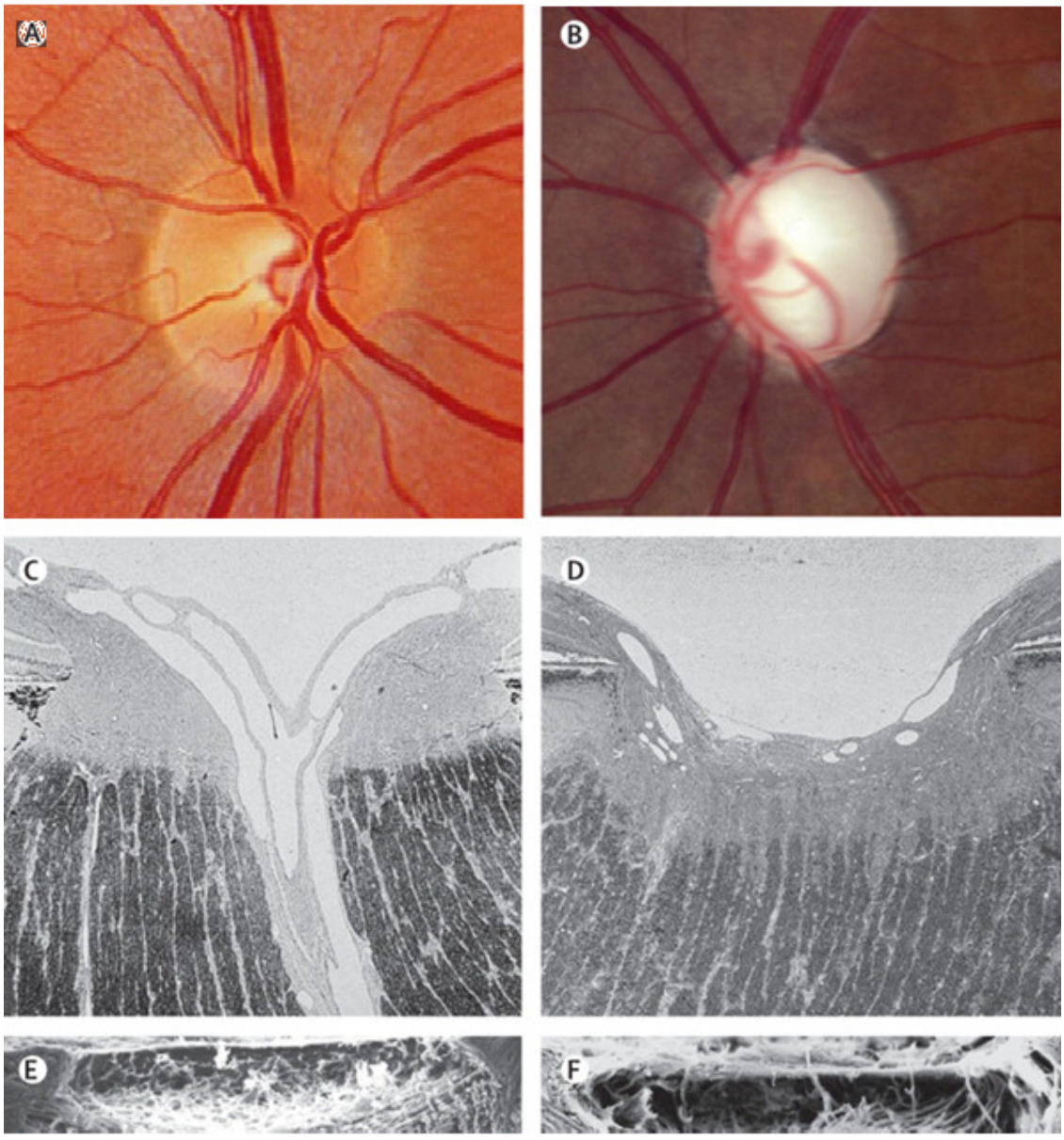

Fig 1.10: Typical features of the eye in healthy individuals and in patients with glaucoma. The optic disc of individuals without glaucoma has a central pale area (cup) that occupies about half or less of the optic disc with a surrounding orange rim of nerve tissue (A). With glaucomatous damage the cup occupies an increasing proportion of the disc, the rim disappears, and the cup becomes excavated with a deep floor and a rim that may be undermined (B). The typical histological appearance of the optic nerve head (C) changes in glaucoma with tissue loss from the rim and deepening of the cup (D). The connective tissues

of the optic nerve head in healthy individuals, when seen after digestion of neural tissue, are like a thin meshwork across the ONH, perforated by pores for nerve bundles (E). The cup in glaucoma deepens and widens with fixed deformation of the connective tissue, leading to the characteristic excavation seen clinically (F) (Modified from Quigley 2011).

This excavation or abnormal structural deepening of the optic disc connective tissue is one of the main clinical features that separates glaucoma from ischaemic optic neuropathy or chiasmal tumour-induced neuropathy (Danesh-Meyer et al 2010). OAG is also distinguished from other optic neuropathies by slow progression over months to years (Heijl et al 2009). It is usually bilateral, but asymmetric (Broman et al 2008). Glaucoma is sometimes referred to as the "silent blinder", because many people are unaware of having the disease (Tielsch et al 1991). It remains undiagnosed in nine out of ten affected people worldwide and in about 50% of those in developed countries, thus improved case detection is needed. Importantly, the loss of peripheral vision, depth perception and contrast sensitivity associated with glaucoma can have a major effect on an individual's life. Injuries caused by car crashes and falls are associated with the types of visual impairment that arise in glaucoma and such injuries can occur even if a person has excellent central acuity (Glynn et al 1991, Owsley et al 1998).

1.2.4 Risk factors (overview) and relevance to the optic nerve head

The pattern and progression of VF loss due to ganglion cell death varies among glaucoma patients suggesting that there is some variability in the magnitude of the insult responsible for the cell loss. Data derived from clinical observations

and from animal experiments suggest that the axons of the optic nerve and the RGC somata do not die at the same time but that death can vary between months and many years (Osborne et al 1999). It seems therefore reasonable to assume that when a patient is diagnosed initially as having glaucoma, only some ganglion cells are dead, whereas others may range from being slightly affected to completely normal (Neufeld 1998).

IOP is a major, and currently the only modifiable, risk factor for VF loss in glaucoma, whether raised (high tension glaucoma) or within the normal range (normal tension glaucoma), which accounts for one third to one half of all cases (Klein et al 1992a, Tielsch et al 1991). This would suggest that, although glaucoma may be associated with increased IOP, its diagnosis does not rely on a specific level of IOP (Coleman 2000) and patients are known to progress at varying rates at all levels of IOP. While there has been success in slowing progression by lowering IOP in both high tension and normal tension glaucoma (Heijl et al 2002, CNTGS AJO 1998) and at both the early and late stages of the disease (Weinreb and Khaw 2006), additional factors (Douglas 1998) must be sought to explain why IOP lowering does not always prevent deterioration. Several possible mechanisms have been proposed for glaucomatous RGC damage (section 1.3 below), which is thought to occur at the ONH (Fig 1.10). The lamina cribrosa of the ONH is likely to be at risk because of the transition between an efficient (myelinated axons) and a not so efficient (unmyelinated axons) energy system of action potential transmission (Osborne et al 1999), and a variable reduction of ATP is likely to exist in the RGCs over time with the greatest effect being in the ONH region. This may cause a reduced normal resting membrane potential with homeostasis of the RGCs now maintained at a lower status, so making them more susceptible to further insults. There is also strong support for a vascular mechanism in which impairment of blood

flow at the ONH is due either to raised IOP (Yamazaki et al 1996, Grunwald et al 1998, Kerr et al 1998) or to intrinsic vascular factors (Osborne et al 2001, Spaeth 1977, Hayreh 1985, Flammer et al 1998, Flammer et al 1999, Chung et al 1999, Yamamoto et al 1998) (Fig 1.11).

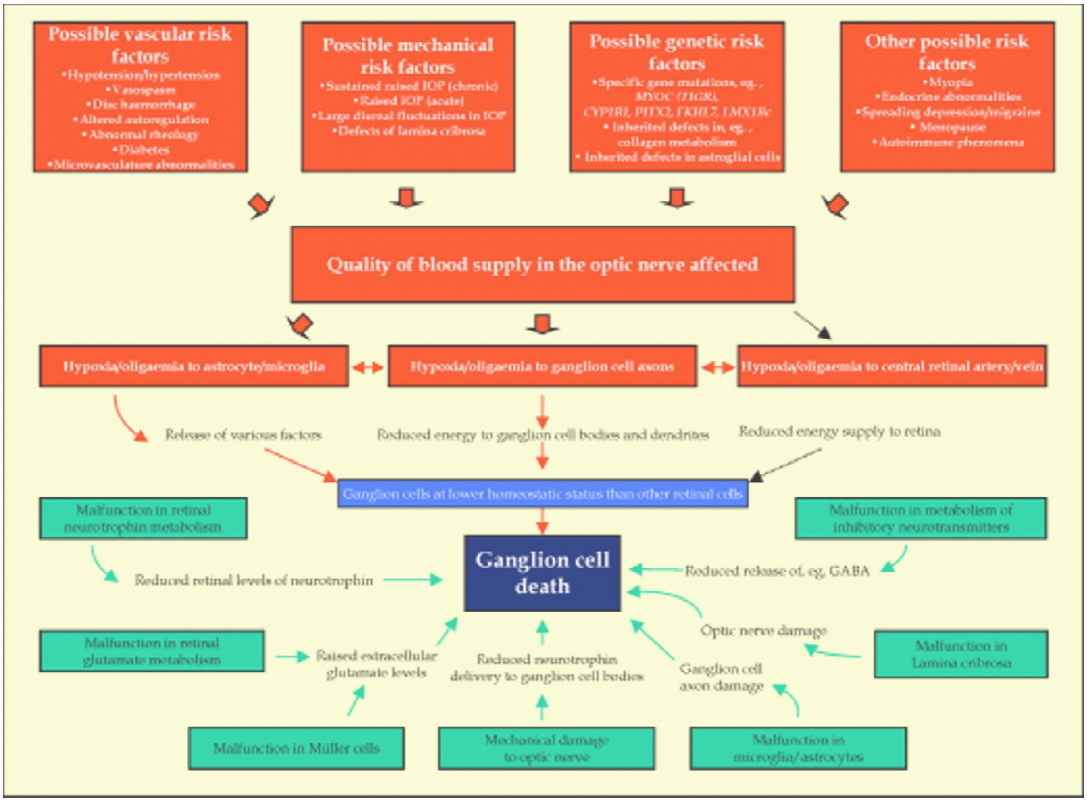

Fig 1.11: Possible causes of ganglion cell death in glaucoma. It is suggested that activation of sufficient risk factors causes the quality of blood supply in the ONH to be affected. As a result, the nutritional supply to the ONH is slowly compromised (oligaemia/hypoxia) particularly affecting astrocytes, microglia and RGC axons. Such insults eventually lead to the death of RGCs. One may also envisage other modes of stimulating ganglion cell death in glaucoma (lighter green boxes) where the vascular system does not have a direct role. Some of these possibilities may also be linked to certain risk factors, such as black race, ageing, history of steroid use and sleep-related breathing disorders, but these are not indicated (Osborne et al 2001).

1.2.5 Management

The goal in the treatment of OAG is to prevent further loss of functional vision during the remainder of a patient's life and to avoid an adverse impact on the patient's quality of life (EGS 1998, AAO 1996). The prevention of loss of vision is mainly achieved by lowering the IOP to a threshold that is deemed to be safe for the RGCs given the current amount of damage in the ONH (target IOP) (Jampel 1997). Once this has been achieved, the patient should be monitored every 4–12 months, although more frequent monitoring might be required for patients who are monocular or have advanced bilateral VF loss. Preferred practice patterns from professional organisations suggest monitoring structural glaucoma damage by clinical observation of the optic disc and by photography or digital imaging of the optic disc and nerve fibre layer. Automated visual field testing with threshold strategies is repeated regularly to establish the rate of progressive worsening as a means to judge the success of treatments that lower IOP (Chauhan et al 2008, Heijl et al 2008). A consensus panel in the UK, the National Institute of Clinical Excellence (NICE), based its recommendations for whether to treat patients with IOP greater than 21 mmHg on assessment of risk factors, including age and central corneal thickness (NICE 2009). Lowering of IOP is accomplished by daily eye drops, laser treatment to the trabecular meshwork or ciliary body, or surgery. The effectiveness of these approaches has been compared pair-wise in randomised controlled trials, with the main differences being the rate and type of side effects (GLT 1995, Ederer et al 2004, Lichter et al 2001). Because patients with OAG can continue to lose vision despite reductions of IOP, the role of neuroprotection in the management of OAG warrants consideration (Caprioli

1997, Levin 2003). In the not so distant future, sustained delivery of treatment may prove beneficial, either through depot placement of sustained-release treatment or by placement of cells engineered to produce IOP-lowering and/or neuroprotective substances (Tao et al 2002).

1.3 Pathways involved in retinal ganglion cell loss in glaucoma

1.3.1 The role of mitochondria

RGCs, because of their high energy requirement, are heavily dependent on mitochondria for survival and function (Raichle et al 2002, Yu et al 2001). Mitochondria play a pivotal role in the maintenance of cellular homeostasis regulating death signalling pathways (Kroemer et al 2000, Naoi et al 2009) and various metabolic functions that include oxidative energy metabolism, intracellular pH maintenance, calcium signalling (Pozzan et al 2000) and neuronal excitability (Chan 2006, Schapira 2006). Mitochondria are also involved in the control of synaptic transmission and the production of reactive oxygen species (ROS) that promote and regulate apoptosis (Halliwell et al 1999).

Oxidative phosphorylation (oxphos) is a major metabolic pathway in the mitochondria, that uses an electrochemical or chemiosmotic gradient of protons (H^+) across the inner mitochondrial membrane to generate the energy-rich molecule ATP from ADP (Knowles 1980). Functionally, the mitochondrial oxphos system comprises around 85 different gene products assembled into five multimeric protein-lipid enzyme complexes (Hatefi 1985): i) At complex I (NADH dehydrogenase) NADH is oxidised to NAD^+, a process that releases

electrons and reduces Q (ubiquinone) to QH_2 (ubiquinol), while at the same time four protons are pumped from the mitochondrial matrix to the intermembrane space (Fig 1.12). ii) At complex II (succinate dehydrogenase) succinate is oxidised to fumarate, a process that releases electrons and reduces FAD to $FADH_2$, which carries the original electrons to reduce Q to QH_2. Again protons are pumped into the intermembrane space. iii) At complex III (ubiquinone cytochrome c oxidoreductase) Q-cycle transfers electrons from QH_2 to cytochrome c (cyt c), while protons are again pumped into the intermembrane space. iv) At complex IV (cytochrome c oxidase) cyt c transfers electrons to oxygen with the release of water. Again protons are pumped into the intermembrane space. v) At complex V (ATP synthase) protons pumped into the intermembrane space now return to the matrix, while this rotary complex combines ADP and inorganic phosphate into ATP. Complex I is the largest complex of the electron transport system and is composed of 46 subunits that are encoded by both mitochondrial DNA and nuclear genes, and defects in this complex are the most frequent cause of oxphos impairment underlying mitochondrial disease (Smeitink et al 2001). All the other complexes are also derived from both nuclear and mitochondrial DNA, with the exception of complex II which is entirely nuclear-gene derived.

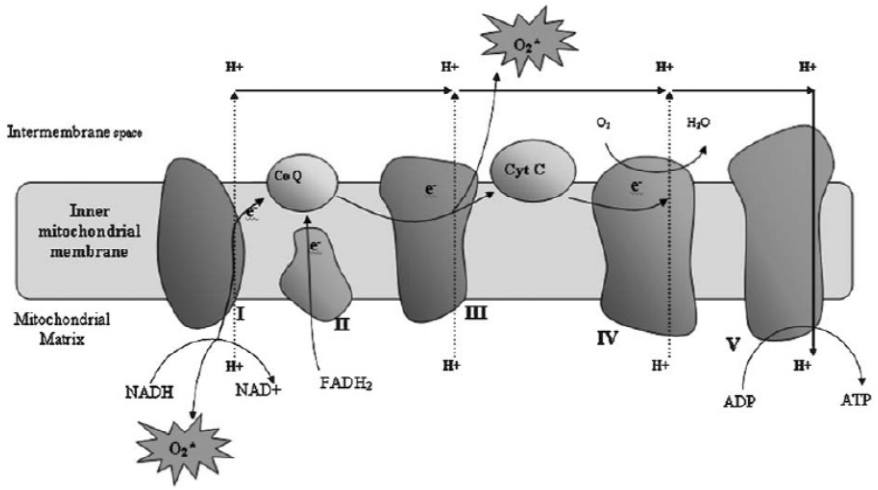

Fig 1.12: The oxidative phosphorylation pathway. The concentration gradient of hydrogen ions across the inner mitochondrial membrane is formed by complexes I to IV. This concentration gradient provides the driving force for ATP production through complex V. Leakage of electrons at complexes I and III are major sites of reactive oxygen species formation (Kong et al 2009). NAD: nicotinamide adenine dinucleotide; FAD: flavin adenine dinucleotide, CoQ: coenzyme Q; O_2: oxygen; H^+: proton; e^-: electron; H_2O: water; CytC: cytochrome C; ADP: adenosine diphosphate; ATP: adenosine triphosphate.

Significantly, and as mentioned previously (1.1.3), RGC axons are unmyelinated within the ocular globe and have mitochondria-enriched axon varicosities (Barron et al 2004, Wang et al 2003), which are interpreted as functional sites with local high-energy demand, critical for maintaining the transmission of action potentials along the pre-laminar axons within the globe (Andrews et al 1999, Bristow et al 2002, Carelli et al 2004) and for axoplasmic flow (Hollander et al 1995, Minckler et al 1977). The high concentration of mitochondria at the optic nerve head also implies dependency on some aspect of mitochondrial function (Barron et al 2004). It is therefore clear that alteration in the functional status of these RGC axon mitochondria may influence ganglion cell survival in a disease like glaucoma (Osborne 2008). RGCs are thought to die by

apoptosis at varying rates depending on, for example, the ganglion cells' receptor profile (Osborne et al 1999) and other factors, such as the number and spatial distribution of the RGC mitochondria (Yu-Wai-Man et al 2005) and their axonal length and position within the globe (Osborne 2010). This may explain why the preferential loss of RGCs in glaucoma is also a key pathological feature found in the two most common inherited mitochondrial optic neuropathies, Leber hereditary optic neuropathy (LHON; MIM#535000), mostly caused by a defect in oxidative phosphorylation (OXPHOS) complex-I (Mackey et al 1996), and autosomal dominant optic atrophy (ADOA; MIM#165500) (Yu-Wai-Man et al 2009), caused by mutations in the nuclear genes encoding the mitochondrial fusion protein OPA1 (Alexander et al 2000, Delettre et al 2000). Both these diseases share phenotypic similarities and may be mistaken for glaucoma (O'Neill et al 2011). It is also interesting that murine RGCs have been found to be more sensitive to the downstream events of mitochondrial fragmentation and pro-apoptotic stimuli than other neuronal populations (Kamei et al 2005), thus emphasising the potential importance of mitochondrial integrity in preventing or delaying glaucomatous optic neuropathies.

Importantly, mitochondrial dysfunction has been implicated in RGC loss in experimental animal models of glaucoma (Tatton et al 2001, Ju et al 2008, Mittag et al 2000) and in transformed ganglion cell cultures (Ju et al 2007). Pre-existing mitochondrial dysfunction, either congenital or acquired, has been proposed to increase the vulnerability of RGCs to stress from other risk factors, including raised IOP, vascular insufficiency and light exposure (Kong et al 2009). In the case of raised IOP, Kong et al have shown recently that a mouse with neuronal expression of a mutant polymerase gamma gene (POLG) has increased mtDNA mutations in the retina and a greater injury response when

subjected to acute IOP elevation (Kong et al 2011). Experimentally increased IOP has also been shown to result in reduction in ATP levels both in RGC-5 cells (Ju et al 2007) and in animal models (Baltan et al 2010). This finding suggests that OXPHOS impairment limits the optic nerve's ability to withstand injury from raised IOP and could contribute to the pathogenesis of the glaucoma, especially in the presence of such insults.

It is also notable that, as discussed later in section 1.5.5, ageing is a major risk factor for OAG and, since mitochondrial function declines with ageing (Kopsidas et al 1998, Li et al 2013), it has been proposed that mitochondrial dysfunction could serve as one of the links between ageing and glaucoma (Lascaratos et al 2012). In post-mitotic non- replicating cells, including the neurons of the retina, the mtDNA, in contrast to the nuclear DNA, is continuously replicated as mitochondria are turned over, increasing the likelihood of ongoing replication errors and mtDNA mutations. Therefore, mtDNA changes are considered relevant to the mitochondrial theory of ageing (Druzhyna et al 2008, Harman 1972, Moosmann et al 2008) particularly as somatic mutations can be propagated during replacement of the mitochondria (Liang et al 2003). Indeed, mtDNA mutations have been shown to accumulate with age (Wei 1992), a phenomenon which may in part be a consequence of the age-related diminishment of autophagic activity (Terman 1995), the process that sequesters and degrades organelles and macromolecular constituents of cytoplasm for cellular restructuring and repair. Moreover, mitophagy (the autophagic destruction of mitochondria) may be important for the elimination of dysfunctional mitochondria and mutated mtDNA (Weber et al 2010); certain mtDNA mutations decrease recognition signals for mitophagy and, therefore, accumulate with age (Lemasters 2005). Age-associated mtDNA mutations include large-scale deletions and point mutations (Corral-Debrinski

et al 1992, Lin et al 2002), as well as oxidative modification with the formation of 8-hydroxy-2'-deoxyguanosine (Wei 1998). The mutant mtDNA often coexists with the wild-type mtDNA in affected tissues, a condition termed heteroplasmy (Lightowlers et al 1997). The clinical severity of glaucoma may therefore be correlated with the proportion of the mutant mtDNA in the target tissue, the type of mutations, the pattern of distribution of the mutant mtDNA and the energy demand of the RGCs.

1.3.2 Reactive oxygen species

ROS, at low levels, are considered critical signalling molecules, while oxidative stress refers to excessive levels of ROS that arise from the imbalance between the processes that generate ROS and those responsible for their removal (Chrysostomou et al 2013). Oxidative stress damages macromolecules including DNA, proteins and lipids and is thought to contribute to the pathogenesis of a number of age-related neurodegenerative diseases (Schapira 1996). Raised IOP is a major risk factor for RGC loss in glaucoma and, in several animal glaucoma models, increasing IOP led to the development of oxidative stress. For example, elevated IOP following intracameral hyaluronic acid injection in rats has been shown to result in a significant decrease in retinal antioxidants and an increase in retinal lipid peroxidation (Moreno et al 2004), while ocular hypertension in rats in other studies has also led to a marked increase in ROS and nitrite levels, lipid peroxidation (Ferreira et al 2010, Ko et al 2005) and protein oxidation localised to the inner retinal layers containing the RGCs (Tezel et al 2005).

It is also important to note that the pathways leading to RGC injury under conditions of oxidative stress are likely to be complex, varied and interrelated, and it is often difficult to distinguish cause from consequence (Fig 1.12). For example, ROS have been shown to be implicated indirectly in RGC damage by causing vascular changes that disrupt the autoregulation of blood flow to the optic nerve, impaired aqueous humour outflow as a result of oxidative injury to the trabecular meshwork (Izzotti et al 2006) and aberrant immune responses and glial cell dysfunction (Tezel 2009), as discussed later (1.3.7-1.3.8) in more detail. Moreover, ROS are able to activate apoptotic pathways when in excess and have been found to affect RGCs directly, by triggering apoptosis *in vitro* via caspase-independent pathways (Li et al 2008). In another study, reduction of ROS generation temporarily protected RGCs from apoptosis (Tezel et al 2004), while Martin et al have shown that oxidative stress alters retinal glutamate/glutamine cycling, leading to the accumulation of neurotoxic levels of glutamate (Martin et al 2002), as described in more detail in section 1.3.5 below.

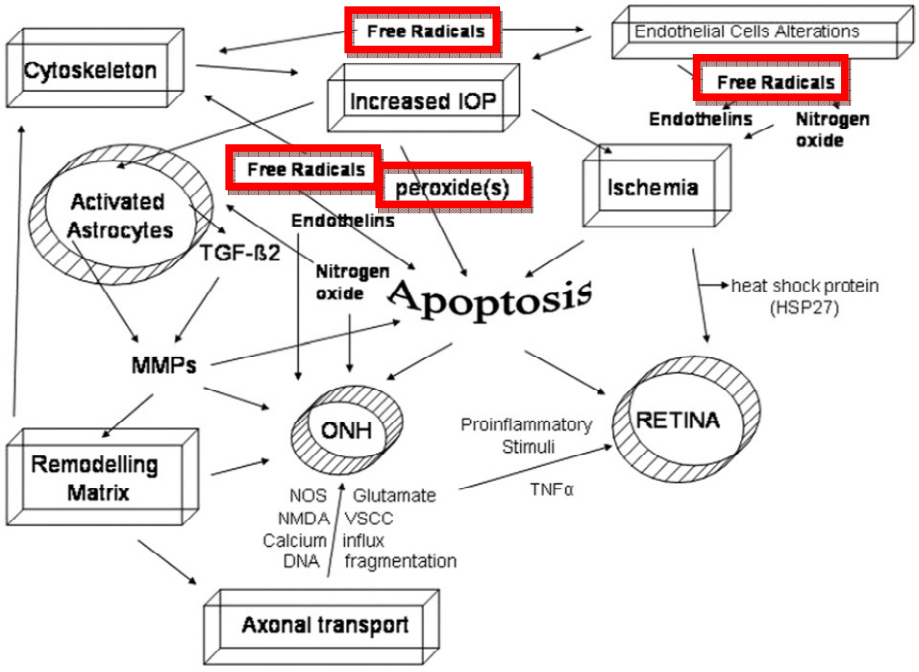

Fig 1.13: RGC death and axon degeneration represent the principal event in the course of glaucoma. The mechanisms that control the loss of this specific neuron population remain largely unclear. From a pathophysiological point of view, the main steps in glaucoma pathogenesis include raised IOP, ischaemia, glial cell activation, apoptosis and structural optic nerve head changes. A common denominator (highlighted in red) is the free radical-generated oxidative damage, which is known to influence these glaucomatous targets (Sacca et al 2008).

1.3.3 Apoptosis - necrosis

The hallmarks of apoptosis are condensation of nuclear and cytoplasmic contents, nuclear DNA fragmentation, cell blebbing and autophagy of membrane-bound bodies. This process typically requires energy and is characterised by clearly distinguishable changes in the nucleus, but not in the cytoplasmic organelles, at least in the initial stages (Kroemer et al 1995, Wyllie et al 1980). Apoptosis appears to occur via different pathways. A mitochondrion-mediated (intrinsic) pathway has been described, where an external insult - such as elevated cytosolic calcium - acts to cause a release of cytochrome c, located in the inner membrane space of the mitochondria. Cytosolic cytochrome c can then bind apoptotic protease-activating factor 1 (APAF-1), which in turn binds to the inactive form of caspase-9 (Fig 1.13). This complex “apoptosome” can then activate a cascade of events, including the activation of caspase-3, and ultimately results in the hallmarks of apoptosis (Acehan et al 2002). Mitochondrion-mediated activation of caspase-9 can also occur via extracellular receptor-mediated signals (extrinsic pathway) to target various ligands - such as Bid and Bax - to the mitochondrion, thereby causing

cytochrome c release (Luo et al 1998). Under certain circumstances, a separate mitochondrial-independent pathway also operates, which involves the activation of caspase-8 and caspase-3 (Stennicke et al 1998). In addition, a caspase-independent/mitochondrial-dependent pathway exists where apoptosis-inducing factor (AIF), confined to mitochondria, is released and translocates to the nucleus to cause chromatin condensation and DNA degradation (Susin et al 1996). The activation of the tumour suppressor protein p53 has also been proposed as one of the molecular events leading to the up-regulation of the pro-apoptotic gene bax and down-regulation of the anti-apoptotic gene brl-2, thus causing changes in mitochondria that ultimately activate caspases and induce neuronal apoptosis in glaucoma (Nickells et al 1999).

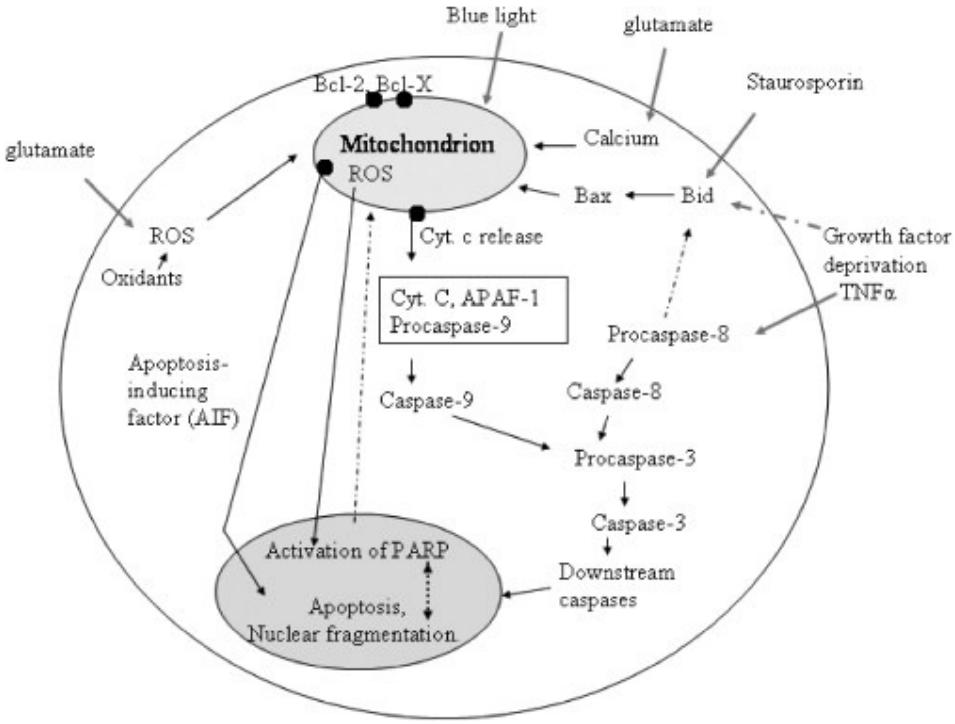

Fig 1.14: Schematic view of the main mitochondria-dependent and -independent (through caspase-8) apoptotic pathways. Mitochondria-dependent apoptosis often involves the release of cytochrome c and the activation of caspase-9, but can also occur through mitochondrial release of cleaved AIF or ROS. AIF, apoptosis-inducing factor; PARP, poly(ADP-ribose) polymerase 1; ROS, reactive oxygen species; APAF-1, apoptotic protease-activating factor 1; Cyt c, cytochrome c; Bid, BH3 interacting-domain; Bax, Bcl-2-associated X; TNF-a, tumour necrosis factor-a; Bcl-2, B-cell lymphoma 2 (Osborne 2008).

Necrosis is characterised by a compromised membrane integrity caused by ATP energy depletion; swelling eventually occurs and the mitochondria become dysfunctional. Eventually, the cell lyses and lysosomal enzymes are released into the extracellular space. Unlike apoptosis, changes in the nucleus of a necrotic cell appear relatively unremarkable, at least during the early stage, but there is some swelling associated with the nuclear membrane followed by a scattering of materials into small masses (Wyllie et al 1981). The main factors thought to differentiate between apoptosis and necrosis are summarised in Fig 1.14 below. Since the rate of glaucomatous damage is relatively slow, it is hypothesised that very few RGCs would be expected to be found actually dying from apoptosis. In support of this, several studies have indeed shown that the number of TUNEL positive ganglion cells in glaucomatous patients is small, although it is greater than in control retinas (Kerrigan et al 1997, Okisaka et al 1997). Another study has also shown that immunoreactivity for the inflammation-associated enzyme, cyclo-oxygenase-2, in the human glaucomatous optic nerve is unchanged compared with controls (Neufeld et al 1997). This argues for an absence of inflammation and endorses the idea that ganglion cell death in glaucoma is by apoptosis. It is, however, possible that in

reality apoptosis and necrosis form a continuum at the extremes of a biochemically overlapping death pathway rather than being totally separate modes of death with only limited molecular and cellular biological overlap (Raffray et al 1997).

Necrosis	***Apoptosis***
• Occurs in groups of cells	• Occurs in isolated cells
• Gene expression not a prerequisite	• Genetically controlled
• Late stage random DNA cleavage	• Precise internucleosomal cleavage of DNA
• Inflammatory response	• No inflammation
• Phagocytosis of debris by macrophages	• Phagocytosis of apoptotic bodies by tissue cells and/or macrophages

Fig 1.15: Factors thought to differentiate between necrosis and apoptosis (Osborne et al 1999).

1.3.4 Neurotrophic factor deprivation

Axonal injury is known to result in retrograde neuronal degeneration (Silveira et al 1994). A common explanation for neuron degeneration after axotomy is that the cell body is deprived of growth factors that it receives from the target field. Consistent with this idea is the finding that ganglion cell degeneration can be partially prevented by intravitreal administration of large doses of growth factors, such as fibroblast growth factors (Sievers et al 1987), nerve growth factor (Carmignoto et al 1989) and ciliary neurotrophic factor (Mey et al 1993). Since axons within the rat optic nerve show a capacity for regrowth following transection (Villegas-Pérez et al 1988, Bray et al 1991), and certain growth factors promote this growth and survival (Thanos et al 1989), the

suggestion has been made that ganglion cells die in glaucoma because of a lack of specific growth factors.

Brain derived neurotrophic growth factor (BDNF) has been particularly discussed in this respect because this neurotrophin and its high affinity receptor TrkB are associated with ganglion cells. Moreover, BDNF is known to be transported by the CNS neurons (Di Stefano et al 1992) and when BDNF is injected into the superior colliculus it reduces developmental ganglion cell death (Ma et al 1998). It has been suggested that in glaucoma the retrograde transport of growth factors from the brain to the ganglion cell somata is altered resulting in RGC death. BDNF transport in the optic nerve head has indeed been found to be altered after chronic IOP elevation in monkeys (Pease et al 2000) and after acute IOP elevation in rats (Quigley et al 1976, Quigley et al 2000), and intravitreal injection of BDNF reduces ganglion cell degeneration (Mansour-Robaey et al 1994). Similar RGC rescue was observed using viral vectors to achieve continuous synthesis of BDNF in the retinas of rats with experimental glaucoma (Martin et al 2003). Partial rescue of RGCs was also reported after the application of ciliary neurotrophic factor in ocular hypertensive (Ji et al 2004) and axotomised adult rat eyes (Van Adel et al 2003). It has, however, also been reported that ganglion cell numbers are unaffected in knockout mice lacking BDNF, suggesting that a decrease in the BDNF activity in a healthy retina may have little effect on ganglion cell survival (Callerino et al 1997), while, in another study, RGC apoptosis was observed before axonal transport obstruction and alterations in neurotrophin levels (Johnson et al 2000).

1.3.5 Glutamate excitotoxicity

ROS-induced neuronal damage can cause cell death accompanied by a release of glutamate into the extracellular space. Glutamate is the major neurotransmitter of the retina and is produced by a variety of retinal neurons that include PRs, bipolar cells, amacrine cells and ganglion cells. Glutamate is released from synapses under normal physiological conditions to act as a neurotransmitter and is immediately inactivated thereafter by being taken up by retinal astrocytes and Müller cells (Rauen et al 1998, Bouvier et al 1992, Barnett et al 2000). However, should the extracellular concentration of glutamate become abnormally high, glutamate can elicit a toxic effect on the RGCs (Lipton et al 1994). Importantly, elevated glutamate levels have been found in the vitreous of glaucoma patients and in animal models of glaucoma (Brooks et al 1997), although subsequent investigations could not corroborate the initial findings (Carter-Dawson et al 2002, Wamsley et al 2005).

Glutamate activates two classes of glutamate receptors: ionotropic and metabotropic. There are three subtypes of ionotropic glutamate receptors found on neurons, identified by their preferred agonists: N-methyl-D-aspartate (NMDA), alpha-amino-3 hydroxy 5-methyl 4-isoxandeproprionic acid (AMPA) and kainate (KA). The ionotropic receptor subtype that appears to be primarily involved in excitotoxicity is the NMDA receptor. AMPA/KA receptors are often situated presynaptically, which on stimulation leads to an excessive activation of postsynaptic NMDA receptors, thus playing a part in the cascade of events involving the role of NMDA receptors in RGC excitotoxicity (Mosinger et al 1991). The NMDA receptor is a ligand-gated ion channel, which is activated physiologically by glutamate. Glycine modulates the influence of glutamate positively, acting as a co-agonist. Activation of the NMDA receptor results in

depolarisation of the neurons caused by an influx of sodium and calcium. When the extracellular concentration of glutamate is elevated above a certain level, the receptor is hyperstimulated with an excess of calcium and sodium entering the RGCs not only via the NMDA channels but also via voltage-dependent Na^+ and Ca^{2+} channels (Bonne et al 1997). Increased cellular Ca^{2+} also leads to an accumulation of the cation within the mitochondria thereby disturbing its oxphos processes and thus decreasing the synthesis of ATP (Kruman et al 1998, Fiskum et al 2000). Consequently, anaerobic metabolism ensues leading to lactate accumulation, metabolic acidosis, compromised buffering capacity within the cell and eventually neuronal death. Lack of available ATP is also known to cause dysfunction of the sodium-potassium-ATPase pump and the calcium pump, as well as reversal of glutamate uptake (Osborne et al 2004).

There is also evidence for ROS causing an increase in glutamate levels by preventing the deamination of glutamate by the mitochondrial enzyme glutamate dehydrogenase (Fig 1.15). In the amino acid metabolism, all nitrogen is channelled through glutamate, which is then normally deaminated in the mitochondria. However, excessive amounts of ROS may hinder this process, since they can cause local damage to the (iron-sulfur) Fe-S centre of mitochondrial respiratory enzymes, mtDNA damage (Carelli et al 2004) and mitochondrial membrane destruction by lipid peroxidation (Kowaltowski et al 2001, Kowaltowski et al 1999).

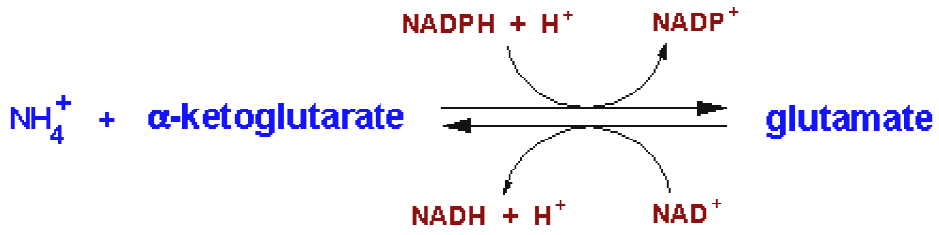

Fig 1.16: The reaction catalysed by the mitochondrial glutamate dehydrogenase.

1.3.6 Hypoperfusion and ischaemia of the optic nerve

The word ischaemia was coined by Virchow, who combined the Greek iskho, meaning “I hold back”, with háima, meaning “blood”. Hence, ischaemia refers to a pathological situation involving an inadequacy (not necessarily a complete lack of) blood flow to a tissue, thus depriving the tissue of three requirements: oxygen, metabolic substrates and removal of waste products. In experimental studies, multiple retinal ischaemic models have been described to result in loss of RGCs (Akiyama et al 2002, Goto et al 2002, Lafuente et al 2002, Wang et al 2002, Chidlow et al 2003, Inoue-Matsuhisa et al 2003). A link between ischaemia and excitotoxicity has also been proposed, as in ischaemia extracellular transmitter levels (particularly glutamate and GABA in case of the retina) are known to be elevated (Louzada-Junior et al 1992, Neal et al 1994) and cells that are excessively affected by these transmitters would be most likely to be susceptible (Fig 1.16) (Kalloniatis 1995, Osborne et al 1999). The particular susceptibility of neurones of the inner retina, and RGCs in particular, to ischemia is thought to be partly due to the fact that these cells express high levels of ionotropic glutamate receptors (Brandstatter et al 1994), as discussed previously (1.3.5). There is also evidence that magnocellular neurons are damaged more effectively than parvocellular neurons in glaucoma (Quigley et al 1987, Luo et al 2001), although this is considered controversial. This difference has been suggested to occur as a result of the greater NMDA receptor density on the magnocellular neurons, which also appear to be more susceptible to NMDA toxicity (Sucher et al 1997).

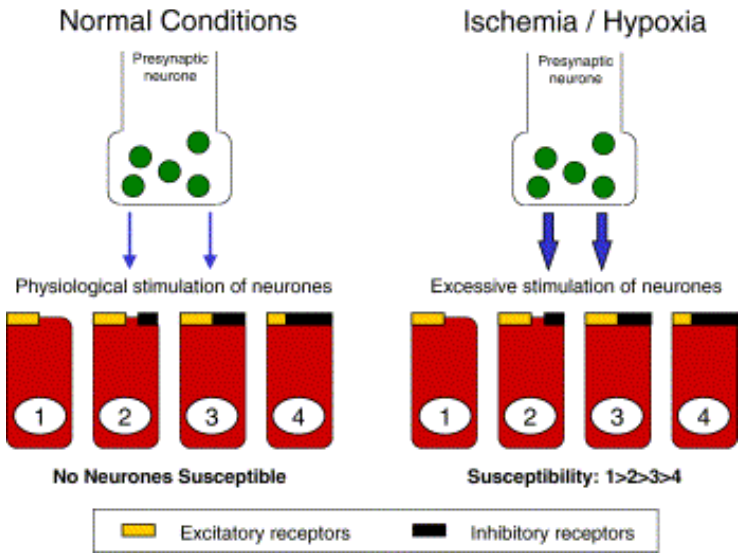

Fig 1.17: The importance of the balance between excitatory and inhibitory neurotransmitter input to retinal neurons. Under physiological conditions, the balance between inhibitory (e.g. GABA) and excitatory (e.g. glutamate) input to neurones is un-important: cellular functioning remains normal. When the neuron is subjected to an ischaemic or hypoxic insult, however, then survival may be favoured by the summed relative proportion of inhibitory to excitatory receptors expressed at synaptic terminals. Susceptibility to the insult will be in the order of 1>2>3>4 since the relative proportion of inhibitory receptors increases in that order (Osborne et al 2004).

Moreover, several non-ocular features consistent with vasospasm (eg, migraine, Raynaud's phenomenon) reportedly occur at higher frequency in patients with NTG, suggesting a role for vascular factors and decreased perfusion of the optic nerve in the pathogenesis of glaucoma. Calcium channel blockers may improve the perfusion of the optic nerve by vasodilation of the cerebral vasculature. Interestingly, glaucoma patients treated with this class of drugs were noted to experience fewer ONH and VF changes than those not taking the medication (Kitazawa et al 1989, Netland et al 1993, Sawada et al

1996). Also, nimodipine, a calcium channel blocker, has been shown to acutely improve contrast sensitivity in patients with NTG, further supporting the importance of vascular factors in glaucoma (Bose et al 1995).

1.3.7 Glial cell activation

Glial cell activation may be an important factor contributing to RGC death in glaucoma. Under normal conditions, glial cells support neuronal function through a variety of mechanisms, as described in section 1.1.5. Glial fibrillary acidic protein (GFAP), an intermediate filament, is a cell specific marker that distinguishes astrocytes from other glial cells. It is expressed by retinal astrocytes under normal conditions, but its synthesis is significantly elevated in glaucoma by astrocytes and Muller cells (Fig 1.17) (Wang et al 2000). Increased retinal expression of GFAP appears to be an early event in the pathogenesis of glaucoma; in animal models, it can be observed as early as 4 days after the induction of elevated IOP, before widespread RGC apoptosis (Woldemussie et al 2004).

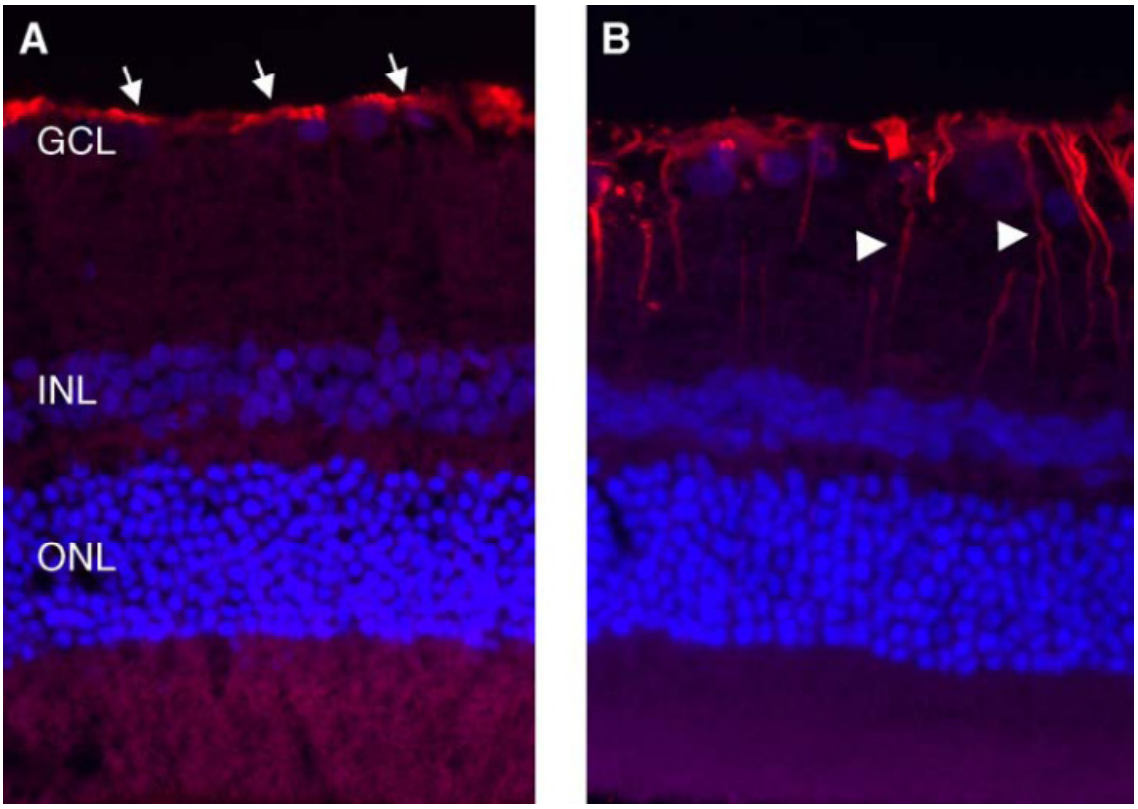

Fig 1.18: Immunohistochemical localisation of glial fibrillary acidic protein (GFAP) in the normal (A) and glaucomatous (B) rat retina. In the healthy retina, GFAP is restricted to retinal astrocytes (arrow). IOP elevation induces glial cell activation and synthesis of GFAP by Muller cells (arrowheads); GCL, ganglion cell layer; INL, inner nuclear layer; ONL, outer nuclear layer (Kuehn et al 2005).

This activation of retinal glial cells is thought to result in the active synthesis of substances that are harmful to RGCs, such as cytokines, reactive oxygen species or nitric oxide. Interestingly, studies on primary co-cultures of RGCs and glial cells suggest that tumour necrosis factor alpha (TNFa), a proinflammatory cytokine, is secreted by glial cells in response to elevated pressure to cause the apoptotic death of RGCs (Tezel et al 2000). Exposure of RGCs to TNF has been shown to reduce their mitochondrial membrane potential (Tezel et al 2004), while intravitreal injections of TNFa have been shown to cause degeneration of the optic nerve (Madigan et al 1996).

Moreover, an immunohistochemical study of human eyes with and without glaucoma showed that TNFa is synthesised by retinal glial cells in glaucoma and that the TNFa receptor is present on RGCs (Tezel et al 2001).

Another glial cell–mediated apoptotic stimulus may be the increased production of nitric oxide (NO). NO serves a variety of physiologic functions, including regulation of vascular tone, neurotransmitter release and synaptic plasticity. Excessive levels of this molecule can lead to cell death in a variety of cell types, including RGCs (Morgan et al 1999). NO has been found to inhibit mitochondrial complexes I and IV (Cleeter et al 2001), while excess plasma NO-mediated neurotoxicity (Liu et al 2003) and elevated levels of NOS activity have been implicated in glaucomatous optic neuropathy in humans (Liu et al 2000, Neufeld et al 1997) and in animal glaucoma models (Shareef et al 1999, Franco-Bourland et al 1998). Inhibition of NO production appears to reduce RGC damage in a rat model of glaucoma (Neufeld et al 1999, Neufeld et al 2002). Increased NOS levels, however, were not detected, and inhibition of NOS did not confer protection to RGCs, in a different rat model of glaucoma induced by hypertonic saline injection into the episcleral veins (Morrison et al 2005, Pang et al 2005).

1.3.8 Abnormal immune response

Evidence from clinical and experimental studies implicates the involvement of the immune system in glaucoma (Tezel et al 2004, Tezel et al 2007, Grus et al 2008, Wax et al 2000) and other neurodegenerative diseases (Scofield 2004). Glaucoma is marked by consistent profiles of up- and down-regulated serum antibodies against retinal and optic nerve antigens (Grus et al 2008, Wax et al

2001, Yang et al 2001). In more detail, antibodies against ocular antigens that have been shown to play a possible neurodegenerative role in glaucoma include antibodies against heat shock proteins (HSPs) (Tezel et al 2000), alpha-fodrin (Grus et al 2006), rhodopsin (Romano et al 1995), γ-enolase (Maruyama et al 2000), glutathione-S-transferase (GST) (Yang et al 2001), TNF-α (Tezel et al 2001), antiphosphatidylserine (Kremmer et al 2001) and γ-synuclein (Surgucheva et al 2002). Importantly, another recent finding was a higher likelihood of glaucoma progression in patients with raised anticardiolipin antibodies (Chauhan et al 2008). Moreover, in NTG elevated serum titres of autoantibodies against small HSPs (25 to 30 kDa) (Tezel et al 2000, Tezel et al 1998) and anti-Ro/SS-A have been found (Wax et al 1998). HSP-27 antibodies are known to trigger apoptotic cell death in RGCs in culture by inactivating or attenuating the ability of native HSP-27 to stabilise the actin cytoskeleton (Tezel et al 2000). In a more recent study by Reichelt et al, raised autoantibodies against histone-H4 were identified in POAG patients, while a decrease in the level of antibodies against the retinal S-antigen was also noted in this group (Reichelt et al 2008). Furthermore, the sera of NTG and POAG patients have been found to exhibit increased levels of soluble interleukin 2 receptors (Yang et al 2001), known to be elevated in autoimmune diseases (Mariotti et al 1992, Ferrarini et al 1998).

Autoantibodies to ONH proteoglycans in the sera of patients with glaucoma have also been reported (Tezel et al 1999). Proteoglycans perform various functions, including the formation of a spatial framework to support the optic nerve and blood vessels. It has therefore been suggested that an immune response directed against proteoglycans may weaken the extracellular matrix supporting the lamina cribrosa and induce or increase optic nerve cupping. Proteoglycans are also present in the cell walls of blood vessels and their

dysfunction could contribute to the development of splinter optic disc haemorrhages or disturbances in the autoregulation of blood flow in glaucoma (Tezel et al 1999).

1.4 Major susceptibility factors for glaucoma onset from large epidemiological studies

Progression from the healthy status to OAG has been assessed by longitudinal population-based studies in which a randomly chosen population living in a well-defined geographical area is examined at baseline, and re-examined after a certain period of time (Coleman et al 2008). One of the advantages of population-based epidemiological studies, unlike case-control studies, is the lack of control selection bias, in which the characteristics of the controls differ significantly from the characteristics of the population that is the target of inferences drawn from the study results. Below, the main risk factors are presented for glaucoma identified from the Barbados Incidence Study of Eye Diseases (BISED) on the African descent population in Barbados (Leske et al 2008), the Melbourne Visual Impairment Project (VIP) on white patients in Melbourne – Australia (Le et al 2003), the Rotterdam Eye Study (RES) on white patients in Rotterdam – Netherlands (deVoogd et al 2006, Muskens et al 2007), and other epidemiological studies. The BISED, VIP and RES studies estimated the incidence of OAG over 9, 5 and 6.5 years, respectively.

1.4.1 Baseline IOP

Baseline IOP was identified as one of the main risk factors for glaucoma in all three studies (BISED, VIP and RES), with the average baseline IOP being 18.0mmHg (SD 4.1), 15.1mmHg (SD 3.1) and 15.0mmHg (SD 3.1), respectively. Notably, a 10% to 14% increased risk of developing OAG was found in subjects with baseline IOPs ≥1mmHg higher than the average for the population over the following 5 to 9 years.

1.4.2 Age

Age at baseline was highlighted as a major risk factor for glaucoma in the BISED and RES studies, where the risk of developing OAG increased by 4% and 6%, respectively, in subjects who were 1 year older at baseline. The baseline mean age was 56.9 years (SD 11.3) in the BISED (Leske et al 2008) and 65.7 years (SD 6.9) in the RES (Muskens et al 2007). Also, in the VIP, where the baseline mean age was 58.7 years (SD 11.4), subjects with an age of 70-79 years old at baseline had a 12-fold increased 5-year risk of developing OAG compared to subjects aged 40-49 years old (Le et al 2007). In the population-based Baltimore Eye Survey, white people and African-Americans aged 70 years or older were 3.5 and 7.4 times more likely to have glaucoma than white people and African-Americans aged 40–50 years, respectively (Tielsch et al 1991). Additional evidence for the association between ageing and the increasing prevalence of OAG was also provided by the Blue Mountains Eye Study in Australia (Mitchell et al 1996) and the Los Angeles Latino Eye Study (LALES) (Varma et al 2004).

1.4.3 Systemic hypertension

The Baltimore Eye Survey reported a positive, although non-significant association of SBP and DBP with POAG in elderly individuals, but found a possible protective role of systemic hypertension in younger ages (Tielsch et al 1995). The Egna-Neumarkt study reported correlation between hypertensive POAG and systemic hypertension, regardless of the age of patients (Bonomi et al 2000). Moreover, the LALES, a large (n=6130) population-based study of adult Latinos, identified high SBP and mean arterial pressure (MAP) to be associated with a higher prevalence of OAG, while in the same study low DBP, DPP, SPP and were also linked to OAG (Memarzadeh et al 2010). In contrast, the 9-year follow-up from the Barbados Eye Study did not confirm the role of systemic hypertension as a risk factor for glaucoma (Leske et al 1995, Leske et al 2001) and revealed a weak negative association with SBP [RR= 0.91 (95% CI 0.84, 1.00) per 10 mmHg] (Leske 2009). Blood pressure and IOP have been reported to be positively associated (Hennis et al 2003, Klein et al 2005) and, since increased IOP is a risk factor for POAG (Sommer et al 1991), it is possible that increased BP and POAG could also be associated through this BP-IOP relationship. Thus, the reported link between BP and POAG may be confounded by IOP.

1.4.4 Family history

In the Baltimore Eye Survey, first-degree relatives of patients with POAG had 2·9 times greater odds of having glaucoma than non-relatives (Tielsch et al 1994). In a population-based familial aggregation study in Rotterdam (Wolfs et al 1998), the lifetime risk of glaucoma was 9.2 times higher in siblings and

offspring of glaucoma patients than in siblings and offspring of controls. Family history was also identified as a risk factor for OAG in the BISED [RR: 2.4, 95% CI (1.3-4.6)].

1.4.5 Other

Other risk factors found in the BISED were a thinner CCT [RR: 1.41, 95% CI (1.01-1.96) per 40µm thinner] and lower MOPP [RR: 2.6, 95% CI (1.4-4.6)] (Leske et al 2008). These results were not repeated in either the VIP or the RES studies. However, the RES reported an association between the use of systemic calcium channel blockers for the treatment of systemic hypertension [RR: 1.9, 95% CI (1.1--3.3)] and the development of OAG (Muskens et al 2007). Moreover, the VIP reported a markedly increased risk of OAG in individuals with pseudoexfoliation [RR: 11.2, 95% CI (2.0-63.3)] and large cup-to-disc ratios (>0.7) [RR: 7.9, 95% CI (4.4-14.1)], while the use of systemic alpha-blockers was also significantly associated with the onset of OAG [RR: 4.8, 95% CI (1.2-18.8)] (Le et al 2003). Diabetes was not a risk factor in any of the three studies (BISED, RES, VIP) (deVoogd et al 2006). An additional demographic risk factor for OAG from the Baltimore Eye Survey (Tielsch et al 1991) and other studies (Leske et al 1994, Mason et al 1989) was African descent, with African-Americans being four times more likely to have glaucoma than white people.

1.5 Major susceptibility factors for glaucoma progression from large clinical trials and smaller studies

Risk factors for the progression of OAG have been explored in four large multicenter randomised clinical trials: the Collaborative Normal Tension Glaucoma Study (CNTGS) (CNTGS AJO 1998), the Early Manifest Glaucoma Trial (EMGT) (Heijl et al 2002), the Advanced Glaucoma Intervention Study (AGIS) (AGIS AJO 2000) and the Collaborative Initial Glaucoma Treatment Study (CIGTS) (Lichter et al 2001). To date, although several risk factors for OAG progression have been established, some of the results have been inconsistent. This may be explained partly by differences in study designs, the variety of definitions used for glaucoma, and the fact that few variables have been included consistently in risk factor analyses across studies (Coleman et al 2008). The stage of OAG differed among the four trials with AGIS (MD of -10.5) (AGIS 1998) and CNTGS (MD of -8 dB) (CNTGS 1998) having the most advanced damage, and CIGTS (MD of -5.5) (Gillespie et al 2003) and EMGT (MD of -4.7 dB) the least. Also, VF progression was defined differently between studies, making useful comparisons challenging. In the AGIS and EMGT, VF progression was defined uniquely to each study, and then treated as a binary outcome in assessing risk factors, while in the CIGTS the definition of progression relied on the mean deviation, rather than the threshold sensitivity change at two or more specific points (AGIS) or pattern deviation change at three or more points (EMGT) (Heijl et al 2008). Despite these differences in study design and definitions, the discrepancies between the above studies could also reflect differences among populations in terms of genetic predisposition and exposure to environmental factors.

1.5.1 Baseline IOP

In the CIGTS, the level of baseline IOP, which was required by inclusion criteria to be at least 20 mmHg, was not significantly associated with subsequent VF loss. However, the range (maximum IOP – minimum IOP) of the six IOP measurements taken at baseline, which varied from 0.5 to 25 mmHg with a median of 6.5 mmHg, did relate to subsequent VF progression (Musch et al 2009). In more detail, as the range of the six baseline IOPs increased, VF loss increased (P=0.0184), while participants whose range was 8.5 mmHg or greater had a 96% greater risk of substantial VF loss (P=0.0006) when compared to those with a lesser IOP range at baseline. During follow-up, in the CIGTS, three IOP measures (increased maximum IOP, SD of IOP and range of IOP) were also significantly associated with VF progression, with higher baseline IOP being one of the main predictors of these three IOP measures (Musch et al 2011). In support of the trial findings, in a recent retrospective study involving 140 Tunisian patients with POAG, IOP at diagnosis was statistically higher in subjects with VF progression, as compared to stable cases (P=0.03; OR=5.25) (Loukil et al 2012).

1.5.2 Mean IOP

Higher mean IOP has been shown to be predictive of progressive VF loss in patients with newly diagnosed glaucoma in the EMGT (HRs, 1.12–1.13 per mmHg higher) (Leske et al 2003, Leske et al 2007), with normotensive glaucoma in the CNTGS (CNTGS 1998) and with advanced glaucoma in the AGIS (AGIS 2000). Similarly, in a smaller prospective, randomised clinical trial

comparing primary laser trabeculoplasty with medication, VF decay showed greater correlation to mean IOP and IOP variation (range and peak) than to baseline IOP or degree of IOP reduction (Bergea et al 1999). The relation between mean IOP and VF loss in the whole group was not quite linear, with more decay at higher IOP levels. Moreover, two retrospective studies by Stewart et al reported that mean IOP, as well as the range and the average SD of IOP measurements over the follow-up period, significantly differed in progressing POAG subjects, as compared to those who were stable (Stewart et al 1993, Stewart et al 2000).

1.5.3 Effect of treatment on IOP

To date, the only two large, randomised, multi-center clinical trials that compared the reduction of IOP in OAG patients to an observation group were the EMGT and CNTGS, while the AGIS, the Low-Pressure Glaucoma Treatment Study (LoGTS) and the CIGTS compared between different treatments. In the EMGT, where patients were randomised to either laser trabeculoplasty plus topical betaxolol (n = 129) or no initial treatment (n = 126), the potential effect of cataracts was minimised by the emphasis on VF pattern loss. On average, treatment reduced the IOP by 5.1mmHg and progression was less frequent in the treatment group (58/129; 45%) as compared to the controls (78/126; 62%) (p=0.007) and occurred significantly later in treated patients (Heijl et al 2002). In the CNTGS, where 145 patients with progressing NTG were randomised to either no treatment or treatment aiming for IOP reduction of 30% within 6 months and maintenance for 4 years by surgical and/or medical means, the protective effect of IOP-lowering treatment was noted only when subjects with cataract progression were censored or removed from the analysis (CNTGS AJO

1998). In the Low-Pressure Glaucoma Treatment Study (LoGTS), no significant association was found between IOP and VF progression and the authors argued that, once the IOP is reduced to relatively low values (mean follow-up IOP was 14mmHg), the importance of other risk factors may become either more apparent or important for determining progression (De Moraes et al 2012).

1.5.4 Long- and short-term IOP fluctuation

In the AGIS, large variations in the IOP from visit to visit were associated with OAG progression (Nouri-Mahdavi et al 2004), whereas in the EMGT fluctuations in IOP were not associated with increased risk of progression (Bengtsson et al 2007). Factors to account for this discrepancy would include the differences in the stage of the disease and in the population ethnicity between the two studies, as well as the fact that the EMGT analyses did not include post-progression IOP values, which would be biased towards larger fluctuations because of more intensive treatment. Although in AGIS the authors did not initially censor or exclude IOP measurements after the second or third surgical intervention, in 2008 it was reported that long-term IOP fluctuation was associated with VF progression in patients with low mean IOP, but not in patients with high mean IOP (Caprioli et al 2008). Long-term IOP fluctuation was also shown to act as a risk factor for progressive VF deterioration even in glaucoma patients with low IOPs (<18mmHg) after a triple procedure (phacoemulsification, posterior chamber intraocular lens implantation, and trabeculectomy) (Hong et al 2007b). Similarly, in 2007 a study by Lee et al revealed IOP SD as a predictor for glaucoma progression in two cohorts of glaucoma patients. After controlling for age, mean IOP, VF stage

and other covariates, the authors found that each unit increase in IOP SD resulted in 4.2 to 5.5 times higher risk of glaucoma progression (Lee et al 2007). Moreover, O'Brien et al. found that three measures of IOP variation showed significant correlation with the rate of VF deterioration in 10 patients whose VF loss worsened during treatment: the standard error of the mean (SEM), the SD, and the range of IOP (O'Brien et al 1991). More recently, in the multicenter Latanoprost/Bimatoprost/Travoprost Study, Varma et al showed that the inter-visit IOP range was associated with risk factors for glaucomatous change, such as African-American race and high baseline IOP (Varma et al 2008). Finally, in the CIGTS increased IOP fluctuation (SD or range) and maximum IOP were important predictors of progressive VF loss (Musch et al 2011). In clinical practice, this would be easiest to measure by observing the inter-visit range of IOP over time, as advocated by Varma et al (Varma et al 2009) and commented on by Katz and Myers (Katz et al 2009).

An additional risk factor for glaucoma progression identified from retrospective studies was higher short-term (diurnal) IOP fluctuation (Asrani et al 2000, Bergea et al 1999). In the study by Bergea et al, which included 82 OAG patients, VF decay showed a greater correlation with IOP variation (range and peak) and mean IOP, than with baseline IOP or degree of IOP reduction (Bergea et al 1999). Similarly, the study by Asrani et al, with only 64 glaucoma patients, showed that baseline IOP had no predictive value, while the diurnal IOP range and the IOP range over multiple days were significant risk factors for progression, even after adjusting for baseline IOP, age, race, gender and baseline VF damage (Asrani et al 2000).

1.5.5 Greater age

Older age was reported to be associated with an increased risk of VF progression in the AGIS (Nouri-Mahdavi et al 2004) and the EMGT (Leske et al 2003, Leske et al 2007), but not in the CNTGS (Drance et al 2001). In the AGIS, each 5 year increment in age increased by 30% the risk of a 1.0dB or greater worsening of the VF. In the EMGT, subjects who were 68 years or older were at a 51% increased risk of progression, as compared to participants <68 years old. In the CIGTS, older age at baseline was associated with VF progression (Musch et al 2009), with the age effect being modified by time ($P<0.0001$), such that the effect of age on VF loss increased over time. For every 10 year increase in age, the risk of a 3 dB worsening of MD increased 35% ($P=0.0006$). Although VF progression was measured in different ways in these clinical trials, the AGIS, EMGT and CIGTS all show more VF progression with increasing age.

1.5.6 More severe visual field MD at baseline

In the EMGT, eyes presenting with a baseline MD worse than −4.0dB progressed faster ($P=0.05$) than eyes with better MD (Leske et al 2007), while more advanced visual field score appeared to be protective in AGIS. This could have resulted from a ceiling effect, where there is little room for subjects to lose VF or to get worse because they are closer to the top of the scale. Similarly to the EMGT, in a very recent retrospective study by Loukil et al, eyes with initial VF defect more than 8.2dB were found 4.8 times more likely to progress ($P=0.07$), while eyes diagnosed at an early glaucoma stage had 4 times the chance of maintaining a stable VF ($P=0.003$) (Loukil et al 2012). However, another retrospective study by Forchheimer et al found no relationship

between the rate of VF change (dB/year) and the severity of the baseline VF MD, with the authors suggesting that more aggressive IOP lowering in eyes with more advanced glaucoma could have masked this relationship (Forchheimer et al 2011).

1.5.7 Lower ocular perfusion pressure

The EMGT showed that lower systolic perfusion pressure (SPP) (≤160 mmHg; HR 1.42; 95% CI 1.04–1.94) was a risk factor for progression. Similar, although non-significant, trends were also observed for the diastolic perfusion pressure (DPP) and mean ocular perfusion pressure (MOPP) (Leske 2009). One could argue that the association of SPP to progression was due to the effect of high IOP alone, regardless of systolic blood pressure (SBP), but the EMGT found that low SBP (≤125 mmHg; HR 0.46; 95% CI 0.21–1.02) was independently associated with progression, even in patients with low IOP. Low SBP is known to cause an increase in vascular resistance, which diminishes blood flow to the ONH (Hayreh et al 2001), and compensatory vasoconstriction of peripheral organs and tissues (Lindholm et al 2005), including the eye and the retinal and choroidal circulation. Another progression factor in the EMGT was history of cardiovascular disease, significant in patients with IOP over the median value (HR 2.75; 95% CI 1.44–5.26). Taken together, these results were consistent with the hypothesised effect of vascular factors on glaucoma progression (Flammer et al 2002). Similarly, in the LoGTS, lower MOPP during follow-up was significantly associated with VF progression and this effect was not significantly affected by other covariates, such as use of systemic antihypertensives and randomisation arm (De Moraes et al 2012). The authors suggested that an imbalance between IOP mechanical stress and blood supply

could lead to hypoxia, which might be responsible, at least partially, for axonal damage and RGC death (Ramdas et al 2011a). Lower DPP has also been linked to glaucoma (Leske et al 2001). It is interesting to note that, even in people without glaucoma, lower DBP (<90mmHg) secondary to antihypertensive treatment has been found to be associated with increased disc cupping and decreased rim area (Topouzis et al 2006). In the CNTGS and AGIS, no association between systemic hypertension and OAG progression was noted.

1.5.8 Presence of pseudoexfoliation (PXF)

PXF was a risk factor in the EMGT and was not evaluated in other large prospective randomised trials. In the EMGT, PXF had a prominent role in the higher baseline IOP group, with 18 of the 19 PXF patients progressing. Also, although only 4 patients with lower baseline IOP had PXF, all progressed, again confirming the importance of this condition on progression (Leske et al 2007). Similarly, in a recent retrospective study involving 140 Tunisian POAG patients, PXF was also identified as a risk factor for progression (OR=2.84; P=0.05) (Loukil et al 2012).

1.5.9 Optic disc haemorrhages

The association between splinter-shaped haemorrhages on the optic disc rim and glaucoma is well known (Drance et al 1989, Bengtsson et al 1981). Although the aetiology of disc haemorrhages is unclear, many investigators suspect a pathogenic link to rim notching (Airaksinen et al 1981) or a localised RNFL defect (Sugiyama et al 1997). In the EMGT, presence of disc haemorrhages at follow-up was a significant factor for progression (Leske et al

2003, Leske et al 2007) and was significantly associated with time to progression (HR=1.02; CI 1.01–1.04). In a smaller retrospective study from Japan on 70 NTG patients, the cumulative probability of VF progression was significantly greater for patients with disc haemorrhages as compared to those without (Ishida et al 2000). In more detail, all eyes with at least two occurrences of disc haemorrhage showed progression using the glaucoma change probability analysis, whereas only three of nine eyes showed progression in the non-recurrent disc haemorrhage group ($P<0.0001$). Furthermore, a significant relationship was found between the location of the disc haemorrhage and the area of the progression of the VF loss in 65.4% of progressive patients with disc haemorrhage (Ishida et al 2000). Moreover, the study by Rasker et al suggested that a history of disc haemorrhage increases the risk of progression more than 5-fold in treated patients with NTG (Rasker et al 1997), while similar results were also reported by Siegner and Netland in cases of NTG and POAG (Siegner et al 1996). Nevertheless, there are conflicting reports regarding the prognostic significance of disc haemorrhage, with some researchers believing that these are completely unrelated to VF progression (Hoyng et al 1992, Heijl et al 1986, Rasker et al 2000).

1.5.10 Thinner central corneal thickness (CCT)

Investigation of the effect of CCT on glaucoma progression is complicated by the relationship between CCT and both IOP measurement and ageing (Foster et al 1998). To date, it remains unclear whether CCT is indeed an independent risk factor for glaucoma progression, a phenotypic marker of diverse ethnic groups with differing inherent glaucoma risk, or just a source of error in clinical tonometry (Brandt et al 2007). In the EMGT, thinner CCT (HR 1.25; 95% CI

1.01–1.55 per 40µm lower) was a significant risk factor for progression, especially in patients with higher baseline IOP (HR 1.42; 95% CI 1.05–1.92 per 40µm lower), but not lower baseline IOP (Leske et al 2007). Moreover, in 2004, a case-control patient population study by Kim et al demonstrated that VF progression in 88 patients with OAG was significantly associated with thinner CCT (Kim et al 2004). Similarly, in another retrospective study involving 163 eyes with chronic PACG, patients with a thinner cornea were at greater risk for VF progression even if they maintained a low IOP (<18mmHg) after treatment (Hong et al 2007a). In a large prospective observational study by Jonas et al, CCT correlated significantly ($P<0.001$) and positively with the neuroretinal rim area and negatively with the amount of VF loss at the time of referral, while VF progression was statistically independent of CCT (Jonas et al 2005). Similarly, other smaller studies have also failed to find an association between CCT and glaucoma progression (Shah et al 2007, Chauhan et al 2005).

1.5.11 Diabetes

Diabetes as a risk factor for progressive VF loss was assessed in the AGIS (Nouri-Mahdavi 2004, AGIS AJO 2002) and found to not differ between those who progressed (21.2% were diabetic) and those who did not progress (21.5% were diabetic). Self-report of diabetes was associated with OAG progression in the CIGTS (Lichter et al 2001), but not in the CNTGS (Drance et al 2001) and EMGT (Leske et al 2007). In the latter study, diabetes was not listed among the factors evaluated for VF progression, which likely relates to the fact that only nine (3.5%) of the 255 enrolled participants reported a history of diabetes. In the CIGTS, while black subjects were over-represented among diabetics (60%, 61/102, of diabetics were black), diabetes was more predictive of VF loss than

race in models with each variable included separately or combined (Musch et al 2009). The authors suggested as a possible explanation the fact that diabetics are more prone to scarring after trabeculectomy, as proposed previously by Hugkulstone et al (Hugkulstone et al 1993).

1.5.12 Race

In the CIGTS, while a subject's race was not significantly associated with the risk or timing of cataract extraction, the impact of race as a risk factor for VF progression was only evident in those subjects who required cataract surgery during the course of follow-up. More specifically, blacks who underwent cataract extraction showed more VF loss than whites undergoing the same procedure (Musch et al 2009). According to the authors, this could relate either to differing thresholds for surgery or differing responses to that procedure. Other likely contributing factors to the greater progression of OAG in African-derived persons is their longer average duration of disease (2.3 years longer) as compared to European-derived persons, as well as differences in access to care and acceptance of and response to treatment (Broman et al 2008). Similarly, in a retrospective study by Wilson et al, both VF loss at initial diagnosis and VF progression appeared to be worse in black patients with OAG, as compared to white (Wilson et al 1985). However, several other glaucoma studies were unable to show that race was a risk factor for disease progression (Katz et al 1997, Stewart et al 2000, Schulz et al 1987), while the role of ethnicity was not evaluated in the EMGT.

1.5.13 Gender

In the AGIS, it is puzzling that male gender was a significant risk factor for VF progression only in the ATT (argon laser trabeculoplasty – trabeculectomy – trabeculectomy) sequence (AGIS 2002). Many other glaucoma studies (Ishida et al 1998, Martinez-Bello et al 2000, Suzuki et al 1999, Araie et al 1994, Katz et al 1997, Stewart et al 2000) and the TAT (trabeculectomy – argon laser trebeculoplasty - trabeculectomy) sequence of AGIS indicated that gender is not a significant risk factor for disease progression. In contrast, two studies found female gender, rather than male gender, to be a risk factor for VF loss (Wilson et al 1982, Drance et al 2001); in one of these studies, gender was significant in univariate Kaplan–Meier analysis, but not in multivariate Cox proportional hazards analysis (Drance et al 2001).

1.5.14 Myopia

The large, abnormally shaped and tilted myopic scleral canal and the thinning of the myopic lamina cribrosa and peripapillary sclera are some of the anatomical factors thought to predispose myopic eyes to glaucomatous damage (Jonas et al 2004, Bellezza et al 2000). However, clinical results to date are not conclusive, with Jonas et al finding no significant association between mean visual field loss and refractive error, and suggesting that, for eyes less myopic than −8 D, refractive error may not contribute much to the optic nerve head susceptibility to IOP (Jonas et al 2002). Similarly, several Japanese studies have been unable to show a link between VF progression and refractive error (Ishida et al 1998, Suzuki et al 1999, Araie et al 1994). However, a Taiwanese retrospective study on 515 POAG patients demonstrated a significant

association between myopia greater than −6 D and VF progression (Lee et al 2008). Similarly, Chihara et al found that moderate-to-severe myopia (>−4 D), but not mild myopia, was a significant risk factor for VF progression in glaucoma (Chihara et al 1997).

1.5.15 Other

Other risk factors for progression, identified from retrospective studies, include optic disc features, such as a smaller neuroretinal rim area (Jonas et al 2004), peripapillary atrophy (Uchida et al 1998, Teng et al 2011) and the presence of acquired optic disc pits (Ugurlu et al 1998). It is perhaps relevant to note that the results of retrospective studies should be taken cautiously, due to limitations in study design, inadequate sample sizes, large rates of loss to follow-up, and other considerations. They may provide interesting and often clinically useful hypotheses, but need to be confirmed by larger randomised longitudinal studies.

More recently, in the LoGTS a significant association was found between the use of topical timolol maleate 0.5% and the risk of progression in patients with low-pressure glaucoma compared to the use of brimonidine tartrate 0.2% (Krupin et al 2011), which was independent from other known risk factors for glaucoma progression (disc haemorrhage, older age, and lower systemic blood pressure) despite similar mean IOP during follow-up. This finding could suggest that brimonidine has an effect on IOP-independent mechanisms that decrease or delay the rate of VF progression in glaucoma patients with IOPs in the statistically normal range and that this possibly neuroprotective effect is independent of ocular perfusion pressure (De Moraes et al 2012).

Alternatively, it is possible that topical beta-blockers have no benefit or are detrimental. It is also particularly interesting that the brimonidine group had higher untreated mean and peak IOP at baseline, as well as higher peak and fluctuation during follow-up, and still progressed at slower rates than the timolol group. Use of systemic antihypertensives was also independently associated with disease progression in the LoGTS (De Moraes et al 2012). Similarly to LoGTS, in a recent retrospective study in the Tunisian population the use of topical beta-blockers was highlighted as a risk factor for progression (Loukil et al 2012).

In the EMGT, an additional risk factor for progression was bilateral disease at baseline (Leske et al 2007). Also, low formal educational achievement was identified as a risk factor for progression in both intervention sequences in the AGIS, with the authors suggesting that this could be explained at least in part by the association between low educational achievement and cataract. This association has been shown in other studies (Hiller et al 1986, Kahn et al 1977, Leske et al 1991), although not found in the AGIS (AGIS 2001).

1.6 Potential additional susceptibility factors for glaucoma development and progression

1.6.1 Mitochondrial dysfunction and mtDNA changes

Emerging evidence suggests that mitochondrial dysfunction may contribute to the pathogenesis of a range of neurodegenerative diseases (Lin et al 2006), including Parkinson's disease, Alzheimer's disease and glaucomatous optic neuropathy (Kong et al 2009, Lascaratos et al 2012). A maternal family history

of POAG is more likely than a paternal family history, suggesting a possible mitochondrial genetic influence (Charliat et al 1994, Mitchell et al 2002, Nemesure et al 1996, Shin et al 1977). This is unexpected, as there is no sex predilection to POAG prevalence and there is no maternal influence on IOP, and so Mendelian inheritance cannot explain these epidemiological differences. However, a study from the North East of England has failed to show an association between mitochondrial haplogroups and POAG in Caucasian patients (Andrews et al 2006). Similarly, a recent study from the same group involving 137 POAG patients has not found an association between the mtDNA haplogroups H, T, J and U and either NTG or high tension glaucoma (HTG), although there was a tendency for haplogroup J to be over-represented amongst the NTG group compared with controls (Yu-Wai-Man et al 2010). This is an interesting observation considering the link between haplogroup J and increased risk of visual loss in Caucasian LHON mutation carriers (Hudson et al 2007) and also the role of mtDNA background in modulating the assembly kinetics of oxphos complexes (Pello et al 2008). Recently, the mtDNA haplogroups have been implicated in the pathogenesis of other types of glaucoma, with haplogroups T and L2 conferring susceptibility to pseudoexfoliation glaucoma in the Saudi Arabian population (Abu-Amero et al 2011) and haplogroup U being associated with a reduced risk for pseudoexfoliation glaucoma in the German population (Wolf et al 2010).

Other research teams have also screened glaucoma cohorts for mitochondrial mutations implicated in LHON. In one study involving 551 Japanese POAG patients and 284 controls, 5 LHON-associated mitochondrial DNA mutations were identified in the glaucoma group, whereas no such mutations were found in the control group. However, the difference was not statistically significant and the study was not conclusive as to whether these mtDNA mutations were

a risk factor for POAG (Inagaki et al 2006). Equally, in a Swiss population, no mtDNA mutations at nucleotides 11778, 3460 and 14484, typically associated with LHON, were identified amongst 54 unselected patients with NTG (Opial et al 2001).

Age-associated somatic mutations in mitochondria have also been shown to potentially contribute to glaucoma pathogenesis. Indeed, in a study by Abu-Amero et al, a decrease was noted in the mitochondrial mean respiratory activity in 24 of the 27 POAG patients, suggesting a role for mitochondrial dysfunction in the pathogenesis of POAG (Abu-Amero et al 2006). Interestingly, the same group was unable to show significant mtDNA derangements in primary angle closure glaucoma (Abu-Amero et al 2007), consistent with the idea that anatomic factors may be more important determinants for primary angle closure than mitochondrial genetics. Moreover, in primary congenital glaucoma patients from the Indian subcontinent, 8 (22.9%) of 35 patients had potentially pathogenic mtDNA sequence variants (Tanwar et al 2010). It is important to note that these studies have been performed on mtDNA isolated from peripheral blood leucocytes, while tissue specific mutations in the trabecular meshwork, RGC compartment and optic nerve head may contribute more significantly to glaucoma pathogenesis. Indeed, mtDNA deletion has been shown to be increased more than 5-fold in the trabecular meshwork of POAG patients comparing to controls, accompanied by a significant decrease in the number of mitochondria per cell and by cell loss (Izzotti et al 2010).

Very recently, Lee et al have shown that lymphoblasts from POAG patients exhibit a defect in the complex-I of the oxphos pathway, leading to decreased rates of respiration and ATP production (Lee et al 2012). Complex-II-driven ATP synthesis was not reduced in the POAG lymphoblasts, as compared to control.

When cells were grown in galactose media, where they were forced to rely on mitochondrial ATP production, no significant differences were noted between the control and POAG cohorts. Thus, the authors concluded that while complex-I defects did not impact lymphoblast growth when the cells were forced to rely on oxidative ATP supply, it remains possible that in the presence of a multitude of cellular stressors as seen in the early stages of POAG, these defects may lead to a bioenergetic crisis in retinal ganglion cells and an increased susceptibility to cell death (Lee et al 2012).

1.6.2 Oxidative stress

It is more than two decades since oxidative stress was first proposed to contribute to glaucoma pathogenesis (Alvarado et al 1981). In 2006, in the study by Abu-Amero et al, 127 different novel non-synonymous mtDNA changes were found in the lymphocytes of patients with POAG with none found in control subjects, while 22 of the identified mutations were potentially pathogenic (Abu-Amero et al 2006). Importantly, these POAG patients had a high frequency of mtDNA transversion mutations (73.5%). This is in contrast to LHON patients, where mtDNA transition changes comprise almost 70% of the mutations reported in MitoMap (Brandon et al 2005), and to NAION patients, where 75% of nonsynonymous mtDNA changes found are transitions (Bosley et al 2004). Abu-Amero et al argued that the guanine base has the lowest oxidation potential of the four DNA nucleobases, making G:C to T:A or G:C to C:G transversion mutations frequent in the setting of oxidative stress (Sekiguchi et al 2002). The presence of mtDNA transversions in POAG may be evidence of increased oxidative stress in these patients and would suggest that alternative mitochondrial damage and repair mechanisms are involved, which

may contribute to the unique optic nerve damage noted in POAG. Moreover, increased serum total antioxidant levels and decreased urinary 8-hydroxy-2-deoxyguanosine, a marker of oxidative DNA damage, have been reported in NTG patients as compared to healthy controls, attributed by the authors to compensatory alterations in response to increased systemic oxidative stress in glaucoma (Yuki et al 2010).

Oxidative stress in the human trabecular meshwork (TM) has also been implicated in the pathogenesis of OAG. More specifically, oxidative stress has been reported to induce human TM degenerative changes that favour increased IOP, with increased DNA oxidative damage noted in the TM of patients with POAG, as compared to controls. Interestingly, a statistically significant correlation was found among human trabecular meshwork DNA oxidative damage, VF damage and IOP (Sacca et al 2005). Hydrogen peroxide has also been shown to induce rearrangement of human TM cells and compromise their integrity (Sacca et al 2007). The human TM was found to be more sensitive to oxidative damage induced by hydrogen peroxide than the cornea or the iris, with the authors arguing that the cornea and lens are directly exposed to light and therefore possess antioxidant defence mechanisms that may not be activated in the TM (Izzotti et al 2009). The same group also demonstrated a link between oxidative stress and mitochondrial dysfunction in the TM of POAG patients by finding that the glutathione-S-transferase (GST) M1-null genotype was associated with increased amounts of mtDNA deletion in the TM of these patients and a decreased number of mitochondria per cell, as compared with GSTM1-positive subjects (Izzotti et al 2010).

More recently, the aqueous humour of ten POAG patients has been shown to have increased levels of glutamine synthase (GS) and nitric oxide synthase (NOS), as compared to an equal number of controls (senile cataract patients) (Bagnis et al 2012). The GS overproduction might be linked to neuronal injury or to the potential role of glutamate as a modulator in the ciliary body signalling, while the NO increase through inducible NOS could form toxic products changing the metabolic conditions of the TM. In the same study, a significant reduction was noted in the levels of antioxidant enzymes superoxide dismutase (SOD) and GST in the aqueous humour of POAG patients, as compared to controls, which, as argued by the authors, could aggravate the imbalance between both oxygen- and nitrogen-derived ROS production and detoxification (Bagnis et al 2012). The reduction in SOD could not be replicated in two other studies, showing a significant increase in SOD (Ghanem et al 2010, Ferreira et al 2004), as well as the antioxidant enzymes glutathione peroxidase (GPO) (Ghanem et al 2010, Ferreira et al 2004) and malondialdehyde (MDA) (Ghanem et al 2010), in the aqueous humour of POAG patients, as compared to cataract patients. No difference was noted in the activity of the catalase (CAT) enzyme in the aqueous humour between the two groups, in either study (Ghanem et al 2010, Ferreira et al 2004). The total reactive antioxidant potential (TRAP) was significantly lower in the aqueous humour of POAG patients, as compared to the cataract cohort (Ferreira et al 2004). Lower total antioxidant status (TAS) levels in the serum and aqueous humour of glaucoma patients, as compared to age-similar cataract patients, was also found in an Iranian cohort (Sorkhabi et al 2011). These studies only included a relatively small number of patients and it was not clear whether these changes were only a result of the glaucomatous process or contributed to the pathogenesis of the disease.

1.6.3 Corneal biomechanics

Apart from the role of thinner CCT in glaucoma progression (1.5.10), a lower corneal hysteresis (CH) was also found to predict VF deterioration in a retrospective study, suggesting that corneal resistance itself may influence progression and that the CCT might be an indicator of anatomical structure reflecting distensibility and elasticity of ocular tissues (Congdon et al 2006). In more detail, each mmHg increase in CH was associated with a 20% decrease in progression, whereas CCT showed no association with progression. However, this association became non significant after adjusting for the axial length, which could favour a potential association between CH and the elasticity of other ocular tissues (Congdon et al 2006). Similarly, in a very recent retrospective study by De Moraes et al, a significant correlation was found between CH and CCT, and CH [OR (95%CI): 1.55 (1.14-2.10) per mmHg lower] was more strongly associated with VF progression than CCT (De Moraes et al 2012). Notably, despite losing their strength when compared with a stronger variable (CH) in the multivariate analysis, both corneal resistance factor (CRF) and the difference between IOPcc and IOPg were associated with progression in the univariate analyses.

The use of CH as a measure of corneal biomechanical properties has been investigated in various studies (Wells et al 2008, Ang et al 2008, Broman et al 2007) and CH is known to decline with ageing (Kotecha et al 2006). However, the relationship between CH and VF progression remains obscure. In the OHTS, a thinner CCT may result in underestimation of the transcorneal pressure gradient measured by GAT and, since CCT correlates with CH, the same argument could also apply to the latter measurement. It is also possible that

the corneal biomechanical properties are a surrogate parameter of the susceptibility of the optic nerve to IOP-dependent and IOP-independent factors associated with glaucomatous loss. For example, it has been suggested that CH (but not CCT) is associated with increased deformation of the optic nerve surface during transient elevations of IOP (Wells et al 2008), while Bochmann et al have shown in a prospective study that acquired pit-like changes of the optic nerve are more frequent in eyes with lower CH (Bochmann et al 2008). Moreover, Leite et al in 2010 reported that healthy individuals of African ancestry, a group known to be at increased risk of glaucoma onset, showed lower CH than healthy individuals of European ancestry (Leite et al 2010). In addition, it has been shown that among eyes with asymmetric glaucomatous VF loss, CH was lower in eyes with worse VF damage independently of its effect on IOP measurements (Anand et al 2010). It is still unclear, however, whether the relationship between CH and VF loss is cause-effect or mere association. Perhaps corneal thinning and decrease of CH could be a consequence of the glaucomatous process, similarly to optic disc cupping and nerve fibre layer loss. Ideally, prospective studies that assess the CH at baseline should address whether lower CH is indeed a risk factor for progression, as was shown with CCT in the OHTS (Gordon et al 2002).

1.6.4 Genetic factors

As discussed previously, family history is a risk factor for the development of glaucoma, and there is a higher prevalence in both first and second degree relatives of patients (Coleman et al 2008, Wang et al 2010). In 1996 and 1997, the first major gene loci for POAG, GLC1A and GLC1B, were described (Stoilova et al 1996, Stone et al 1997). The GLC1A gene encodes myocilin, the trabecular

meshwork-induced glucocorticoid response protein. GLC1A is mapped to chromosome 1 and although the exact role of myocilin in the pathogenesis of glaucoma is not clear (Stone et al 1997), it is thought to interact with the trabecular extracellular matrix affecting aqueous outflow (Fautsch et al 2000, Tamm 2002). The GLC1B gene, located on chromosome 2, is associated with normal to moderately raised IOP and optic nerve damage (Stoilova et al 1996). Several other genes that increase the risk of POAG have since been identified: The GLC1C gene, located on chromosome 3, is associated with increased IOPs and cup-to-disc ratios ≥0.7 or an abnormal result on a VF test (Wirtz et al 1997). The GLC1D gene on chromosome 8 and the GLC1E gene on chromosome 10 are associated with mild to moderately raised IOP in individuals with optic nerve damage (Trifan et al 1998, Sarfarazi et al 1998). In 1999, Wirtz et al mapped the GLC1F gene to chromosome 7 and found it to be associated with raised IOP or VF loss and a cup-to-disc ratio of 0.6 (Wirtz et al 1999).

More recently, many genetic studies in large extended pedigree families have demonstrated that POAG is genetically heterogeneous, with genetics linkage reported to at least 22 genetic loci (Fan et al 2006, Hewitt et al 2006). To date, the only three genes identified for POAG from these reported genetic loci are myocilin (MYOC, OMIM 601652), optineurin (OPTN, OMIM 602432) and WD repeat-domain 36 (WDR36, OMIM 609669) (Fingert et al 2002, Rezaie et al 2002, Monemi et al 2005). The majority of these genes represent rare monogenic forms of glaucoma and are estimated to account for less than 10% of all glaucoma cases (Hewitt et al 2006). The common forms of adult-onset glaucoma appear to have a complex trait inheritance and several POAG genome-wide association studies (GWAS) have flagged variants in CAV 1 and 2 (Thorleifsson et al 2010, Wiggs et al 2011), TMCO1 and CDKN2B-AS1 (Burdon

et al 2011, Nakano et al 2012) and ZP4, PLXDC2 and DKFZp762A217 in a Japanese population (Nakano et al 2009), though the latter three genes were found not to be associated with POAG in an Indian population (Rao et al 2009). A single NTG paper reported common variants in SRBD1 and ELOVL5 (Meguro et al 2010). Because POAG is a heterogeneous disease, with some individuals exhibiting features, such as raised IOP, and others without these features, it would not be surprising if more gene loci were identified in POAG families. The role of genetics is also important in other types of glaucoma, such as pigmentary glaucoma, as described from our group in more detail elsewhere (Lascaratos et al 2013).

1.6.5 Light

It has long been known that exposure of biological systems to high energy ultaviolet (UV) light can result in the photochemical release of toxic as well as mutagenic end products (Smith et al 2005). Recently, however, studies have shown that components of the visible spectrum can be absorbed by biologic chromophores (Hockberger et al 1999) in cells, such as astrocytes (Jou et al 2004) and epithelial cells (Godley et al 2005), to cause cellular dysfunction and even death. It is believed that the blue region of the spectrum (approximately 400–500 nm) is particularly likely to induce these reactions, since it has relatively high energy and can penetrate through tissues to cells and their organelles. It can be theorised, therefore, that mitochondria, which are laden with prominent chromophores (COX, flavins and flavoproteins) may be affected in a detrimental way by components of visible light (Egorov et al 1999, Boulton et al 2001). This is supported by observations that isolated light-exposed mitochondria release several ROS, including singlet oxygen,

superoxide and hydroxyl radicals (Jung et al 1990, Godley et al 2005). It is likely that light will have a greater detrimental effect to RGC axons than to more external cellular elements, in part because the RGC axons form the most internal layer and are rich in mitochondria and in part because absorption by this layer will attenuate the delivery of energy to outer layers. Mitochondrial dysfunction, as a result of light exposure, would be particularly problematic in long nerve fibres, such as those of the peripheral nervous system, or in axons of very narrow calibre, those with minimal or no myelin, and those with a rapid rate of firing. These last three features are all found in intra-retinal RGCs, whose high and constant firing rate increases energy demands, whose high surface area to volume ratio favours energy consumption over energy production and whose lack of myelination deprives them of the efficiency of saltatory conduction (Bristow et al 2002). Therefore, the retinal components that will be most susceptible to any possible light-induced damage are the intraocular ganglion cell axons and in particular, their mitochondria.

The human retina is protected from shorter wavelength radiation by the cornea and lens, which absorb UV light below 400 nm (Boulton et al 2001). It is likely that under normal circumstances there is insufficient energy in this light that impinges on the retina to directly cause death of otherwise healthy neurons. It is more likely that light radiation may merely serve as an additional strain for cells already compromised in some way. In glaucoma, for example, it is believed that minor insults residing in the ONH serve to lower the functional status of affected RGC axons (Whitmore et al 2005, Quigley 1999). This compromised energetic state is thought to impact on selected RGCs during the evolution of glaucoma and the RGCs of the papillomacular bundle in patients with inherited mitochondrial optic neuropathies. The vasogenic hypothesis of glaucoma implies that RGC axons are metabolically compromised by the

impaired ONH blood flow, and the distribution of affected axons may be determined by these initiating vascular factors. It has been suggested that once a bioenergetic defect is established, these axons are at risk of additional damage through the photochemical mechanism described above. In this case, light damage is invoked as a mechanism which accelerates the progression of the established disease (Osborne et al 2006). Laboratory studies on RGC-5 cells in culture (Wood et al 2008) and primary rat retinal cultures (Lascaratos et al 2007) provide support for this notion.

1.7 Aims of the thesis

The purpose of this thesis was to a) evaluate the efficacy of IOP-lowering treatment in delaying glaucoma progression within the United Kingdom Glaucoma Treatment Study (UKGTS) and investigate whether average IOP (as measured by GAT, DCT and ORA) during follow-up is associated with the rate of glaucoma progression (Chapter 3), and b) explore the role of mitochondrial dysfunction and oxidative stress as risk factors for glaucoma progression within an exploratory study (Chapter 4).

With regards to point a) above, elevated IOP is a major risk factor for the deterioration of OAG and medical IOP reduction is the standard treatment, yet no randomised placebo-controlled study of medical IOP reduction has been undertaken previously. The UKGTS, a randomised, double-masked, placebo-controlled, multicenter treatment trial for OAG, tests the hypothesis that treatment with a topical prostaglandin analogue, compared with placebo, reduces the frequency of VF deterioration events in OAG patients by 50% over a 2-year period. Five hundred sixteen newly diagnosed (previously untreated)

patients with OAG were recruited prospectively at 10 UK centres between 2007 and 2010. The primary outcome was time to VF deterioration within 24 months. In summary, the UKGTS is the first randomised, placebo-controlled trial to evaluate the efficacy of medical treatment in reducing VF deterioration in OAG.

Other than raised IOP, the risk factor with the largest effect for more rapid progression, consistently determined from epidemiologic studies and clinical trials, is patient age. There is a strong rationale for considering mitochondrial function as a susceptibility factor given the pathological models of optic neuropathies caused by mitochondrial defects (Leber's hereditary optic neuropathy, dominant optic atrophy). Furthermore, ageing is associated with structural and functional changes to the mitochondria and data from clinical and experimental studies have implicated mitochondrial dysfunction and oxidative stress in glaucoma development and progression. To address point b) above, an exploratory study was designed to measure for the first time systemic mitochondrial function and oxidative stress in a unique cohort of patients, contrasting individuals at the extremes of IOP susceptibility – rapidly progressing patients with NTG and non-progressing patients with OHT.

Chapter 2

Materials and Methods

Chapter 2: Materials and Methods

2.1 General materials

2.1.1 General reagents

Reagent	Supplier	Location
ATP Bioluminesence Assay kit CLSII	Roche	Mannheim, Germany
BCA (bicinchoninic acid) Protein Assay Kit	Thermo Scientific	Northumberland, UK
Lymphoprep	Axis-Shield	Oslo, Norway
PBS (Phosphate-buffered saline)	Gibco, Life Technologies Ltd	Paisley, UK
Polyvinylidene difluoride (PVDF) membrane	Millipore	Billerica, MA
PathScan Total mTOR and Phospho-mTOR (Ser2448) Sandwich ELISA kit	Cell Signaling Technology Inc	Danvers, MA
8-OHdG DNA Damage ELISA kit	Cell Biolabs Inc	San Diego, CA
Fluo3, rhod2, pluronic acid, 2', 7'-dihydroethidium (DHE) and tetramethylrhodamine methyl ester (TMRM)	Molecular Probes, Life Technologies Ltd	Paisley, UK
Horseradish peroxidase (HRP) conjugated chemiluminescence kit and Hyperfilm ECL films	GE Healthcare Life Sciences	Buckinghamshire, UK
Halt protease inhibitor cocktail	Thermo Scientific	Rockford, IL
NuPage Protein gels	Novex, Life Technologies Ltd	Paisley, UK

Table 2.1: List of general reagents, the suppliers and their location.

Unless otherwise stated, all other chemicals were obtained from Sigma Chemical Co (Gillingham, Dorset, UK) and were of the best quality available.

2.1.2 Immunochemicals

Immunochemical	Supplier	Location
Primary (rabbit) polyclonal antibody to b-actin (1:5000, PC: ab8227) and primary (rabbit) polyclonal antibody to porin (1:1000, PC: ab15895)	Abcam	Cambridge, UK
Primary (rabbit) polyclonal antibody to superoxide dismutase 2 (SOD2) (1:1000, PC: sc30080) and primary (rabbit) polyclonal antibody to TOM20 (1:1000, PC: sc11415)	Santa Cruz Biotechnology Inc	Santa Cruz, CA
Secondary (goat) polyclonal antibodies anti-rabbit IgG (PC: PO448) with HRP conjugate	Dako UK	Cambridgeshire, UK

Table 2.2: List of immunochemicals, the suppliers and their location.

2.1.3 Cell culture materials

Cell culture material	Supplier	Location
Foetal bovine serum (FBS) and foetal calf serum (FCS)	Biosera, Labtech International Ltd	Uckfield, UK
75cm^2 tissue culture flasks	PAA Laboratories Ltd	Somerset, UK
6-, 48- and 96-well plates, and eppendorfs	Greiner Bio-One	Frickenhausen, Germany
15mls and 50mls Falcon tubes	BD Biosciences	Oxford, UK
Petri dishes	Sarstedt	Leicester, UK
Single channel pipettes (Pipetman P2, P10, P100, P200 and P1000)	Gilson Inc	Middleton, WI
HBSS (Hank's Balanced Salt Solution), penicillin, streptomycin, and RPMI (Roswell Park Memorial	Gibco, Life Technologies Ltd	Paisley, UK

Institute) 1640 medium supplemented with glutamax and HEPES (hydroxyethyl piperazineethanesulfonic acid)

Table 2.3: List of cell culture materials, the suppliers and their location.

2.1.4 Laboratory equipment

Laboratory equipment	Supplier	Location
Synergy HT multi-mode microplate reader for BCA, DHE and aconitase assays	Biotek	Bedfordshire, UK
Jade tube luminometer for ATP measurements	LabTech	Uckfield, UK
Beckman GPR refrigerated centrifuge	Beckman Coulter Ltd	High Wycombe, UK
Heracell 240i CO_2 incubator	Thermo Scientific	Rockford, IL
FACS Calibur flow cytometer	BD Biosciences	Oxford, UK
LS50B Luminescence Spectrometer	Perkin Elmer	Cambridge, UK

Table 2.4: List of laboratory equipment, the suppliers and their location.

2.1.5 Clinical devices

The Heidelberg Retina Tomograph (HRT) was from Heidelberg Engineering (Heidelberg, Germany; HRT3 image acquisition software version 3.0.60). The Stratus Optical Coherence Tomography (OCT) and the GDx Enhanced Corneal Compensation scanning laser polarimetry devices were from Carl Zeiss Meditec (Dublin, CA; software version 5.0). The Humphrey Field Analyzer/HFA™ II-i Series was also from Carl Zeiss Meditec. Goldmann applanation tonometry (GAT) was performed with a Haag Streit slit lamp (Koeniz, Switzerland). The Pascal Dynamic Contour Tonometre (DCT) was from Ziemer Ophthalmic

Systems AG (Zurich, Switzerland) and the Ocular Response Analyzer (ORA) from Reichert (Buffalo, NY; software version 2.10). The Omron M7 Blood Pressure Monitor was from Matsusaka (Mie, Japan). The Welch Allyn Ambulatory Blood Pressure Monitor 6100 was from Welch Allyn UK (Aston Abbotts, Buckinghamshire, UK; software version 1.6.0.489). The IOL Master was from Carl Zeiss Meditec (Dublic, CA; software version 5.4.3.0002). The ultrasound pachymeter for Central Corneal Thickness (CCT) measurements was from DGH Technology Inc (Exton, PA).

2.1.6 Participants and other materials

1. UKGTS participants

Five hundred sixteen newly diagnosed (previously untreated) patients with OAG were recruited prospectively at 10 UK centers between 2007 and 2010, as described in more detail in chapter 3.

2. Participants/materials for experiments to optimise laboratory techniques

Two well established immortalised human B- and T- lymphocyte cell lines (Raji and Jurkat, respectively) were used to optimise the experimental techniques of measuring mitochondrial function and oxidative stress (see section 4.1). At a later stage, and before embarking on the main laboratory experiments, the experimental techniques were also optimised using lymphocytes isolated from the peripheral blood of healthy volunteers (see section 4.2).

3. Study participants (control, NTG, OHT) for main laboratory experiments (mitochondrial exploratory study)

Two cohorts of 30 consecutive subjects with normal tension glaucoma (NTG) and ocular hypertension (OHT) were recruited prospectively from the Moorfields Eye Hospital NTG and OHT clinics, respectively, for the mitochondrial exploratory study, as described in more detail in section 4.3. An equal number of age-similar subjects with normal IOP, healthy discs and no family history of glaucoma was also recruited as controls for the same study. These were either spouses or friends of patients, or were recruited from the Friends of Moorfields. Raji cells were used in many cases as reference (internal control) during the main laboratory experiments, as explained in more detail in section 2.3.

2.2 Clinical Methods

2.2.1 Introduction

The clinical methods described in this section (2.2) were employed both in the mitochondrial exploratory study and in the UKGTS cohort, as explained later in more detail. The laboratory methods described in the next section (2.3) apply exclusively to the mitochondrial exploratory study.

2.2.2 Goldmann applanation tonometry (GAT)

In the UKGTS, two diastolic IOP readings were recorded, with a third measurement obtained if the difference between the first 2 was more than 1mmHg. In the mitochondrial pilot study, 1 diastolic IOP reading was

recorded. 2-hourly diurnal GAT IOP measurements (between 9 AM and 5 PM) were performed twice in the UKGTS [at Visit 1, six weeks after commencing the study drops, and at Visit 8a] and once in the mitochondrial pilot study.

2.2.3 Dynamic Contour Tonometry (DCT)

Goldmann applanation tonometry measurements are known to be affected by the CCT and age-related corneal stiffening (Kotecha et al 2005). Therefore, additional IOP measurements were made with the Pascal DCT, a more accurate and precise tonometry device that reduces the effects of corneal biomechanics during IOP measurement (Fig 2.1) (Kotecha et al 2010). Three readings with a quality value of 3 or better were recorded at each UKGTS visit and as part of the mitochondrial pilot study. Phasing with DCT was performed once in the mitochondrial pilot study.

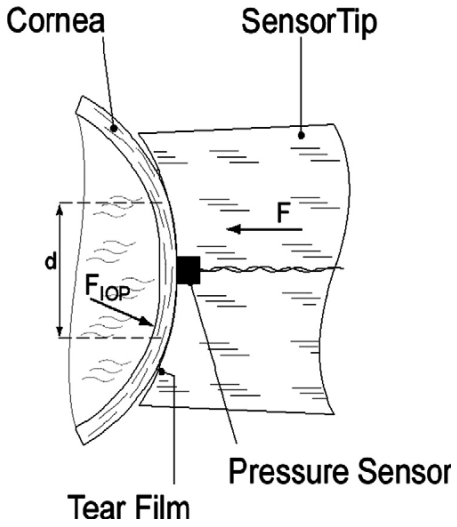

Fig 2.1: The Pascal DCT uses a concave tip to “contour match,” rather than applanate, a convex segment of the central cornea. When this match is achieved, the law of Pascal states that tangential forces are theoretically neutralised. A microchip- enabled solid-state sensing element in the tonometer

tip then measures IOP. The instrument then dynamically records more than 100 IOP measurements per second, measuring IOP fluctuations throughout the cardiac cycle and digitally displaying the average diastolic IOP. The ocular pulse amplitude (OPA), the difference in IOP between systole and diastole (IOP systolic - IOP diastolic), is also reported and is thought to be a marker for overall ocular rigidity (Kanngiesser et al 2005, Pallikaris et al 2005) although it may also be affected by ocular blood flow.

2.2.4 Perkins tonometry

Supine IOP measurements with the Perkins tonometer were made at the UKGTS visit 1 and at the mitochondrial pilot study visit after the participant had been lying down for at least 15 minutes.

2.2.5 Ocular Response Analyser (ORA) (Fig 2.2)

The ORA is a non-contact tonometer that measures two applanation events: one as the air jet pressure rises and one as it falls. These applanation signals are used to derive a Goldmann-correlated IOP (IOPg), an IOP corrected for biomechanical properties (corneal-compensated IOP or IOPcc), and measurements related to the ocular biomechanics (corneal hysteresis or CH, and corneal resistance factor or CRF). Three IOPg, IOPcc, CH and CRF readings with good quality traces were recorded at each UKGTS visit and and as part of the mitochondrial pilot study.

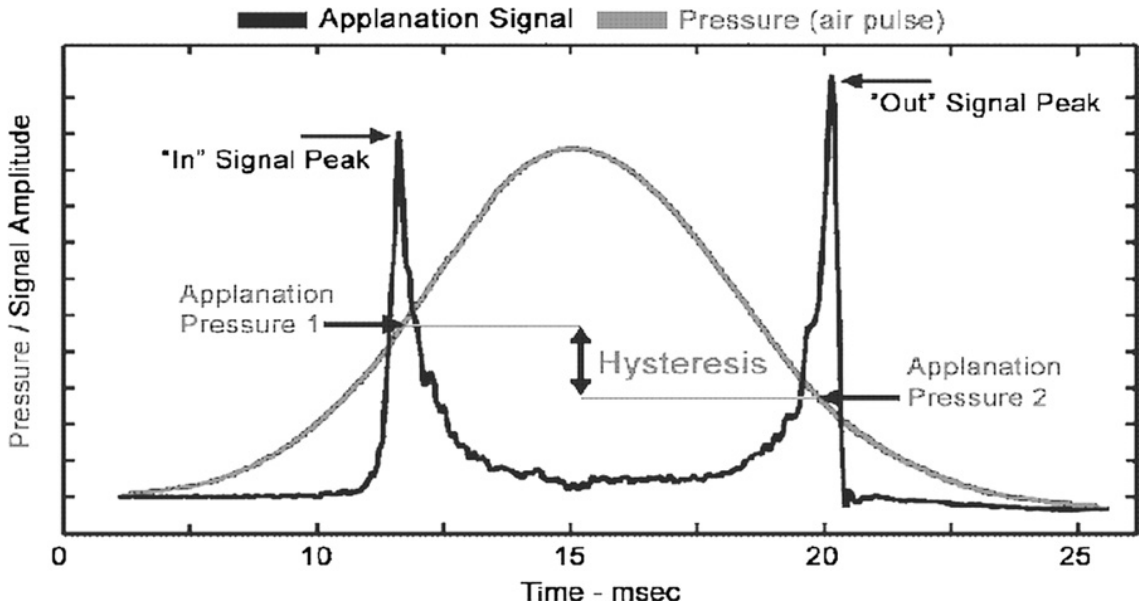

Fig 2.2: The ORA uses a metered collimated air pulse to applanate the cornea and an infrared electrooptical system to record inward and outward applanation events. The air pulse deforms the cornea through an initial applanation event (peak 1), then beyond into concavity, and gradually subsides allowing the cornea to rebound through a second applanation (peak 2) (Figure 1). Corneal hysteresis is defined as the difference in pressure between peak 1 (P1) and peak 2 (P2). This dynamic assessment of corneal biomechanical properties yields metrics of both the cornea's viscous and elastic qualities. Whereas CH may reflect mostly corneal viscosity, CRF, defined as a linear function of P1 and P2 by the formula: P1− (k × P2) where k is an empirically derived constant (Shah et al 2007), may predominantly relate to the elastic properties of the cornea. Although CH and CRF are, on average, the same for a normal population, they differ from person to person, providing us with distinct corneal information. The IOPcc is an IOP measurement thought to be less influenced by the cornea and derived from the equation P2 – (0.43 × P1). The IOPg is the average of the two pressure values derived from the inward and outward applanation events (P1+P2)/2.

2.2.6 Central Corneal Thickness (CCT)

CCT was measured with an ultrasound pachymeter at the UKGTS visit 1 and at the mitochondrial pilot study visit.

2.2.7 Automated perimetry

All tests for the UKGTS were performed with the Humphrey Field Analyzer Mark II (or II-i) and the Swedish interactive threshold algorithm standard 24-2 program. A reliable VF was one with a false-positive rate of less than 15% and 20% fixation losses (for fixation losses >20%, reliability was based on subjective judgment, including assessment of the eye tracker trace). Unreliable tests were repeated, either on the same day (with a break of at least 30 minutes) or at a visit within 1 month.

2.2.8 Progressor software

To estimate the rate of VF progression of subjects recruited in the mitochondrial pilot study, the PROGRESSOR software package (Medisoft) was used. This package analyses VF progression using pointwise linear regression of sensitivity on time. The pointwise linear model has been demonstrated to provide a valid framework for detecting glaucomatous loss (Viswanathan et al 1997). PROGRESSOR produces a cumulative graphical output as shown below.

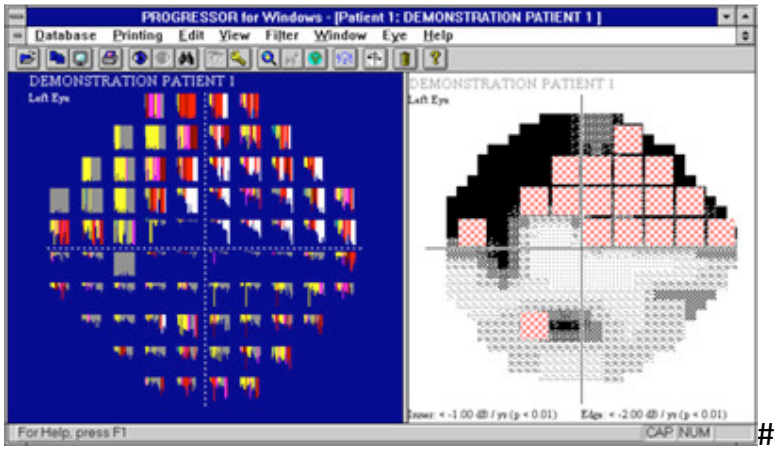

#

Fig 2.3: Graphical output from the Progressor software.

Each test location is shown as a bar graph in which each bar represents one test. The length of the bar relates to the depth of the defect (longer bars represent lower sensitivities) and the colour of the bar relates to the p value of the regression slope. Thus, undamaged locations are seen as series of short grey bars.

2.2.9 Ocular biometry

At the UKGTS visit 1 and the mitochondrial pilot study visit, refractive error was recorded, either with an available autorefractor or from spectacle focimetry, and axial length measured with the IOLMaster.

2.2.10 24-hr Ambulatory Blood Pressure (ABP)

At each UKGTS visit, blood pressure (BP) was recorded in the left arm with the patient seated after at least 5 minutes of rest with the Omron M7 Blood Pressure Monitor. 24-hour BP measurements were made at the 4-month

UKGTS visit and at the mitochondrial pilot study visit with the Welch Allyn Ambulatory Blood Pressure Monitor 6100.

2.2.11 Body Mass Index (BMI)

The height (m) and weight (Kg) of each participant for the mitochondrial pilot study was measured and the BMI was calculated by dividing each individual's weight by their height squared. Height and weight were measured in participants wearing light clothing and no footwear.

2.2.12 Structural Imaging

Structural imaging was carried out in the UKGTS as follows:

1. Confocal scanning laser ophthalmoscopy was carried out using the HRT. Image quality of mean pixel height standard deviation (MPHSD) 40µm or less was required; if necessary, pupils were dilated to obtain adequate image quality.

2. Scanning laser polarimetry was carried out with the GDx Enhanced Corneal Compensation scanning laser polarimetry device. Imaging was performed through an undilated pupil and a scan quality score of 8 or more was required.

3. Optical coherence tomography (OCT) with the Stratus OCT. Images were acquired through dilated pupils with the fast RNFL thickness (3.4) scanning protocol and using the landmark function. A signal strength of 7 or more was required. In addition, spectral-domain OCT imaging was performed where available.

4. Monoscopic optic disc photography was used to identify disc haemorrhages.

5. Fundus photography was performed if a patient reached a VF deterioration or visual acuity change end point.

A summary of the UKGTS investigations' schedule is shown in Table 3.2.

2.3 Laboratory Methods

2.3.1 Cell cultures

1. Immortalised human B- and T-lymphocyte cell lines

Both cell lines were cultured in RPMI 1640 medium, supplemented with 10% FCS, 2mM glutamax, 12.5mM HEPES, 50U/mL penicillin and 50µg/mL streptomycin in 75-cm^2 flasks at 37°C in an atmosphere of 5% CO_2. Doubling time of these cells was approximately 20 hours under these conditions and they were generally passaged at a ratio of 1:8. Cells were maintained at a density of approximately 1million/ml for use in experiments. The Raji cell line was originally derived from the B-lymphocytes of an 11-year-old Nigerian Burkitt's lymphoma male patient in 1963 (Karpova et al 2005), while the Jurkat cell line (originally called JM) was established in the late 1970s from the peripheral blood of a 14-year-old boy with T cell leukemia (Schneider et al 1977). Both Raji and Jurkat are suspension cells that can grow as single, doublets, or form large aggregates when in culture (Fig 2.4). The cells, which tend to clump, are relatively large in diameter (5-8 µm) and have irregular indented nuclei.

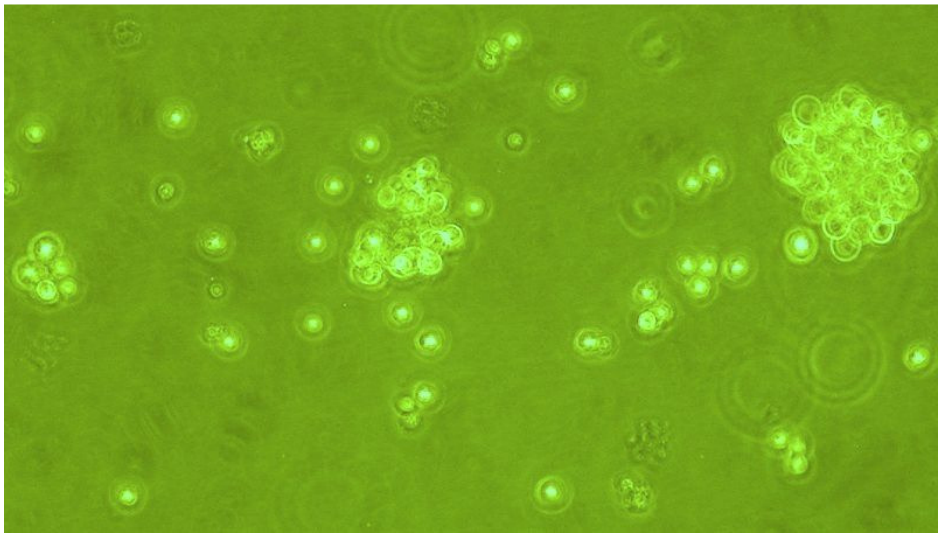

Fig 2.4: A Raji cell line in culture (at an early cultural stage).

2. Healthy volunteers' and study participants' lymphocytes

Lymphocytes were isolated, after the removal of monocytes, from anticoagulated peripheral blood of healthy volunteers and study participants (control, NTG and OHT) using Lymphoprep (see section 2.3.2), and maintained in petri dishes in the incubator overnight under unstimulated conditions for subsequent experiments. The isolated lymphocytes were resuspended in phenol red-free RPMI 1640 medium supplemented with 2mM glutamax, 12.5mM HEPES, 50U/mL penicillin and 50µg/mL streptomycin, to create a cell density of approximately 1million lymphocytes/ml.

3. Treatment with rotenone and paraquat

For some experiments, to model mitochondrial dusfunction and oxidative stress in our system, cells were treated with 0.5µM rotenone for 24hrs and with 100µM paraquat for 24hrs, respectively. This dose was based on our laboratory's previous experience with these agents on different cell types and no dose-response experiments were conducted. Cell viability after exposure to these agents was assessed with trypan blue on a weekly basis prior to starting

the experiments and cell death was noted in less than 5% of the lymphocytes. Rotenone, a flavonoid often used as a pesticide, is a neurotoxin that induces neurodegeneration and has been used *in vivo* in animals and *in vitro* neurogeneration disease models to replicate certain features of Parkinson's disease (PD) (Betarbet et al 2000, Inden et al 2011) and Alzheimer's disease (AD) (Chaves et al 2010). Apart from the well known role of rotenone as a mitochondrial complex I inhibitor, it has also been shown to affect microtubule stability and Ca^{2+} homeostasis (Choi et al 2011), induce oxidative stress, alter proteasome function (Shamoto-Nagai et al 2003), and cause DNA damage, inflammatory response and apoptosis (Newhouse et al 2004). Paraquat, a quaternary ammonium bipyridyl herbicide, is known to generate reactive oxygen species (including superoxide anion, hydrogen peroxide and hydroxyl radicals) highly reactive to cellular macromolecules and cause the oxidation of reducing equivalents (such as NADPH and reduced glutathione) necessary for normal cellular function (Bus et al 1984, Lee et al 2012).

2.3.2 Lymphoprep

For the isolation of lymphocytes from anticoagulated peripheral blood, a ready-made, sterile and endotoxin tested solution (Lymphoprep) was used, as described by Thorsby and Bratlie (Thorsby and Bratlie 1970). This solution contains sodium diatrizoate 9.1% (w/v) and sodium diatrizoate polysaccharide 5.7% (w/v). These compounds aggregate the erythrocytes, when mixed with blood, thereby increasing their sedimentation rate. The sedimentation of leucocytes is only slightly affected and these can be collected from the upper part of the tube, when the erythrocytes have settled.

Blood was collected in an EDTA (purple top) tube and transferred from Moorfields Eye Hospital to the Department of Clinical Neurosciences, Royal Free Hospital within 1-2 hours from collection. The blood was diluted by the addition of an equal volume of HBSS. A certain volume of the diluted blood was then carefully layered over half the volume of Lymphoprep in a 50mls Falcon tube. The tube was centrifuged at 800 x g for 20 minutes at 20°C in a swing-out rotor. After centrifugation the peripheral blood mononuclear cells (PBMCs) formed a distinct band at the sample/medium interface and were removed from the interface using a single channel pipette. After washing in HBSS twice to remove any remaining Lymphoprep solution, the PBMC from each patient were resuspended in medium (phenol red-free RPMI 1640 medium, 2mM Glutamax, 12.5mM HEPES, 50U/mL penicillin and 50µg/mL streptomycin) to a final cell density of approximately 1million PBMC/ml. The PBMC in RPMI medium were incubated overnight in petri dishes with and without rotenone/paraquat treatment. This overnight incubation allowed monocytes to adhere to the petri dish walls, while lymphocytes remained in suspension and were easily removed on the following day for use in subsequent experiments.

2.3.3 BCA protein assay

The BCA Protein Assay was used to measure total protein concentration compared to a protein standard. This assay combines the well-known reduction of Cu^{2+} to Cu^{1+} by protein in an alkaline medium with the highly sensitive and selective colourimetric detection of the cuprous cation (Cu^{1+}) by bicinchoninic acid (BCA) (Smith et al 1985). The first step is the chelation of copper with protein to form a light blue complex. In the second step of the

colour development reaction, BCA reacts with the reduced cuprous cation to form a purple-coloured reaction product (Wiechelman et al 1988). The BCA/copper complex is water-soluble and exhibits a strong linear absorbance at 562 nm with increasing protein concentrations.

During the BCA protein assay, 5µl from each sample were added into each well of a 96-well plate containing 45µl of water, to produce a final volume of 50µl per well. A standard curve (Figure 2.5) was also prepared with the use of serial dilutions of Bovine Serum Albumin (BSA) (2mg/ml). Subsequently, 50µl of the reagent mix were added into each well and incubated at 37^{o}C for 30min. A plate reader was used to read the 96-well plate at 562nm.

A	BSA (µL)	3	2	1	0
B	[BSA] mg/ml	0.12	0.08	0.04	0
C	Spectrophotometer reading or OD	0.384	0.322	0.15	0.015
D	Net OD: OD – Background OD	0.369	0.307	0.135	0

Table 2.5: Data required for BSA standard curve. Row A shows the amount of BSA inserted in each of the BSA wells of the 96-well plate. Row B shows the [BSA] concentration in each of these wells. Row C shows examples of spectrophotometer readings (optical density - OD) for each well. Row D shows the net OD for each well, which is calculated by subtracting the blank OD from the OD of each well. The blank OD is the OD of the background (in this case 0.015).

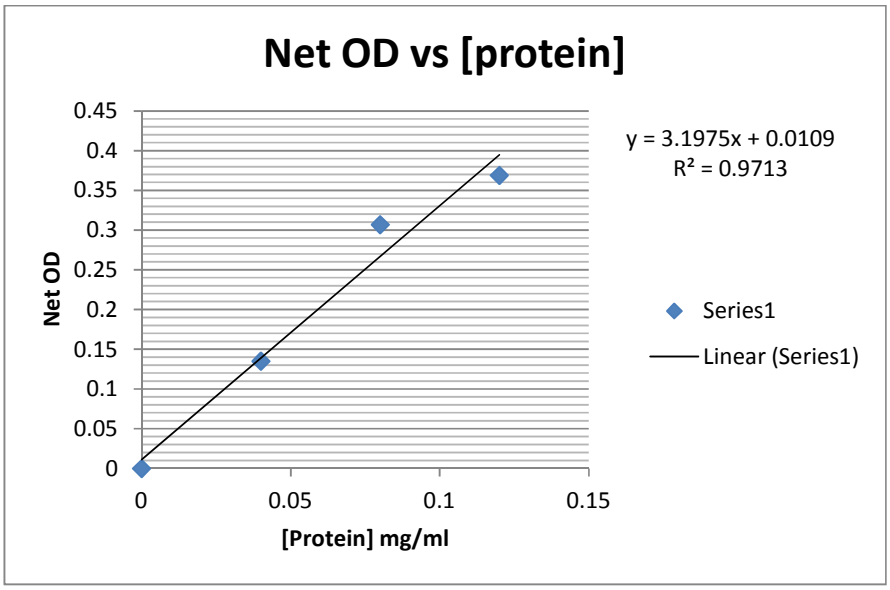

Fig 2.5: Example of a BSA standard curve, based on Table 2.5. Axis X represents the [BSA] mg/ml and axis Y represents the net OD. The equation shows the correlation between the net OD and [protein] concentration (mg/ml).

Based on the BSA standard curve above, the amount of protein in each sample well was calculated, as shown below (Table 2.6).

Well	OD	Net OD	[Sample Protein] in the Well	[Sample Protein]
A	0.158	0.143	0.0413mg/ml	0.413mg/ml

Table 2.6: Example of [Sample Protein] calculation in each well (in this case Well A). If the OD of the well is, for instance, 0.158, then after subtracting the blank OD (0.015 according to Table 2.5) the Net OD is 0.143. Using the BSA standard curve equation from Figure 2.5, the [sample protein] in well A is calculated to be 0.0413. Since the sample volume in the well represents 1/10 of the total volume of the content of the well, the [sample protein] = 10* [sample protein] in the well = 0.413mg/ml.

2.3.4 ADP phosphorylation assay

1. Basic principles

ADP phosphorylation describes a type of substrate-level phosphorylation that results in the formation of adenosine triphosphate (ATP) by the direct transfer and donation of a phosphoryl (PO_3^{2-}) group to adenosine diphosphate (ADP) from a phosphorylated reactive intermediate (Fig 2.6), such as 1,3-bisphosphoglycerate and phosphoenolpyruvate.

Fig 2.6: Substrate-level phosphorylation generating ATP.

In addition to the substrate-level phosphorylation that occurs during glycolysis and the Krebs cycle, an alternative way to create ATP is through oxphos, which takes place during the process of cellular respiration. The ADP phosphorylation assay is designed to measure complex-specific ATP synthesis in live cells over a given period of incubation time, based on the exogenous supply of substrates, such as a) glutamate-malate (for complex I), b) succinate-rotenone (for complexes II/III) and c) ascorbate-TMPD (for complex IV). Subsequently, the measurement of generated ATP over that period is based on the principle of luminescence, where ATP reacts with luciferin to produce light, measured by a tube-luminometer. The ATP Bioluminescence Assay Kit CLS II was used, which includes lyophilised luciferase reagent. This kit uses the ATP dependency of the

light emitting, luciferase catalysed, oxidation of luciferin for the measurement of extremely low concentrations of ATP (Fig 2.7).

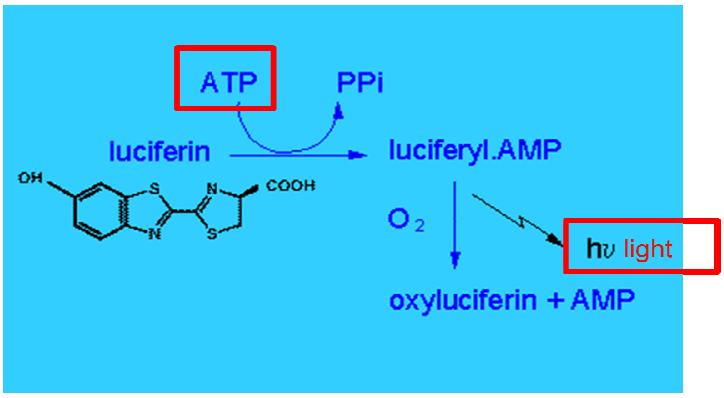

Fig 2.7: The ATP measurement is based on the principle of luminescence, where ATP produced by the cells reacts with luciferin to produce light, which is then measured by a tube-luminometer (modified from http://ase.tufts.edu/biology).

Prior to performing the substrate-linked ADP phosporylation assay, we attempted to quantify the amount of digitonin that would provide the maximal ATP measurements for a given cell type. Digitonin is a glycoside obtained from digitalis purpurea and is commonly used in this assay to solubilise cell and mitochondrial membranes, in order to allow substrate penetration and ATP release.

2. Methodology

2a) Optimisation experiments

As mentioned in section 2.1.6, the two immortalised cell lines (Raji and Jurkat) and lymphocytes from healthy volunteers were used to optimise the ADP

phosporylation assay. Prior to starting this assay, a digitonin titration experiment was performed on the cell lines to identify the optimum concentration of digitonin required to solubilise the mitochondrial membrane and enable the penetration of the substrates into the cells.

Digitonin titration: For cell preparation, 5 million Raji and Jurkat cells from each flask were spun at 1000 x g for 10min. The cell pellet was washed in HBSS and spun again at 1000 x g for 10min. The pellet was resuspended in ATP buffer (150mM KCl, 2mM K_2EDTA, 10mM K_2HPO_4, 5mM Tris base, pH 7.4). For each reaction (performed in triplicate) 0.25mls of reaction buffer (10mM Glutamate pH 7.4, 10mM Malate pH 7.4 and 1mM ADP in ATP buffer) were allowed to react with 0.25mls of cells suspended in ATP buffer for 20 minutes at 37°C with shaking. For each cell line 8 reactions were performed using 8 different doses of digitonin (0, 10, 25, 50, 75, 100, 150, 200µg per reaction). The reaction was terminated after 20min by adding 28.5 µl of perchloric acid (70%) into each eppendorf. The acid was then neutralised with the addition of 76µl of K_2CO3/TEA 3M/0.5M in two steps (38µl added twice with a 10 min gap) to prevent the creation of large amounts of CO_2. 50µl of luciferin from the ATP Bioluminescence Assay Kit CLS II were allowed to react with 5µl of cell lysate (cells in ATP/reaction buffer after the end of the reaction) for 10 seconds and the emitted luminescence was measured by a Jade Tube Luminometer. The measurements provided by the luminometer are in RLU (relative luminescence units), which are arbitrary units. The digitonin titration results for Raji (Fig 2.8) and Jurkat (Fig 2.9) suggest that the rate of ATP synthesis was maximum when 10-25µg of digitonin per reaction were used to solubilise the mitochondrial membrane and enable the penetration of the substrates, while higher digitonin concentrations led to a reduction in ATP synthesis. Considering the data from both cell lines together, 10µg of digitonin per 0.5ml reaction was

considered the optimum concentration to allow the substrates to penetrate into the cells without damaging their integrity and was used in subsequent experiments.

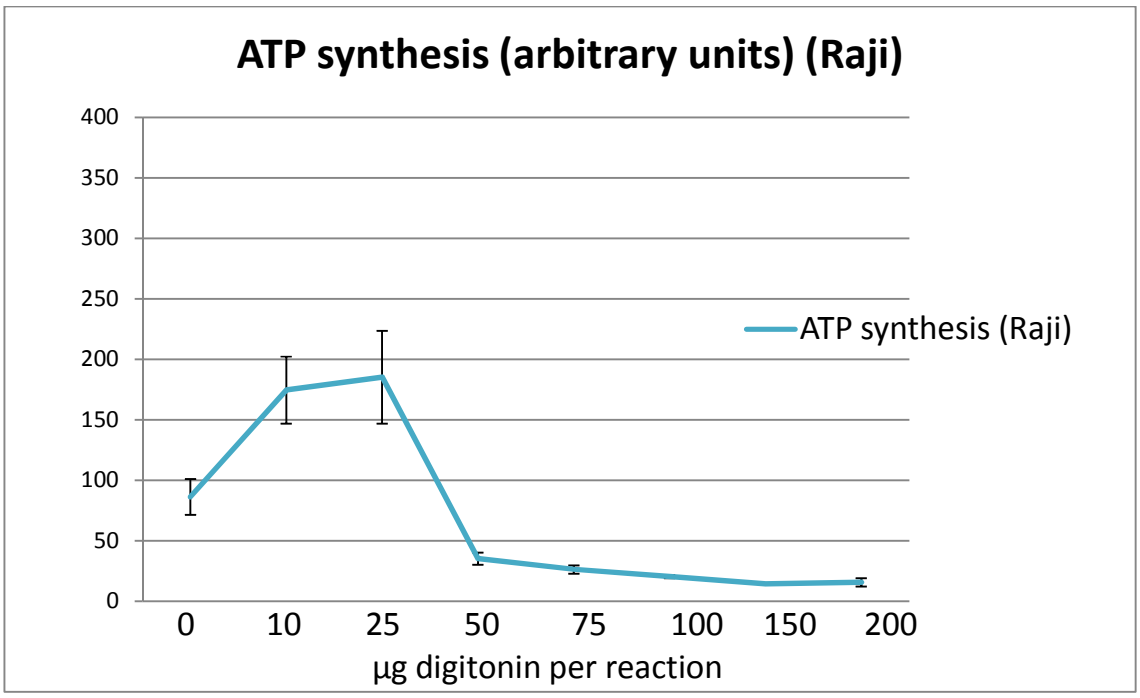

Fig 2.8: Graph showing the rate of ATP synthesis for different concentrations of digitonin (range 0 to 200µg per reaction) in the Raji cell line. The arbitrary measurements provided by the luminometer are expressed in RLU (relative luminescence units). Error bars represent the SEM (n=3).

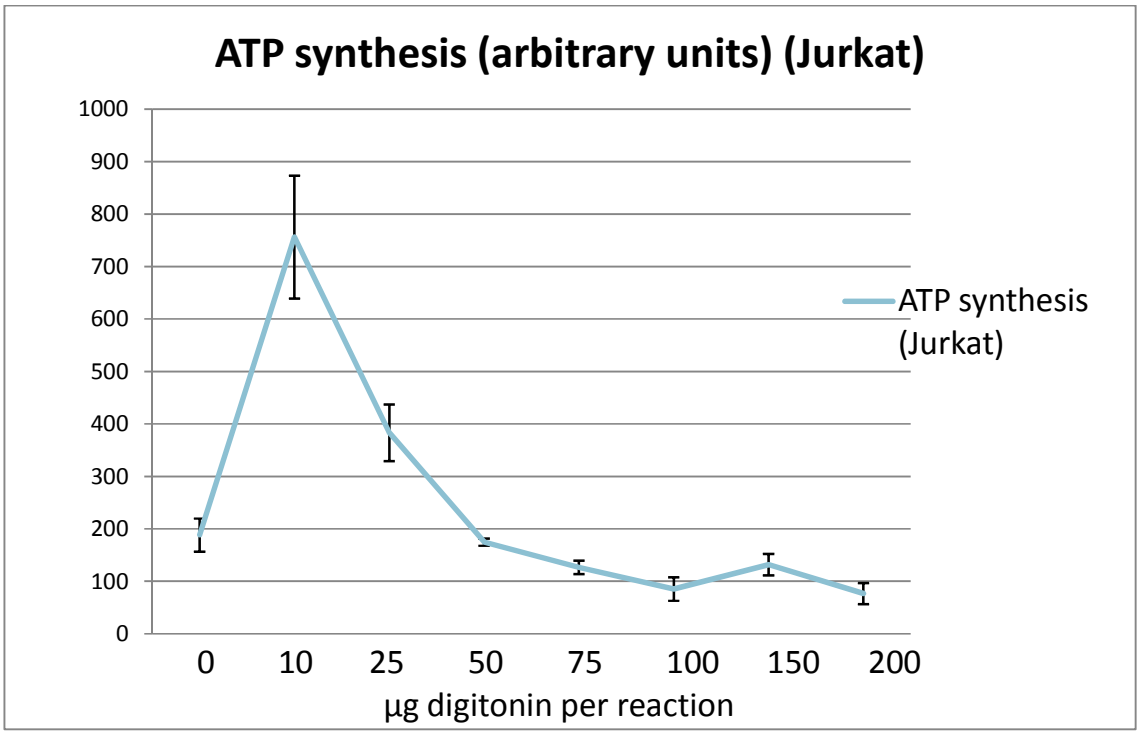

Fig 2.9: Graph showing the rate of ATP synthesis for different concentrations of digitonin (range 0 to 200µg per reaction) in the Jurkat cell line. The arbitrary measurements provided by the luminometer are expressed in RLU (relative luminescence units). Error bars represent the SEM (n=3).

ADP Phosphorylation Assay: Cells in suspension were spun at 1000 x g for 10min, washed in 1xPBS and spun again at 1000 x g for 10min. The pellet was resuspended in ATP buffer. For each reaction one eppendorf was used and 0.25mls of reaction buffer were allowed to react for 20 minutes with 0.25mls of cells suspended in ATP buffer. For each cell line and for the healthy volunteers' lymphocytes 3 reactions were performed for complex I, 3 for complexes II/III, 3 for complex IV and 2 for control (reaction buffer with no substrate). The corresponding reaction buffers required were as follows: Complex I (10mM glutamate pH 7.4, 10mM malate pH 7.4, 1mM ADP, 10 µg digitonin per reaction and ATP buffer), Complexes II/III (10mM succinate pH 7.4, 10µM rotenone in ethanol, 1mM ADP, 10 µg digitonin per reaction and

ATP buffer), Complex IV (2mM ascorbate pH 7.4, 50µM TMPD pH 7.4, 1mM ADP, 10 µg digitonin per reaction and ATP buffer) and Buffer with no substrate (1mM ADP, 10 µg digitonin per reaction and ATP buffer). The latter served as a negative control, with this background measurement being subtracted from the complex-related measurements. The reaction was terminated after 20min by adding 28.5 µl of perchloric acid (70%) into each eppendorf. The acid was then neutralised with the addition of 76µl of 3M/0.5M K2CO3/TEA in two steps. 50µl of luciferin were allowed to react with 2.5µl of cell lysate for 10 seconds and the emitted luminescence was measured by a Jade Tube Luminometer. Rotenone (0.5µM 24hrs), known to reduce mitochondrial function, was used as a positive control.

To reduce measurement variability, repeat readings were taken and averaged. 1.25µl of cell lysate were also tested, ensuring that the ATP readings were approximately half as compared to 2.5µl. Duplicate measurements were performed for both 2.5µl and 1.25µl. The mean of the 4 measurements taken per eppendorf was used for further analysis.

In the case of the Raji and Jurkat immortalised cell lines, triplicate eppendorfs were used for each experimental condition (with the exception of acid control where duplicate eppendorfs were used), as shown schematically below (Fig 2.10).

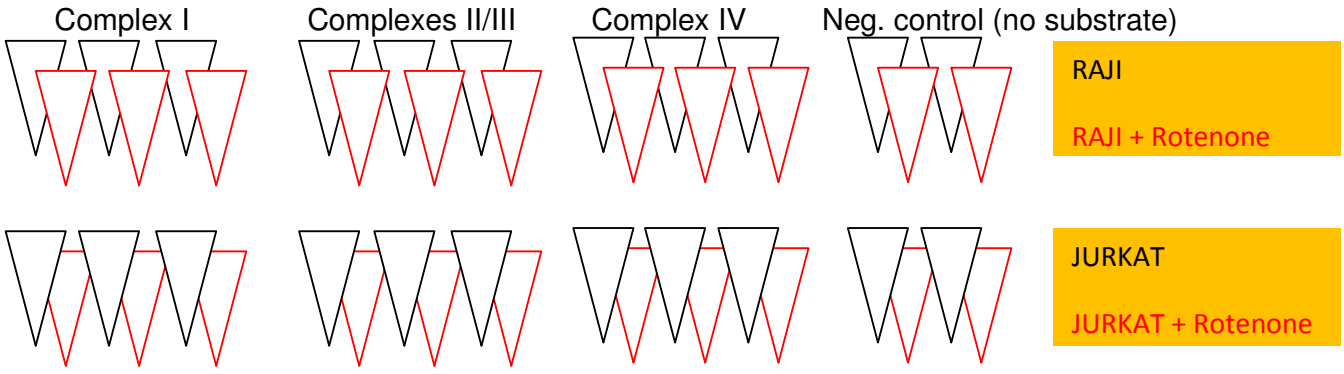

Fig 2.10: Schematic representation of the experimental design for the ADP phosphorylation assay in the Raji and Jurkat cell lines. Triangles represent eppendorfs.

The same design applied to the ATP experiments on the healthy volunteers' lymphocytes, where Raji cells were also used as an internal control (Fig 2.11).

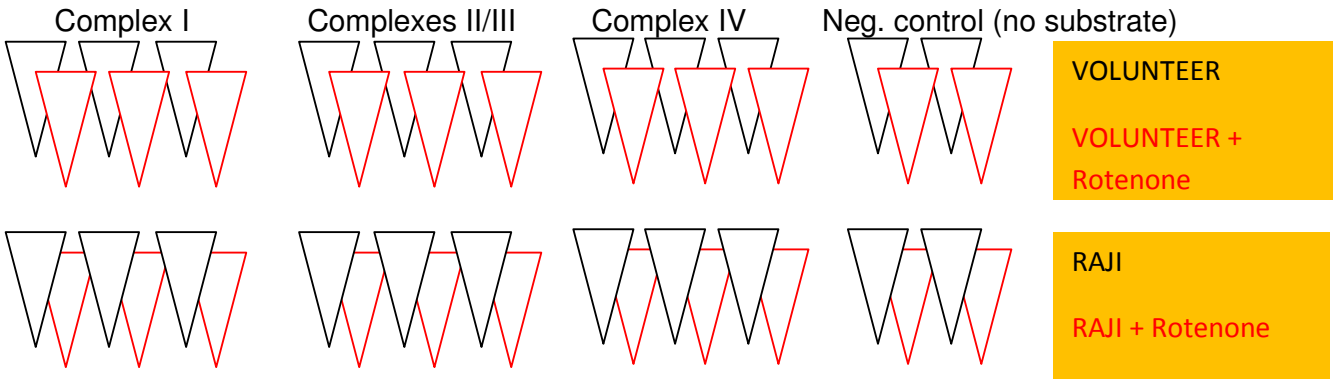

Fig 2.11: Schematic representation of the experimental design for the ADP phosphorylation assay in the Raji cells and the healthy volunteers' lymphocytes.

The arbitrary measurements provided by the luminometer in RLU (relative luminescence units) were converted into ATP concentrations using a calibration (standard) curve upon measuring known ATP levels. The ATP standard was included in the kit and each bottle contained 10mg of ATP. The content of the bottle was dissolved in Lysis Buffer, again provided with the kit, to a final concentration of 1nmol ATP/ml. Next, 50µl of luciferase were allowed to react with 0, 1.25, 2.5, 5 and 10µl of ATP standard for 10 sec and the emitted luminescence was measured by a Jade Tube Luminometer. With increasing concentrations of ATP, different luminescence readings were generated, for example 0.085, 1053, 2224, 3875 and 6596, respectively (Table 2.7).

A	ATP standard (µl)	0	1.25	2.5	5	10
B	[ATP] pmol/ml	0	25	50	100	200
C	Bioluminescence (Luminometer reading)	0.085	1053	2224	3875	6596

Table 2.7: The components of an ATP standard curve. Row A shows the amount of ATP standard inserted into each cuvette for the creation of an ATP standard curve. Row B shows the [ATP] in each cuvette with ATP standard. Row C shows examples of luminometer readings for the respective [ATP].

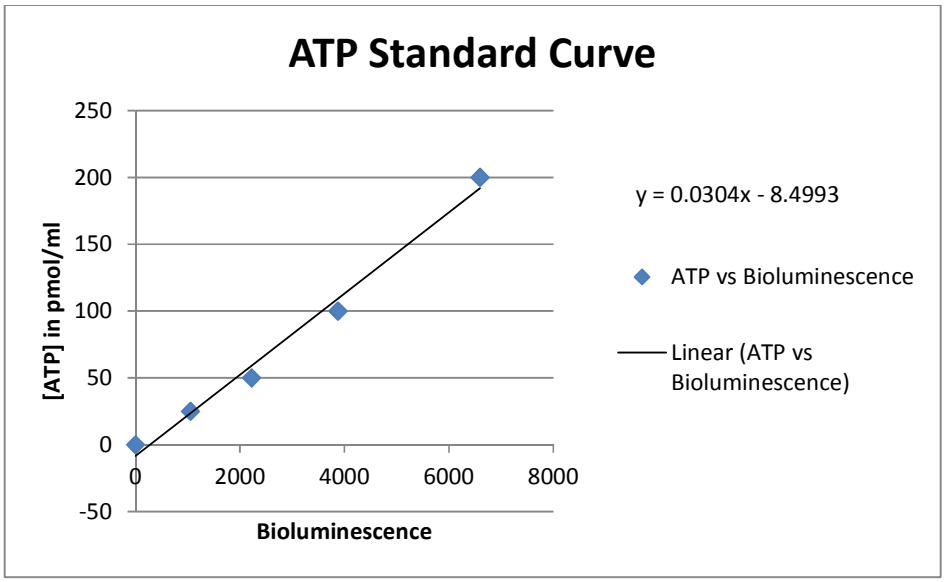

Fig 2.13: Example of ATP standard curve, based on Table 2.7. The X axis represents bioluminescence (luminometer readings). The Y axis represents [ATP]. The equation shows the correlation between bioluminescence and [ATP].

Using the ATP standard curve, the [ATP] in each cuvette was calculated, as shown below (Table 2.8).

Cuvette	Bioluminescence	[ATP]
A	4250 Luminescence Units	120.7 pmol/ml

Table 2.8: Example of the calculation of the [ATP] in cuvette A. If the luminometer reading for the cuvette A is 4250 Luminescence Units, then by using the ATP standard curve above (Figure 2.13), the [ATP] for the cuvette A is estimated to be 120.7 pmol/ml.

Next, a BCA protein assay (see section 2.3.3) was performed to the neutralised cell lysates, in order to express the ATP production rate in pmol of ATP/min/mg of cell lysate. By dividing the amount of ATP produced in each cuvette, with the amount of protein in each 2.5µl sample, the total ATP produced per 1ml of each sample was estimated (Table 2.9).

Sample	Luminometer reading	[ATP] in cuvette	[Sample protein]	[ATP]/[Sample Protein]	[ATP] in 1ml	Rate of ATP synthesis per min
A	4250 Luminescence Units	120.7 pmol/ml	0.413 mg/ml	292.25 pmol/mg of cell lysate	116900.72 pmol/mg of cell lysate	5845.04 pmol/min/mg of cell lysate

Table 2.9: Example of calculating the rate of ATP synthesis for sample A. The luminometer reading for sample A is 4250 Luminescence Units (Table 2.8). The [ATP] in the cuvette is 120.7 pmol/ml (Table 2.8). The [protein] in sample A has been estimated to be 0.413mg/ml (Table 2.6). Normalisation for protein is performed by dividing the [ATP] in the cuvette by the [protein] in sample A. This gives an ATP result of 292.25 pmol/mg of cell lysate. This amount of ATP has been produced by 2.5µl of sample A. Therefore, the amount of ATP produced per 1ml of sample A, is 400* 292.25 pmol/mg of tissue= 116900.72 pmol/mg of cell lysate. To correct for the amount of time (20min) required for this ATP to be produced, the [ATP] is divided by 20, giving a final rate of ATP synthesis of 5845.04 pmol of ATP/min/mg of cell lysate.

2b) Main experiments

As discussed in section 2.1.6, lymphocytes isolated from the study participants (NTG, OHT, controls) were used for the main ADP phosphorylation experiments. The same methodology was followed, as described for the optimisation experiments, with the only exception being the use of duplicate (instead of triplicate) eppendorfs for each experimental condition (apart from acid control where a single eppendorf was used), as shown schematically below (Fig 2.12). Raji cells were again used as an internal control helping to standardise the assays over time.

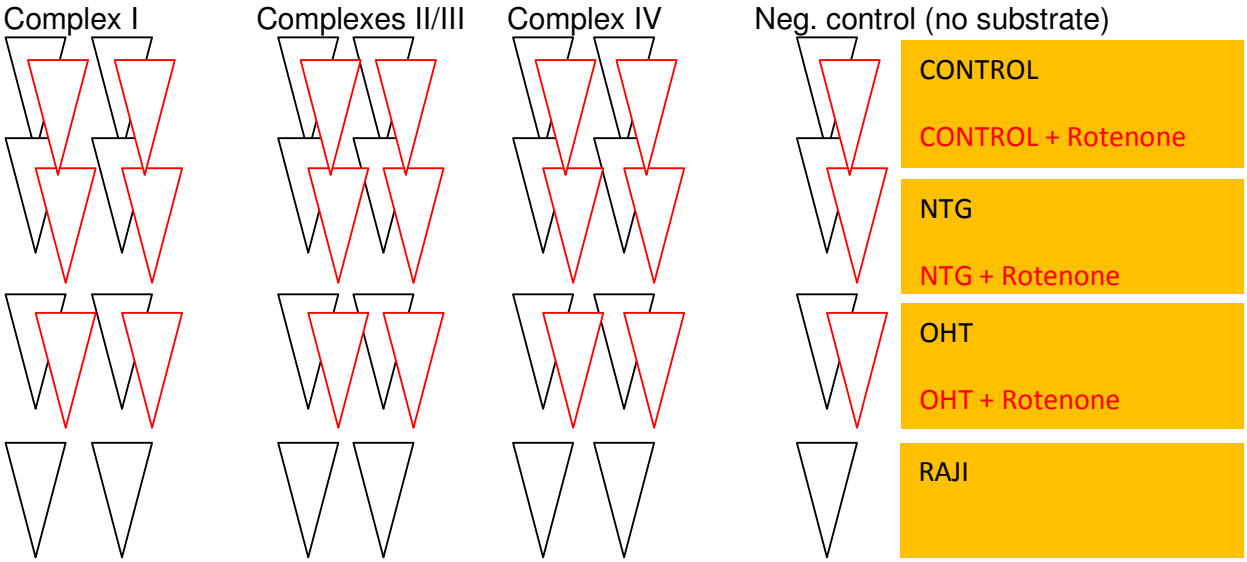

Fig 2.12: Schematic representation of the experimental design for the ADP phosphorylation assay in the Raji cells and the study participants' (NTG, OHT, control) lymphocytes.

2.3.5 Mitochondrial membrane potential using flow cytometry (TMRM)

1. Basic principles

Energy obtained through the transfer of electrons down the electron transport chain is used to pump protons from the mitochondrial matrix into the intermembrane space of the mitochondria, creating an electrochemical proton gradient across the mitochondrial inner membrane, called the mitochondrial membrane potential (ΔΨm). This electrochemical proton gradient allows ATP synthase to use the flow of protons through the enzyme back into the matrix to generate ATP (Fig 2.14). The ΔΨm is a key indicator of mitochondrial function and the characterisation of ΔΨm in live cells allows for an accurate determination of mitochondrial bioenergetics and cellular metabolism (Chen 1988). To measure changes in the ΔΨm in our cells we employed the monovalent cationic fluorescent red dye TMRM (Scaduto et al 1999). The uncoupler FCCP was used to depolarise the mitochondria and affect their ability to maintain a negative ΔΨm across the mitochondrial inner membrane, thus serving as a positive control.

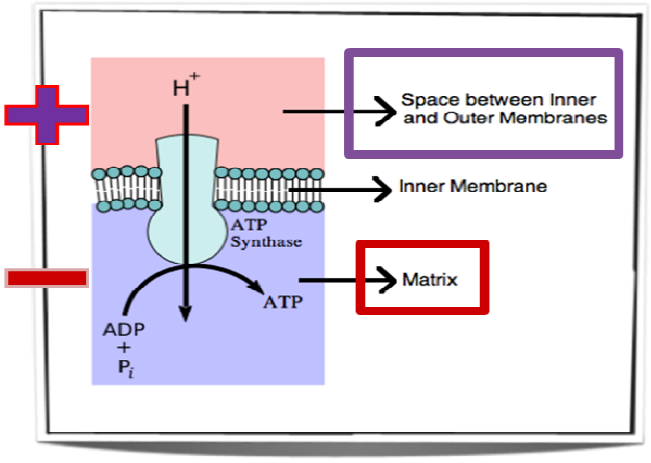

Fig 2.14: The negative ΔΨm between the matrix and the mitochondrial intermembrane space allows the ATP synthase (Complex V), located on the inner mitochondrial membrane, to use the flow of protons (H^+) through the enzyme into the matrix to generate ATP (http://www.ibguides.com/biology/notes/cell-respiration).

2. Methodology

2a) Optimisation experiments

As discussed in section 2.1.6, the two immortalised cell lines (Raji and Jurkat) and lymphocytes from healthy volunteers were used to optimise the TMRM assay, before embarking on the main experiments using the study participants' (NTG, OHT, control) lymphocytes.

Cells were spun at 1000 x g for 10min, washed in 1xPBS and spun again using the same settings. The pellet was resuspended in PBS to a final volume of 1ml per cuvette. It is important to note that we used a relatively low concentration of TMRM (25nM) to ensure the staining was mitochondria specific (Cleeter et al 2013). At higher TMRM concentrations it is possible that non-mitochondrial cellular membranes may also be stained, resulting in non-specific staining. FCCP was used at a final concentration of 10μM. The ΔΨm was quantified by the steady-state fluorescence of the mitochondrial patterns produced by live cells stained with TMRM at room temperature for 45 min. The samples were read using the FACS Calibur Flow cytometer running the CellQuest software using the same gate and gain. Data were collected in the FL2-H channel and 50,000 events were counted for each sample. Analysis was performed using the WinMDI software, version 2.5 (Joseph Trotter, La Jolla, CA).

In the case of the Raji and Jurkat cell lines, the following seven experimental conditions were represented for each of the two cell lines in each experiment in triplicate:

- Cells without TMRM (negative control)
- Cells with TMRM
- Cells with TMRM + 0.5µM rotenone 24hrs
- Cells with TMRM + 100µM paraquat 24hrs
- Cells with TMRM + 10µM FCCP (positive control)
- Cells with TMRM + 0.5µM rotenone 24hrs +10µM FCCP
- Cells with TMRM +100µM paraquat 24hrs +10µM FCCP

In all cases, the background fluorescence recorded for cells without TMRM was subtracted from the fluorescence measured for TMRM-stained live cells. In the case of the healthy volunteers' lymphocytes, duplicate measurements were made for each experimental condition, as shown schematically below (Fig 2.15). Raji cells stained with TMRM were used as an internal control helping to standardise the assays over time, while cells exposed to FCCP served as a positive control.

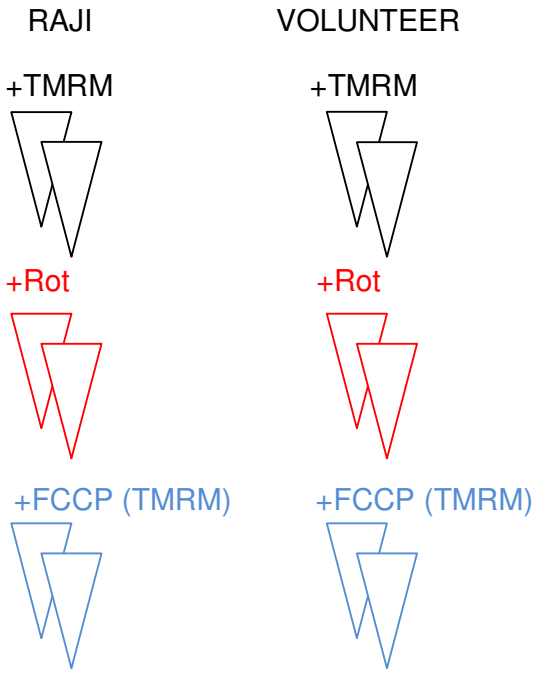

Fig 2.15: Schematic representation of the experimental design for the mitochondrial membrane potential assay in the human volunteers' lymphocytes and the Raji cells. Cells without TMRM were also used in all cases as background controls (not shown here).

2b) Main experiments

As discussed in section 2.1.6, lymphocytes isolated from the study participants (NTG, OHT, controls) were used for the main TMRM experiments. The same methodology was followed, as described for the optimisation experiments. In the case of the study participants' lymphocytes, duplicate measurements were made for each experimental condition, as shown schematically below (Fig 2.16). In all cases, the background fluorescence recorded for cells without TMRM (not shown schematically) was subtracted from the fluorescence measured for TMRM-stained live cells. Again, Raji was used as an internal control, with results being expressed as the mean red fluorescence % change from Raji (100%) (see section 4.3.3.3).

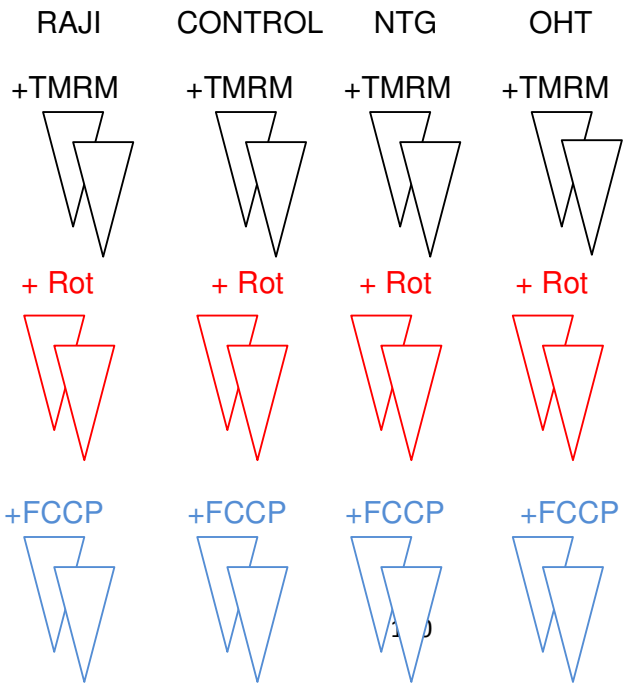

Fig 2.16: Schematic representation of the experimental design for the mitochondrial membrane potential assay in the patients' and controls' lymphocytes and the Raji cells. Cells without TMRM were also used in all cases as background controls (not shown here).

2.3.6 Dihydroethidium (DHE) staining

1. Basic principles

DHE, by virtue of its ability to freely permeate cell membranes, is used extensively to monitor the production of superoxide free radicals. DHE present in the cytosol in its reduced state (prior to contact with ROS) emits a blue fluorescence, whereas in the presence of superoxide anions it becomes oxidised and converts to ethidium bromide, which enters the nucleus and interacts with the DNA to emit a red fluorescence (Bindokas et al 1996) (Fig 2.17).

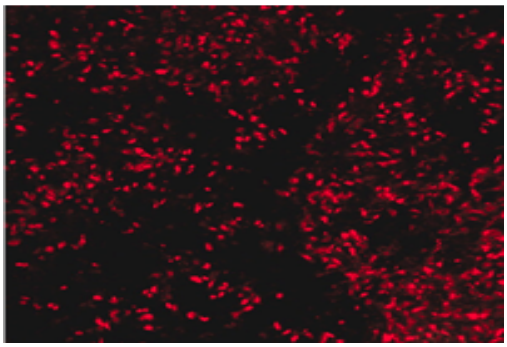

Fig 2.17: In the presence of superoxide, cells stained with DHE emit a red fluorescence.

2. Methodology

2a) Optimisation experiments

Similarly to the ADP phosphorylation and TMRM experiments, the two immortalised cell lines (Raji and Jurkat) and lymphocytes from healthy volunteers were used to optimise the DHE assay, before embarking on the main experiments using the study participants' (NTG, OHT, control) lymphocytes.

Cell suspensions were spun at 1000 x g for 10min, washed in 0.1M PBS and spun again at 1000 x g for 10min. After resuspending the pellet in PBS the cells were counted and the volume of cell suspension required for each experimental condition was selected to achieve a final cell density of 50,000cells/well. The final volume of cell suspension per well of the 96-well plate was 50µl made up in PBS. 50µl of DHE were then added into each well to produce final concentrations of 10µM and 20µM in the case of the Raji and Jurkat cells. A final concentration of 40µM was used in experiments involving healthy volunteers' lymphocytes to ensure there was no limitation in substrate supply. The rate of red fluorescence emission after staining live cells with DHE was used for subsequent analysis. Duplicate wells were employed for each experimental condition in each experiment. A Synergy HT Microplate Reader was used for measuring fluorescence kinetics on the 96-well plastic plates using the following filter (red fluorescence): excitation 485/20 and emission 590/25. The run time for each plate was 30 minutes with measuring intervals of 37 seconds. Sensitivity of 100 was used and the plate was shaken once for 2 seconds prior to each measurement.

In the case of Raji and Jurkat cells, the following experimental design was followed (Table 2.10). Three different treatments were used as positive controls to generate ROS and cause oxidative stress (Li et al 2003): 5μM rotenone (instantly), 0.5μM rotenone for 24hrs and 100μM paraquat for 24hrs.

	Control (cells without treatment)	**Rotenone 0.5 μM 24hrs**	**Paraquat 100 μM 24hrs**	**Rotenone 5μM instantly**	
DHE 10μM					Raji cells
DHE 20μM					Raji cells
DHE 10μM					Jurkat cells
DHE 20μM					Jurkat cells

Table 2.10: Schematic representation of the experimental design for the DHE assay in the Raji and Jurkat cells.

In the case of healthy volunteers' lymphocytes, four different treatments were used to produce ROS, and therefore an increase in DHE staining, thus serving as positive controls. The Raji cells served as an internal control and the following experimental design was followed (Table 2.11).

	Control (cells without treatment)	**0.5 μM Rotenone 24hrs**	**100 μM Paraquat 24hrs**	**5microM Rotenone instantly**	**5microM Rotenone 2hrs**	
DHE 40μM						Raji cells
DHE 40μM						Volunteer Lymphocytes

Table 2.11: Schematic representation of the experimental design for the DHE assay in the healthy volunteers' lymphocytes and the Raji cells.

2b) Main experiments

Lymphocytes isolated from the study participants (NTG, OHT, controls) were used for the main DHE experiments. The same methodology was followed, as described for the optimisation experiments. In the study participants' lymphocytes only one treatment was used to produce ROS, 0.5µM rotenone (24hrs), which was found from previous experiments to be associated with the largest increase in DHE staining in the Raji cells and healthy volunteers' lymphocytes (see section 4.2.4). Again, the Raji cells served as an internal control helping to standardise the assays over time, with the results being expressed as the percentage change from Raji (100%). The following experimental design was followed (Fig 2.18).

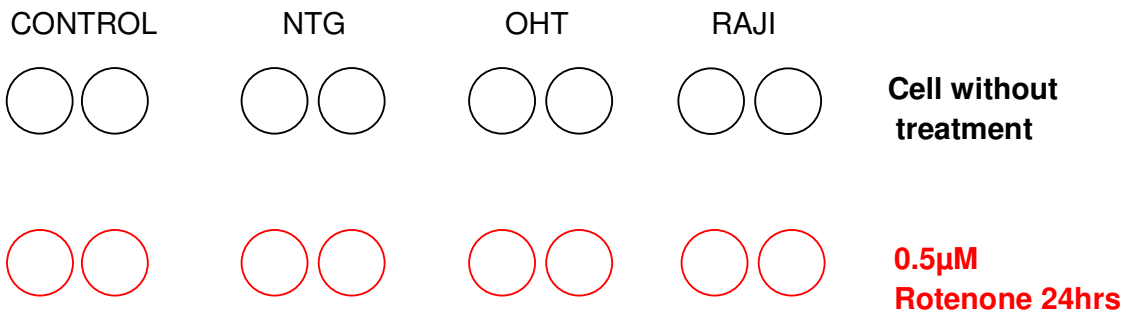

Fig 2.18: Schematic representation of the experimental design for the DHE assay in the patients' and controls' lymphocytes and the Raji cells (final DHE concentration 40µM). Circles represent wells of a 96-well plate.

2.3.7 Aconitase enzymatic activity

1. Basic principles

Aconitase (aconitate hydratase) is an iron-sulfur protein that catalyses the stereo-specific isomerisation of citrate to isocitrate via cis-aconitate in the

tricarboxylic acid cycle (Fig 2.19). In this assay citrate is catalysed by aconitase into isocitrate, and then the isocitrate catalysed by isocitrate dehydrogenase, to form alpha-ketoglutarate in the presence of NADP+ (colourless). The resulting increase of NADPH (yellow) can be detected by spectrophotometry using a plate reader. Aconitase is known to be sensitive to oxidation and thus reduction in its activity serves as an indicator of increased oxidative damage to the cells (Gardner et al 1994). The aconitase enzymatic activity was therefore used as a marker of background oxidative damage to the Raji and Jurkat cells, and human lymphocytes. Paraquat (PQ) is known to cause oxidative damage by generating superoxide and was used at a relatively low concentration (100µM, 24hrs) adequate to reduce aconitase function without killing the cells. It thereby served as a positive control.

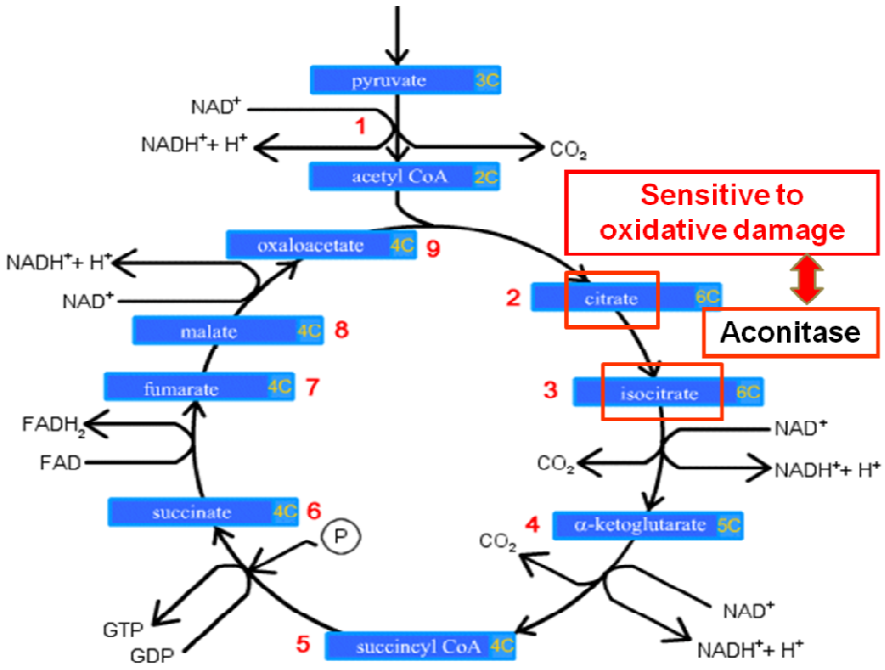

Fig 2.19: Aconitase catalyses the stereo-specific isomerisation of citrate to isocitrate in the tricarboxylic acid (Krebs) cycle and is known to be sensitive to

oxidative damage. Thus, reduced aconitase activity is associated with increased oxidative damage in our system (modified from http://library.thinkquest.org).

2. Methodology

2a) Optimisation experiments

Similarly to previous experiments, the two immortalised cell lines (Raji and Jurkat) and lymphocytes from healthy volunteers were used to optimise the aconitase enzymatic assay, before embarking on the main experiments using the study participants' (NTG, OHT, control) lymphocytes.

Cells in suspension were spun at 1000 x g for 10min, washed in 1xPBS and spun again at 1000 x g for 10min. Each pellet was then resuspended in distilled water (dH_2O) to a final cell density of 2million lymphocytes/ml, sufficient to exceed the threshold of the measurement. 207µl of cells were added into each well of the 48-well plate and duplicate measurements were taken for each experimental condition. An additional 2 wells contained only 207µl of distilled water without cells and acted as a negative control. 701µl of reaction buffer was added into each well leading to a total volume of 908µl per well. The reaction buffer included 0.4mM NADP, 50mM Tris-HCl pH 7.4, 5mM tri-Na Citrate, 0.6mM $MgCl_2$ and 0.1% Triton X-100 (final concentrations). 1 unit of citrate dehydrogenase per reaction was also added to the reaction buffer. The Synergy HT Microplate Reader, prewarmed at 37°C, was used for measuring absorbance kinetics on the 48-well plastic plate, at 340nm. Both the reaction buffer and the cells were placed in an incubator at 37°C prior to each measurement to optimise the reaction kinetics. Run time for each plate was 30

minutes with measuring intervals of 37 seconds. A BCA assay was performed to estimate the amount of protein in each sample and normalise the readings.

Raji and Jurkat cells were treated with 100µM paraquat for 24hrs and 0.5µM rotenone for 24 hrs to measure the susceptibility of lymphocytes to oxidative stress. Cell density was checked in the flasks treated with rotenone and PQ prior to starting each experiment to ensure no excessive cell loss. The following six experimental conditions were explored:

- Raji control
- Raji + 0.5 µM Rotenone 24hrs
- Raji + 100µM PQ 24hrs
- Jurkat control
- Jurkat + 0.5 µM Rotenone 24hrs
- Jurkat + 100µM PQ 24hrs

In the case of the healthy volunteers' lymphocytes, the experimental design is shown in Fig 2.20. Cells were again treated with paraquat (100µM 24hrs), as a positive control, and Raji cells without PQ treatment were used as a reference (internal control).

VOLUNTEERS	RAJI	No cells
+/-100µM PQ 24hrs	+/-100µM PQ 24hrs	(Negative control)

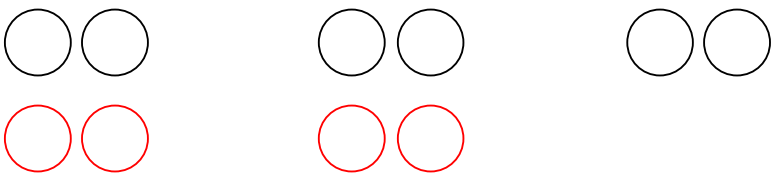

Fig 2.20: Schematic representation of the experimental design for the aconitase assay in the human volunteers' lymphocytes and the Raji cells. Circles represent wells of the 48-well plate. Duplicate measurements were taken for each experimental condition.

2b) Main experiments

Lymphocytes isolated from the study participants (NTG, OHT, controls) were used for the main aconitase experiments. The same methodology was followed, as described for the optimisation experiments. In the case of the study participants' lymphocytes, the experimental design is shown in Fig 2.21. Again, paraquat (100µM 24hrs) served as a positive control and Raji cells without PQ treatment served as an internal control helping to standardise the assays over time.

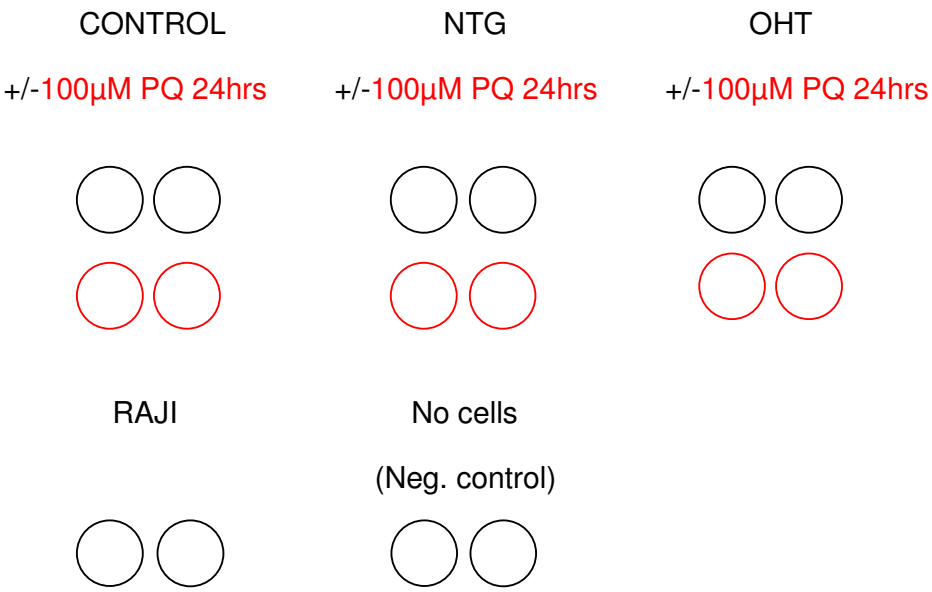

Fig 2.21: Schematic representation of the experimental design for the aconitase assay in the patients' and controls' lymphocytes and the Raji cells. Duplicate measurements were taken for each experimental condition.

2.3.8 Western blot analysis to quantify protein levels

1. Basic principles

The separation of charged molecules in solution in response to an electric field is called electrophoresis. A very common method for separating proteins by electrophoresis uses a discontinuous polyacrylamide gel as a support medium and sodium dodecyl sulfate (SDS) to denature the proteins. The method is called sodium dodecyl sulfate polyacrylamide gel electrophoresis (SDS-PAGE) (Schapiro et al 1967). The rate of migration of the charged molecules depends on the strength of the field, on the size and shape of the molecules, as well as on the viscosity and the temperature of the medium in which the molecules are moving (Weber et al 1969).

Proteins need to be transferred to membranes from gels so as to allow various probes to interact with individual macromolecules. The most used type of probes to interact with immobilised proteins are antibodies with specific affinity to given antigens. This can be implemented by incubating a membrane with transferred fractionated protein from a gel in a diluted antibody solution to recognise a defined protein (Fig 2.22). This is followed by washing of the membrane and incubation with a conjugated secondary antibody. Exposure to ECL (enhanced chemiluminescence) reagent allows the protein bound to the secondary antibody to emit light, captured on an x-ray film. A defined specific protein can then be quantified by densitometry.

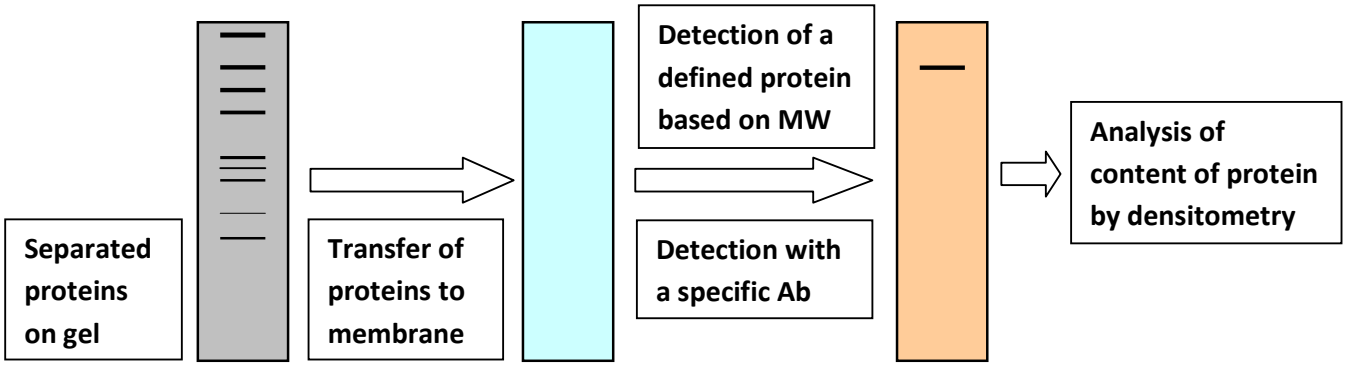

Fig 2.22: Detection of protein on a gel by Western blotting. Proteins on an SDS-polyacrylamide gel are transferred to a sheet of nitrocellulose paper and stained by a specific antibody. MW, molecular weight; Ab, antibody

2. Methodology

Cells in suspension were spun at 1000 x g for 10min, washed in 1xPBS and spun again at 1000 x g for 10min. The pellets were then lysed on ice with 50 µl of 10mM Tris pH7.5 and 1% (v/v) Triton X-100, and centrifuged at 15000 x g for 10 min. The supernatant was then aliquoted. Protein levels in the lysates were assayed with a BCA kit. Lysates were diluted so each lane was loaded with the same amount of protein. Lysates were mixed with loading dye and reducing agents according to the Novex system (Life Technologies) and heated at 70^{o}C for 10 minutes. Lysates were then loaded on a 4-12% NuPage gel and electrophoresed in the MES buffer at 200V for 35 minutes. Proteins were blotted onto PVDF membranes, blocked in non-fat milk (5%) in 1xPBS and then incubated with the primary antibody for 1hr in 1xPBS with 2.5% milk and 0.2% Tween-20. After washing with 1xPBS with 0.4% Tween-20 twice, the blot was incubated with HRP labelled secondary antibody for 1hr in 1xPBS with 2.5% milk and 0.2% Tween-20. The bound antibody was detected using the ECL

Chemiluminescence kit. Membranes were exposed to the Hyperfilm ECL film for the appropriate duration. Primary antibodies to actin, SOD2, TOM20 and porin were used, as detailed in section 2.1.2. Band intensity was quantified using Image-J (NIH, Bethesda, http://rsbweb.nih.gov/ij/). The intensity of the band for the protein of interest was divided by the intensity of the band for b-actin (loading control) in the same lane to quantify the amount of the protein (Fig 4.29).

2.3.9 Citrate synthase enzymatic activity

1. Basic principles

Citrate synthase is a pace-maker enzyme in the Krebs cycle (citric acid cycle) and is localised in the mitochondrial matrix. CS is nuclear encoded, synthesised on cytoplasmic ribosomes and transported into the mitochondrial matrix. Thus, CS enzymatic activity is commonly used as a quantitative measurement for the content of intact mitochondria (Holloszy et al 1970, Williams et al 1986), although this role of CS has been questioned in developmental (Drahota et al 2004) and age-related studies (Marin-Garcia et al 1998). In the latter study, the developmental increase in CS activity noted in cardiac tissue during the progression from early childhood to adulthood paralleled increasing CS polypeptide content, but was not related to overall increases in mitochondrial number or in cardiac mitochondrial respiratory enzyme activity (Marin-Garcia et al 1998).

2. Methodology

Cell suspensions were spun at 1000 x g for 10min, washed in 1xPBS and spun again at 1000 x g for 10min. The pellets were then lysed on ice with 50 µl of

10mM Tris pH7.5 and 1% (v/v) Triton X-100 and centrifuged at 15000 x g for 10 min. The supernatant was then aliquoted. For samples from each participant, 10µl of supernatant was mixed with 240µl of reaction mix (0.1M Tris-HCl pH=8, 0.2M acetyl coenzyme A, 0.2M DTNB, 0.1M oxaloacetic acid and 0.1% Triton X-100 in dH_2O). The assay was performed on a 96-well plate using a Synergy HT plate reader preheated to 30^{o}C. 250µl of the reaction mixture was added to each well, while blanks consisting of reaction mix without cell lysates were also assayed. The protein concentration for each sample was measured using the BCA kit described in 2.2.3. Citrate synthase enzymatic activity was calculated as nmol/min/mg protein.

2.3.10 Calcium mobilisation

1. Basic principles

Calcium (Ca^{2+}) homeostasis is fundamental for cell metabolism, proliferation, differentiation, and cell death. Elevation in intracellular Ca^{2+} concentration is dependent either on Ca^{2+} influx from the extracellular space (which has a concentration of around 1-2mM) through the plasma membrane or on Ca^{2+} release from intracellular Ca^{2+} stores, such as the endoplasmic reticulum (ER) with concentrations of 250-600µM (Giorgi et al 2009). Mitochondria are major components of calcium signalling, capable of modulating both the amplitude and the spatio-temporal patterns of Ca^{2+} signals. Mitochondrial Ca^{2+} uptake is due to the large electrochemical gradient provided by the negative inner mitochondrial membrane potential, usually between -150 and -180 mV, and is thus dependent on the integrity of the $\Delta\Psi_m$. Mitochondrial Ca^{2+} uptake has therefore been used as another measurement of mitochondrial function and is

known to play a key role in the regulation of many cellular functions, ranging from ATP production to cell death (Patergnani et al 2011). An increase in mitochondrial Ca^{2+} activates several dehydrogenases and carriers, inducing an increase in the respiratory rate, H^+ extrusion and ATP production. However, Ca^{2+} overload or prolonged increase in mitochondrial Ca^{2+} leads to the opening of the mitochondrial permeability transition pore (mPTP) and causes cell death either by energetic collapse and ATP depletion or by initiating mitochondrial swelling, cytochrome c release and apoptotic cascades (Giorgi et al 2008, Abramov et al 2003), although Ca^{2+} can also inhibit apoptotic cell death (Reimertz et al 2001).

Ionomycin is a Ca^{2+} ionophore often applied to cells in order to increase cytosolic Ca^{2+} and induce Ca^{2+}-dependent processes in the mitochondria in situ. Ionomycin, at concentrations less than 1µM, is thought to act primarily at the level of the internal Ca^{2+} stores, mainly the ER, and not the plasma membrane (Morgan et al 1994). However, actions of Ca^{2+} ionophores in intact cells are more complex, given the diversity of ionic gradients between the different membrane-bound compartments within the cell. It has also been reported that ionomycin at a standard dose of 10µM can cause mitochondrial depolarisation in intact cells, although this was often modest and highly variable and dependent on the prior state of mitochondrial calcium loading (Abramov et al 2003). The concentration used in our experiments was only 0.06µM and is less likely to have impacted significantly on mitochondrial function. Rhod2 and fluo3, two fluorescent Ca^{2+} indicators, were employed for measurements of mitochondrial and cytosolic Ca^{2+}, respectively (Kao et al 1989, Minta et al 1989). Rhod2 is a rhodamine-based dye and its ester forms are known to be cationic, resulting in potential-driven uptake into the mitochondria and its use as a selective indicator for mitochondrial calcium (Hoth et al 1997, Babcock et

al 1997). Pluronic acid was used to facilitate dye entry, eliminating any possible hydrolysis of the dyes by external esterases, and more efficient loading while maintaining cell integrity.

2. Methodology

One million cells were spun at 1000 x g for 10min and the pellet was resuspended in 0.5ml HBSS to which fluo3, rhod2 and pluronic acid were added to a final concentration of 5µg/ml, 5µg/ml and 0.025%, respectively. After incubating at room temperature for 30min, the cells were spun at 1000 x g for 10min, the supernatant removed, and the pellet resuspended in HBSS and incubated at room temperature for another 30min to remove any dye that was nonspecifically associated with the cell surface. The cells were again spun at 1000 x g for 10min, the pellet resuspended in 2ml HBSS and the cell suspension loaded into a cuvette. Measurements of resting fluorescence for fluo3 (fluo3 Fo) and rhod 2 (rhod2 Fo) were made within 30mins with a fluorometer and corrected for protein level, as measured with a BCA kit. For rhod2, the fluorescence excitation and emission maxima were 552nm and 581nm, respectively. For fluo3, the fluorescence excitation and emission maxima were 506nm and 526nm, respectively. After measuring the resting fluorescence, ionomycin was added (final concentration 0.06µM) for kinetic measurements (Fig 2.23). Upon ionomycin treatment, a significant rise was noted in both the cytosolic (expressed as the change in fluo3 fluorescence upon ionomycin treatment divided by the baseline fluo3 fluorescence: fluo3 ΔF/Fo) and mitochondrial (rhod2 ΔF/Fo) calcium (acute phase). This was followed by a more chronic phase of slow rise (chronic phase) and the rate of increase in the rhod2 fluorescence during this phase was divided by the rate of increase in the fluo3 fluorescence (Δrhod2 chr/ Δfluo3 chr). This observed preferential

coupling between increases in cytosolic and mitochondrial Ca^{2+} is one proposed mechanism to coordinate mitochondrial ATP production with cellular energy demand (Robb-Gaspers et al 1998).

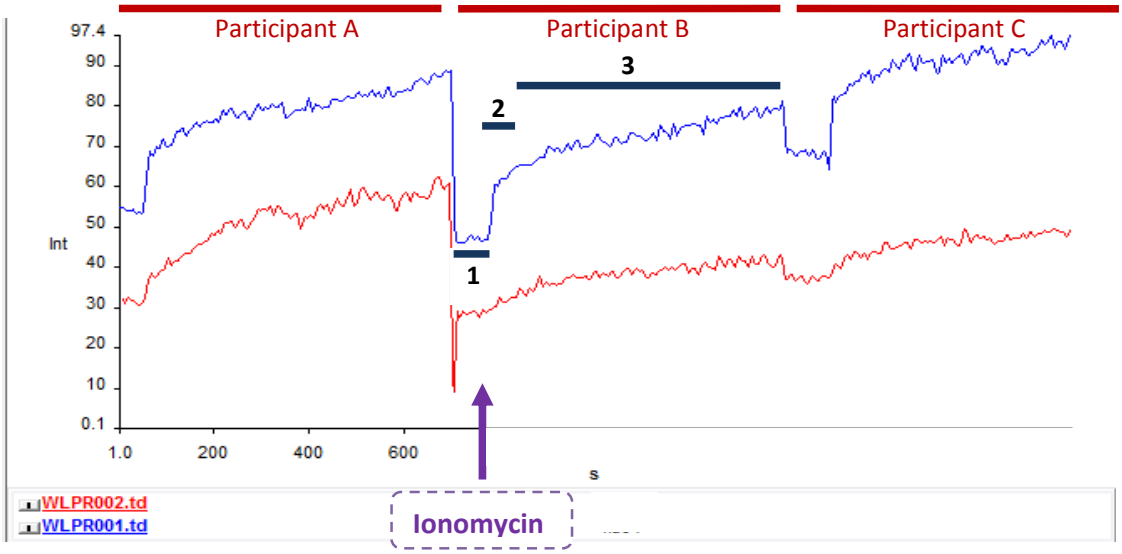

Fig 2.23: Example of resting fluorescence and kinetic fluorescence measurements upon ionomycin treatment for Participant B. Rhod2 is shown in red and fluo3 in blue. The y axis represents the intensity of fluorescence and the x axis the time (in sec). The purple arrow represents the timepoint when ionomycin was added. 1 represents the baseline (resting) fluorescence for fluo3 (fluo3 Fo), 2 represents the acute phase, where fluo3 staining rises suddenly upon ionomycin treatment (fluo3 $\Delta F/Fo$) and 3 represents the chronic phase of slow rise in the fluo3 fluorescence.

2.3.11 Enzyme-linked immunosorbent assay (ELISA)

1. Basic principles

The Enzyme-Linked Immunosorbent Assay (ELISA) is a commonly used technique for the determination of known analytes. The success of an ELISA

assay is dependent upon the underlying level of immunoreactivity of the capture and detection antibodies to the target analyte. The basic principles of ELISA are described in more detail in the legend of Fig 2.24 below.

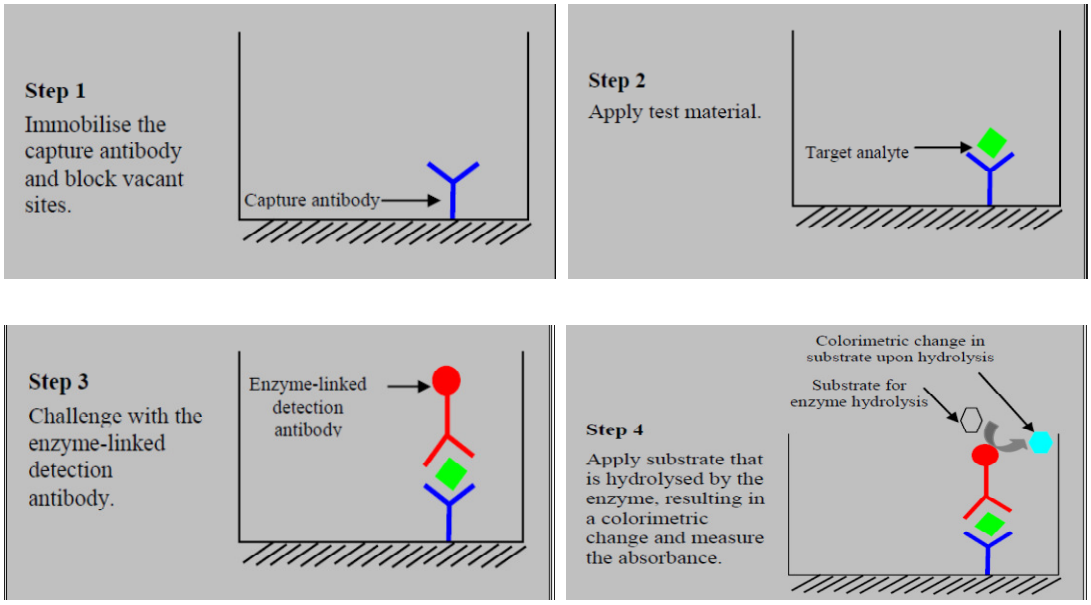

Fig 2.24: The basic principles of ELISA. In Step 1, the capture antibody is applied to the well of a microtitre plate and binds to the plate via passive absorption. A blocking solution [typically milk protein (casein), BSA or fish gelatine] is also applied, which adheres to any vacant sites on the plastic surface of the well that are not occupied by capture antibodies, thereby minimising the effect of non-specific binding by other reagents to the plate surface during subsequent incubation steps. Excess blocking agent is removed, the plate is rinsed and the test sample is added. Wash steps are incorporated between all incubation steps to minimise the background signal due to non-specific binding. In Step 2, the target analyte in the test sample is bound by the capture antibody that is anchored to the plate. After the incubation step with the test sample, the plate is washed prior to the addition of the enzyme-linked detection antibody (commonly used enzymes include horseradish peroxidise, alkaline phosphatase or β-D-galactosidase) (Step 3). These enzymes are proteins that catalyse the

hydrolysis of a chromogenic substrate, such as 3, 3', 5, 5'-tetramethylbenzidine (TMB), which undergoes a colourimetric change measurable using a spectrophotometric plate reader at specified wavelengths (Step 4). With the catalysis of the traditional chromogenic substrates, the reaction is terminated by the addition of a stop solution prior to measuring the absorbance of each of the wells of the microtitre plate (modified from Analytical Methods Committee Technical Briefings, No 45, 2010).

2. Background and Methodology for mTOR ELISA

The mammalian target of rapamycin (mTOR) is a highly conserved serine/threonine kinase that controls cell growth and metabolism in response to nutrients, growth factors, cellular energy and stress (Khalil et al 2012). Two structurally and functionally distinct multiprotein complexes are found: a) mTOR Complex 1 (mTORC1) is inhibited by rapamycin and mediates temporal control of cell growth by regulating translation, transcription, ribosome biogenesis, nutrient transport and autophagy, through the downstream targets 4E-binding protein 1 (4E-BP1) and p70 S6 kinase (Fig 2.25); b) mTOR Complex 2 (mTORC2) is rapamycin insensitive and mediates spatial control of cell growth by regulating the actin cytoskeleton. Such a physiological response is important for cell adaptation under stress and protection from death.

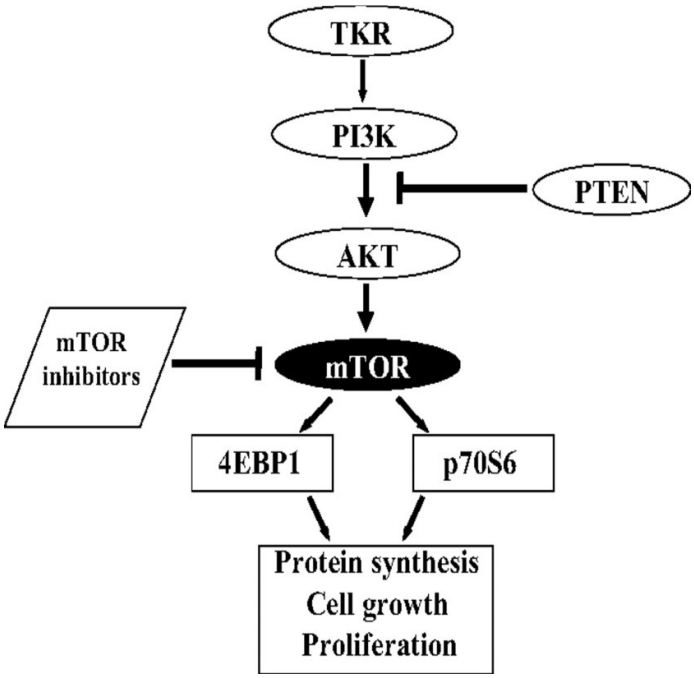

Fig 2.25: The mTOR pathway. Growth factor induced activation of phosphoinositide 3-kinase (PI3K) and protein kinase B (PKB or AKT) leads to increased activity of the mammalian target of rapamycin (mTOR). This subsequently leads to increased phosphorylation of the eIF4E binding protein-1 (4EBP1) and activation of the p70 ribosomal S6 protein kinase (p70S6K), both of which are important steps in the stimulation of protein translation (Navé et al 1999). mTOR is also regulated upstream by PTEN (phosphatase and tensin homologue deleted on chromosome ten); TKR: tyrosine kinase receptor.

As discussed in section 1.6.1, systemic mitochondrial dysfunction has been implicated as a potential susceptibility factor for glaucoma, given the role of increasing age as a major risk factor for glaucoma and the fact that ageing is well known to be associated with structural and functional changes to the mitochondria (Kong et al 2009, Yu-Wai-Man 2012, Lascaratos et al 2012). It is well established that upon stress, cells suppress the mTOR signalling in order to maintain energy homeostasis for survival. mTOR colocalises with the outer mitochondrial membrane (Desai et al 2002) and mTOR suppression has been

found to result in increased autophagy, reduced mitochondrial function (Ramanathan et al 2009) and decreased mitochondrial respiration (Schieke et al 2006). This direct effect of mTOR on mitochondrial function is thought to be mediated to a certain extent by its ability to form complexes with the mitochondrial outer membrane proteins Bcl-xl (B-cell lymphoma-extra large) and VDAC1 (voltage-dependent anion-selective channel protein 1) (Ramanathan et al 2009). Importantly, mTOR has also been shown to affect cellular metabolism by means of the transcriptional control of mitochondrial oxidative function through a YY1-PGC1α (yin-yang 1-peroxisome-proliferator-activated receptor coactivator 1α) transcriptional complex (Cunningham et al 2007). Based on this link between mTOR activity and mitochondrial function, the mTOR activity in the lymphocytes of our study participants was measured to explore the potential role of this kinase in mitochondrial dysfunction in glaucoma. mTOR is known to be phosphorylated at Ser2448 via the PI3 (phosphoinositide 3)-kinase/Akt signaling pathway (Fig 2.25) (Navé et al 1999). The mTOR activity in these experiments was expressed as the ratio between phosphorylated (active) mTOR and total mTOR.

In more detail, the PathScan Total mTOR and Phospho-mTOR (Ser2448) Sandwich ELISA kits were used to measure total and phospho-mTOR, respectively. Unlike previous experiments and in order to maintain the phospho-activity, peripheral blood mononuclear cells (PBMCs) isolated from our study participants were not incubated overnight. Immediately after isolation of the PBMCs, 1 million cells were spun at 1000 x g for 10min, washed in PBS and spun again using the same settings. The pellet was resuspended in 100µl of lysis buffer provided with the kit. The lysate was then microcentrifuged at 15000 x g for 10 min at 4°C and the supernatant transferred to a new tube and stored at -80^{o}C for future analysis. 100 µl of the

cell lysate were added into each well of a 96-well plate pre-coated with mTOR mouse antibody, sealed with tape and incubated at 4°C overnight. After washing twice with wash buffer supplied with the kit (200µl each time per well), 100 µl of mTOR rabbit antibody was added to each well to detect the captured mTOR protein. After a second incubation at 37°C for 1hr and repeat wash, 100 µl of anti-rabbit IgG, HRP-linked antibody was added to each well to recognise the bound detection antibody. The plate was again incubated at 37°C for 30min, washed as previously and 100 µl of TMB substrate was added to each well, in order to develop the colour (blue). The plate was again incubated at 37°C for about 10min to reach the desired colour intensity and the reaction was terminated by the addition of an acidic STOP solution, which changed the solution colour from blue to yellow. The absorbance for the developed colour was proportional to the quantity of mTOR protein and a plate reader was used to read the 96-well plate at 450nm.

3. Background and Methodology for 8OHdG ELISA

For several decades 8-OH-deoxy-Guanosine (8OHdG) has been considered a pivotal indicator of oxidative stress and more specifically oxidative DNA damage (Ames et al 1991, Loft et al 1992). Among all purine and pyrimidine bases, guanine is the most prone to oxidation, upon which a hydroxyl group is added to the 8th position of the guanine molecule (Cadet et al 2000) to produce the oxidatively modified product 8OHdG (Fig 2.26). This DNA alteration can induce point mutations, such as G-C transversions, but also the formation of apurinic/apyrimidinic sites. Although specific repair pathways are recognised for these lesions (Floyd et al 1990), whenever these mechanisms are overwhelmed by excessive levels of 8OHdG, stable DNA alterations can

occur. Upon DNA repair, 8OHdG is known to be excreted in the urine and urinary 8OHdG is widely used as a biomarker of generalised cellular oxidative stress (Patel et al 2007). Elevated urinary 8OHdG has been found in patients with various types of cancer (Chiou et al 2003, Wu et al 2004), cardiovascular disease (Negishi et al 2001) and diabetes, while the level of urinary 8OHdG was also found to be correlated with the severity of diabetic nephropathy (Hinokio et al 2002). Increased 8OHdG has also been, interestingly, linked to ageing (Hamilton et al 2001) and neurodegeneration (De Flora et al 1996). Smoking has also been shown to increase the levels of 8OHdG in several studies (Pilger et al 2001, Pourcelot et al 1999, Howard et al 1998), although this was not repeatable in other studies (Musarrat et al 1996, Wu et al 2004).

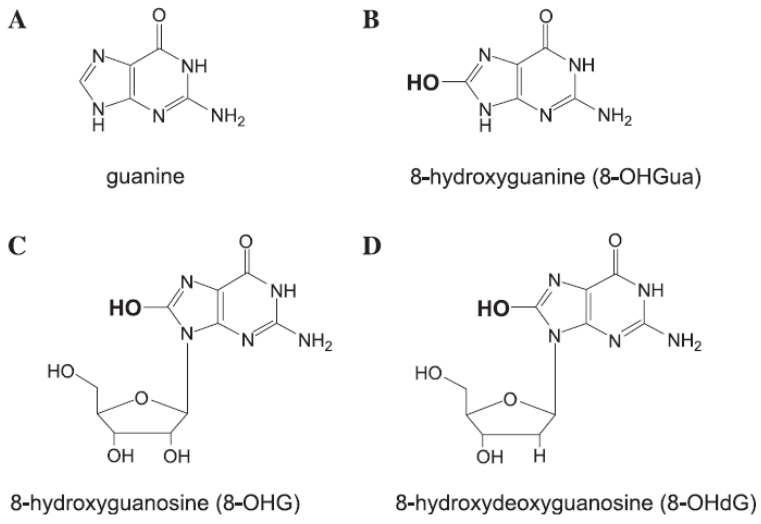

Fig 2.26: Chemical structure of 8OHdG and its analogues: (A) structure of an unmodified guanine base; (B) structure of an oxidised base; (C) analogue of 8OHdG derived from RNA, called 8OHG; (D) structure of 8OHdG derived from DNA (Wu et al 2004).

In 2003, elevated 8OHdG was noted for the first time in the TM of 42 glaucoma patients (angle recession, neovascular, juvenile, pseudoexfoliative syndrome

and POAG), as compared to 45 age-similar controls (Izzotti et al 2003). Interestingly, oxidative DNA damage among these patients correlated significantly with IOP fluctuation and maximum IOP values, as well as with VF damage in the POAG subgroup, suggesting a role for localised oxidative stress in glaucoma pathogenesis. 8OHdG levels were also significantly higher in the TM of patients with the GSTM1 gene deletion, which has been associated with an increased risk of cancer and atherosclerosis. The finding of increased oxidative DNA damage in the human TM in glaucoma was later confirmed by another study from the same group focusing on POAG patients, where elevated 8OHdG (5-fold) was found in 17 glaucoma patients, as compared to 21 controls (Sacca et al 2005). In another study from Iran, the aqueous levels of 8OHdG were found to be significantly (2.1 fold) higher in 28 glaucoma patients (15 with POAG and 13 with pseudoexfoliative glaucoma) as compared to 27 age-similar cataract patients (p=0.002), while the serum levels of 8OHdG in the glaucoma group were only marginally higher (p=0.046) than in the cataract group (Sorkhabi et al 2011). Also, recently, urinary 8OHdG was reported to be reduced in 43 NTG patients as compared to 40 healthy controls, indicating, according to the authors, a compensatory response to increased systemic oxidative stress in glaucoma (Yuki et al 2010). The measurement of urinary 8OHdG in this study was employed as an additional measure of generalised oxidative stress in our cohort and was performed with the use of a previously described competitive ELISA kit (Subash et al 2010).

Similarly to the ELISA steps presented above for mTOR, 50µl of each sample diluted to 1:80 and 1:320 were added into an 8OHdG/BSA conjugate coated 96-well plate. After a 10min incubation, 50µl of the anti-8OHdG monoclonal antibody were added and incubated for 1hr. After washing, 100µl of the HRP conjugated secondary antibody were loaded and the plate was incubated for

another hour. After washing, 100µl of substrate solution were added to develop the colour and after about 10min the reaction was terminated by adding 100µl of stop solution. The absorbance was read on a plate reader at 450nm. A first morning mid-stream urine sample was collected from each participant and the level of 8OHdG was corrected for urine creatinine and expressed in ng/mg creatinine. Each sample was assayed in duplicate and the quantity of 8OHdG in each sample was determined by comparing its absorbance with that of an 8OHdG standard curve. The detection range of the ELISA assay was 0 to 20 ng/ml and all of the 8OHdG measurements were performed within 3 months of urine collection.

2.3.12 Other laboratory tests (vitamins, homocysteine, urate)

The following laboratory tests were performed by TDL (The Doctors' Laboratory), Whitfield Street, London W1T 4EU: plasma homocysteine, urate, serum folate, red blood cell (RBC) folate, vitamin B12 (cobalamin), vitamin A (retinol), vitamin B6 (pyridoxine), vitamin C (ascorbate) and urine creatinine. Peripheral blood was collected at Moorfields Eye Hospital from the mitochondrial study participants and sent to TDL for further analyses. EDTA blood in a purple top tube was collected for the homocysteine, RBC folate and B6 measurements, while for the remaining measurements blood was collected in serum separator tubes (SSTs - yellow top). For vitamin measurements, the samples were protected from light by wrapping the tubes in aluminium foil.

2.4 Statistical analysis

In the UKGTS, the sample size estimation, randomisation, and study design were based on the patient as the unit of observation; the event time to deterioration was defined by the first deterioration in either eye. For eye-based analyses, two approaches were taken: (1) worse eye analysis (Kamal et al 2003) and (2) analysis of both eyes. Except for patients for whom no data were available, analyses were carried out on all patients in the treatment group to which they were randomised, using all the available data up to the point that they withdrew, to retain the validity of the randomisation process.

For the analysis of the UKGTS baseline characteristics, summary measures for continuous variables have been presented as mean and standard deviation (SD) for normally distributed measures and as median and interquartile range (IQR) for data that are not normally distributed. Frequencies (n) and percentages (%) were used for categorical variables. A two sample t-test was used to compare the mean values for continuous variable and a chi-square test for categorical variables. The STATA software (version 11, StataCorp LP) was employed for data analysis by the trial statisticians.

The primary UKGTS analysis concerned the incidence of primary deterioration events in latanoprost-treated eyes versus placebo-treated eyes over 24 months after entry to the trial. Survival analysis, conducted by a statistician, compared the differences in time from baseline to the event of confirmed VF deterioration between treatment groups and a Kaplan-Meier survival curve was constructed. Treatment effect was estimated as a hazard ratio with 95% confidence intervals computed by a Cox proportional hazards model. The survival analysis took into account subjects who were observed only for part of the trial period. A comparison of the proportion of subjects with deterioration

events in the treatment groups was made using univariate tests. In a clinical trial over a 2-year time frame, patients inevitably were lost to follow-up and reasons for loss to follow-up were investigated. Summary measures for continuous normally distributed outcome measures were differences in means and 95% confidence intervals for differences in means. Nonparametric equivalents were used for non-normally distributed outcome measures. For categorical variables, the Pearson's chi-square test or Fisher exact test was used.

For the IOP-related UKGTS analysis in section 3.5, the Pearson's correlation coefficient, also known as Pearson's R, was used as a measure of the strength and direction of the linear relationship between the median IOP and MD slope. The Akaike Information Criterion (AIC) value was used by the study statistician to compare models. The AIC, originally developed by Hirotugu Akaike in 1974 (Akaike 1974), is considered a measure of the relative goodness of fit of a statistical model, and is grounded in the concept of information entropy, in effect offering a relative measure of the information lost when a given model is used to describe reality. Therefore, the AIC values provide a means for model selection and models with smaller AIC values are preferred. However, the AIC 'raw' values make it difficult to unambiguously interpret the observed AIC differences in terms of a continuous measure, such as probability. Therefore, Akaike weights are also presented for each model, which can be directly interpreted as the probabilities of each model being the most likely model to describe the relationship (Wagenmakers et al 2004). In this case, the models with higher Akaike weights are preferred.

In chapter 4, the Wilcoxon signed rank test, a non-parametric counterpart of paired t-test, was used by the candidate for comparisons between two groups.

For comparisons between all three groups (control, NTG, OHT) in the mitochondrial pilot study, the Kruskal Wallis test was used as the equivalent of one-way non-parametric ANOVA. Clinical data are presented as mean ± standard deviation (SD) for normally distributed measures and as median ± interquartile range (IQR) for data that are not normally distributed. Experimental data are presented as median ± IQR. For the western blotting data the densitometric reading of the protein of interest was expressed as a percentage of the control gene product (b-actin). Box plots for the mitochondrial pilot study were prepared by the candidate using the SPSS 20.0 Inc software (IBM, Somner, NY). In all experiments a p-value of <0.05 was generally considered statistically significant.

2.5 Ethics approval

Consent was obtained from all the participants for the mitochondrial pilot study and the relevant Ethics Committee approval (REC Ref: 11/H0715/10) was granted. For the UKGTS, ethics committee approval was granted by the Moorfields and Whittington Research Ethics Committee on June 1, 2006 (REC Ref: 09/H0721/56) and an independent data and safety monitoring committee was appointed by the steering committee. Both studies adhered to the tenets of the Declaration of Helsinki.

Chapter 3

Intraocular pressure as a risk factor for glaucoma progression in the UKGTS

Chapter 3: Intraocular pressure as a risk factor for glaucoma progression in the UKGTS

3.1 Introduction

In 1993, Rossetti et al, in a systematic review of the literature, identified the paucity of evidence for the medical management of OAG and OHT (Rossetti et al 1993); their report stimulated the initiation of a number of treatment trials. A more recent Cochrane systematic review of medical interventions for OAG and OHT found evidence to support the use of IOP-lowering treatment to prevent the onset of VF loss in patients with OHT (Vass et al 2007), but identified no randomised, placebo-controlled trials assessing VF preservation in OAG. The authors concluded: "There is especially no evidence of a protective effect of prostaglandins. Further efforts should be directed to proving visual field preservation for these drugs." The UKGTS is the first randomised, double-masked, placebo controlled trial for the medical treatment of OAG and assesses the impact of treatment with prostaglandin analogues on VF preservation.

To date, medical treatment trials in OAG have compared a treatment with either no treatment or an active control, but not with a placebo (Vass et al 2007). Randomised, double masked, placebo controlled trials provide the highest level of evidence to guide clinical practice. Unmasked studies tend to be biased towards beneficial effects only if the outcomes are subjective and especially if there is inadequate allocation concealment. There are only 2 published trials comparing medical IOP-lowering treatment of OAG with no treatment (Holmin et al 1988, Leske et al 1999). These studies were unmasked

and had an objective primary outcome measure (computerised perimetry). The study by Holmin et al was very small (only 16 patients enrolled). To date, the best evidence for the beneficial effect of IOP-lowering treatment in OAG with established VF loss comes from the EMGT (Leske et al 1999), where patients with early OAG were randomised to argon laser trabeculoplasty plus betaxolol (n=129) or no immediate treatment (n=126) and were examined every 3 months for a median of 6 years (Heijl et al 2002).

With conventional trial design, the typical observation period for therapeutic trials in OHT and OAG with VF deterioration as an outcome has been 5 years or longer (Heijl et al 2002, CNTGS 1998, Kass et al 2002, Musch et al 1999, Kamal et al 2003). Long observation periods increase the cost of clinical trials, delay evidence in establishing efficacy for new treatments and considerably increase the cost for development of new therapies. There is, therefore, a great need for trial designs that reduce the observation period required. The UKGTS has two principal novel design features that may make much shorter observation periods possible. The first modifies the frequency and interval of VF tests to maximise power to measure the velocity of deterioration; the justification for measuring deterioration velocity is that OAG is a chronic progressive disease, so that more rapid deterioration infers greater vision loss over longer observation periods. The second includes quantitative imaging of the ONH and RNFL structure. To date, all clinical trials in OAG with VF deterioration as an outcome have used a VF change event criterion as an end point (CNTGS 1998, Musch et al 1999, AGIS 1994, Leske at al 2003, Krupin et al 2005); the velocity of VF deterioration itself has yet to be used as a trial outcome. The velocity of deterioration has been used as an outcome in clinical trials of other chronic progressive conditions seeking to identify disease modifying effects of therapy (Cheah et al 2011). The UKGTS study design allows a comparison of study

power when data analysis is based on survival analysis and on deterioration velocity.

OAG deterioration is characterised by changes in visual function and in the structure of the ONH and RNFL (Read et al 1974). Visual function outcomes generally are regarded to be more relevant to the patient. Some clinical trials have included both vision function and ONH structure end points (Kass et al 2002, Read et al 1974). However, agreement between structural and functional measurements of deterioration is poor over short periods (relative to the time course of the disease) (Artes et al 2005, Strouthidis et al 2006), so the application of structure end points in a clinical trial of therapy makes it difficult to evaluate the true effect of treatment on vision function. Over short periods, even clinically significant vision function deterioration may be masked by measurement imprecision, resulting in failure to identify the deterioration. Provided structural and functional parameters are sufficiently well correlated (and cross-sectional studies across the disease spectrum suggest this is the case) (Bartz-Schmidt et al 1999, Schlottmann et al 2004), analysis of structural parameter outcomes in the same model as outcome measurements of visual function may increase the power of a clinical trial to identify treatment effects in the preferred domain (visual function). Modeling of joint outcomes has shown potential in other diseases (Wilson et al 2000). In the UKGTS, the trial end point was VF deterioration, but frequent quantitative imaging was undertaken, for the first time in a medical treatment trial for OAG, to permit analysis of joint outcomes.

Apart from establishing the VF-preserving effect of a prostaglandin analogue, the UKGTS also aimed to quantify important risk factors for OAG deterioration. As discussed in more detail in section 1.5, known risk factors for deterioration

are higher IOP, greater subject age, lower ocular perfusion pressure, presence of pseudoexfoliation, optic disc hemorrhages and thinner CCT. Known risk factors have low power to predict OAG deterioration and patients deteriorate at varying rates at all levels of IOP, suggesting that factors other than IOP influence susceptibility for OAG deterioration. In the UKGTS, new potential risk factors are investigated and existing risk factors are measured with greater precision than previously. In the EMGT, no deterioration was detected in 38% of untreated subjects over a follow-up period of 6 years (Heijl et al 2002), and in the CNTGS 50% of untreated normal-tension glaucoma patients showed no deterioration over 5 years (CNTGS 1998). A secondary goal of the UKGTS was to evaluate whether risk profiling and stratifying patients is able to identify which patients do not need immediate treatment and which patients may benefit from more vigorous treatment.

3.2 The UKGTS design and methodology

Study Design

The UKGTS was a multicenter, randomised, double-masked, placebo-controlled medical treatment trial for OAG. Eligible patients were randomised in a 1:1 ratio to receive either latanoprost 0.005% or placebo once in the evening in both eyes for 24 months or until reaching an end point. After 24 months, subjects who had not reached an end point were invited to continue for a further 24 months either with latanoprost (open-label) or without treatment (no drops) to provide greater power for risk factor analyses (the UK Glaucoma Risk Factor Study).

Objectives

Primary: The primary objective was to test the hypothesis that medical treatment with a topical prostaglandin analogue reduces the incidence of VF deterioration events compared with placebo by 50% over a 2-year observation period.

Secondary: Secondary objectives were: (1) to evaluate the velocity of deterioration as a trial outcome, (2) to evaluate quantitative imaging measurements as additional trial outcomes, (3) to identify risk factors for OAG deterioration, (4) to establish whether initial observation, rather than immediate treatment, is feasible for selected patients, and (5) to evaluate the association of VF loss with measures of quality of life (QoL).

Eligibility Criteria

Eligibility criteria were modeled on those for the EMGT. OAG was defined as glaucomatous VF defects (defined below) in at least 1 eye with corresponding damage to the ONH (cup-to-disc ratio of ≥0.7, focal narrowing of the neural rim, or both), with an open angle on gonioscopy and the absence of retinal or neurologic condition that could account for VF loss. A glaucomatous VF defect, for trial inclusion, was defined as a reproducible (in at least 2 consecutive reliable post screening VFs) reduction in sensitivity at 2 or more contiguous points with $P<0.01$ loss or more, 3 or more contiguous points with $P<0.05$ loss or more, or a 10dB difference across the nasal horisontal midline at 2 or more adjacent points in the total deviation plot (Greaney et al 2002).

Inclusion Criteria

Inclusion criteria were the following: newly detected, previously untreated OAG (including primary OAG, NTG and pseudoexfoliation glaucoma) in either eye; age older than 18 years; Snellen visual acuity of 20/40 or better; VF mean

deviation (MD; location-weighted mean difference from average age-corrected VF sensitivity) of 2 post-screening VFs differing by no more than 3 dB, for an MD of better than -6.0 dB, or by no more than 4 dB, for an MD worse than -6.0 dB; and the ability to give informed consent and to attend for the duration of the study.

Exclusion Criteria

Exclusion criteria were the following: moderately advanced VF loss (MD worse than -10 dB in the better eye or worse than -16 dB in the other eye) or a threat to fixation (a paracentral point with sensitivity of <10 dB in both the upper and lower hemifields) in either eye; IOP of >35mmHg on 2 consecutive occasions in either eye or mean (2 visits) baseline IOP of ≥30mmHg; inability to perform reliable VF testing; poor-quality Heidelberg Retina Tomograph (HRT) images (see section 2.2.12), cataractous lens gradings of more than N1, C2, or P1 according to the Lens Opacities Classification System III grading; previous intraocular surgery (other than uncomplicated cataract extraction more than 1 year previously); and diabetic retinopathy.

Recruitment

Consecutive potentially eligible patients were identified at the new patient clinics of participating centers (Table 3.1). Potentially eligible subjects attended a training visit where VF tests were repeated twice and ONH imaging was performed; the results of these tests were assessed for eligibility at the accredited Moorfields Eye Hospital Reading Centre. After eligibility was confirmed and informed consent was obtained, a study identification number was assigned by the Moorfields Clinical Trials Unit. Patients were enrolled between 1 December 2006 and 16 March 2010.

Participating Centres	Local Principal Investigator	Screening start date	Screening end date
Moorfields Eye Hospital	Professor DF Garway-Heath	December 2006	March 2010
Aberdeen Royal Infirmary	Professor A Azuara-Blanco	March 2007	March 2010
Addenbrookes Hospital	Professor K Martin	December 2008	March 2010
Birmingham Heartlands and Solihull	Mr I Cunliffe Mr A Negi	May 2007	March 2010
Bristol Eye Hospital	Mr J Diamond Dr P Spry	November 2007	March 2010
Cheltenham General Hospital	Professor A McNaught	December 2007	March 2010
Hinchingbrooke Hospital	Professor R Bourne	April 2007	March 2010
Huddersfield/Halifax	Mr N Anand	February 2009	March 2010
Norfolk and Norwich University Hospital	Mr DC Broadway	February 2007	March 2010
Sunderland Eye Infirmary	Mr S Fraser	March 2007	March 2010
West of England Eye Unit, Exeter	Mr D Byles	January 2009	March 2010

Table 3.1: The UKGTS participating centres.

Randomisation

A randomisation schedule was drawn up by the statisticians in the R&D Department at Moorfields Eye Hospital using randomised permuted blocks of

varying centres with stratification by center. The randomisation schedule then was sent to the Pharmaceutical Manufacturing Unit for labeling of treatments. The unit of randomisation was the patient, with both eyes allocated to receiving treatment.

Allocation Concealment

Pfizer provided latanoprost and placebo drops in identical containers with tear-off labels identifying the container contents; the tear-off labels were removed by the Moorfields Pharmaceutical Manufacturing Unit and were replaced with the study identification number (according to the randomisation schedule) before packaging. The randomisation codes were held securely by the Moorfields Pharmaceutical Manufacturing Unit and Moorfields R&D Department and were not available to study personnel. In an attempt to maintain masking, investigators were encouraged not to tell patients their IOP measurements. On exiting the study (at deterioration or at 24 months), patients were asked to guess whether they had been taking the active or placebo drops.

Formulation

The active formulation was as follows per 1 ml: latanoprost, 50µg; benzalkonium chloride 0.20mg; sodium chloride; sodium dihydrogen phosphate monohydrate; disodium phosphate anhydrous; and water for injection. The placebo formulation was as follows per 1 ml: benzalkonium chloride 0.20mg; sodium chloride; sodium dihydrogen phosphate monohydrate; disodium phosphate anhydrous; hydrochloric acid; sodium hydroxide; and water for injection.

Adherence

Trial participants were asked at each visit whether they had taken the study drops the previous evening and how frequently they thought that they had forgotten their drops.

Blinding

This was a double-masked study. In an attempt to maintain masking, investigators were encouraged not to tell patients their IOP measurements.

Adverse Events

The trial manager monitored adverse events and reported them immediately to the Data and Safety Monitoring Committee. Serious adverse events were reported to the Medicines and Healthcare Products Regulatory Agency.

Quality Assurance

Eligibility and deterioration status were assessed independently at the Moorfields Eye Hospital Reading Centre. Data collection was standardised and procedures for all investigations were set out in the trial Manual of Procedures and the Manual of Standard Operating Procedures. Technicians and clinicians performing the investigations underwent training and certification before initiation of recruitment. Case report forms were collected at the Data Centre and primary data entry into the electronic database was performed by the trial manager; primary outcomes were double-data entered by a data entry clerk. The trial manager monitored adherence to trial protocols, and completeness and validity of data and contacted sites, to recover missing data.

Participant flow

A diagram describing participant flow can be found below (Fig 3.1).

UKGTS Flow Diagram

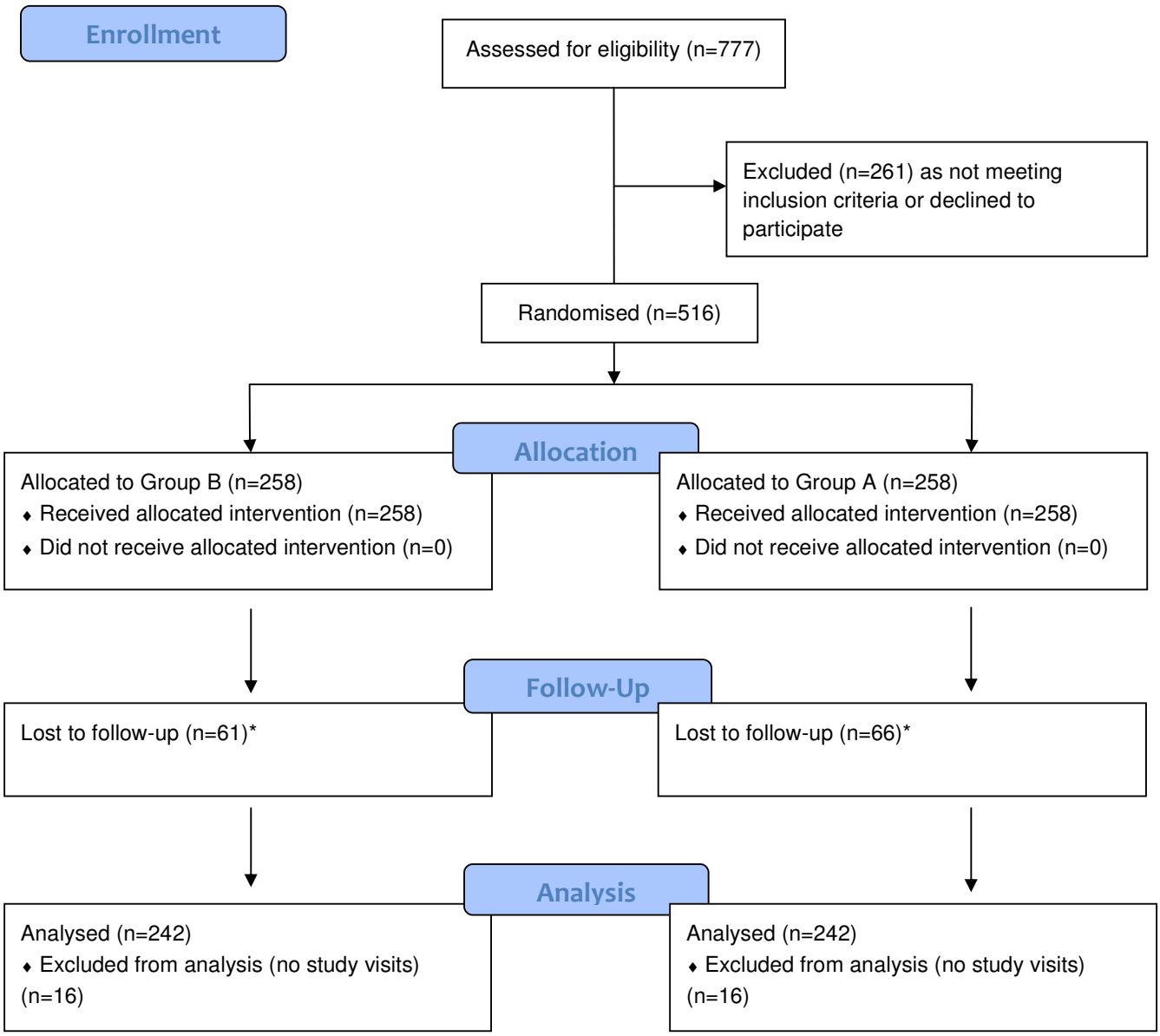

Fig 3.1: The UKGTS participant flow diagram. *Reasons for loss to follow-up are presented in table 3.8.

The UKGTS schedule of investigations is given in Table 3.2 below.

	Training Visit 0 Week -8	Visit 1 Month 0	Visit 2 Month 2	Visit 3 Month 4	Visit 4 Month 7	Visit 5 Month 10	Visit 6 Month 13	Visit 7 Month 16	Visit 8a Month 18	Visit 8b Month 18	Visit 9 Month 20	Visit 10 Month 22	Visit 11 Month 24
Phenotyping													
Screening													
Consent Randomisation	X												
Visual Fields	X2	X2	X2	X	X	X	X	X2	X2	X2	X	X	X2
Visual Acuity	X	X	X	X	X	X	X	X	X	X	X	X	X
Standard clinical exam, including GAT	X	X	X	X	X	X	X	X	X	X	X	X	X
Questionnaire (visual function health status)		X							X				X
LOCS III lens grading	X								X				X
Pascal DCT		X	X	X	X	X	X	X	X	X	X	X	X
IOP: ORA		X	X	X	X	X	X	X	X	X	X	X	X
Biometry, inc CCT		X											
HRT	X	X3	X2	X	X	X	X	X2	X3	X2	X	X	X
Disc photography		X	X	X	X	X	X	X	X	X	X	X	X
GDxECC		X3	X2	X	X	X	X	X2	X3	X2	X	X	X
OCT		X5	X3	X3	X3	X3	X3	X3	X5	X3	X3	X3	X5
Phasing		X							X				X
24-hour BP				X									
Phlebotomy for DNA, B12, folate, HbA1c			X										

Table 3.2: The UKGTS schedule of investigations; GAT: Goldmann Applanation Tonometry; LOCS: Lens Opacities Classification System; DCT: Dynamic Contour Tonometre; IOP: intraocular pressure; ORA: Ocular Response Analyzer; CCT: central corneal thickness; HRT: Heidelberg Retina Tomography; OCT: Optical Coherence Tomography; GDxECC: scanning laser polarimetry enhanced corneal compensation; BP: blood pressure.

Eleven visits over 24 months were planned, with VF and imaging tests clustered at the beginning and end of the observation period, as statistical modelling demonstrates that clustering increases the precision of estimates of the velocity of deterioration (Crabb et al 2009). Additional tests were clustered at the 18-month time point to assess whether trial durations could be reduced further. The maximum interval between visits was 3 months.

Additional Investigations for Secondary Analyses

Blood tests related to cardiovascular and neurodegenerative risk: Blood samples to assess various lipid (total cholesterol, low-density lipoprotein cholesterol, high-density lipoprotein cholesterol and triglycerides) and non-lipid (including fasting glucose, glycosylated hemoglobin, vitamin B12, red cell folate, homocysteine, high-sensitivity C-reactive protein and thyroid function) risk factors were obtained (Herrmann et al 2011). The rationale for these investigations is that glaucoma, as a neurodegenerative condition, may share risk factors for cognitive decline of degenerative or vascular origin (Solfrizzi et al 2006). Additional samples were taken for future DNA and proteomics analyses.

Cardiovascular history and examination: A history was taken to elicit evidence for hypertension, stroke, generalised arteriosclerosis, smoking, alcohol intake, migraine, Raynaud's phenomenon, diabetes mellitus, use of BP medications and statins. In addition to BP measurements, height, weight and waist circumference measurements were obtained.

End Points

End points included (1) visual field deterioration (therapeutic end point); (2) IOP of >35mmHg on 2 successive occasions (safety end point); and (3) decline

of best-corrected visual acuity to less than 20/60 (non-glaucomatous end point). On the basis of fundus photographs and the pattern of VF loss, 2 independent glaucoma fellowship-trained ophthalmologists confirmed that the VF deterioration was consistent with OAG, rather than a non-glaucomatous process such as vein occlusion, stroke or age-related macular degeneration.

Outcome Measures

The primary outcome was time to confirmed VF deterioration. VF deterioration was based on the GPA pattern deviation maps and defined as, in either eye, at least 3 test points showing significant negative change compared with baseline ($P<0.05$), at the same location in 2 consecutive VFs (tentative deterioration) and deterioration according to the same criterion present in the next 2 VFs (confirmed deterioration). In more detail, if tentative deterioration was identified, confirmation tests were performed within 1 month and, if the same criteria were satisfied in these confirmation tests, then the patient was considered to have progressed. An exit visit was scheduled within 1 month of the confirmation visit. Two VFs were performed at this visit and then treatment started (or augmented). The tests after the confirmation tests were included in the analysis of the velocity of VF deterioration, but not in the analysis of incident deterioration.

The secondary outcomes were velocity of uniocular and binocular VF loss, rate of confocal scanning laser ophthalmoscopy neural rim area loss, rate of RNFL loss (OCT and scanning laser polarimetry) and change in IOP from baseline at 4 and 24 months (or time of deterioration).

The outcomes for the substudy investigations were (1) the identification of risk factors for glaucomatous deterioration, including IOP level, IOP fluctuation,

age, race, degree of glaucoma damage at baseline (MD in dB), and other ocular and systemic variables, and (2) the association of visual function with measures of QoL.

Trial Size

The trial sample size was based on the outcome of the EMGT (Heijl et al 2002): Deterioration rates at 24 months were 24% in the untreated group and 11% in the treated group, and IOP reduction was 25% in the treated group. Latanoprost typically achieves a 20% to 30% IOP reduction, depending on the baseline IOP. Based on 90% power (1–β) at a 2-sided error α=0.05 to detect the difference between 24% and 11% in incident deterioration over a 24-month follow-up, 193 patients were needed in each arm (386 total). Allowing for a 25% attrition over the study period, 516 patients needed to be recruited to the study.

Protocol Amendments

Trial size: At the initiation of the trial, the sample size was determined for an outcome at 18 months, based on the EMGT (15% vs. 7%, 85% power, 2-sided error α=0.05, and an attrition rate of 15%). Because recruitment was slower than expected, the sample size was recalculated in October 2008 for an outcome at 24 months (24% vs. 11%, 90% power, 2-sided error α=0.05, and an attrition rate of 15%), and additional study sites were added. The sample size was revised further in June 2009, because of a greater than anticipated attrition rate.

Primary outcome: The trial size was determined from the results of the EMGT. The primary outcome of the EMGT was based on the Humphrey Field Analyzer GPA pattern deviation maps and defined as at least 3 test points showing

significant negative change (P<0.05), as compared with baseline, at the same locations in 3 consecutive VFs in the 30-2 VF. Because the UKGTS used 24-2 VF testing, the EMGT criterion is more stringent than intended and would have resulted in fewer end points than anticipated for the sample size calculation. A less stringent end point (defined above) was adopted and used throughout the study.

Primary analysis: After the publication of the National Institute for Clinical Excellence Guidelines, "Diagnosis and Management of Chronic Open Angle Glaucoma and Ocular Hypertension," the independent Data and Safety Monitoring Committee requested an interim analysis in January 2011 based on time to event, rather than difference in proportions with an event in either arm (the analysis on which the trial was powered). The Steering Committee therefore formally adopted time to event for the primary analysis, and difference in proportions for a secondary analysis, in the Statistical Analysis Plan.

Trial Sponsor and Funding

The trial sponsor was Moorfields Eye Hospital NHS Foundation Trust. The principal funding was through an unrestricted Investigator-Initiated Research grant from Pfizer Inc, with supplementary funding from the UK's National Institute for Health Research Biomedical Research Centre at Moorfields Eye Hospital and UCL Institute of Ophthalmology. Carl Zeiss Meditec provided 6 prototype GDx Enhanced Corneal Compensation scanning laser polarimetry devices and 4 Stratus OCT devices, Heidelberg Engineering provided 3 HRTs, and OptoVue provided 2 RTVue OCTs for the duration of the study. The funding organisations had no role in the design or conduct of this research. Trial registration no: ISRCTN96423140.

Trial Organisation

The Trial Steering Committee monitored and supervised the trial and commented on any proposed major protocol amendments. The study was coordinated by the clinical trials manager in the Clinical Trials Unit at Moorfields Eye Hospital. The trials manager monitored recruitment, data completeness and quality, study end points, and adverse events and produced monthly trial progress reports for the Data and Safety Monitoring Committees. The Data Centre is located in the Glaucoma Research Unit, Moorfields Eye Hospital. The Visual Fields Reading Centre is located at the Reading Centre, Moorfields Eye Hospital. Operational data and safety monitoring was undertaken by the Moorfields Eye Hospital Research Governance Committee.

3.3 The UKGTS baseline data

Introduction

The purpose of this section is to report and discuss the baseline characteristics of the UKGTS cohort. In the present study, baseline characteristics were evaluated by patient (Tables 3.4 and 3.5) and by eye (Tables 3.6 and 3.7). For eye-based baseline data, two approaches were taken: 1) analysis of all eligible eyes (Table 3.6) and 2) 'worse' eye analysis (Table 3.7) to compare the baseline characteristics between the worse and better MD eyes.

Baseline IOP data represent the mean of two pre-allocation diastolic measurements by GAT. A third measurement was obtained, if the difference between the first two was more than 1 mmHg. For the baseline VF data, the mean of the two baseline (post-allocation) VFs performed at Visit 1 was used, while for the 32 patients who failed to attend Visit 1 the mean of the two

screening VFs is presented. Where the Humphrey Field Analyzer (HFA) software excluded a baseline VF, due to learning effects or high false positive rates, the mean of the baseline VFs selected by the HFA software are presented. The baseline spherical equivalent (SE) calculation (algebraic sum of the value of the sphere and half of the value of the cylinder) was based on the refractive error recorded in the case report form from either an autorefractor or from spectacle focimetry. Where neither of these was recorded, the trial lens correction used to perform the VFs was used to estimate the SE in 86 eligible eyes, based on the age of the patient.

Source of referrals

The main source of referrals in the UKGTS was optometrists (88%), while only a small percentage of patients were referred from their general practitioner (GP) (3%) or through the hospital (8%) (Table 3.3).

Referral Source	Patients Participated n (%)
GP	15 (3%)
Hospital	43 (8%)
Optometrist	454 (88%)
Unknown	4 (1%)

Table 3.3: Source of referral across all UKGTS sites.

Participant flow

Out of 777 subjects assessed for eligibility, 261 were excluded as not meeting the inclusion criteria or declined to participate (see Fig 3.1 above); 66.4% of

the patients screened took part in the UKGTS. The 516 eligible patients were randomised to latanoprost or placebo.

Baseline patient characteristics (Tables 3.4 and 3.5)

	(n=516)	
	n (%)	Mean ± SD
Centre:		
MEH	91 (17.6%)	
ARI	42 (8.1%)	
NNUH	83 (16.1%)	
BHS	74 (14.4%)	
CGH	24 (4.7%)	
BEH	26 (5%)	
SEI	32 (6.2%)	
HH	109 (21.1%)	
AH	21 (4.1%)	
WEEU*	2 (0.4%)	
H&H	12 (2.3%)	
Family history of glaucoma:		
None	348 (67.4%)	
1st–degree relative	164 (31.8%)	
Other family history	2 (0.4%)	
Unknown	2 (0.4%)	
Age (years):		66 ± 11
20-29	2 (0.4%)	
30-39	4 (0.8%)	
40-49	40 (7.8%)	
50-59	97 (18.8%)	
60-69	181 (35%)	
70-79	162 (31.4%)	
≥80	30 (5.8%)	
Gender:		
Female	243 (47.1%)	
Male	273 (52.9%)	

Education achieved:		
Up to age 16	244 (47.3%)	
Up to age 18	33 (6.4%)	
Apprenticeship/certificate/diploma	137 (26.6%)	
Degree	96 (18.6%)	
Unknown	6 (1.1%)	
Ethnicity:		
White	465 (90.1%)	
Black	27 (5.2%)	
Asian	16 (3.1%)	
Other	3 (0.6%)	
Unknown	5 (1%)	
History of:		
Blood loss	35 (6.8%)	
Myocardial infarction	28 (5.4%)	
Obstructive pulmonary disease	31 (6%)	
Diabetes mellitus	54 (10.5%)	
Concomitant neurological disease (Parkinson's, Alzheimer's, multiple sclerosis, deafness)	65 (12.6%)	
Medication use:		
Antihypertensives	207 (40.1%)	
Corticosteroids	45 (8.7%)	
Statins	140 (27.1%)	
Other (insulin, oestrogen etc.)	304 (58.9%)	

Table 3.4: Baseline clinical characteristics of all the randomised UKGTS patients (n=516). (MEH: Moorfields Eye Hospital, ARI: Aberdeen Royal Infirmary, NNUH: Norfolk and Norwich University Hospital, BHS: Birmingham Heartlands and Solihull, CGH: Cheltenham General Hospital, BEH: Bristol Eye Hospital, SEI: Sunderland Eye Infirmary, HH: Hinchingbrooke Hospital, AH: Addenbrookes

Hospital, WEEH: West of England Eye Unit, H&H: Huddersfield/Halifax) *two patients were recruited at WEEH and they were followed up for only two visits.

The eleven initial participating centres across the UK with the corresponding patient cohorts are presented in Table 3.4. Almost 70% of the participants were recruited and followed up in one of the following four centres: Moorfields Eye Hospital, Norfolk and Norwich University Hospital, Birmingham Heartlands and Solihull Hospital, and Hinchingbrooke Hospital.

The 516 participants had a mean (±SD) age of 66±11 years. The age distribution of all randomised patients at baseline is shown in Fig 3.2.

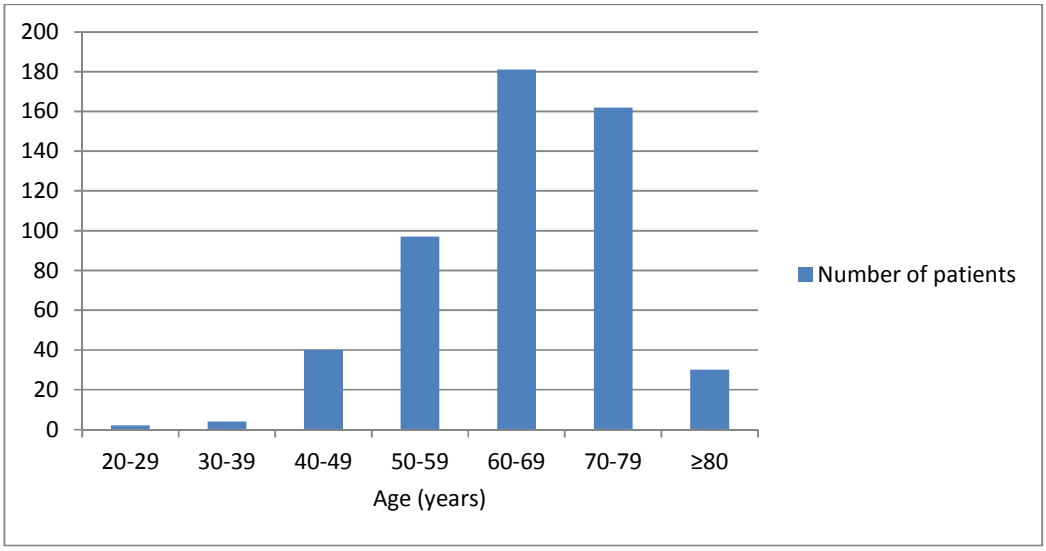

Fig 3.2: Age distribution of patients (n=516) at baseline.

There were slightly more male patients in our cohort (52.9%). Almost a third (32.2%) had a family history of glaucoma. The vast majority in our cohort were white (90.1%). The health status of the participants was generally good; 28 (5.4%) had a history of myocardial infarction, 54 (10.5%) of diabetes mellitus; 31 (6%) obstructive pulmonary disease and 65 (12.6%) concomitant neurological disease (Parkinson's, Alzheimer's, multiple sclerosis or deafness).

Use of antihypertensives was noted in 207 (40.1%) patients; corticosteroids in 45 (8.7%); statins in 140 (27.1%) and other medications in 304 (58.9%).

The measurement of blood pressure, anthropometric measures (body mass index, waist circumference, waist-hip ratio), and the evaluation of history of hypertension, general arteriosclerosis (stroke, angina and intermittent claudication), vasospasm, migraine and Raynaud's phenomenon were undertaken during the first post-treatment allocation study visit; the baseline characteristics for the UKGTS participants attending at least one post-allocation visit (n=484) are summarised in Table 3.5 below.

	(n=483)	
	n (%)	Mean ± SD Median (IQR)
Systolic blood pressure (mmHg)		136 ± 20
Diastolic blood pressure (mmHg)		81 ± 11
Body mass index		26.9 (23.9 to 30.1)
Waist circumference (cm)		98 (88 to 107)
Waist-hip ratio		0.91 (0.84 to 0.96)
Hypertension: Receiving treatment, or Systolic >160mmHg, or Diastolic >95mmHg	279 (57.8%)	
History of:		
General arteriosclerosis (stroke, angina or intermittent claudication)	38 (7.9%)	
Vasospasm, migraine or Raynaud's phenomenon	229 (47.4%)	

Table 3.5: Baseline characteristics of all the UKGTS participants that attended at least one post-allocation visit (visit 1) (n=484).

The median (IQR) body mass index, calculated as the weight in kilograms divided by the height in metres squared, in our cohort was 26.9 (23.9 to 30.1).

The median (IQR) waist-hip ratio, calculated as the ratio of the circumference of the waist in centimetres to that of the hips, was 0.91 (0.84 to 0.96). History of hypertension, defined as systolic blood pressure greater than 160 mmHg or diastolic blood pressure greater than 95 mmHg or antihypertensive treatment history (Leske et al 1999), was noted in 279 (57.8%) patients. History of general arteriosclerosis (stroke, angina or intermittent claudication) was found in 38 (7.9%) patients, while evidence for vasospasm, migraine and/or Raynaud's phenomenon was reported for 229 (47.4%) subjects.

Baseline characteristics for all eligible eyes (n=777) (Table 3.6)

	n (%)	Mean ± SD Median (IQR)
Eyes enrolled of a patient: Both eyes Right eye only Left eye only	 265 117 130	
Refractive error (D): < -1 -1 to 1 > 1	 254 (32.7%) 333 (42.9%) 190 (24.4%)	
Best-corrected visual acuity: <0.5 0.5 to 0.66 0.67 to 0.9 ≥1.0 Unknown	 1 (0.1%) 18 (2.3%) 238 (30.7%) 517 (66.5%) 3 (0.4%)	1 (0.67 to 1.2)
Axial length (mm)		24.1 ± 1.3
SAP MD (dB): All eyes Better eye Worse eye		-2.9 (-1.6 to -4.8) -2.0 (-1.2 to -3.3) -3.5 (-2.1 to -5.9)
GAT IOP (mmHg)*: <15 15-19 20-24 25-29 ≥30	 102 (13.1%) 334 (43.0%) 240 (30.9%) 88 (11.3%) 13 (1.7%)	19.5 ± 4.5
Any iridotrabecular contact	74 (9.5%)	
Van Herick grade: 0-5% ≥ 5% ≥15%	 0 (0%) 2 (0.3%) 23 (2.9%)	

≥25%	166 (21.4%)	
≥40%	578 (74.4%)	
Unknown	8 (1%)	
Trabecular pigmentation grade:		
0-1	607 (78.1%)	
2	142 (18.3%)	
3	22 (2.8%)	
Unknown	6 (0.8%)	
Any peripheral anterior synechiae	5 (0.6%)	
Krukenberg spindle:		
0	760 (97.8%)	
1	9 (1.2%)	
2	4 (0.5%)	
3	3 (0.4%)	
4	0 (0%)	
Unknown	1 (0.1%)	
Posterior embryotoxon (quadrants):		
0	763 (98.2%)	
1	10 (1.3%)	
2	1 (0.1%)	
3	1 (0.1%)	
4	0 (0%)	
Unknown	2 (0.3%)	
Iris colour:		
Blue	363 (46.7%)	
Blue/green	65 (8.4%)	
Green	29 (3.7%)	
Hazel	114 (14.7%)	
Light brown	116 (14.9%)	
Dark brown	86 (11.1%)	
Unknown	4 (0.5%)	
Transillumination – mid-peripheral	16 (2.1%)	
Transillumination – sphincter	6 (0.8%)	
Iris thickness:		
Thick	34 (4.4%)	
Normal	702 (90.4%)	
Hypoplastic	40 (5.1%)	
Unknown	1 (0.1%)	
Pseudoexfoliation:		
0	760 (97.8%)	
1	3 (0.4%)	
2	1 (0.1%)	
Unknown	13 (1.7%)	
LOCS lens grading:		
N>1	19 (2.4%)	
C>2	1 (0.1%)	
P>1	0 (0%)	

Table 3.6: Baseline clinical characteristics for all eligible eyes (n=777) in enrolled patients (D: dioptres, SAP: standard automated perimetry, GAT: Goldmann applanation tonometry, LOCS: Lens Opacities Classification System,

N: nuclear, C: cortical, P: posterior subcapsular). *27.4% of the participants had IOP>21mmHg at baseline.

The number of right and left eyes meeting the study eligibility criteria at baseline was almost equal, while both eyes met eligibility criteria in over two thirds (68.2%) of subjects. Approximately a third of the eligible eyes (32.7%) had a myopic refractive error [SE<-1D] and about a quarter (24.4%) were hypermetropic (SE>1D). The vast majority of patients (97.2%) had a best-corrected visual acuity (BCVA) of 0.67 or better. The mean (±SD) axial length was 24.1±1.3mm.

Two baseline VFs were performed in each eye at visit 1 (first post-allocation visit). Amongst the UKGTS eligible eyes, the median (IQR) for the mean MD (average of the two baseline visual fields for each eye) of the better and worse eyes was -2.0dB (-1.2 to -3.3) and -3.5dB (-2.1 to -5.9), respectively. The median (IQR) for the mean MD of all eligible eyes was -2.9dB (-1.6 to -4.8). In the case of the right eyes, the mean difference (95% CI) between the two baseline VFs was 0.16dB (0.04, 0.28), with the first VF being slightly more sensitive than the second. In the left eyes, which were tested after the right eyes, this difference was slightly larger at 0.31dB (0.20, 0.42). The baseline VFs comprised 874 eyes (90.5%) with VFs taken on the same day and 92 eyes (9.5%) with the second VF taken on a subsequent occasion, because the second field at the baseline visit was excluded by the perimeter software because of learning effects. Of the baseline VFs, the first had only slightly higher sensitivity than the second in the right eye, suggesting that any learning and fatigue effects, in patients with the level of experience represented in this cohort, are evenly balanced. The difference was slightly larger in the LE, which was tested after the RE, suggesting a small fatigue effect. The perimeter

software removed some VFs considered to show learning, likely contributing to an impression of a slight overall fatigue effect. The good agreement found between the first and second VFs suggests that performing duplicate VFs on the same day is probably compatible with clinical practice.

The mean (±SD) GAT IOP for all eligible eyes was 19.5±4.5 mmHg. The baseline GAT IOP distribution in all eligible eyes is shown in Figure 3.3. 87% of eligible eyes had a baseline IOP of less than 25mmHg and 56.1% of less than 20mmHg.

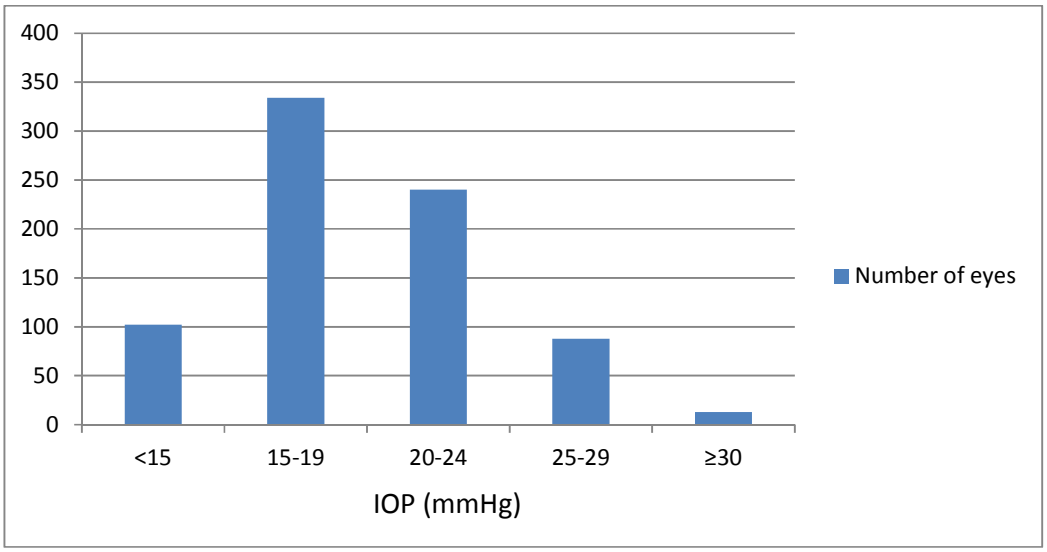

Fig 3.3: Baseline intraocular pressure distribution in all eligible eyes (n=777).

Any iridotrabecular contact was noted in almost a tenth of all eligible eyes (9.5%), while peripheral anterior synechiae (0.6%) and a posterior embryotoxon of any grade (1.5%) were rare in our cohort. The vast majority of cases had 'wide' open angles, with only 3.3% having a Van Herick grade of less than 25%. Significant trabecular pigmentation was uncommon (2.8%), with the majority of eligible eyes (78.1%) having either no, or very mild, pigmentation. Similarly, a Krukenberg spindle of any grade and mid-peripheral iris transillumination were found in only 2.1% of the UKGTS eligible eyes. The most common iris colour was blue (46.7%), followed by light brown (15.0%) and

hazel (14.7%). Eligible eyes with any degree of pseudoexfoliation (0.5%) and iris sphincter transillumination (0.8%) were very rare in this UK cohort. Protocol violations were noted in one eye with BCVA worse than 0.5, in one eye with baseline MD<-16dB, and in 19 eyes with nuclear cataract (N)>1 and one eye with cortical cataract (C)>2.

Better versus worse MD eyes

	Better MD (n = 516)		Worse MD (n = 516)	
	n (%)	Mean ± SD	n (%)	Mean ± SD
Number of right eyes	312 (60.5%)		204 (39.5%)	
Axial length		24.07 ± 1.26		24.11 ± 1.29
*GAT IOP (mmHg):		18.9 ± 4.1		19.9 ± 4.7
<15	80 (15.5%)		65 (12.6%)	
15-19	228 (44.2%)		209 (40.5%)	
20-24	166 (32.2%)		163 (31.6%)	
25-29	41 (7.9%)		66 (12.8%)	
≥30	1 (0.2%)		13 (2.5%)	
CCT (µm)		542 ± 34		541 ± 34
PXF present	3 (0.6%)		2 (0.4%)	

Table 3.7: Baseline characteristics of the better MD versus worse MD eyes in the UKGTS (GAT: Goldmann applanation tonometry, CCT: Central corneal thickness, PXF: Pseudoexfoliation).

The baseline characteristics of the better MD versus worse MD (n=516) eyes in the UKGTS are presented in Table 3.7. Right eyes were more likely to have a better MD at baseline (60.5%) ($p<0.0001$). The mean IOP (±SD) at baseline was lower in the better (18.9±4.1mmHg) than the worse (19.9±4.7mmHg) MD

eyes (p=0.0053). More than half of both the better (59.7%) and worse MD (53.1%) eyes presented with an IOP of less than 20mmHg at baseline. Axial length and central corneal thickness (CCT) were very similar between the better and worse MD eyes, while pseudoexfoliation (PXF) was very rare in both groups.

Discussion

The primary source of referrals in the UKGTS was community optometrists (88%). This is in contrast with the EMGT where the majority of subjects (85%) were recruited by actively screening 70% of the local population fulfilling the age criteria for eligibility. Recruitment from clinical centres (6.6%) and practitioners (8.6%) in the EMGT represented the minority of cases, similarly to the UKGTS, where only 8% of the study patients were referred from the hospital and 3% from their GP.

More than half of the UKGTS patients had both eyes eligible, unlike the EMGT where only 24% of cases were bilateral. A refractive error more myopic than -1D at baseline was found in 32.7% of our cohort and was more common that in the EMGT (13%). Hypermetropia of more than 1D was over-represented in the EMGT cohort (57%), as compared to the UKGTS (24.4%). As expected for a clinical trial recruiting newly diagnosed OAG cases, and given the eligibility criteria, the BCVA was equal or better than 0.67 in the majority of our cohort (97.2%), similarly to the EMGT (99%). The mean axial length in the UKGTS (24.1±1.3mm) was slightly longer than the average reported for a British population in the EPIC-Norfolk study (23.8mm males, 23.3mm females) (Foster et al 2010), thus reflecting the higher percentage of axial myopia in our cohort.

A possible explanation for the difference is the referral source (optometry), with myopes being more used to visiting optometry for refractive error correction than emmetropes or low hypermetropes, who may be more likely to buy off-the-shelf reading glasses.

The median (IQR) MD for all UKGTS eligible eyes was -2.9dB (-1.6 to -4.8), and represents earlier disease than in the EMGT (MD of -4.7 dB) and the CIGTS (MD of -5.5dB) (Gillespie et al 2003) cohorts, while the AGIS (MD of -10.5dB) (AGIS 1998) and CNTGS (MD of -8dB) (CNTGS 1998) included subjects with more advanced glaucomatous damage at baseline. The IOP distribution in the UKGTS showed that 86.9% of eligible eyes had a baseline IOP<25mmHg, which is in line with the EMGT (80%). The mean IOP (±SD) at baseline was 19.5±4.5mmHg, a little lower than in the EMGT (20.7±4.1mmHg). As expected, the UKGTS mean IOP was higher than the one recorded at baseline in studies focusing on normal tension glaucoma, such as the CNTGS (16.1±2.3mmHg for the control and 16.9±2.1mmHg for the treated group). The early stage of the glaucoma and relatively low IOP at diagnosis suggests remarkably sensitive case-finding by community optometrists in the UK.

The vast majority of eligible eyes had wide open angles (≥40%) on Van Herick grading (74.4%), similarly to the EMGT (82%). Significant trabecular pigmentation was relatively uncommon, both in our cohort (2.8%) and in the EMGT (6%). Pseudoexfoliation was extremely rare in our cohort (0.5%), unlike the EMGT or the CIGTS, where it was noted in 8% of eligible eyes and 4.8% of enrolled patients, respectively. However, unlike the EMGT and the other major glaucoma clinical trials, the UKGTS is the first to report detailed baseline phenotypic data, to include the Krukenberg spindle grade, embryotoxon grade,

presence of any iridotrabecular contact, and iris thickness, colour and transillumination.

The mean age of the participants was 66 years and was almost identical with the mean age of participants in the CNTGS (CNTGS 1998) and very similar with the EMGT mean age of 68.1 years (Leske et al 1999). Both genders were almost equally represented in our cohort, as opposed to the EMGT where participants were predominantly female (66%). Family history of glaucoma was relatively common in our study, with almost one third of the participants reporting a first degree relative with the disease. This was almost identical with the family history rate reported in the CIGTS (Musch et al 1999) but higher than the EMGT (Leske et al 1999), where a positive family history was noted in only one fifth of the participants. With regards to education, almost half of the UKGTS participants did not pursue education beyond the age of 16, while in the AGIS almost three quarters (71.3%) of the subjects had not been to any college or graduate school. The vast majority in our cohort was white, similar to the Swedish cohort described in the EMGT. Unlike the CIGTS and AGIS (AGIS 1994), where a substantial proportion of the study groups (38% and 56%, respectively) were black, only 5.2% of the UKGTS participants were black, the second most common ethnicity in our cohort.

Hypertension (defined as in the EMGT to allow for comparisons) at baseline was more common in our cohort (57.8%) than in the EMGT (38%) and the AGIS (50%). The mean systolic and diastolic blood pressures in the UKGTS (136±20 and 81±11mmHg, respectively) were lower as compared to the EMGT (148.0±18.8 and 85.7±10.3mmHg, respectively). This is likely explained by the fact that more than a third of our participants were on antihypertensive medications, as compared to only 24% in the EMGT, while the nowadays

widely prescribed statins were taken by more than a quarter of the UKGTS patients. The median body mass index (BMI) was 26.9 in our cohort, suggesting that the majority of patients were overweight (BMI>25), in line with the latest Health Survey for England (HSE), showing that in 2009, 61.3% of adults in England were overweight. Similarly to the BMI results, the waist circumference, thought to assess the proportion of body fat located intra-abdominally, as opposed to subcutaneously, and to better reflect cardiovascular risk (Lean et al 1995), was also found to be higher in the UKGTS cohort (median 98cm), as compared to the recommended limits (<94 for men and <80cm for women). The median waist-hip ratio (WHR), considered a more efficient predictor of mortality in older people than waist circumference or BMI (Price et al 2006), was 0.91 in our cohort, suggesting that the majority of UKGTS patients has abdominal obesity (defined as a WHR >0.90 for males and >0.85 for females by the World Health Organisation) (WHO 2008).

History of myocardial infarction was similar in the UKGTS (5.4%) and EMGT (6%) cohorts, while diabetes mellitus was more frequent in the UKGTS (10.5%) than in the EMGT (4%) cohort, but less frequent when compared to the AGIS (20%). Obstructive pulmonary disease was also more frequent in our study population (8%) as compared to the EMGT (1%). General arteriosclerosis (defined more broadly than in the EMGT to include stroke, angina and/or intermittent claudication) was noted in more patients (7.9%) in the UKGTS than in the EMGT (5%). Moreover, almost half of our participants reported a history suggestive of peripheral vasospasm, migraine and/or Raynaud's, while these conditions were only encountered in 19% of cases in the EMGT. In the UKGTS, recognised standardised protocols were used to elicit a history of these conditions, such as the Rose questionnaire for angina and intermittent claudication (Rose et al 1977), the International Headache Society diagnostic

criteria for migraine (IHS 1988) and protocols derived from well established definitions for vasospasm and Raynaud's (Flammer et al 2001). Concomitant neurological disease was reported in 12.6% of the UKGTS cohort, which is higher than that reported in the literature for the UK population (6%) (MacDonald et al 2000).

Left eyes were slightly more likely to be associated with a worse MD at baseline in our cohort, in line with a retrospective cross-sectional study in NTG that found the left eye 2.1 times more likely to present a greater field defect than the right eye (Poinoosawmy et al 1998). In contrast, in high tension glaucoma right and left eyes had an equal chance of being the side of more advanced field damage (Poinoosawmy et al 1998). The mean IOP at baseline was 1mmHg lower in the better (18.9±4.1mmHg) as compared to the worse (19.9±4.7mmHg) MD eyes, as expected by the link between raised IOP and glaucoma, although other studies have suggested only poor correlation between IOP and VF damage (Greenfield et al 2007, Orgul et al 1994b). Just over half of both the better and worse MD eyes demonstrated an IOP of less than 20mmHg at baseline, largely in line with the EMGT where 46% of eligible eyes fell below this same IOP threshold. The mean CCT in our cohort was consistent with the mean CCT reported in epidemiological studies (Wolfs et al 1997) and meta-analyses (Doughty et al 2000).

In summary, the UKGTS is the first randomised, placebo-controlled trial to evaluate the efficacy of medical treatment in reducing VF deterioration in OAG. The outcome will provide evidence for the efficacy of the most widely prescribed class of IOP-reducing medication (prostaglandin analogues) in preserving the visual field in patients with glaucoma; it will also allow the quantification of risk factors for deterioration, enabling more precise risk

profiling of patients and the development of patient management protocols. Some groups of patients were under-represented in our cohort, such as those with high IOP (>30mmHg) or pseudoexfoliation, and black subjects. However, the study will provide useful information on the effectiveness of IOP-lowering treatment in the majority of patients with OAG.

3.4 Time to confirmed VF deterioration in the UKGTS

In January 2011, the Data and Safety Monitoring Committee (DSMC) requested an interim analysis. This revealed a significant difference between treatment arms and the DSMC requested that the trial be terminated. Patients were scheduled for exit visits over the following 6 months.

Survival analysis showed a statistically significant difference in the time from baseline to the event of confirmed VF progression between the two groups over 24 months following entry to the trial (p=0.001). The adjusted Hazard Ratio by site was 0.48 (95% CI 0.31, 0.74) (Fig 3.4). A statistically significant difference in the time from baseline to the event of confirmed VF progression was also noted at 18 months (p=0.049).

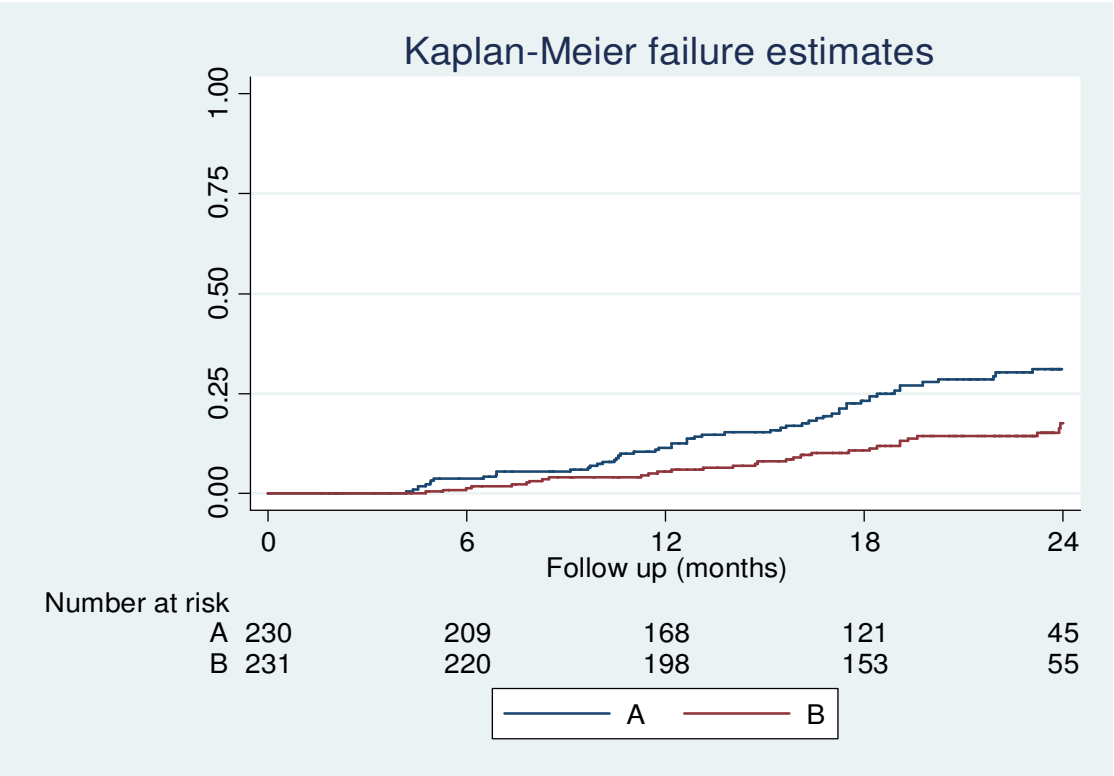

Fig 3.4: Kaplan-Meier curve showing the time from baseline to the event of confirmed VF progression for the placebo (A) and latanoprost (B) groups.

Out of 516 patients, 55 were excluded from the survival analysis (28 from the placebo and 27 from the latanoprost group), due to insufficient data to obtain an endpoint. In more detail, amongst the 55 patients, 32 did not attend the 1st post treatment allocation visit (visit 1) and 23 only attended visit 1, but no further visits.

As shown in Table 3.8 below, only 7 patients showed a possible or established reaction to a study drug for which they had to be withdrawn from the study. No serious adverse events definitely related to the study intervention were noted. 2 cases of life-threatening events were reported and included an asthma attack and a suspected stroke.

Reasons	(n = 127) n (%)
Adverse reaction to study drug (possible or established)	7 (5.5%)
Ill health	32 (25.2%)
Death	7 (5.5%)
Ocular co-morbidity*	11 (8.7%)
Other	70 (55.1%)

Table 3.8: Reasons for loss to follow-up in the UKGTS (*includes cataract, angle closure or uveitis).

3.5 IOP as a risk factor for glaucoma progression

3.5.1 The effect of treatment on IOP

The IOP change from the pre-allocation visit to the first visit post-allocation is shown in Table 3.9 below.

	Placebo (A)	Latanoprost (B)
IOP before allocated treatment	19.4 ± 4.7	19.0 ± 4.6
IOP at 1st visit post-allocation	18.8 ± 5.2	14.5 ± 3.3

Table 3.9: IOP (±SD) in mmHg before and at the 1st visit after treatment in Groups A and B.

3.5.2 Is average IOP (as measured by GAT, DCT and ORA) associated with the rate of glaucoma progression?

In the EMGT, the mean GAT IOP during the follow-up period was positively associated with the risk for progression, with an average 12% increase with every mmHg of mean IOP higher (HR 1.12, 95% CI 1.07–1.16, p<0.0001) (Leske et al 2007). Also, mean GAT IOP was a significant predictor of progression in both the higher (≥21mmHg) and lower baseline IOP groups, indicating very clearly the relevance of follow-up IOP in patient management, regardless of the IOP levels at baseline. CCT was another significant predictor for progression in the EMGT, with an average 25% increase with every 40µm reduction in CCT (HR: 1.25, 95% CI 1.01–1.55, p=0.0422). However, CCT was not evaluated in the EMGT as an independent risk factor and was only highlighted as a significant predictor, when controlling for the effects of mean follow-up GAT IOP. Unlike previous large clinical trials in glaucoma, in the UKGTS IOP data were collected at each visit by three devices: GAT (2 measurements per visit within 1mmHg), DCT (3 measurements per visit), and ORA (IOPcc and IOPg; 3 measurements per visit). Additional GAT IOP measurements were available for visits 1 and 8 (phasing visits), where 10 measurements were performed; two at each of the following time points: 9am, 11am, 12pm (midday), 2pm and 4pm. Also, data were collected on CCT (3 measurements at visit 1), and ORA CH and CRF (3 measurements per visit).

The purpose of this analysis was 1) to assess the association between median GAT IOP over the follow-up period and the rate of progression (change in MD over time) for each participant and whether including covariates CCT or CH in the GAT IOP model improves prediction and 2) to evaluate which IOP model (GAT, DCT, IOPcc, IOPg) better predicts glaucoma progression and to what

extent the inclusion of covariates in each of the above models (CCT, CRF, CH and AL) improves prediction. Only DCT values with a quality score of 1 or 2 were included in the analysis and only participants with VF data available over at least 5 clinic visits (n=379) were considered, to provide a more precise measure of visual field progression rate.

The Pearson's R of MD slope against median GAT IOP across all the UKGTS sites was 0.250 ($p<0.001$), suggesting that the GAT IOP measurement was significantly, but weakly, correlated with visual field progression (AIC=1337.0, Akaike weight=0.48) (Fig 3.5).

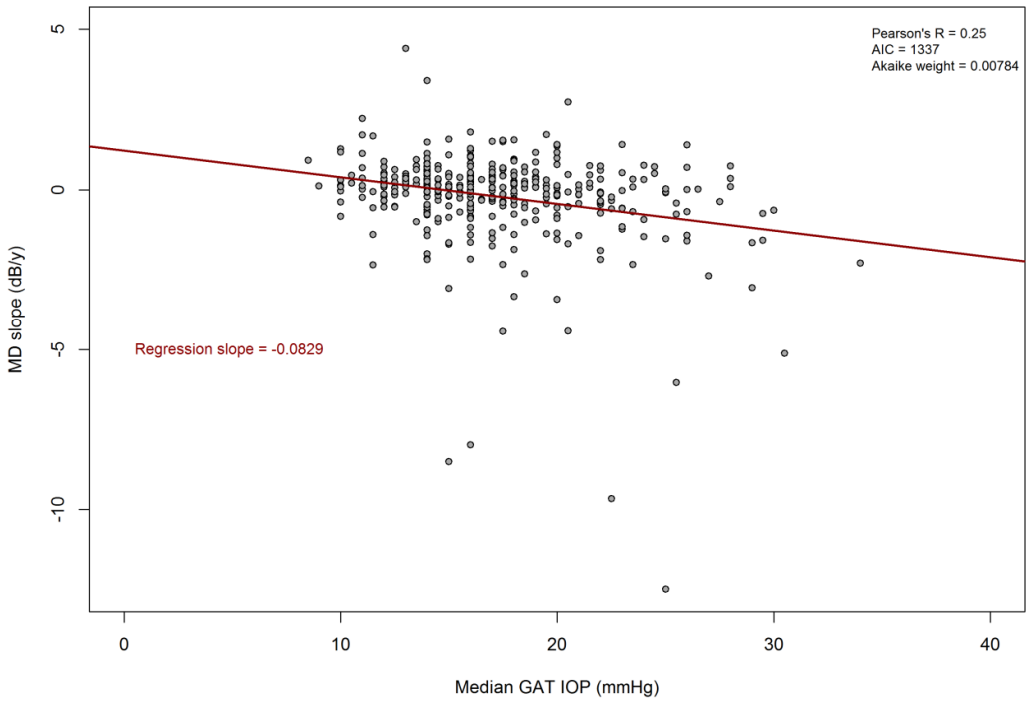

Fig 3.5: Graph showing the median GAT IOP across all visits against the MD slope for each participant (n=379) for all the UKGTS sites.

In line with the EMGT analysis for CCT, when CCT was included in the model with GAT IOP to predict the MD slope, the AIC value was found to be

marginally lower (AIC=1336.8) and the Akaike weight marginally higher (Akaike weight=0.52), suggesting that the addition of CCT slightly improves the GAT prediction model. However, although GAT IOP remained a significant predictor of progression in the GAT+CCT model, the CCT was not (P = 0.137). To test the hypothesis that CCT is an independent predictor of progression, the MD slope was plotted against CCT across all the UKGTS sites. CCT was not correlated to the MD slope (R = 0.02) and was not a significant predictor of progression (AIC=1361.4, Akaike weight ~0) (Fig 3.6). In light of this finding, it could be argued that the benefit gained by including CCT in the GAT IOP model most likely arises from the reduction in the GAT measurement error associated with CCT, rather than any genuine association between CCT and glaucoma progression.

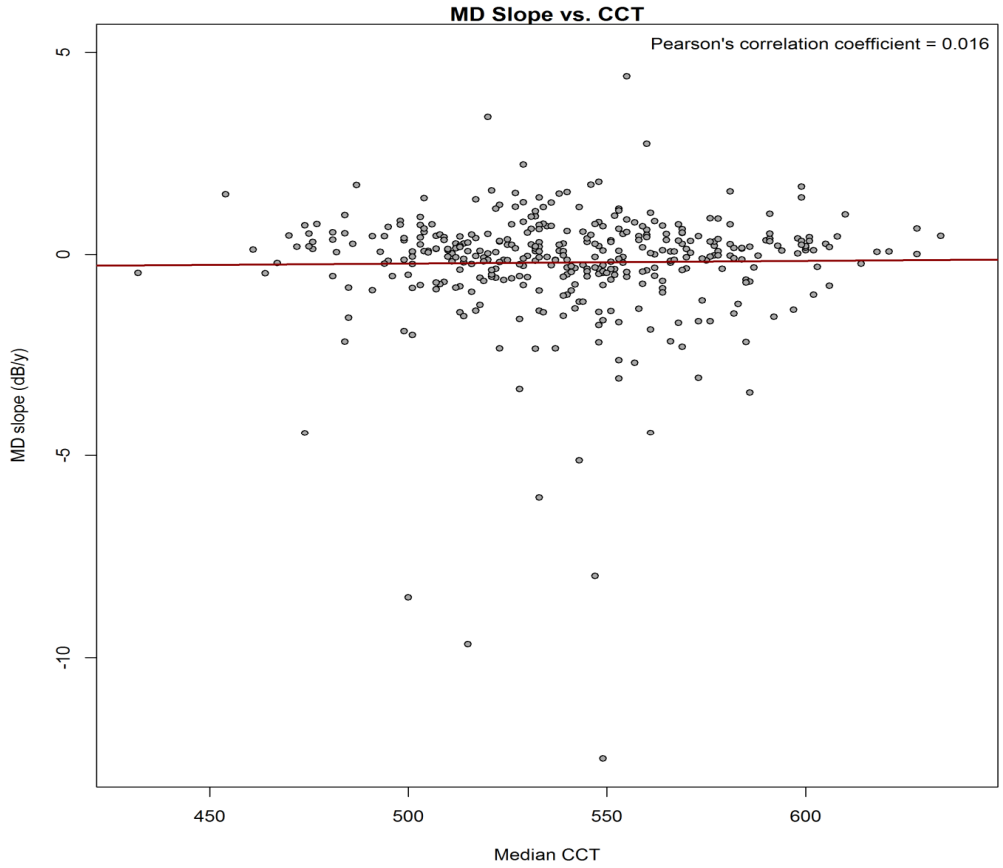

Fig 3.6: Graph showing the median CCT across all visits against the MD slope for each participant (n=379) for all the UKGTS sites.

During the second stage of the analysis, the different IOP models (GAT, DCT, IOPcc, IOPg) were compared in their ability to predict glaucoma progression. The Pearson's R of MD slope against GAT, DCT, IOPcc and IOPg across all the UKGTS sites, was 0.250, 0.199, 0.276 and 0.239, respectively ($p<0.001$ in all cases), suggesting that the IOP measurements by all devices were significantly correlated with visual field progression (Fig 3.7).

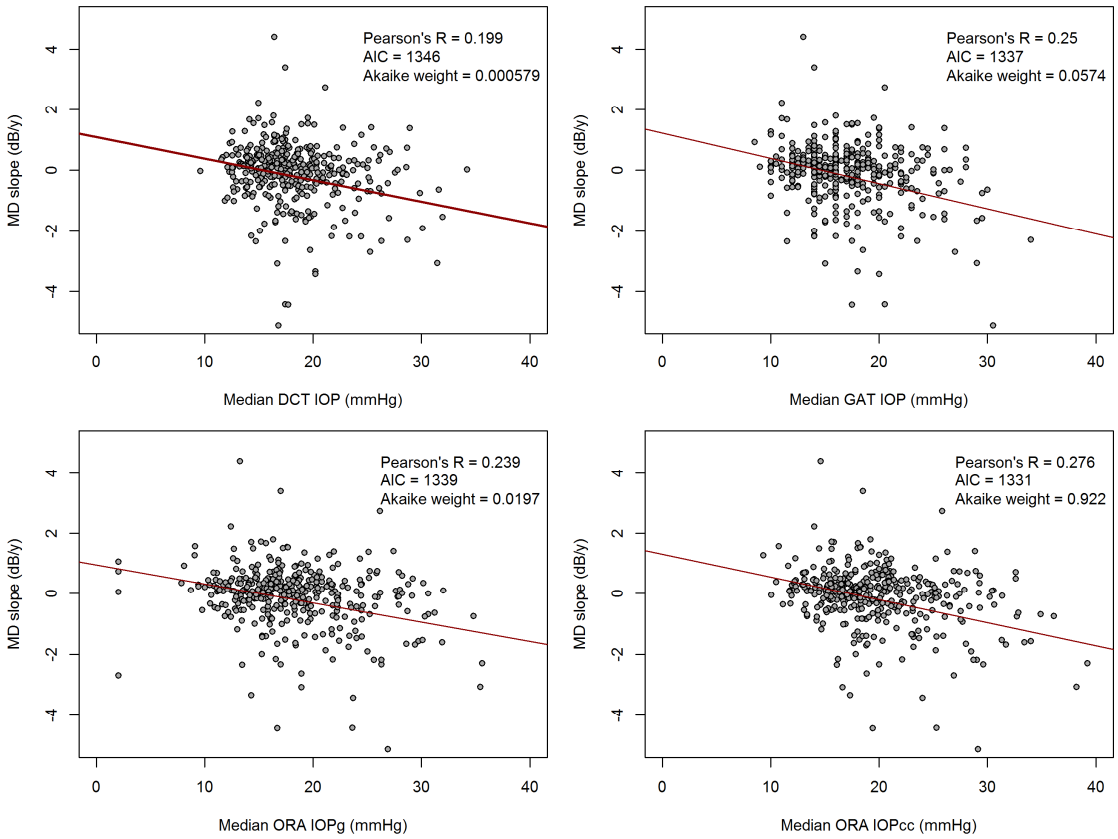

Fig 3.7: Graph showing the median IOP (GAT, DCT, IOPcc, IOPg) across all visits against the MD slope for each participant (n=379) for all the UKGTS sites.

As expected, and similarly to GAT IOP, the correlation was negative in all cases, showing that an increase in median IOP is associated with a more negative MD slope, suggesting faster VF progression. The correlation was significant, but weak, for all the IOP measures tested, with IOPcc having the highest correlation, as compared to GAT, DCT and IOPg.

The AIC value for each model was used to compare models, where the outcome variable was MD slope and the predictor variable was median follow-up IOP, as measured by GAT, DCT and ORA. The AIC values for the GAT, DCT, IOPcc and IOPg models were similar: 1337, 1346, 1331 and 1339, respectively. The lowest AIC value was for IOPcc, suggesting that less information is lost when the IOPcc model is used to predict VF progression. The Akaike weights

for the GAT, DCT, IOPcc and IOPg models were 0.0574, 0.000579, 0.922 and 0.0197, respectively, suggesting that the IOPcc model has a 92.2% probability of being the 'best' model.

When data were analysed for each site separately, IOPcc was not the most likely model for most of these sites, with sites A1, B2, F6 and G7 having DCT as the preferred model, and sites D4, E5, H8 and M12 having GAT as the preferred model (Table 3.10).

Site	Number of patients	GAT	DCT	IOPcc	IOPg
A1	71	0.230	**0.455**	0.237	0.078
B2	29	0.232	**0.303**	0.231	0.233
C3	78	0.230	0.144	**0.343**	0.283
D4	45	**0.965**	0.003	0.018	0.015
E5	21	**0.435**	0.111	0.384	0.070
F6	10	0.160	**0.551**	0.150	0.139
G7	24	0.117	**0.467**	0.093	0.324
H8	78	**0.555**	0.040	0.148	0.257
J9	16	0.247	0.226	**0.281**	0.246
M12	7	**0.268**	0.245	0.266	0.221

Table 3.10: Akaike weights for each IOP model (GAT, DCT, IOPcc, IOPg) per site with the model having the largest Akaike weight being highlighted in bold.

An example of a site where DCT was the preferred model is shown below (Fig 3.8).

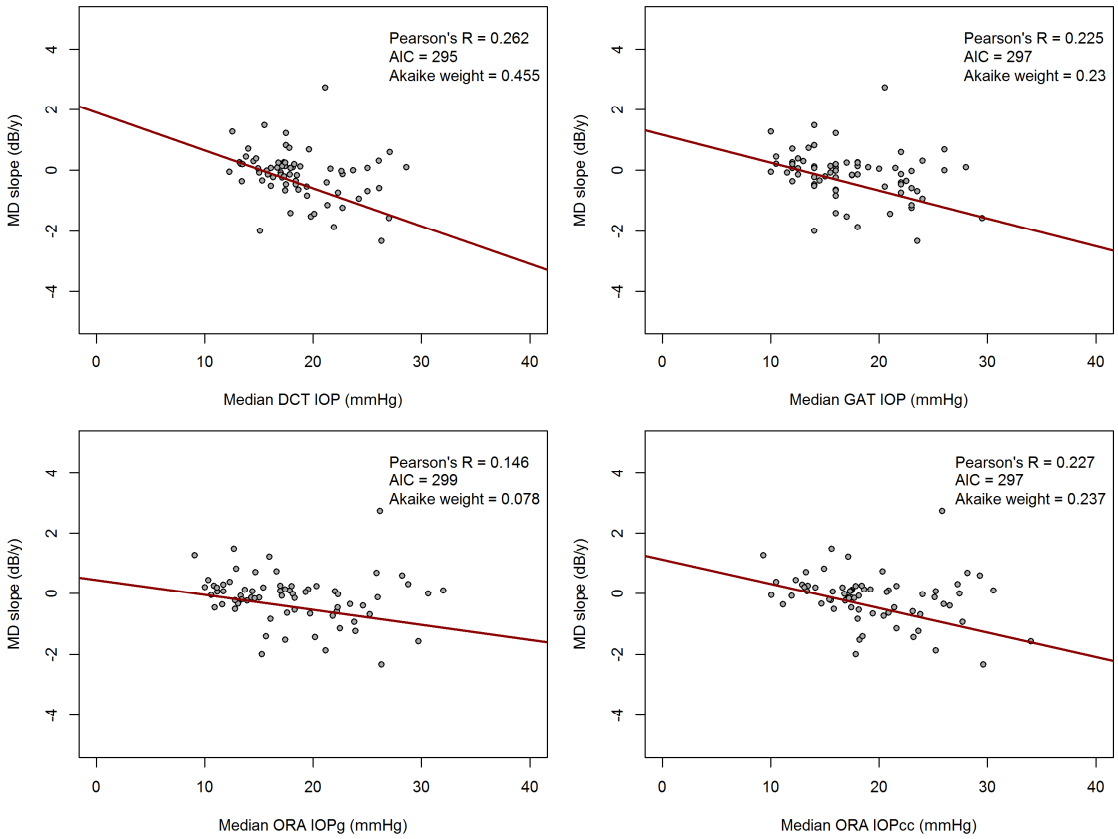

Fig 3.8: Graph showing the median IOP (GAT, DCT, IOPcc, IOPg) across all visits against the MD slope for each participant (n=71) for site A1 (Moorfields).

However, across all sites, IOPcc was by far the most likely model, according to the Akaike weights. This may be explained by the observation that the relationship between IOPcc and the MD slope was much more consistent across sites (data not shown). These results suggest there may be differences between sites in the way DCT and GAT were operated (eg calibration issues), while ORA IOPcc may be less operator-dependent. In addition, the two GAT IOP measurements recorded per visit were required by the Standard Operating Procedures to be within 1mmHg. This may have increased the precision of this measurement, which may in turn have increased the strength of the correlation between GAT IOP and the MD slope relative to DCT and ORA. No such requirement applied to the DCT or ORA measurements.

In the third stage of the analysis, each of the aforementioned linear models (GAT, DCT, IOPcc, IOPg) was re-examined, with CCT, CH, CRF and AL included as covariates, and a backward stepwise AIC approach was employed to remove non-significant predictors of VF progression. In the case of the GAT linear model, when CCT, CH, CRF and AL were included as covariates, this model reduced to GAT IOP and CH as significant predictors (AIC=1331.0), suggesting that CCT, CRF and AL added no additional information regarding progression rate. For the DCT model, the model reduced to CRF and CH only (AIC=1337.3), suggesting that CCT, DCT IOP and AL were non-significant predictors when CRF and CH were available. In the case of the IOPcc model, this reduced to only IOPcc, suggesting that all the other parameters were non-significant predictors in the presence of IOPcc, thus reinforcing the idea that corneal parameters have been taken into account in the IOPcc measurement (AIC=1331.4). In the case of IOPg, the model reduced to IOPg, CH and CRF (AIC=1333.6). The AIC value for the GAT IOP-CH model was smaller than any other model, but only marginally less than the IOPcc model. However, it is generally accepted that the most robust model is the one that provides an adequate account of the data while using a minimum number of parameters (Myung et al 2000). Considering this trade-off between descriptive accuracy and parsimony, it could be argued that the model with IOPcc as the only predictor remains the preferred model of progression.

In the UKGTS, the IOPcc, a measurement where metrics of corneal biomechanics are adopted in the IOP calculation, was the best predictor of progression across all sites. This may be the case, either because it provides a more accurate or consistent measure of IOP or because it may better reflect ocular susceptibility to IOP, to the extent that susceptibility is influenced by the material properties of the eye and reflected in the corneal biomechanics.

Moreover, IOPcc appears to be less dependent on the operator, as shown by the relatively consistent relationship between IOP and progression rate across sites.

In controlled experiments, DCT IOP has been shown to be the most accurate and precise IOP measurement, displaying the best repeatability and reproducibility (Kotecha et al 2010) and to have the lowest association with CCT (Boehm et al 2008). This is due to the use of a curved contact surface, which the contour of the cornea matches during measurement. The effects of capillary forces, corneal rigidity and thickness are reduced during contact matching. These beneficial properties of DCT are only apparent at some sites when sites are considered individually, suggesting possible differences in calibration and/or operation across the UKGTS sites. Also, upon the inclusion of covariates (CCT, CH, CRF, AL), the DCT model was reduced to only CRF and CH. This may suggest that DCT IOP provided no additional information of progression rate over and above CRF and CH. However, to reiterate, the relationship between DCT IOP and the MD slope was variable across sites, while the relationship between ORA measurements (including CH and CRF) and MD slope was more consistent, which may contribute to this finding.

That DCT IOP did not contribute to progression rate when CRF and CH were in the model may imply that 'corneal factors' are also important predictors of progression. However, the 'corneal factors' given by the ORA (CH and CRF) themselves vary with IOP (Kotecha et al 2006), so cannot be regarded as reflecting ocular material properties independently of IOP.

The reduction of the GAT model (when CCT, CH, CRF and AL were included as covariates) to GAT and CH as significant predictors, would suggest that CH provides a better model fit than CCT. This is further confirmed by directly

comparing the AIC values of the GAT IOP + CH model (AIC=1331.0) and the GAT IOP + CCT model (AIC=1336.8); the Akaike weights were 0.95 and 0.05, respectively, when these models were compared. This superiority of CH over CCT in improving the GAT model prediction may suggest that CH better reflects the GAT IOP measurement error than CCT or that CH provides an additional measure of IOP susceptibility. To explore this further, GAT IOP + CCT as predictors of DCT IOP were compared with GAT IOP + CH as predictors of DCT IOP. As DCT measurement is thought to be less influenced by corneal biomechanics, the covariate resulting in the better prediction of DCT IOP by GAT IOP may be the one which best reflects the IOP measurement error due to ocular biomechanics. The AIC for the GAT IOP + CH model (1725.6) was significantly better than the GAT IOP + CCT model (1735.3), with Akaike weights of 0.99 and 0.01, respectively. This suggests that CH was a much better predictor of the differences between GAT and DCT IOPs, thus reinforcing the idea that CH explains GAT measurement errors, rather than susceptibility to IOP. Future work will explore the association between additional covariates (CRF and AL) and both IOP and glaucoma progression. Also, the role of the diurnal IOP variation and of the DCT ocular pulse amplitude in glaucoma progression will be investigated.

3.6 Discussion

Primary outcome

The UKGTS is the first randomised, placebo-controlled trial to show the efficacy of medical IOP-lowering treatment in reducing VF deterioration in OAG.

Limitations and generalisability

The intensive testing and visit schedule contributed to a high attrition rate (almost 25%), potentially limiting the generalisability of the findings. Patient masking may have been imperfect because of the effects on IOP, eyelash growth and iris colour change, but the extent of masking at the end of the study has yet to be analysed.

Agreement between baseline VFs

In the case of the right eyes, the mean difference (95% CI) between the two VFs taken at the baseline visit was 0.16dB (0.04, 0.28), with the first VF being slightly more sensitive than the second. In the left eyes, this difference was slightly larger at 0.31dB (0.20, 0.42). The baseline VFs comprised 874 eyes (90.5%) with VFs taken on the same day, while for 92 eyes (9.5%) the second visual field was taken on a subsequent occasion, because the second field at the baseline visit was excluded by the perimeter software due to learning effects. Of the baseline VFs, the first had slightly higher sensitivity than the second in the right eye (0.16dB), suggesting that any learning and fatigue effects, in patients with the level of experience represented in this cohort, are evenly balanced. The difference was slightly larger in the LE (0.31dB), which was tested after the RE, suggesting a small fatigue effect. The perimeter software removed some VFs considered to show learning, likely contributing to an impression of a slight overall fatigue effect. The good agreement found between the first and second VFs, suggests that performing duplicate VFs on the same day is probably compatible with clinical practice.

Interpretation of trial design novelties

The UKGTS has the shortest observation period of all OAG therapeutic trials with a VF outcome to date. This was achieved simply by inflating the sample

size so that differences in the rate of incident deterioration between treatment groups could be identified at the 2-year time point, based on the outcome of the EMGT. However, the trial was designed to assess novel data analysis methods, which may further reduce the trial duration or sample size required to identify treatment effects (Chauhan et al 2008a); these design features are related to VF test frequency and interval, selected to maximise the accuracy of estimates of the VF deterioration velocity, and to the inclusion of quantitative imaging of ONH and RNFL structure. Shorter trial durations would reduce considerably the cost of drug development and would increase the likelihood of new therapies being brought to patient benefit.

Several clinical trials in OHT and OAG have included structural endpoints (Leske et al 2003), based on subjectively-identified change in stereoscopic ONH photographs. The OHTS included quantitative imaging in a subset of patients. The UKGTS is the first clinical trial in OAG to include quantitative imaging in all participants. Structural outcomes were not trial endpoints, so that treatment effects on visual function could be assessed without the censoring effect of endpoints based on structural deterioration. However, it is possible to assess whether the inclusion of structural measures as joint outcomes increases statistical power to identify treatment effects and risk factors; statistical methods have been developed to enable the modelling of joint outcomes (Harvey et al 2003) and have shown promise in the analysis of longitudinal VF and imaging data in glaucoma (Russell et al 2012). Based on the improved risk profiling, the relationship between risk and velocity of VF deterioration, and the variability of VF measurements, it is expected that protocols specifying the optimal follow-up frequency and intervals will be developed so that clinically meaningful deterioration can be identified in a timely fashion.

Chapter 4

Mitochondrial dysfunction, oxidative stress and other risk factors for glaucoma progression in a pilot study

Chapter 4: Mitochondrial dysfunction, oxidative stress and other risk factors for glaucoma progression in a pilot study

4.1 Immortalised human B- and T- lymphocyte cell lines

4.1.1 Introduction

The immortalised human B- (Raji) and T- (Jurkat) lymphocyte cell lines were used in this section as a model to test and demonstrate that the four experimental techniques described below are suitable for measuring mitochondrial dysfunction (ADP phosphorylation assay and mitochondrial membrane potential) and oxidative stress (aconitase activity and dihydroethidium staining) in lymphocytes. The lymphocyte cell lines were treated with rotenone to model mitochondrial dysfunction and paraquat to model oxidative stress, as described in the section 2.3.1. The results on the Raji and Jurkat cell lines are presented below.

4.1.2 ADP Phosphorylation Assay (complexes I, II/III and IV)

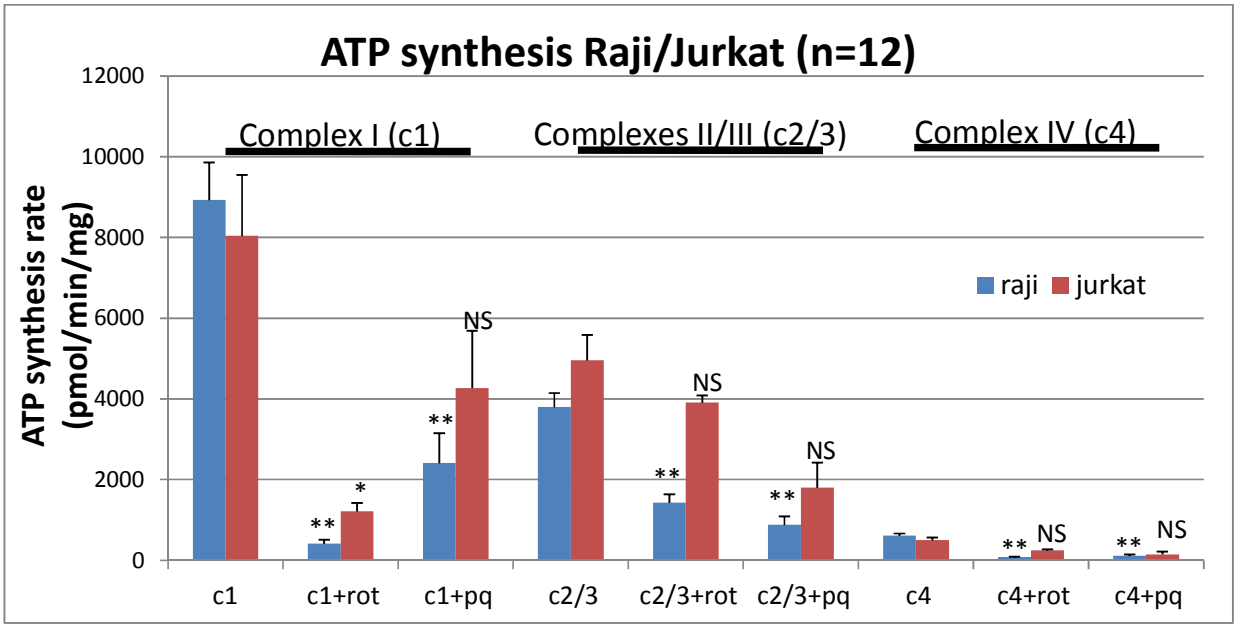

Fig 4.1: The rate of ATP synthesis by complexes I, II/III and IV in the two cell lines, with and without treatment with 0.5μM rotenone for 24 hrs and 100μM paraquat for 24 hrs. The ATP synthesis rate is expressed in pmol/min/mg lysate. Error bars represent the SEM (n=12); *p<0.05, **p<0.01, ***p<0.001, NS: not significant, c1: complex I, c2/3: complex II/III, c4: complex IV, rot: rotenone, pq: paraquat.

Complex I: A statistically significant reduction in the rate of ATP synthesis by complex I was noted in both Raji (from 8928±935 pmol/min/mg to 413±98 pmol/min/mg) and Jurkat cells (from 8043±1511 pmol/min/mg to 1210±215 pmol/min/mg) upon treatment with 0.5μM rotenone for 24hrs. A statistically significant reduction was also found after treatment with 100μM paraquat for 24hrs in the Raji cells (from 8928±935 pmol/min/mg to 2409±746 pmol/min/mg), but not in the Jurkat cells (from 8043±1511 pmol/min/mg to 4270±1425 pmol/min/mg).

Complexes II/III: Raji cells demonstrated a statistically significant reduction in the rate of ATP synthesis by complexes II/III, upon treatment with 0.5μM rotenone (from 3799±351 pmol/min/mg to 1430±213 pmol/min/mg) and 100μM pq (from 3799±351 pmol/min/mg to 881±215 pmol/min/mg) for 24 hrs. The effect on the Jurkat cells was not significant, with 0.5μM rotenone causing a reduction from 4954±637 pmol/min/mg to 3909±182 pmol/min/mg and 100μM pq from 4954±637 pmol/min/mg to 1802±624 pmol/min/mg.

Complex IV: Similarly to complexes II/III, a statistically significant reduction in the rate of ATP synthesis by complex IV was noted in the Raji cells upon treatment with 0.5μM rotenone (from 609±60 pmol/min/mg to 82±11 pmol/min/mg) and 100μM pq for 24hrs (from 609±60 pmol/min/mg to 110±43 pmol/min/mg). The effect on the Jurkat cells was not significant, with 0.5μM

rotenone causing a reduction from 502±64 pmol/min/mg to 248±32 pmol/min/mg and 100µM pq from 502±64 pmol/min/mg to 149±74 pmol/min/mg.

Discussion: Rotenone, a known complex I inhibitor (Choi et al 2011), was found to cause a statistically significant reduction in the rate of ATP synthesis by complex I in both cell lines. In the case of complexes II/III and IV, the effect of rotenone was still significant in the Raji cells, but not the Jurkat cells, suggesting that the inhibitory effect of rotenone on complex I in the Raji cells could also influence the activity of the other complexes. Paraquat significantly reduced the ADP phosphorylation rate by all complexes only in the Raji cells, but not the Jurkat cells. The effect of rotenone and paraquat on the ATP synthesis rate in all the different complexes appears greater in the Raji than in the Jurkat cells.

4.1.3 Mitochondrial Membrane Potential (steady-state TMRM staining)

Addition of 25nM TMRM caused a shift of the peak of the histogram to the right (Fig 4.2 a, b). Addition of 0.5µM rotenone over 24hrs caused a shift of the histogram to the left in the Raji cells (b, c), whereas addition of 100µM PQ over 24hrs did not cause a significant shift to the histogram peak (b, d). 10µM FCCP caused a significant shift to the left, both in the absence (b, e) and presence of rotenone (c, f) and PQ (d, g).

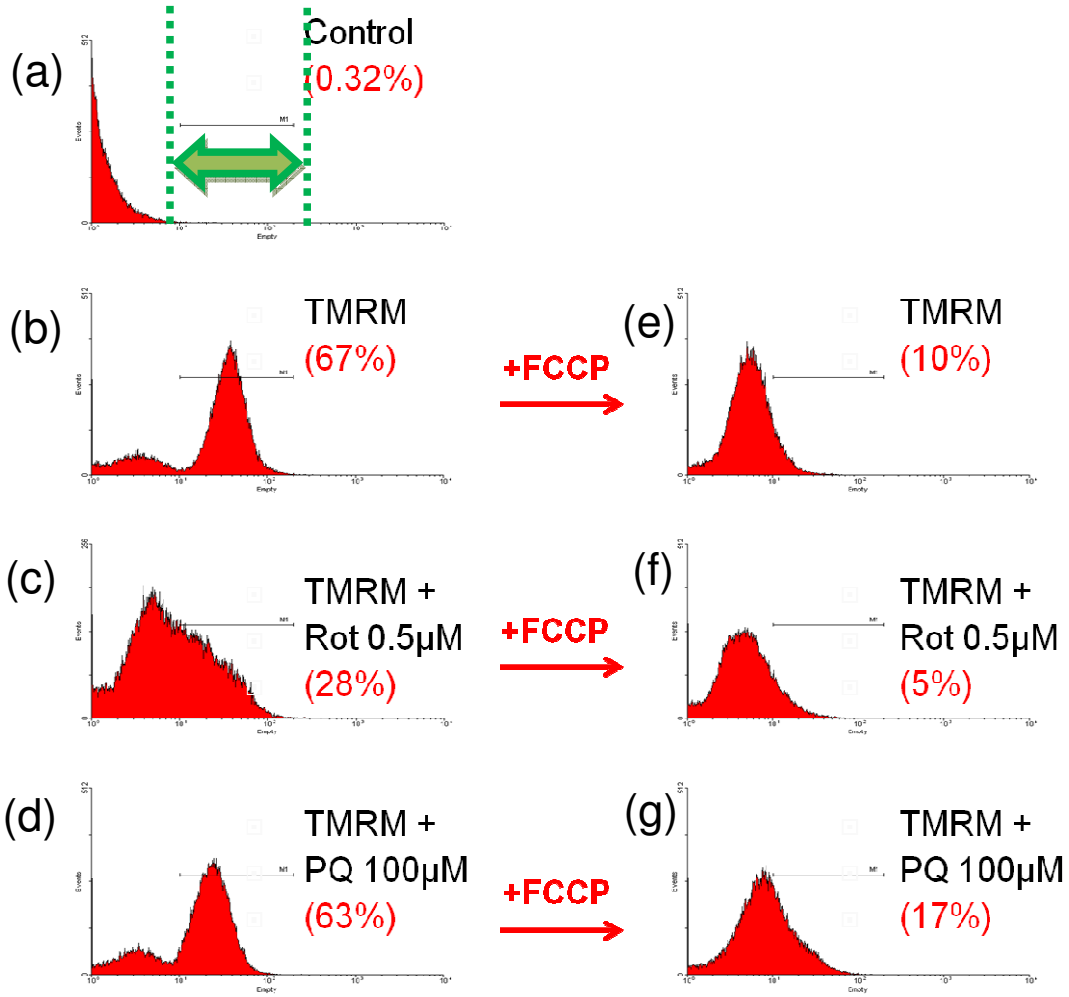

Fig 4.2: Representative histograms in the Raji cells for each of the seven experimental conditions (a-g). Values in red brackets represent the % of total events included in the gated area (green arrows in figure a). The same gate was used in all experiments.

Similarly to the Raji cells, addition of 25nM TMRM caused a shift of the peak of the histogram to the right (Fig 4.3 a, b) in the Jurkat cells. Addition of 0.5µM rotenone over 24hrs caused a shift of the histogram to the left (b, c), whereas addition of 100µM PQ over 24hrs did not cause a significant shift to the

histogram peak (b, d). 10µM FCCP caused a significant shift to the left, both in the absence (b, e) and presence of rotenone (c, f) and PQ (d, g).

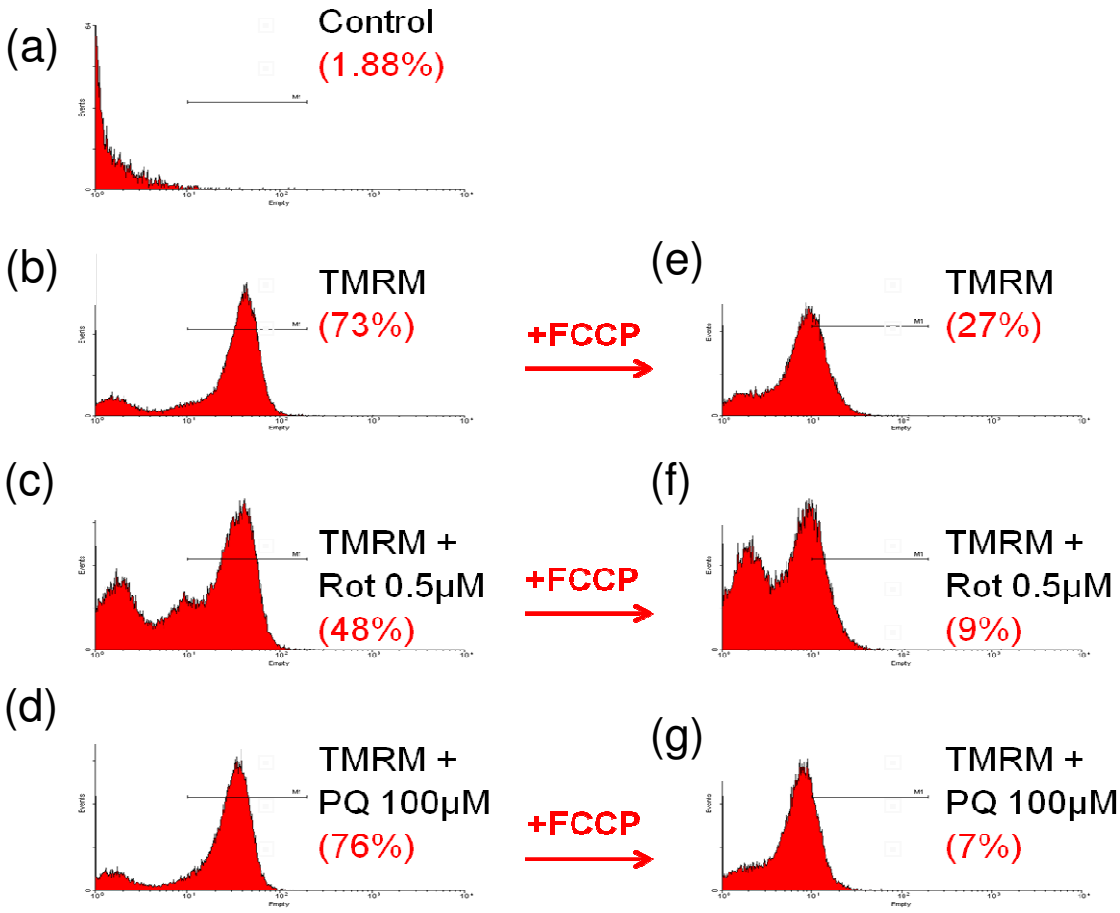

Fig 4.3: Representative histograms in the Jurkat cells for each of the seven experimental conditions (a-g). Values in red brackets represent the % of total events included in the gated area.

A statistically significant reduction in the TMRM staining was noted in the Raji (from 67±3% to 28±7%) and Jurkat cells (from 73±6% to 48±5%) upon treatment with 0.5µM rotenone for 24hrs (Fig 4.4). 100µM PQ for 24hrs had no significant effect on TMRM staining (Raji cells showed a change from 67±3% to 64±5% and Jurkat cells from 73±6% to 76±5%). The addition of uncoupler

(FCCP) caused a statistically significant reduction in TMRM staining in both cell lines (Raji cells showed a change from 67±3% to 10±4% and Jurkat cells from 73±6% to 27±11%).

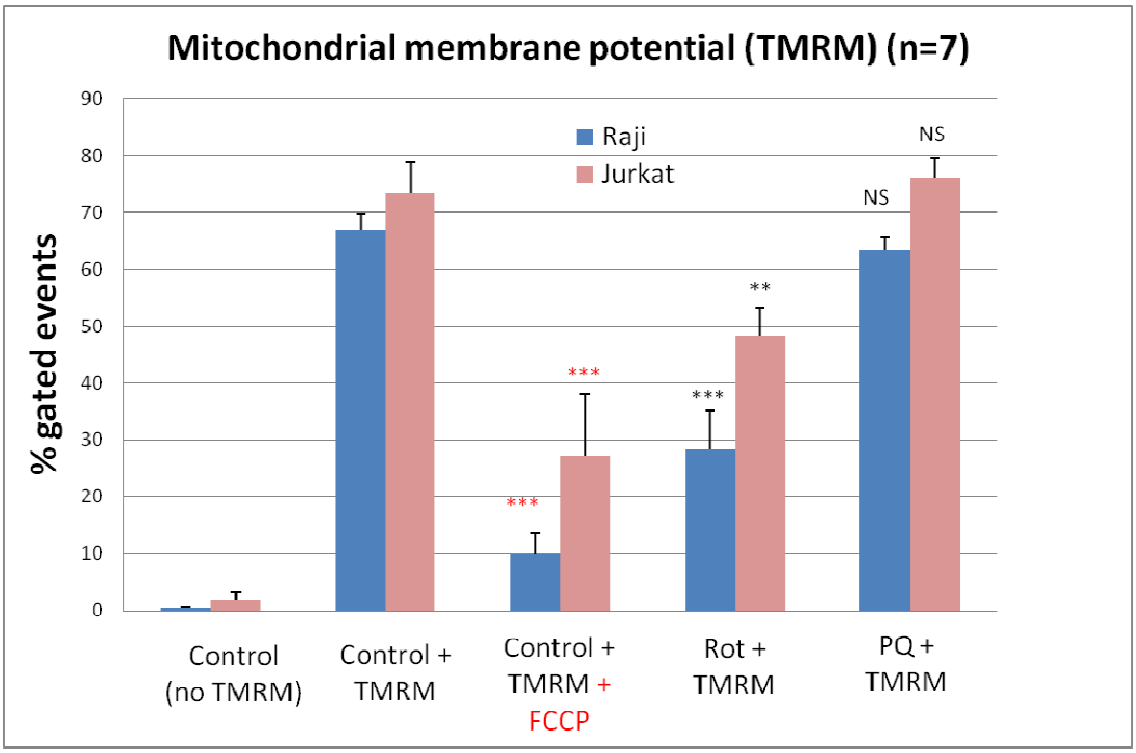

Fig 4.4: Change in the % gated events in the Raji and Jurkat cells upon treatment with 0.5µM rotenone for 24hrs and 100µM paraquat (PQ) for 24hrs, and upon treatment with FCCP (in red). Error bars represent the SEM (n=7);**p<0.01, ***p<0.001, NS: not significant.

Discussion: Flow cytometry appears to be a useful method for measuring the steady-state TMRM staining that represents the mitochondrial membrane potential in Raji and Jurkat cells. The concentration of TMRM used (25nM) was mitochondria-specific and the uncoupler FCCP acted as an effective positive control leading to the depolarisation of the mitochondria and causing the TMRM staining to dissipate. Rotenone, a known complex I inhibitor, led to a statistically significant reduction in TMRM staining in both Raji and Jurkat cells.

Paraquat did not significantly affect the TMRM staining in both cell lines. Similarly to the ADP phosphorylation assay, the Raji cells were more sensitive to rotenone and paraquat than the Jurkat cells.

4.1.4 Dihydroethidium (DHE) staining

A statistically significant increase in rate of superoxide production (as demonstrated by the increase in DHE staining) was noted in the Raji cells upon treatment with 0.5µM rotenone for 24hrs (194±20% for 10µM DHE and 185±11% for 20µM DHE in Fig 4.5 and Fig 4.6, respectively), 100µM PQ for 24 hrs (188±20% for 10µM DHE and 227±46% for 20µM DHE) and 5µM instant rotenone (229±19% for 10µM DHE and 292±28% for 20µM DHE). The Jurkat cells showed a smaller increase in the production of superoxide than the Raji cells in all three experimental conditions: rotenone 24hrs (142±15% for 10µM DHE and 141±13% for 20µM DHE), paraquat 24hrs (145±14% for 10µM DHE and 141±17% for 20µM DHE) and instant rotenone (151±18% for 10µM DHE and 179±39% for 20µM DHE).

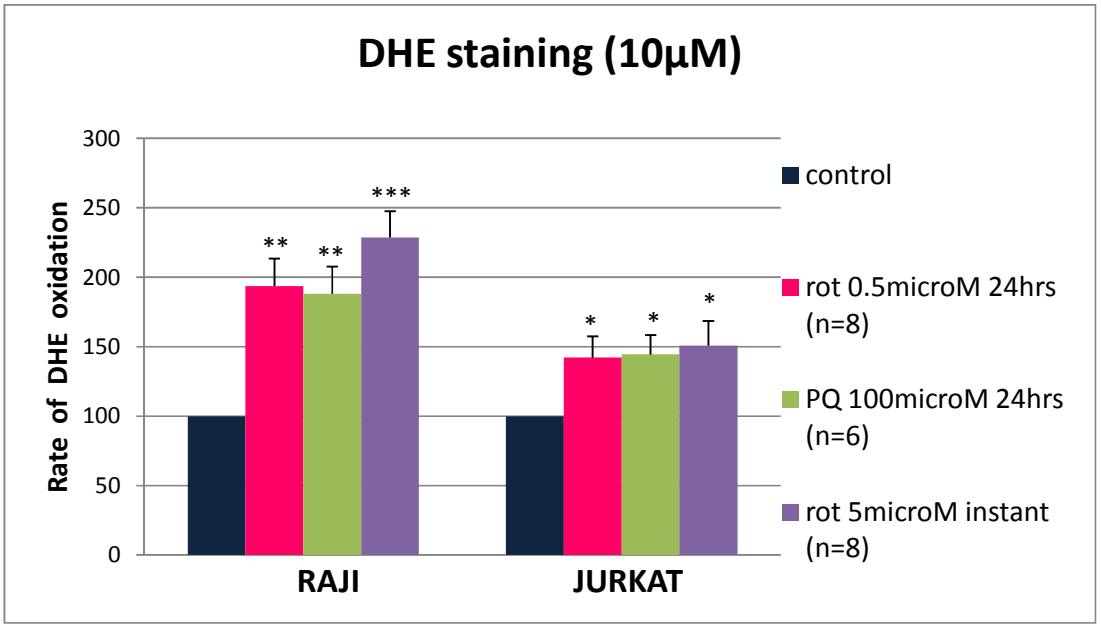

Fig 4.5: Graph representing the percentage change in the rate of DHE oxidation comparing to control (100%) upon treatment of the Raji and Jurkat cells with 0.5µM rotenone for 24 hrs (n=8), 100µM paraquat (PQ) for 24 hrs (n=6) and 5µM instant rotenone (n=8). Error bars represent the SEM; *p<0.05, **p<0.01, ***p<0.001, 10µM DHE was used.

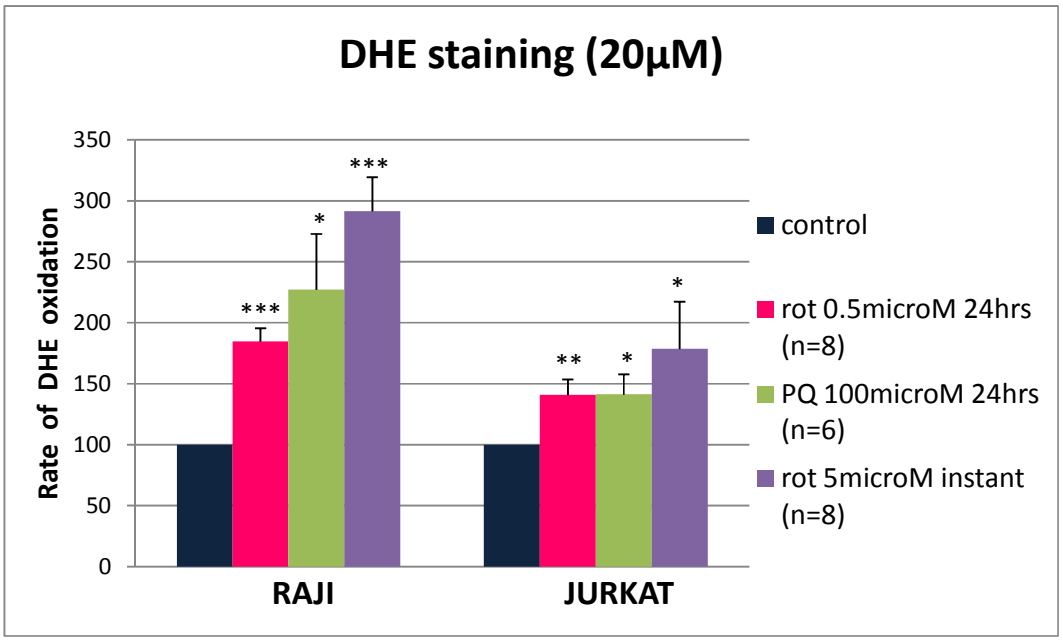

Fig 4.6: Graph representing the percentage change in the rate of DHE oxidation comparing to control (100%) upon treatment of the Raji and Jurkat cells with 0.5µM rotenone for 24hrs (n=8), 100µM paraquat (PQ) for 24hrs (n=6) and 5µM instant rotenone (n=8). Error bars represent the SEM; *p<0.05, **p<0.01, ***p<0.001, 20µM DHE was used.

Discussion: Rotenone administered instantly at a relatively high concentration (5µM) acted as an effective positive control, leading to a statistically significant increase in DHE staining in both cell lines using two different DHE concentrations (10µM and 20µM). Paraquat, known to generate ROS, also caused a statistically significant increase in the rate of red fluorescence emission in both cell lines. Similarly, rotenone over 24hrs caused a statistically

significant increase in DHE staining, mediated by its ability to inhibit complex I, cause mitochondrial dysfunction and thus oxidative stress. The Raji cells were more sensitive than the Jurkat cells to rotenone and paraquat treatment, although the effect was statistically significant in both cell lines.

4.1.5 Aconitase enzymatic assay

A statistically significant reduction in the aconitase enzymatic activity was noted in both the Raji and Jurkat cell lines comparing to control, when the cells were treated with rotenone and paraquat (Fig 4.7).

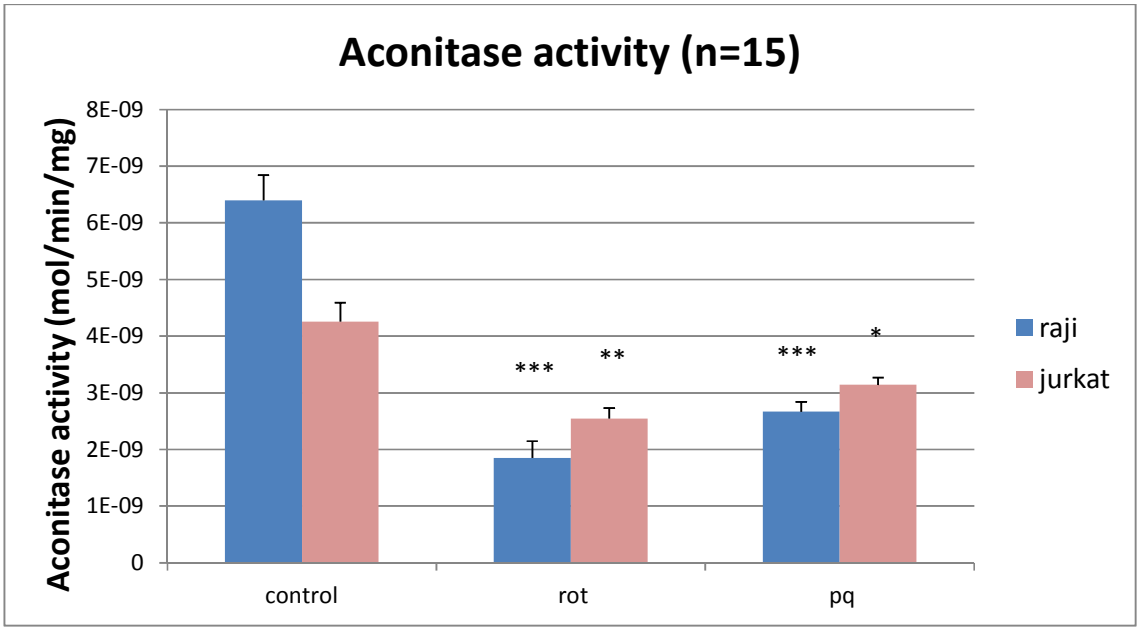

Fig 4.7: Graph showing the change in aconitase enzymatic activity in the Raji and Jurkat cells after treatment with 0.5µM rotenone and 100µM paraquat over 24hrs (n=15). Error bars represent the SEM; *p<0.05, **p<0.01, ***p<0.001. In all measurements, the background (no cells with reaction buffer) has been subtracted. Aconitase activity is expressed in mol/min/mg. All values have been adjusted for the protein level in each sample.

Discussion: Paraquat, a known generator of ROS, caused significant oxidative damage to the two cell lines, as demonstrated by the statistically significant reduction in the aconitase activity. Similarly, rotenone had a statistically significant effect on the aconitase activity in both cell lines, thus suggesting that rotenone at this concentration (0.5µM) can also lead to oxidative damage, which may be linked to its ability to inhibit complex I and cause mitochondrial dysfunction. Interestingly, as already shown with the previous methods, the aconitase activity in the Raji cells was more significantly affected than in the Jurkat cells.

4.1.6 Conclusion

In summary, we have modelled mitochondrial dysfunction and oxidative stress (by using rotenone and paraquat respectively) in B- and T- lymphocyte cell lines and have demonstrated that the four experimental techniques described above (see sections 4.1.2 - 4.1.5) were effective in measuring changes to these cells upon rotenone and paraquat treatment.

4.2 Healthy volunteers

4.2.1 Introduction

The purpose of this section was to demonstrate that the four aforementioned experimental techniques (ADP Phosphorylation, TMRM, DHE and aconitase) can be used to measure mitochondrial dysfunction and oxidative stress not only in a cell line system, but also in human lymphocytes from healthy volunteers. Lymphocytes were isolated, after the removal of monocytes, from

anticoagulated peripheral blood using Lymphoprep (see section 2.3.2), and maintained under unstimulated conditions for subsequent experiments, as shown in the red boxes of the flowchart below (Fig 4.8). Approximately 25-30mls of peripheral blood were collected from each volunteer and the isolated PBMC were resuspended in the appropriate medium (see section 2.3.1) to create a cell density of approximately 1million PBMC/ml. PBMC were treated with 0.5µM rotenone overnight, 100µM paraquat overnight or incubated overnight without treatment (Fig 4.8). The Raji cells were chosen in the volunteers' experiments as a reference, since Raji were found in the previous section to be more sensitive than Jurkat.

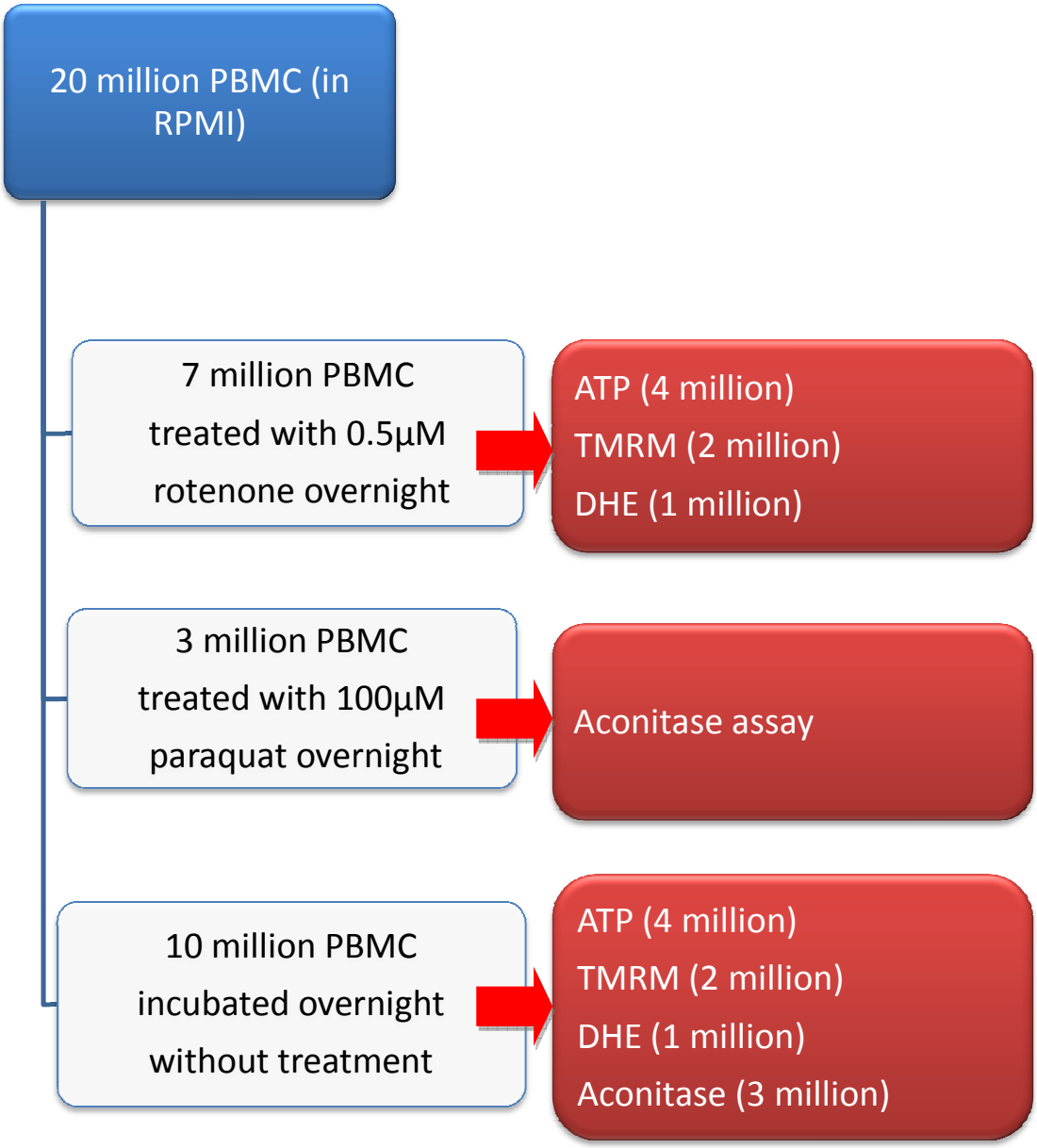

Fig 4.8: Schematic representation of the experimental design used for the PBMC derived from human volunteers.

4.2.2 ADP Phosphorylation Assay (complexes I, II/III and IV)

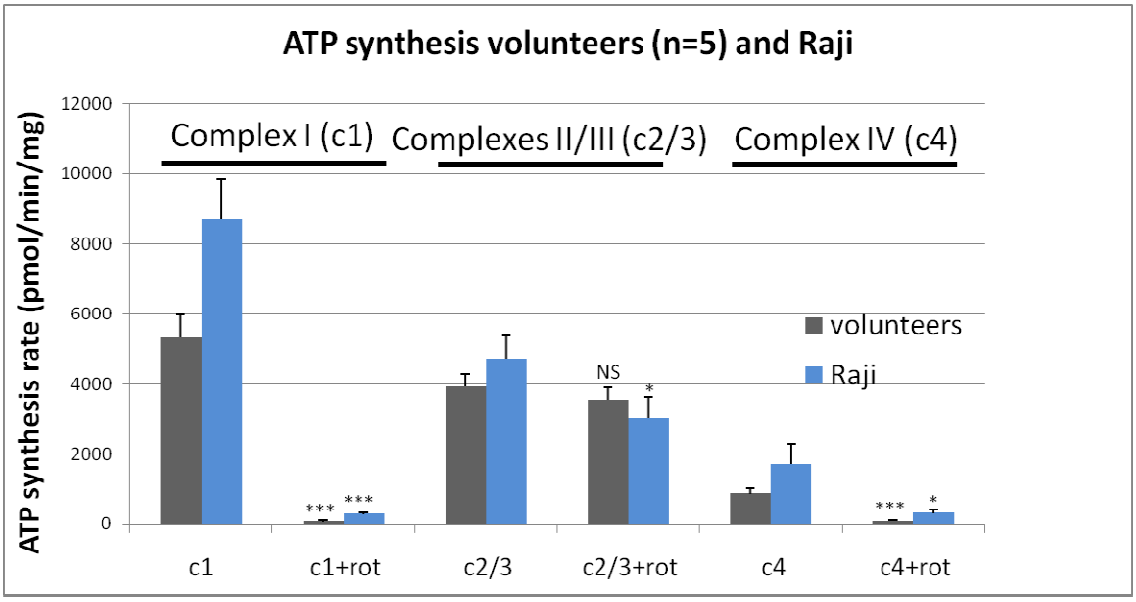

Fig 4.9: Graph showing the rate of ATP synthesis by complexes I, II/III and IV in the volunteers' lymphocytes and in the Raji lymphocytes, with and without treatment with 0.5µM rotenone for 24hrs. The ATP synthesis rate is expressed in pmol/min/mg lysate. Error bars represent the SEM (n=5); *p<0.05, ***p<0.001, NS: not significant, c1: complex I, c2/3: complexes II/III, c4: complex IV, rot: rotenone.

Complex I: A statistically significant reduction in the rate of ATP synthesis by complex I was noted upon treatment with 0.5µM rotenone for 24hrs in both the volunteers' lymphocytes (from 5321±667 pmol/min/mg to 70±55 pmol/min/mg) and Raji cells (from 8724±1105 pmol/min/mg to 286±57 pmol/min/mg).

Complexes II/III: Upon treatment with 0.5µM rotenone for 24hrs, Raji cells demonstrated a statistically significant reduction in the rate of ATP synthesis by complexes II/III (from 4698±670 pmol/min/mg to 3025±601 pmol/min/mg).

The effect on the volunteers' lymphocytes was not significant (from 3921±350 pmol/min/mg to 3554±348 pmol/min/mg).

Complex IV: Similarly to complex I, 0.5μM rotenone for 24hrs caused a statistically significant reduction in the rate of ATP synthesis by complex IV in both the volunteers' lymphocytes (from 881±143 pmol/min/mg to 78±32 pmol/min/mg) and Raji cells (from 1701±588 pmol/min/mg to 311±93 pmol/min/mg).

Discussion: The ADP phosphorylation assay appears to be a useful method in human lymphocytes to measure the mitochondrial dysfunction caused by the complex I inhibitor rotenone. In the case of complex I, rotenone was found to cause a statistically significant reduction in the rate of ATP synthesis by complex I in healthy volunteers' lymphocytes. Upon rotenone treatment, the rate of ATP synthesis by complex IV in healthy volunteers' lymphocytes was also reduced, suggesting that the inhibitory effect of rotenone on complex I could also influence the activity of other complexes. In the case of complexes II/III, the effect of rotenone was significant in the Raji cells, but not in the volunteers' lymphocytes, suggesting that human lymphocytes may be less sensitive to mitochondrial dysfunction and oxidative stress comparing to a B-lymphocytic cell line.

4.2.3 Mitochondrial Membrane Potential (steady-state TMRM staining)

Fig 4.10 presents the results of the mitochondrial membrane potential experiment with the use of the red fluorescent dye TMRM. In the absence of TMRM staining, the % gated events were almost zero. A statistically significant reduction in the TMRM staining was noted in the volunteers' lymphocytes

(from 65±2% to 39±7%) and in the Raji cells (from 71±2% to 48±4%) upon treatment with 0.5µM rotenone for 24hrs. As expected, the addition of uncoupler (FCCP 10 µM) also caused a statistically significant reduction in TMRM staining to 38±4% and 18±6% in the volunteers' lymphocytes and Raji cells, respectively.

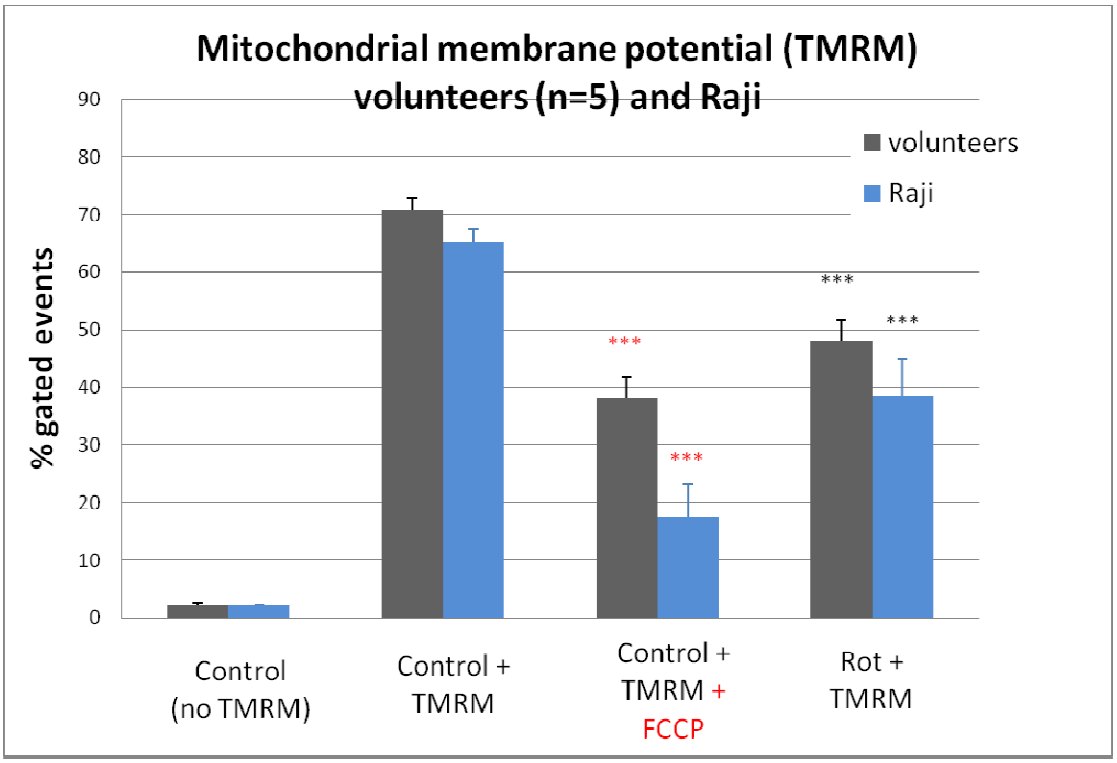

Fig 4.10: Graph representing the change in the % gated events in the human volunteers' lymphocytes and Raji cells upon treatment with 0.5µM rotenone for 24hrs, and upon treatment with FCCP (in red). Error bars represent the SEM (n=5); ***p<0.001, NS: not significant. The same gate was used in all experiments.

Discussion: Flow cytometry is a useful method for measuring the steady-state TMRM staining that represents the mitochondrial membrane potential in human (healthy volunteers') lymphocytes. The concentration of TMRM used (25nM) was mitochondria-specific and the uncoupler FCCP acted as an

effective positive control leading to the depolarisation of the mitochondria and causing the TMRM staining to dissipate. Rotenone led to a statistically significant reduction in TMRM staining in both human lymphocytes and Raji cells. Similarly to the ADP phosphorylation assay for compexes II/III above (section 4.2.2), the mitochondrial membrane potential in the human lymphocytes appears more resistant to the rotenone treatment comparing to the Raji cells.

4.2.4 Dihydroethidium (DHE) staining

Human lymphocytes showed a statistically significant increase in the DHE staining comparing to control human lymphocytes (100%, not shown on Fig 4.11) upon treatment with 5μM instant rotenone (125±4%), 5μM rotenone for 2hrs (114±6%), 0.5μM rotenone for 24 hrs (139±5%) and 100μM paraquat for 24 hrs (120±9%). Raji cells also showed a statistically significant increase in the DHE staining comparing to control Raji (100%, not shown on Fig 4.11) upon treatment with 5μM instant rotenone (205±10%), 5μM rotenone for 2hrs (205±3%), 0.5μM rotenone for 24 hrs (404±2%) and 100μM paraquat for 24 hrs (189±18%).

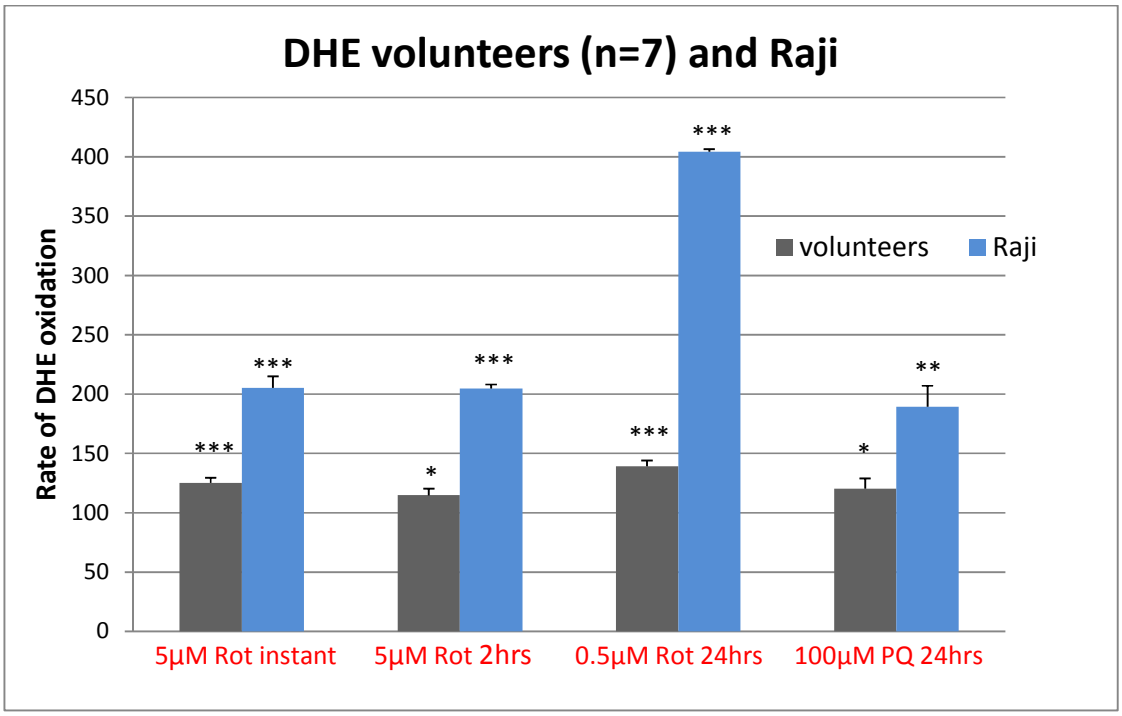

Fig 4.11: Graph representing the percentage change in the rate of DHE staining in the lymphocytes from healthy volunteers and in Raji cells, upon treatment with 5µM instant rotenone, 5µM rotenone for 2hrs, 0.5µM rotenone for 24hrs and 100µM paraquat for 24hrs (n=7). The volunteers' (grey bars) and Raji (blue bars) results are expressed as the percentage change from control human lymphocytes without rotenone (100%, not shown) and control Raji without rotenone (100%, not shown), respectively. Error bars represent the SEM. An equal number of cells was added into each well of the 96-well plate (50,000 cells/well); **p<0.01, **p<0.01, ***p<0.001, Rot: rotenone, PQ: paraquat. 40µM DHE was used in this experiment.

Discussion: A statistically significant increase in the rate of DHE staining, and therefore in the rate of superoxide production, was noted in the volunteers' lymphocytes and the Raji cells upon treatment with 5µM instant rotenone, 5µM rotenone for 2hrs, 0.5µM rotenone for 24 hrs and 100µM paraquat for 24hrs. In all cases, the human healthy volunteers' lymphocytes showed a

smaller increase in the production of superoxide than the Raji cells, suggesting that the human lymphocytes may be less sensitive to oxidative stress comparing to the B-lymphocytic cell line. The highest increase in the level of DHE staining, in both human lymphocytes and Raji cells, was found upon treatment with 0.5μM rotenone for 24hrs and this was used for subsequent DHE experiments in section 4.3.

4.2.5 Aconitase enzymatic assay

The baseline aconitase enzymatic activity in the volunteers' lymphocytes (1.64±0.12pmol/min/mg) appears lower comparing to the Raji cells (5.84±0.95pmol/min/mg) (Fig 4.12). Upon paraquat treatment, the aconitase activity for the volunteers' lymphocytes and Raji cells was reduced to 0.83±0.09pmol/min/mg and 2.3±0.4pmol/min/mg, respectively ($p<0.001$, as compared to baseline).

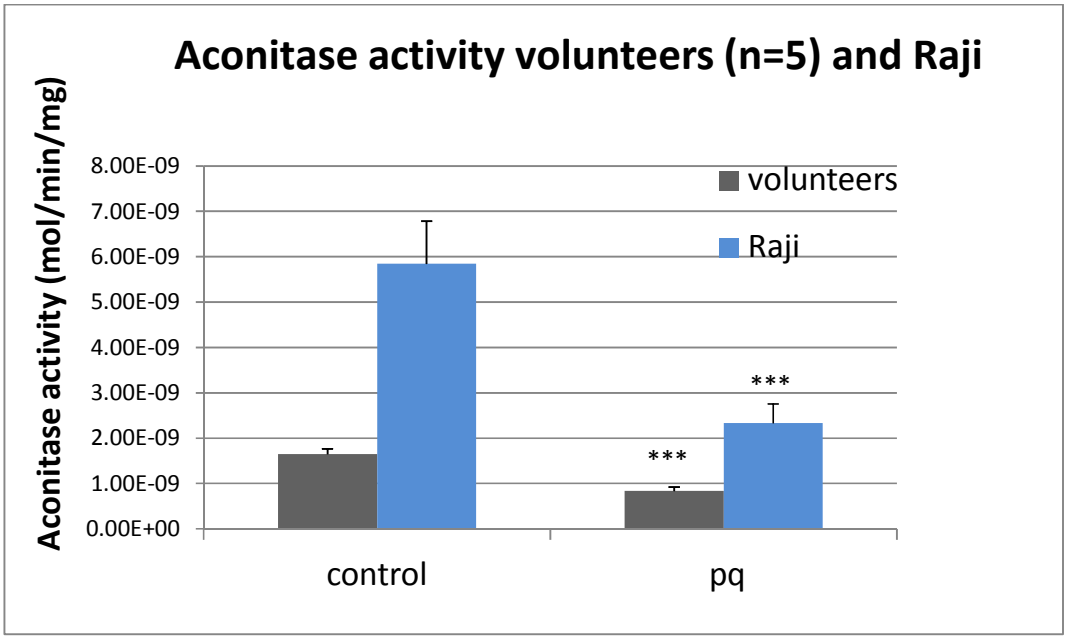

Fig 4.12: Graph showing the change in the aconitase enzymatic activity of volunteers' lymphocytes and Raji cells with and without treatment with 100μM paraquat over 24hrs (n=5). Error bars represent the SEM; ***p<0.001, pq: paraquat. In all measurements, the background (no cells with reaction buffer) has been subtracted. Aconitase activity is expressed in mol/min/mg. All values have been adjusted for the protein level in each sample, as described in section 2.3.7.

Discussion: The lower baseline aconitase enzymatic activity in volunteers' lymphocytes comparing to the Raji cells may reflect the differences between unstimulated human lymphocytes and immortalised lymphocytic cell lines, and suggest that the volunteers' lymphocytes may be under more oxidative stress comparing to the Raji cell line. Upon free-radical induction with paraquat, a statistically significant reduction was noted in the volunteers' lymphocytes, suggesting that this assay is useful in our model for detecting changes in the oxidative stress levels of human lymphocytes.

4.2.6 Conclusion

In summary, in this chapter we have demonstrated that the four experimental techniques described (ATP, TMRM, DHE and aconitase) can measure mitochondrial dysfunction and oxidative stress not only in a cell line system, but also in human lymphocytes from healthy volunteers.

4.3 Patients with normal tension glaucoma, ocular hypertension and controls

4.3.1 Introduction

In this section we present our results on human unstimulated lymphocytes isolated from patients with normal tension glaucoma (NTG), ocular hypertension (OHT) and controls. A series of different assays were employed, as discussed later in more detail, to measure parameters relating to mitochondrial function (ATP for complexes I, II/III and IV, TMRM, calcium mobilisation, mTOR), oxidative stress (DHE, aconitase, 8OHdG) and antioxidant defence (SOD2, vitamins A, B6, B12, C, folate, urate).

Two cohorts of 30 subjects with ≥8 Humphrey 24-2 visual fields over ≥5 years of follow-up were recruited prospectively from Moorfields Eye Hospital:

a) Normal Tension Glaucoma (NTG) group: rapidly progressing patients with Mean Deviation change > -1.0 dB/yr and mean IOP<16;

b) Ocular Hypertension (OHT) group: non-progressing patients with mean IOP>24.

An equal number of age-similar subjects with normal IOP, healthy discs and no family history of glaucoma was also recruited as controls.

Approximately 50-60mls of peripheral blood were collected from each participant and transferred from Moorfields Eye Hospital to the Department of Clinical Neurosciences, Royal Free Hospital within 1-2 hours from collection. The blood was processed as shown in the flowchart below (Fig 4.13). In summary, 8mls of SST blood were spun at 800 x g for 15min to separate the serum, which was frozen in 1ml aliquots at -80^{o}C for future analyses. The remaining blood was used for the isolation of PBMC as described previously

(see section 2.3.2) and maintained under unstimulated conditions in the appropriate medium (see section 2.3.1) to create a cell density of approximately 1million PBMC/ml. A first morning mid-stream urine sample was also collected from each patient. Five 1ml urine aliquots were prepared and both the aliquots and the remaining urine were stored at -80^{o}C for future analyses, including the measurement of 8OHdG.

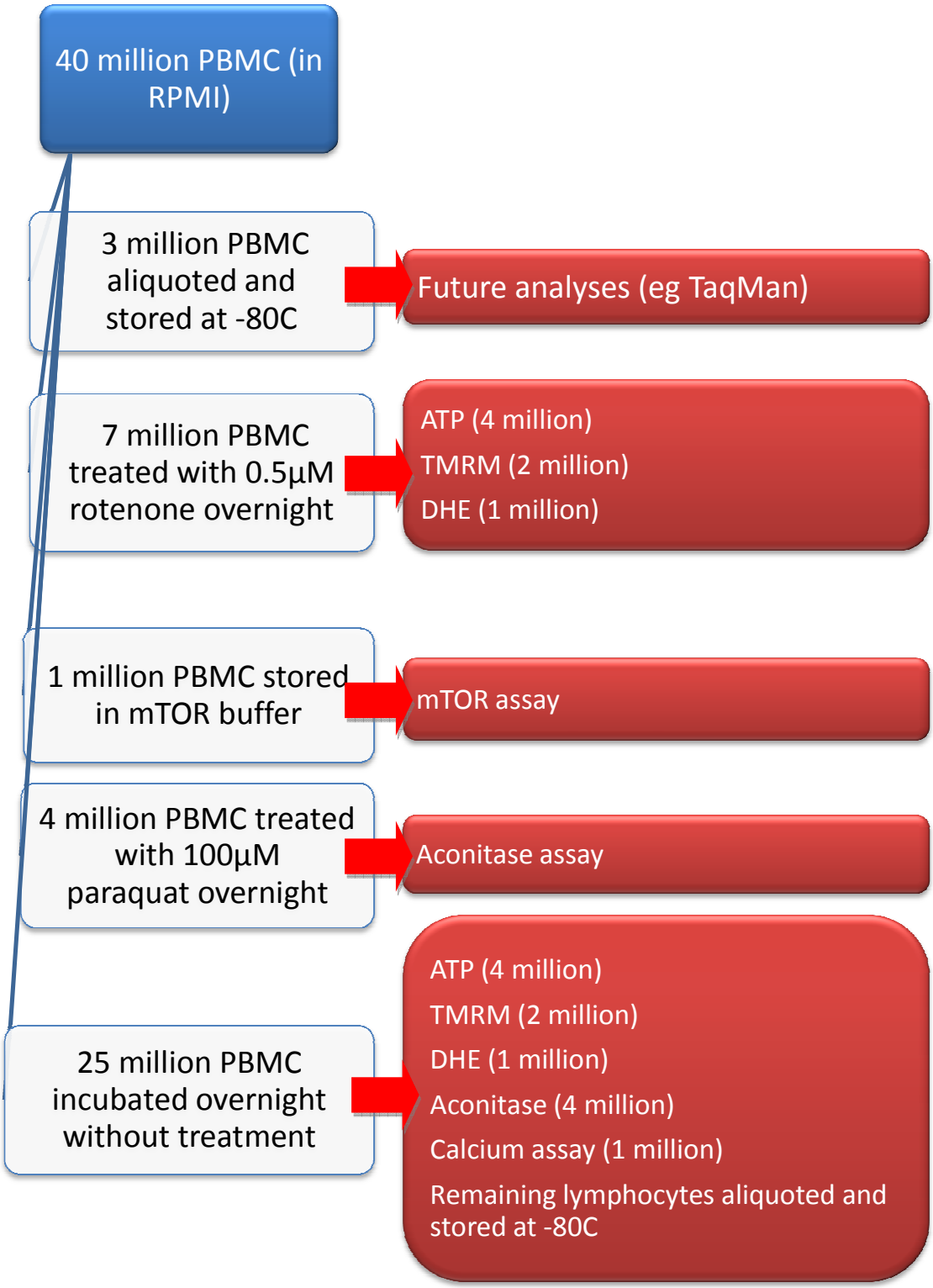

Fig 4.13: Schematic representation of the experimental design used for the patients' and controls' PBMC.

4.3.2 Baseline characteristics

Demographic and other baseline clinical data

The mean age of the subjects (control: 67.8, NTG: 73.9, and OHT: 67.8 years) was similar between the three groups and only slightly higher in the NTG group. Most participants were white, with the exception of 2 controls, 3 NTGs and 2 OHTs of Asian ethnic background, and 3 NTGs and 1 OHT of Carribean background. Right and left eyes were almost equally represented between the three groups. The median rate of VF progression for the whole field over the follow-up period, measured with the Moorfields Progressor software (section 2.2.8), was -1.14dB/year (IQR -1.05 to -1.49) in the NTG group, while the median rate only for the VF progressing points was -3.24dB/year. It is clear that this NTG group was carefully selected to represent a fast-progressing group, while the OHT cohort showed no (or minimal) progression with a median rate of -0.11dB/year (IQR 0.03 to -0.23). It should also be noted that all the OHT patients had full VFs and that a significant number of VFs was performed in the NTG and OHT groups to provide sufficient information for representative progression measurements. Importantly, despite the fast disease progression, the mean IOP in the NTG group over 6 years of follow-up was only 13.2mmHg. In the OHT group, despite no VF progression, the mean IOP over 8.5 years of follow-up was 25.0mmHg. The mean CCT was higher in the OHT group (579.6µm) and lower in the NTG group (528.8µm), as compared to the controls (547.2µm). The mean cup-to-disc ratio in the OHT subjects was very similar to the controls, while the NTG group showed advanced cupping with an almost double cup-to-disc ratio, as compared to the other two groups. By definition, none of the controls had a family history (FH) of glaucoma. Amongst the 16 NTGs and 19 OHTs with a positive FH of glaucoma, first degree relatives were

reported in 15 subjects from each group. Protocol violations were noted in participant n23, whose mean GAT IOP during follow-up was 16.3; in n27, who was 101 years of age and could not be age-matched; and in o29, whose VF progression rate was -0.63dB/year. The records of the latter participant were rechecked to confirm that he does not suffer from glaucoma and the relatively high progression rate was attributed to a Progressor software error. All 30 participants from each group were included in the analysis.

Variable	Control (n=30)	NTG (n=30)	OHT (n=30)
Mean age (±SD)	67.8 (±8.2)	73.9 (±11.7)	67.8 (±8.9)
Ethnicity (white)	28	24	27
Right eyes	18	16	18
Median (IQR) VF progression rate (dB/year)	n/a	-1.14 (-1.05 to -1.49)	-0.11 (0.03 to -0.23)
Median number of VFs (IQR)	n/a	9.5 (8.75 to 11)	10.5 (8 to 11)
Median years of follow-up (IQR)	n/a	6.0 (5.0 to 6.5)	8.5 (7.0 to 10.15)
Mean GAT IOP during follow-up (mmHg) (range)	n/a	13.2 (9.1-16.3)	25.0 (24.0 to 26.6)
Mean maximum reported GAT IOP (mmHg)	n/a	19.8	33.4
Cup-to-disc ratio	0.40	0.88	0.49
Family history	0	16	19

Table 4.1: Demographic and other baseline clinical data for Control, NTG and OHT subjects in the mitochondrial pilot study; n/a: not applicable.

Cardiovascular background and other past medical history

Symptoms of Raynaud's, vasospasm and migraines were significantly over-represented in the NTG cohort. Extreme dippers, defined as subjects whose mean night time SBP was more than 20% lower as compared to the mean day time ambulatory SBP, were equally distributed between the three groups. The mean SBP during the day and at night were higher in the OHT group, as compared to the other two groups, while the mean DBP was lower in the NTG group. The mean body mass index (BMI), which represents a balance between nutrient intake from all sources and energy expenditure, was relatively higher in the OHT subjects, as compared to the other two groups. History of systemic hypertension and diabetes mellitus was more common in the NTG and OHT groups, as compared to the control subjects. Other cardiovascular diseases, including cerebrovascular accident and myocardial infarction, were rare in our cohort. Cancer was slightly over-represented in the OHT cohort, while hypothyroidism was far more common in the NTG group.

	Control	NTG	OHT
Raynaud's or vasospasm	0	6	0
Migraine	4	8	0
Extreme dippers	3	3	3
SBP during day (mmHg) (mean±SD)	133.2±16.6	133.0±13.1	145.5±17.7

DBP during day (mmHg) (mean±SD)	79.5±10.4	70.9±9.5	79.2±9.5
SBP at night (mmHg) (mean±SD)	117.4±17.1	117.7±15.9	127.6±20.6
DBP at night (mmHg) (mean±SD)	64.1±7.7	59.0±8.1	64.0±9.2
Systemic Hypertension	7	14	13
Diabetes mellitus	0	2	5
Other cardiovascular history (CVA, MI)	2	3	0
Body Mass Index (mean±SD)	25.4±4.7	25.0±6.5	27.4±5.0
Cancer	2	4	6
Hypothyroidism	1	7	2

Table 4.2: Cardiovascular background and other past medical history in our cohort; SBP: systolic blood pressure; DBP: diastolic blood pressure; CVA: cerebrovascular accident; MI: myocardial infarction.

Discussion: Symptoms of Raynaud's or vasospasm were significantly over-represented in the NTG cohort. This is interesting, considering evidence from the literature that supports an association between vasospasm and glaucoma, and an abnormal peripheral reactivity to cold in glaucoma patients (Gasser et al 1990), and particularly in NTG (Gasser et al 1991, Drance et al 1988). Migraines were also more common in our NTG group, in line with previous studies (Phelps et al 1985, Cursiefen et al 2000, Orgul et al 1994a), although other studies have not confirmed this association between migraines and NTG

(Usui et al 1991, Wang et al 1997). Also, a history of hypothyroidism was more often encountered in the NTG cohort, consistent with previous studies showing that hypothyroidism can be associated with OAG (Girkin et al 2004, Smith et al 1993, Jämsén 1996) and with changes in ocular blood flow in glaucoma patients that may be reversible upon treatment of the hypothyroidism (Smith et al 1992). Another mechanism for increased OAG risk in hypothyroidism, proposed by Becker et al in 1966, was the presence of myxoedema of the trabecular meshwork in patients with abnormal thyroid function (Becker et al 1966). Similarly to the study by Smith et al, who found that 23% of POAG patients suffered from hypothyroidism (Smith et al 1993), exactly the same percentage of our NTG subjects (n=7) also had a history of thyroid disease. However, other studies have not been able to show a link between hypothyroidism and OAG (Karadimas et al 2001, Munoz-Negrete et al 2000, Motsko et al 2008), with the authors suggesting that the large proportion of patients receiving thyroid replacement therapy may have negated any OAG-related consequences of hypothyroidism.

With regards to systemic blood pressure, SBP both during the day and at night was found to be relatively increased in the OHT group, in line with previous reports that show blood pressure and IOP to be positively associated (Hennis et al 2003, Klein et al 2005). However, the DBP was lower in the NTG cohort, in line with evidence from the Thessaloniki Eye Study that lower DBP secondary to antihypertensive treatment was associated with increased disc cupping and decreased rim area (Topouzis et al 2006). Similarly, a lower DBP was linked to a higher prevalence of OAG in the Los Angeles Latino Eye Study (Memarzadeh et al 2010).

The relatively increased BMI in the OHT group may be consistent with the recently reported finding in the Rotterdam Study that obesity was associated with a higher IOP and a lower risk of developing OAG, although these associations were only present in women (Ramdas et al 2011b). In line with the Rotterdam Study, various other studies also document a positive association between BMI and IOP (Yoshida et al 2003, Klein et al 1992b, Wu et al 1997, Mori et al 2000), while the few studies that have directly studied the relation between BMI and POAG suggest an inverse association between BMI and POAG (Gasser et al 1999, Leske et al 1995). In our study, the mean BMI in the NTG was only marginally lower as compared to the control group and, similarly to the study by Gasser et al, this difference was not statistically significant.

Cancer and diabetes mellitus were slightly more frequent in the OHT group, although it is unclear to what extent these conditions would have affected mitochondrial function in the lymphocytes. Lymphocytes may not be as critically involved in the pathophysiology of certain diseases as other tissues, and type II diabetes, for example, has been associated with mitochondrial dysfunction in insulin-sensitive tissues, including myocytes (Kelley et al 2002), hepatocytes (Sivitz et al 2010, Vester et al 1957) and adipocytes (Choo et al 2006), but not in lymphocytes. It is also important to note the relatively short half life of peripheral blood lymphocytes (usually days to month) and their relatively high turnover, which would perhaps minimise the accumulating impact of chronic diseases on mitochondrial function. Fortunately, no patients in our cohort were suffering from active haematological malignancy or infection at the time of the blood sampling or had undergone recent chemotherapy, factors which, if present, might have impacted more directly on the function of the lymphocytes.

Systemic medications and lifestyle parameters

Smokers were only found in the OHT group and above average alcohol consumption (>21 units/week for males and >14 units/week for females) was slightly more common in the control group. Above average (≥5 cups a day) coffee consumption, the primary dietary source of caffeine, was noted in very few subjects from each cohort. Antioxidant supplements were equally common between the control and NTG groups, while the frequency of antioxidant supplements in the OHT group was significantly lower and almost half, as compared to the other two groups. Intake of NSAIDs was slightly more common in the NTG group, while statins were almost equally represented between the NTG and OHT subjects and were less common in the control group. Topical prostaglandin analogues and b-blockers were slightly more common in the NTG as compared to the OHT group, while none of the controls were on topical medications.

	Control	NTG	OHT
Smoking	0	0	3
Alcohol[1]	6	2	3
Coffee[2]	3	1	3
Antioxidant supplements	15	14	7
NSAIDs	4	8	6
Statins	5	13	12
PG analogues[3]	0	20	17
B-blockers[3]	0	11	7

Table 4.3: Systemic medications and lifestyle parameters in our cohort; [1] >21 units/week for males and >14 units/week for females; [2] ≥5 cups a day; [3] topical medications; NSAIDs: non steroidal anti-inflammatory drugs; PG: prostaglandin.

Discussion: In terms of the role of systemic medications on mitochondrial function, it is important to note the tissue specificity of such medications. Statins, for example, have been shown to be beneficial to heart muscle mitochondria, while having a damaging effect on mitochondria from skeletal muscle and causing rabdomyolysis (Bouitbir et al 2012, Jones et al 2003). Similarly, pioglitazone is thought to improve mitochondrial biogenesis in the adipose tissue, while having the opposite effect in the pancreas (Bogacka et al 2005, Lamontagne et al 2009). Another commonly used group of drugs, b-blockers, improves mitochondrial function in the cardiac muscle, but not in skeletal muscle (Dreisbach et al 1993, Hugel et al 1999). This tissue specificity of medications on mitochondrial function could reflect the different mechanisms of action of drugs and their interaction with other drugs, as well as the diverse energy requirements of different tissues and their unique receptor profiles, which eventually impacts on intracellular signals and mitochondrial function. Also, the fact that NSAIDS were slighty more common in the NTG group may not have impacted significantly on mitochondrial function in this group, since it was not possible to find convincing evidence that NSAIDS affect lymphocytic mitochondria, although NSAIDs are known to affect gastrointestinal mucosa mitochondria (Somasundaram et al 2000) and liver mitochondria (Browne et al 1999). Moreover, no convincing evidence exists to date to suggest that drugs applied topically would have a major impact on human circulating lymphocytes.

By focusing on evidence for systemic medications that could have a direct negative effect on lymphocytic mitochondria, it was discovered that such effect has clearly been reported for amiodarone (Yasuda et al 1996), tetracyclins, chloramphenicol (Riesbeck et al 1990) and antiretroviral drugs (Tolomeo et al 2003). None of our subjects were on any of the above medications at the time of the blood collection. Smoking has also been described to clearly affect lymphocytic mitochondrial function (Miro et al 1999, Cardellach et al 2003), although, in the only 3 OHT patients who smoked, mitochondrial function was not significantly reduced. Nevertheless, it remains possible that the results of enhanced mitochondrial function in the OHT group (see section 4.3.3) have been masked to some extent by the presence of smokers in this group. Interestingly, in a prospective study evaluating the effect of cigarette smoking on the risk of POAG, after controlling for potential risk factors of POAG, including age, hypertension and African American heritage, neither current smokers nor past smokers were at greater risk for POAG than those who had never smoked (Kang et al 2003). Similarly, a systematic literature review concluded that there is little evidence for a causal association between smoking and POAG development, and that there is no evidence of a dose-response relationship with smoking or of reversibility of effect in the studies where this was assessed (Edwards et al 2008).

Ethanol is also known to directly affect lymphocytic mitochondria (Kapasi et al 2003), although the mean rate of ATP synthesis by the different complexes for the 6 controls that exceeded the alcohol limit was very similar to the mean rate of ATP synthesis for the whole control group. However, it could be argued that the presence of more above average alcohol consumers in the control group (n=6) as compared to the NTG group (n=2) could have contributed to the lack of significant reduction in mitochondrial function in the NTG cohort. In the

large prospective Nurses' Health Study and the Health Professionals Follow-up Study, alcohol consumption was not found to influence the risk of POAG (Kang et al 2007). Similarly, in the recently published results from the Rotterdam Study with 3939 eligible participants, smoking and alcohol consumption were not associated with POAG (Ramdas et al 2011b). Additional case-control and prevalence studies provide mixed results regarding the relation between alcohol use and glaucoma, with one showing an inverse relation (Fan et al 2004), others showing no association (Wilson et al 1987, Klein et al 1993, Leske et al 1995) and one actually showing a positive association (Kahn et al 1980). Similarly, the link between alcohol and IOP is not clear, with acute ingestion of alcohol thought to promptly lower IOP in a dose-dependent manner (Peczon et al 1965, Houle et al 1967), while some studies suggest that daily alcohol consumption is associated with increased IOP (Leske et al 1996, Yoshida et al 2003, Lin et al 2005).

With regards to caffeine consumption, in a large prospective population-based sample of health professionals (n=121,172), consumption of ≥5 cups of caffeinated coffee, the primary dietary source of caffeine, daily was associated with 1.6-fold increased risk of POAG, while tea or caffeinated cola intake were not associated (Kang et al 2008). In our cohort only a very small number of subjects from each group consumed ≥5 cups of caffeinated coffee a day making it difficult to draw any conclusions. In the same study by Kang et al, greater caffeine intake was more adversely associated with POAG among those reporting a family history of glaucoma, particularly in relation to POAG with elevated IOP (Kang et al 2008). A typical cup of coffee is thought to cause a 1−4mmHg rise in IOP that lasts for at least 90 minutes (Higginbotham et al 1989, Avisar et al 2002), while in the Blue Mountain Eye Study OAG patients who consumed coffee regularly had higher IOP than their counterparts who

abstained from coffee consumption (19.6mmHg vs 16.8mmHg; p=0.03) (Chandrasekaran et al 2005). The mean number of cups of coffee a day in our cohort was 1.8, 1.2 and 1.3 for the control, NTG and OHT groups, respectively, and did not differ significantly between groups.

In this pilot study, instead of excluding subjects on the basis of co-existing diseases, medications or lifestyle parameters, we selected patients based on VF progression and IOP-related criteria only. This follows a more 'real life' approach, identifying mitochondrial function and related variables as manifest in these patients and then identifying lifestyle factors that may account for any differences identified, despite the relatively small sample size and the multiplicity of potential variables. Lifestyle parameters were often difficult to accurately characterise and measure. Similarly, the contents and strength of antioxidant supplements varied significantly amongst subjects, making more detailed comparisons difficult. An alternative approach followed in this study was to explore the role of antioxidant defences in the three groups of participants by directly measuring the levels of multiple antioxidants (vitamins A, B6, B12, C, folate, urate) in the peripheral blood.

Ocular features

	Control	NTG	OHT
CCT (µm)	547.2±45.9	528.8±36.6	579.6±35.5
AL (mm)	23.8±1.4	24.3±2.2	23.7±1.3
ACD (mm)	3.1±0.4	3.5±0.6	3.2±0.5
SE (Dioptres)	-0.6±3.1	-1.9±3.5	0.2±3.0
Phasing GAT IOP (mmHg)	13.6±2.5	12.6±3.4	22.3±3.0

Phasing DCT IOP (mmHg)	16.2±2.7	15.5±3.0	23.9±2.9
ORA IOPcc (mmHg)	14.4±3.1	15.6±3.8	23.2±3.9
Supine GAT (mmHg)	13.2±2.7	12.3±3.6	22.1±3.9
CRF (mmHg)	10.1±1.9	8.2±1.9	12.1±2.3
CH (mmHg)	10.6±1.8	8.7±1.5	9.7±1.7
Phasing DCT OPA (mmHg)	2.3±0.8	2.3±1.0	4.2±1.3

Table 4.4: Summary (mean±SD) of ocular features for the three groups of participants; CCT: central corneal thickness; AL: axial length; ACD: anterior chamber depth; SE: spherical equivalent; GAT: Goldmann applanation tonometry; DCT: dynamic contour tonometry; CRF: corneal resistance factor; CH: corneal hysteresis; OPA: ocular pulse amplitude; ORA: ocular response analyser; IOPcc: corneal compensated intraocular pressure.

The central corneal thickness was slightly higher in the OHT group and lower in the NTG group, as compared to the controls. The mean CCT in the control group was consistent with the mean CCT reported in epidemiological studies (Wolfs et al 1997) and meta-analyses (Doughty et al 2000). The mean AL, ACD and SE show that the NTG group were a little more myopic than the other two groups. Pseudophakia was noted in 3 controls, 15 NTG patients and 2 OHT patients.

As expected, the mean diurnal GAT and DCT IOPs, calculated from the average of 5 GAT and 5 DCT (mean of three measurements at each time point) IOP measurements taken during daytime phasing (between 9am and 5pm) for each participant, was significantly higher in the OHT group, as compared to the NTG and controls. The DCT IOP, thought to display better repeatability and reproducibility than GAT IOP and ORA IOPcc (Kotecha et al 2010, Wang et al 2013) and be less influenced by the corneal biomechanics (Kotecha et al 2005,

Kotecha et al 2009, Boehm et al 2008), was higher than the GAT IOP in all three groups and this difference was smaller in the group with higher IOP and thicker CCT (OHT group). Also, the difference between DCT and GAT phasing IOPs was highest in our NTG group. Similarly, in a recent study by Ito et al (2012) that did not include phasing, the mean DCT IOP was 2.8 mm Hg higher than the GAT IOP, with the difference being greater with thinner CCT and in the lower IOP group, as compared to the higher IOP group. The standard deviation of the 5 GAT IOP diurnal phasing measurements in the control, NTG and OHT groups was 1.1±0.5, 1.2±0.6 and 1.8±0.7mmHg, respectively. Similarly, a higher variability in the 5 DCT diurnal measurements was noted in the OHT group (standard deviation 1.8±0.7mmHg), as compared to the control (1.0±0.4mmHg) and NTG groups (1.1±0.6mmHg). The variability noted during DCT phasing was similar and not significantly better than that noted during GAT phasing. The mean GAT diurnal supine IOP was similar to the mean phasing diurnal sitting GAT IOP in all three groups.

Similarly to the DCT IOP, the IOPcc was also higher than the GAT IOP in all three groups, in line with previous studies that show GAT to under-read both DCT and ORA IOP measurements (Kotecha et al 2010, Sullivan-Mee et al 2012). Interestingly, the IOPcc was lower than the DCT IOP in both OHT subjects and controls, while in NTG it was marginally higher. This could be explained by the fact that the DCT IOP is known to be correlated with CCT (DCT IOP/CCT slope 0.03 mmHg/μm; 95% CI 0.00-0.05) (Kotecha et al 2009), while the IOPcc is thought to be less affected by CCT (Nessim et al 2013) and believed not to change significantly following laser refractive surgery, although this has not been confirmed in several studies (Pepose et al 2007, Shah et al 2009). A higher IOPcc in NTG was also reported recently in a Japanese cohort, with the authors suggesting that IOP values may be underestimated with GAT and DCT

(Morita et al 2010). The CRF was lower in the NTG group and higher in the OHT group, as compared to the controls. Interestingly, while the CH was similar to the CRF in the controls and NTG subjects, in the OHT patients the mean CH was lower than the CRF, underlying the distinct corneal properties represented by these two parameters. Similarly to our study, lower CRF and CH in glaucoma have also been noted in several previous studies for both NTG (Nessim et al 2013) and POAG (Abitbol et al 2010, Mangouritsas et al 2009).

The mean phasing DCT OPA was significantly higher in the OHT cohort, as compared to the NTG patients and controls. Increased OPA has been shown to correlate with less severe glaucoma (Kynigopoulos et al 2012) and with increased CCT (Weizer et al 2007) and GAT and DCT IOP (Kaufmann et al 2006, Ishii et al 2012), as in our OHT group. No difference was noted in the OPA between the controls and NTG, as reported recently by Lee et al (2012), although other studies have reported a reduction in OPA in NTG patients as compared to controls (Stalmans et al 2008, Schwenn et al 2002). Based on the thinner cornea and lower DCT and GAT IOPs in the NTG group, one might have expected a smaller OPA in NTG as compared to the control group. However, OPA has also been shown to be negatively correlated with DBP (Detry-Morel et al 2007) and the lower DBP in our NTG cohort may have accounted for this lack of difference in the OPA between NTG and control.

4.3.3 Measurements relating to mitochondrial function – content

4.3.3.1 Introduction

In the box-and-whisker plots presented below, the middle (horizontal) line of each box represents the median. The lower and upper horizontal lines of each

box represent the lower and upper quartile values, respectively. The difference between the lower and upper quartiles is the interquartile range (IQR). Results are presented as median (IQR) for each parameter (n=30 from each group); *p<0.05, **p<0.01, ***p<0.001, NS: not significant. Outliers are highlighted with a circle or asterisk on the box-and-whisker plot.

4.3.3.2 ADP Phosphorylation Assay (complexes I, II/III and IV)

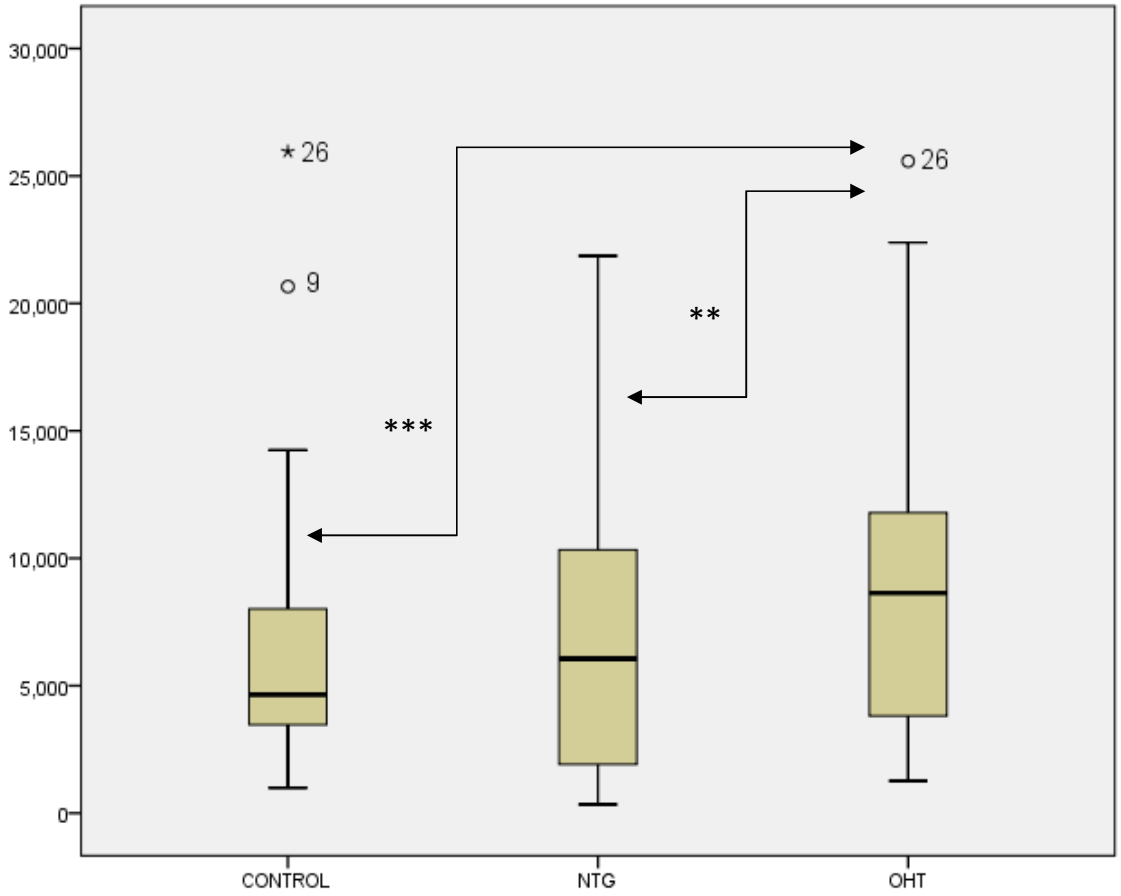

Fig 4.14: The rate of ATP synthesis by complex I in the lymphocytes of NTG, OHT patients and controls. The ATP synthesis rate is expressed in pmol/min/mg lysate.

Complex I: A statistically significant increase in the rate of ATP synthesis by complex I was noted in the OHT group [8632 pmol/min/mg, (3788 to 11798)] as compared to the NTG [6063 pmol/min/mg, (1810 to 10380)] and controls [4646 pmol/min/mg, (3438 to 8148)]. The difference between NTG and controls was not significant (p=0.804).

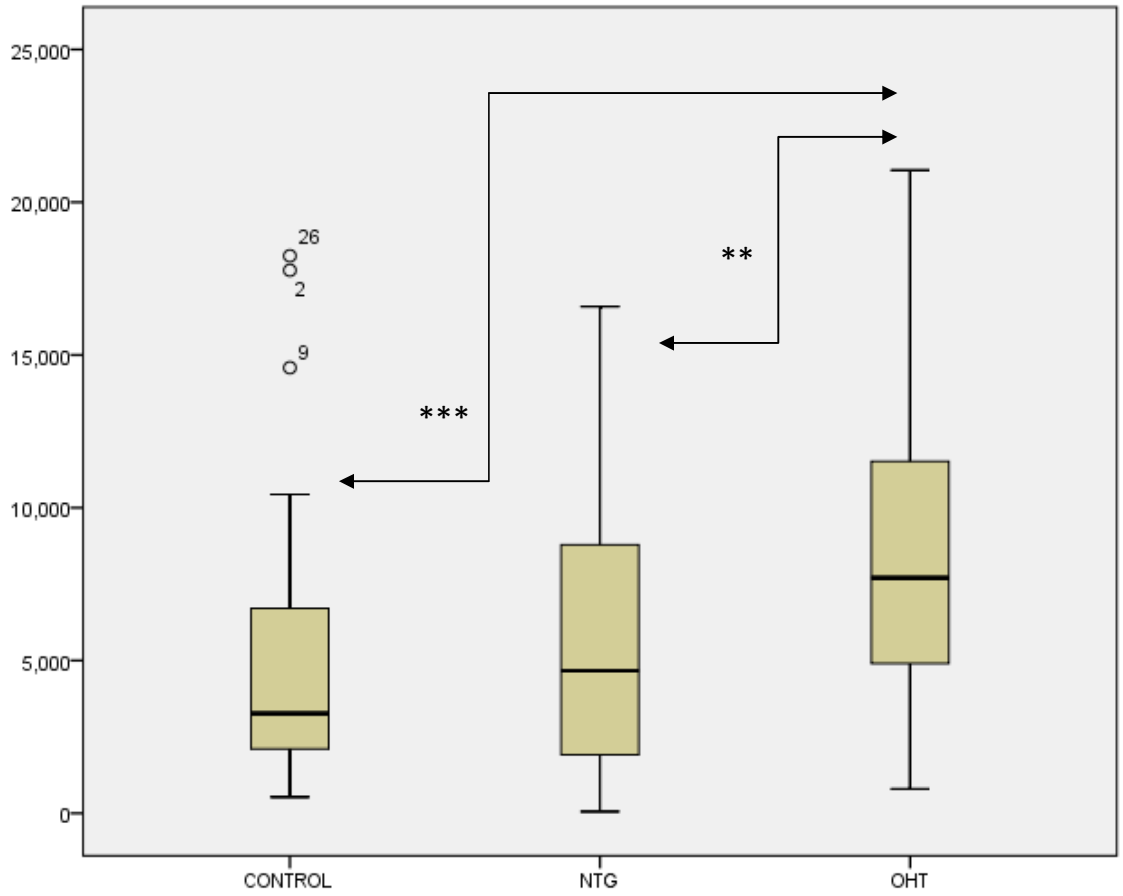

Fig 4.15: The rate of ATP synthesis by complexes II/III in the lymphocytes of NTG, OHT patients and controls. The ATP synthesis rate is expressed in pmol/min/mg lysate.

Complexes II/III: A statistically significant increase in the rate of ATP synthesis by complex I was noted in the OHT group [7709 pmol/min/mg, (4732 to 11640)] as compared to the NTG [4663 pmol/min/mg, (1896 to 8959)] and

controls [3627 pmol/min/mg, (1961 to 7086)]. The difference between NTG and controls was not significant (p=0.509).

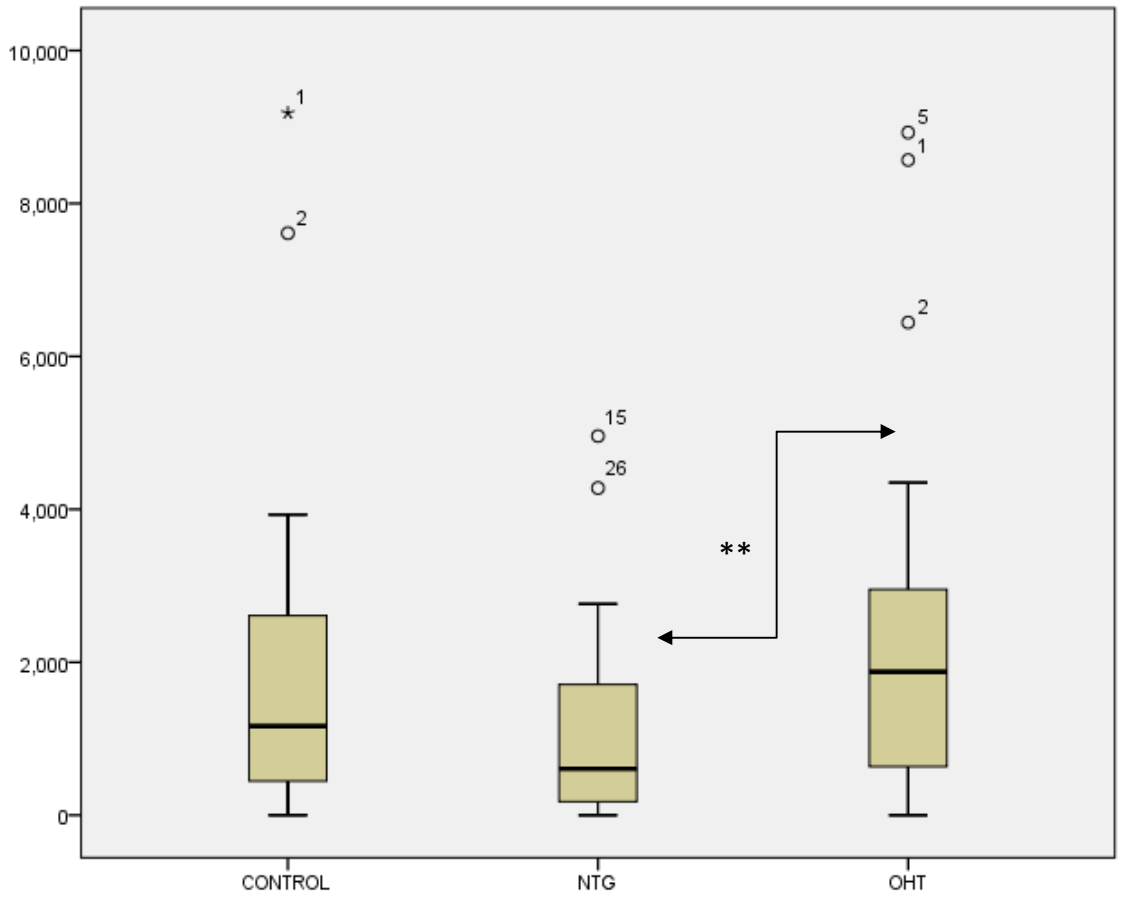

Fig 4.16: The rate of ATP synthesis by complex IV in the lymphocytes of NTG, OHT patients and controls. The ATP synthesis rate is expressed in pmol/min/mg lysate.

Complex IV: A statistically significant increase in the rate of ATP synthesis by complex IV was noted in the OHT group [1876 pmol/min/mg, (610 to 3019)] as compared to the NTG group [605 pmol/min/mg, (172 to 1772)]. The difference between controls [1166 pmol/min/mg, (442 to 2701)] and either NTG or OHT was not significant (p=0.102 and 0.382, respectively), although there was a trend for the NTG group to show lower levels of ATP, as compared to the

controls. Upon correction of the rate of ATP synthesis for mitochondrial content, as measured by porin, the complex IV-driven ATP synthesis was significantly lower in the NTG group, as compared to both the controls (p=0.03) and OHT subjects (p=0.005) (Fig 4.17). In the case of complex I and complexes II/III, upon porin correction all the significant differences in the rate of ATP synthesis noted between the OHT and the other two groups were maintained (data not shown), as described previously.

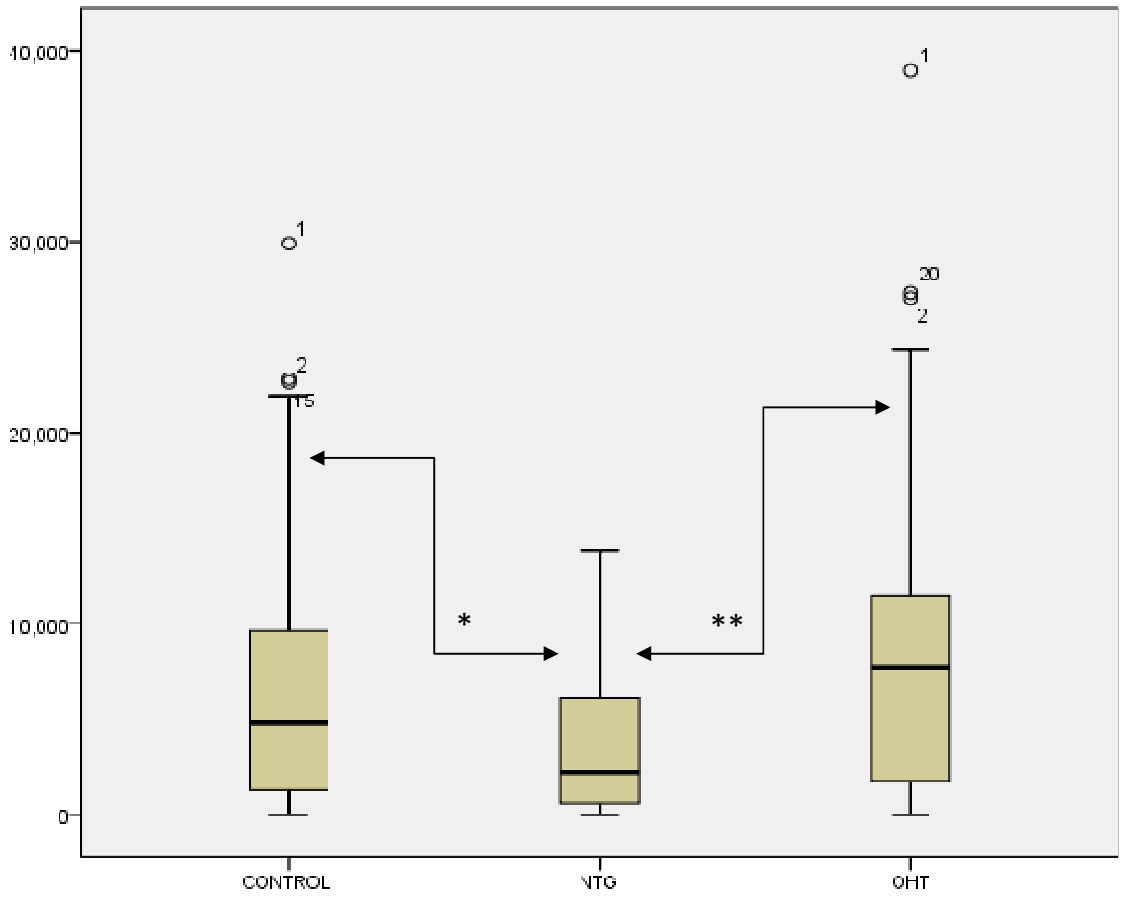

Fig 4.17: The rate of ATP synthesis by complex IV, after correction for porin, in the lymphocytes of NTG, OHT patients and controls. The ATP synthesis rate is expressed in pmol/min/mg lysate.

Discussion: These results suggest for the first time that, compared with the NTG and control groups, lymphocytes from the OHT group may have more efficient mitochondria, capable of producing more energy under conditions of unrestricted substrate supply, or contain a higher percentage of well functioning mitochondria per cell, as demonstrated by the higher levels of ATP produced by mitochondrial complexes I, II/III and IV. RGCs are known to be particularly vulnerable to OXPHOS impairment, especially in the presence of external stressors, such as raised IOP (Kong et al 2011), and the finding of good systemic mitochondrial function in OHT subjects may contribute to the reduced susceptibility of their RGCs and may be implicated in resistance to glaucomatous optic neuropathy and glaucoma progression. Similarly to the study by Lee et al (2012), discussed in more detail in section 1.6.1, complex II driven ATP synthesis was similar in our NTG cohort and the controls. However, unlike the latter study, which showed that POAG lymphoblasts have lower rates of complex I driven ATP synthesis, as compared to controls (Lee et al 2012), the results presented here do not support the presence of a significant defect in complex I in NTG. It should be noted though that the complex I defect in the study by Lee et al was not sufficient to impact negatively on the ability of the POAG lymphoblasts to grow in galactose media, where they were forced to rely on mitochondrial ATP production, and that the EBV-transformed lymphocytes (lymphoblasts) used by Lee et al. may behave differently from the unstimulated fresh lymphocytes employed in our cohort.

4.3.3.3 Mitochondrial Membrane Potential (steady-state TMRM staining)

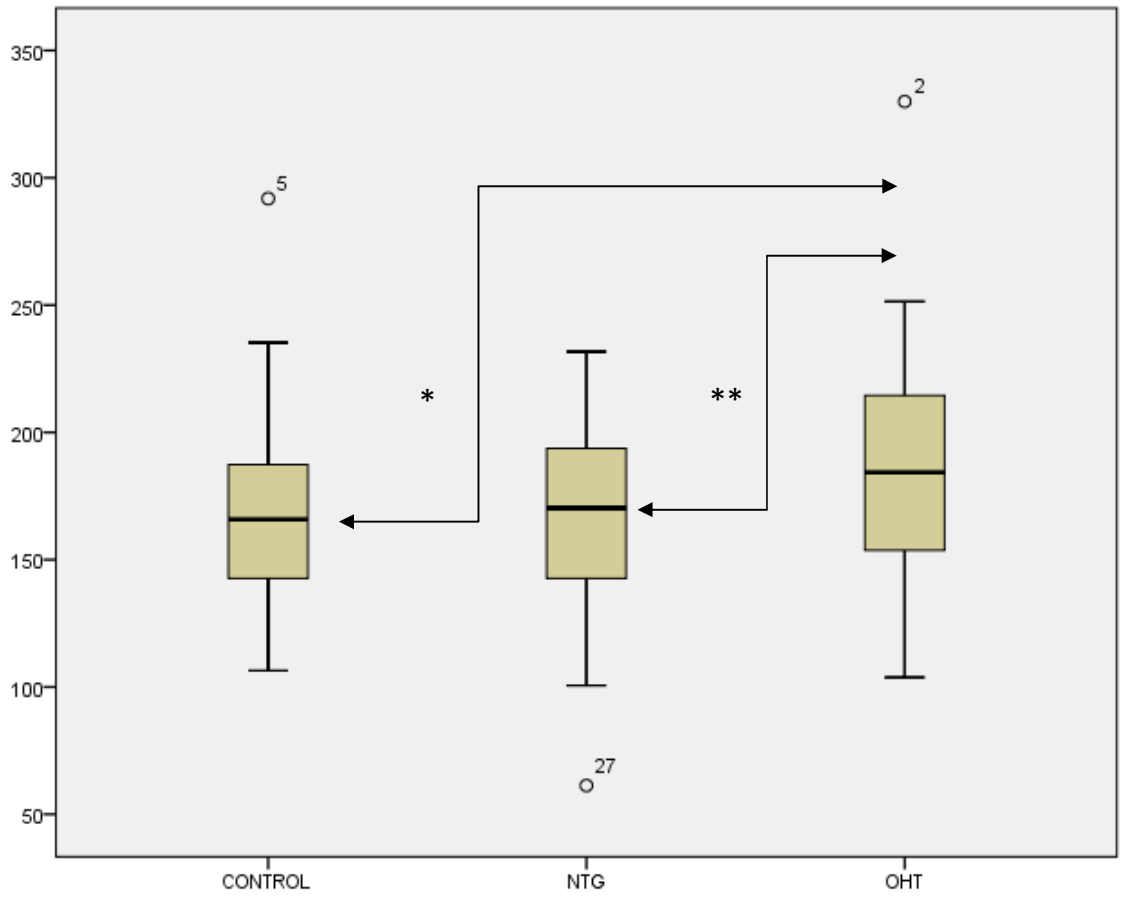

Fig 4.18: This graph presents the TMRM staining in the lymphocytes of controls and NTG and OHT patients. TMRM staining is expressed as the mean red fluorescence % change from Raji, which acts as an internal control (100%, not shown here).

The OHT lymphocyte TMRM staining [184% (152 to 215)] was significantly higher than that in the NTG [170% (140 to 196)] and control [166% (141 to 187)] groups. The difference between NTG and controls was not significant (p=0.716).

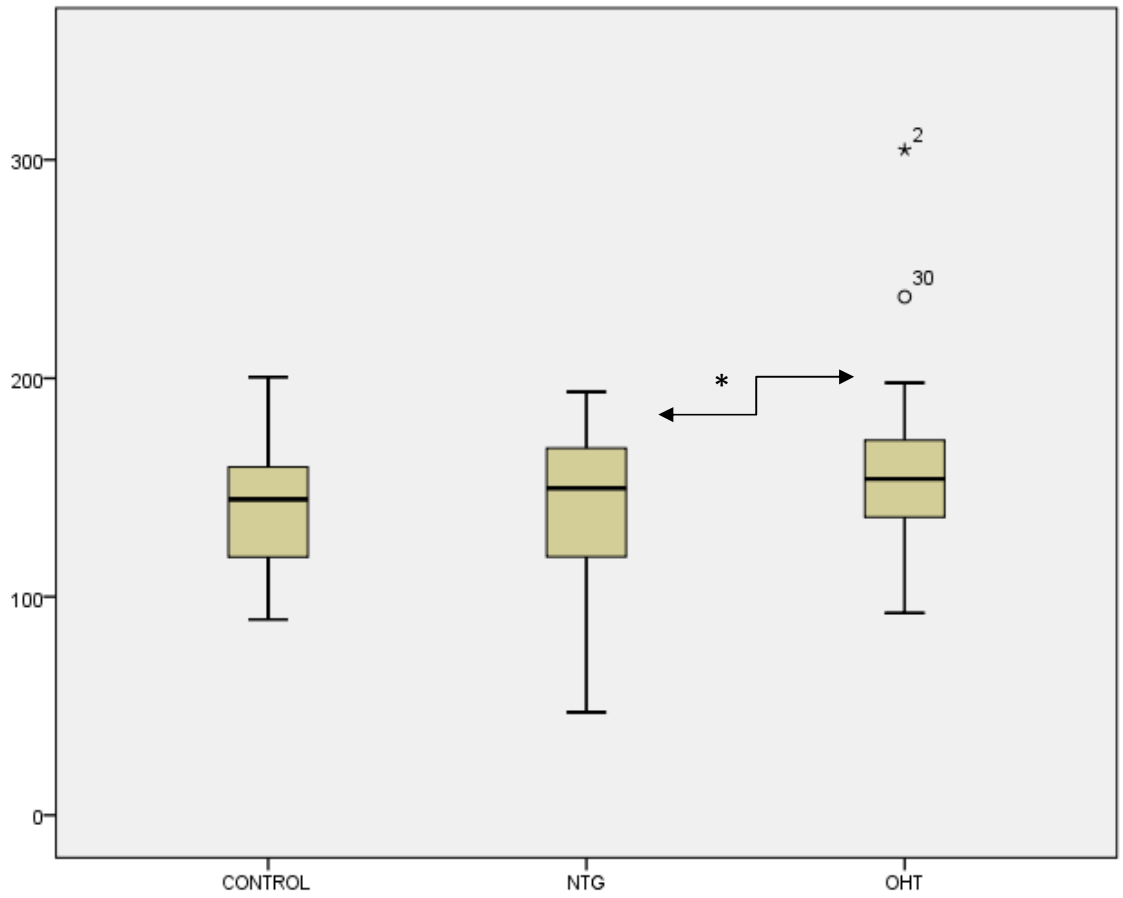

Fig 4.19: The TMRM staining in the lymphocytes of controls and NTG and OHT patients, upon rotenone treatment (0.5µM 24hrs). TMRM staining is expressed as the mean red fluorescence % change from Raji, which acts as an internal control (100%, not shown here).

Upon rotenone treatment, the TMRM staining for the control, NTG and OHT groups was significantly reduced to 145% (118 to 161) ($p<0.001$ comparing to baseline), 150% (115 to 169) ($p<0.001$) and 154% (134 to 173) ($p<0.001$), respectively. Even after rotenone treatment, the OHT group maintained higher levels of TMRM staining than the controls, although the difference was not significant ($p=0.062$), and significantly higher TMRM staining than the NTG group ($p=0.031$).

Discussion: These findings suggest for the first time that lymphocytes from the OHT group demonstrate a higher ΔΨm, as compared to the NTG and control groups. This finding is in line with the increased rate of ATP synthesis in the OHT group and in support of the idea that OHT patients demonstrate healthy and efficient systemic mitochondria, especially since the ΔΨm is a key indicator of mitochondrial function, as discussed in section 2.3.5. Interestingly, however, excessive increase in the ΔΨm is thought to be associated with slowed electron transport, particularly at complex III, prolonged ubiquinol occupancy in the complex and increased electron leak thus favouring ROS production (Zhang et al 2007), while uncouplers of OXPHOS, such as 2,4-dinitrophenol and mitochondrial uncoupling proteins (UCPs), a family of mitochondrial anion carriers that induce proton leak across the inner membrane, suppress the ΔΨm resulting in reduced ROS formation (Fink et al 2005, Duval et al 2002). Nevertheless, in view of the increased ATP production by various mitochondrial complexes (I, II/III and IV) in the OHT cohort, the overall increased ΔΨm reported in this group, as reflected by the TMRM staining, is unlikely to represent the presence of heavily hyperpolarised mitochondria in the OHT lymphocytes, and should be attributed to the presence of more efficient mitochondria or of a higher percentage of well functioning mitochondria per OHT lymphocyte. The increased TMRM staining in OHT could also represent an increase in mitochondrial content in this group, without necessarily an increase in the ΔΨm per mitochondrion, although this is not supported by the lack of any difference in mitochondrial content between the three groups, as measured by porin and citrate synthase enzymatic activity below (see section 4.3.3.6).

4.3.3.4 Calcium mobilisation

Fluo3 (Cytosolic calcium)

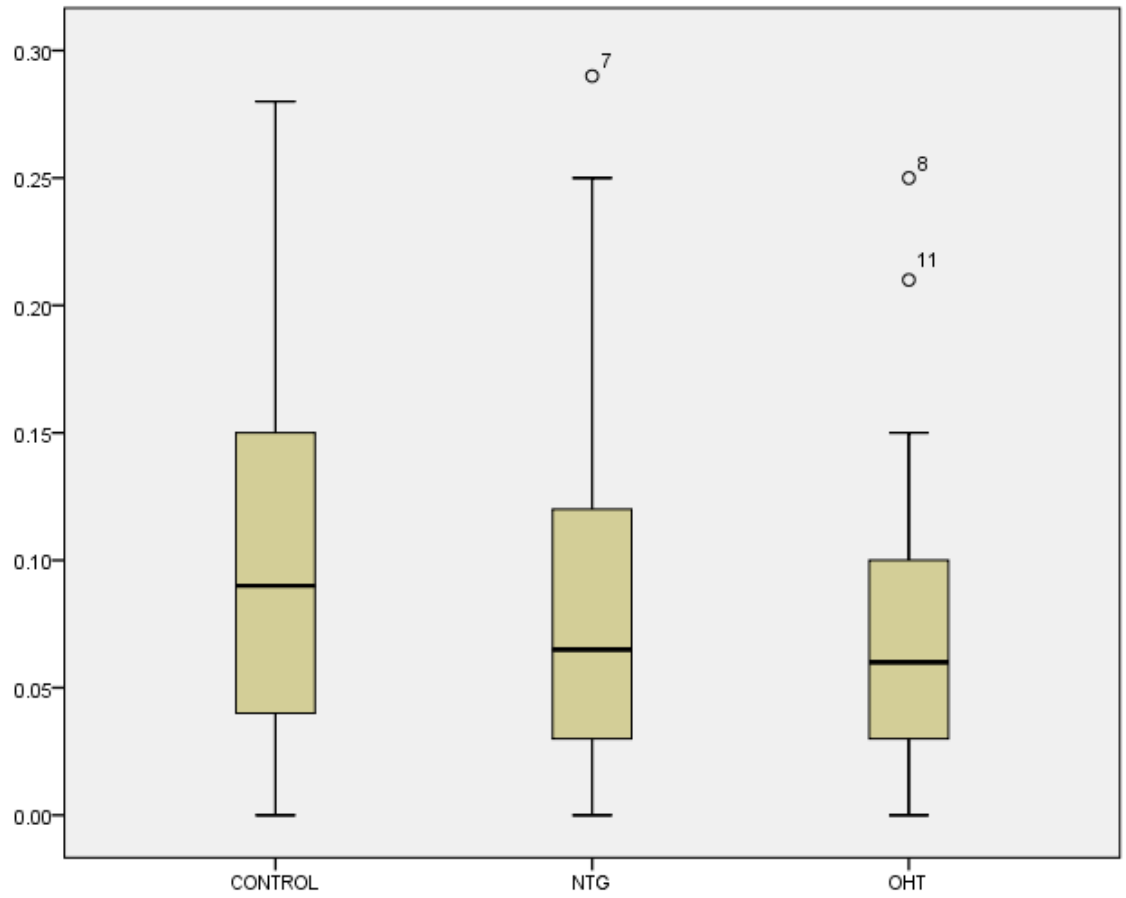

Fig 4.20: Graph showing the change in fluo3 fluorescence upon ionomycin treatment divided by the baseline fluo3 fluorescence (fluo3 ΔF/Fo) in the control, NTG and OHT lymphocytes.

The median (IQR) fluo3 ΔF/Fo for the control, NTG and OHT groups, was 0.09 (0.0375 to 0.15), 0.065 (0.03 to 0.125) and 0.06 (0.025 to 0.115), respectively. Although the difference between the three groups was not significant, the fluo3 ΔF/Fo was lowest in the OHT group. Smoking is known to impact negatively on lymphocytic mitochondrial function (section 4.3.2) and,

interestingly, in a *post-hoc* analysis for non-smokers (all study participants apart from 3 OHT subjects who were active smokers), the fluo3 ΔF/Fo in OHT subjects [0.05 (0.02 to 0.0825)] was significantly lower as compared to the controls (Fig 4.21 below), while there was no difference between NTG subjects and controls. The low fluo3 ΔF/Fo in the OHT lymphocytes would suggest the presence of less free Ca^{+2} in the cytosol after ionomycin treatment, which, in view of the aforementioned better ATP synthesis and ΔΨm in OHT, could potentially represent a better capacity of the OHT mitochondria to take up free Ca^{+2} from the cytosol.

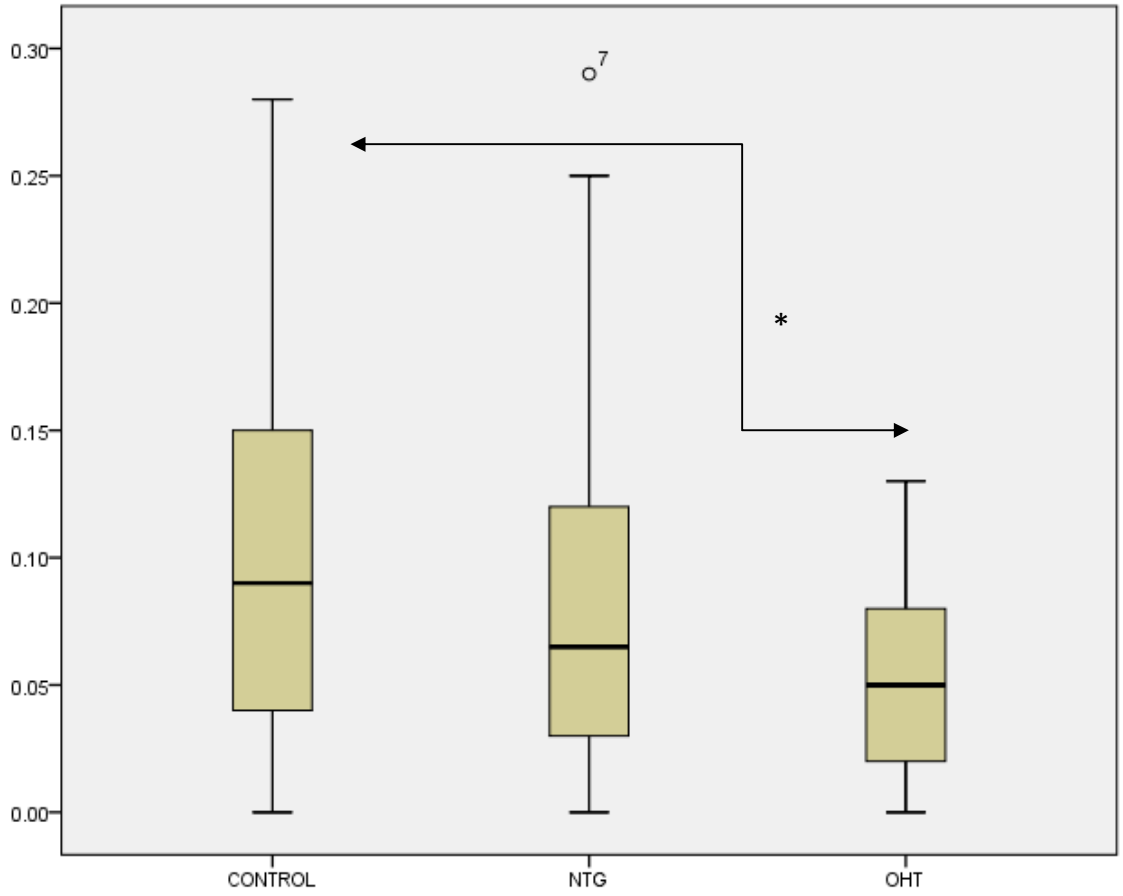

Fig 4.21: Graph showing the fluo3 ΔF/Fo for the control, NTG and OHT lymphocytes, in non-smokers.

Rhod 2 (Mitochondrial calcium)

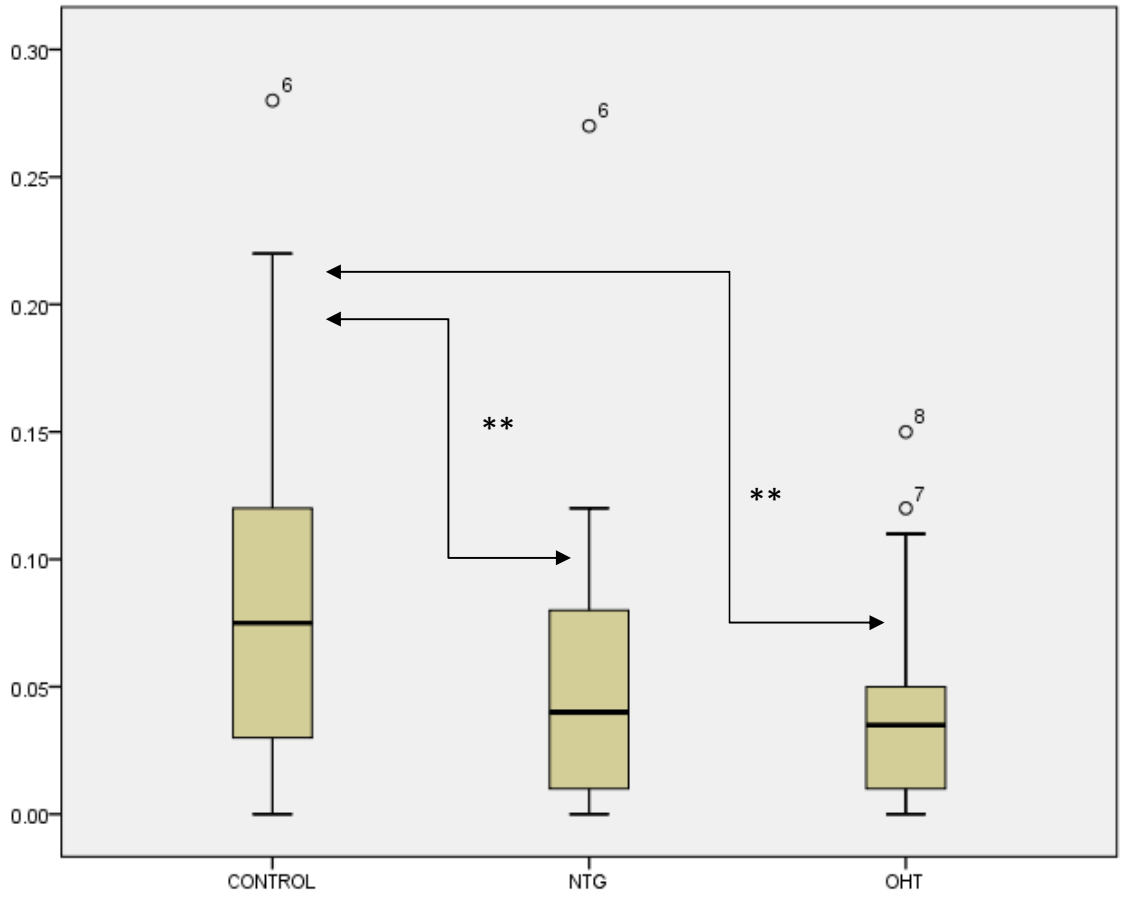

Fig 4.22: Graph showing the change in rhod2 fluorescence upon ionomycin treatment divided by the baseline rhod2 fluorescence (rhod2 ΔF/Fo) in the control, NTG and OHT lymphocytes.

The median (IQR) rhod2 ΔF/Fo for the control, NTG and OHT groups, was 0.075 (0.028 to 0.125), 0.04 (0.01 to 0.083) and 0.035 (0.075 to 0.053), respectively. A significant difference was noted between the control and the other two groups, while, similarly to the fluo3 ΔF/Fo above, the rhod2 ΔF/Fo was lowest in the OHT group. Again, in the absence of smokers, the rhod2 ΔF/Fo in OHT was further reduced [0.03 (0.00 to 0.04)], as compared to the control [0.075 (0.028 to 0.125)] and NTG [0.04 (0.01 to 0.083)] groups (Fig 4.23 below).

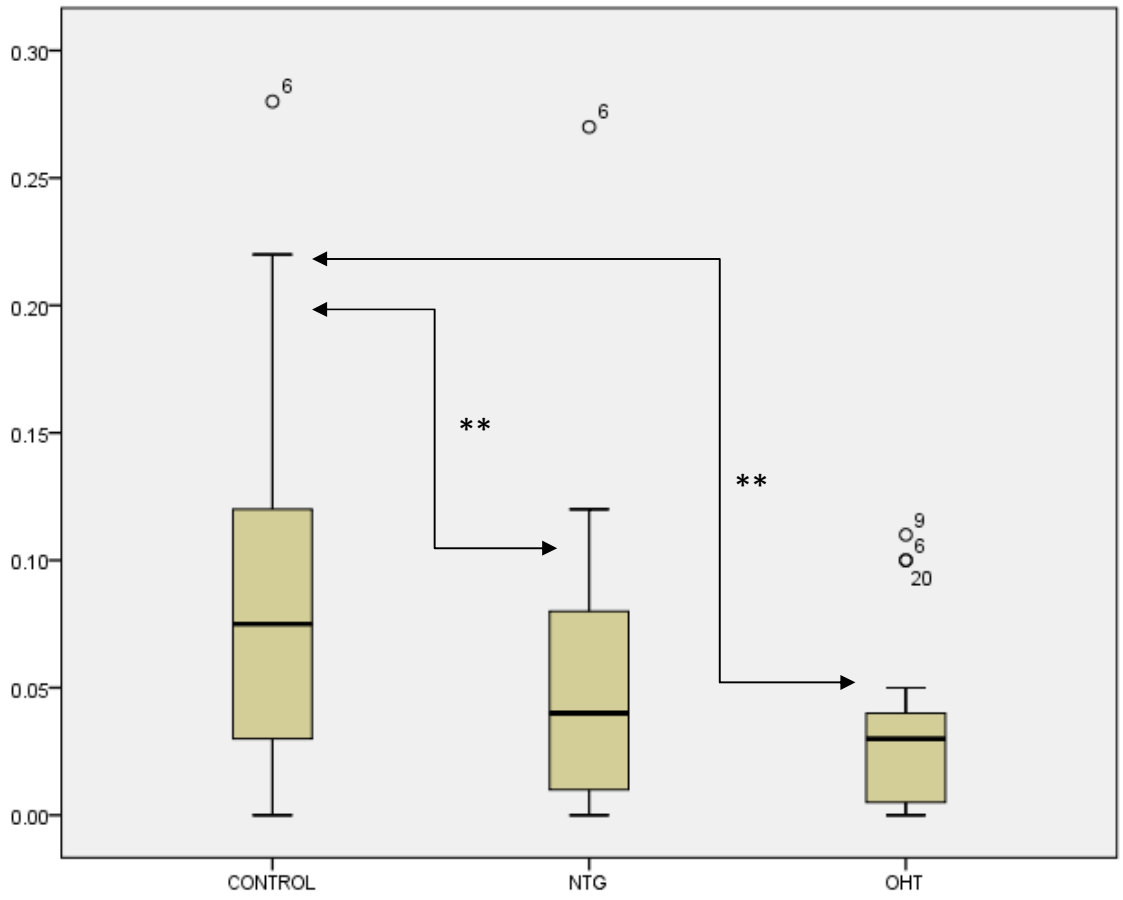

Fig 4.23: Graph showing the rhod2 ΔF/Fo for the control, NTG and OHT lymphocytes, in non–smokers.

The low rhod2 ΔF/Fo in the OHT lymphocytes would suggest the presence of less free mitochondrial Ca^{+2} after ionomycin treatment, which, in view of the aforementioned better ATP synthesis and ΔΨm in OHT, could potentially represent the better capacity of the OHT mitochondria to buffer free mitochondrial Ca^{+2}. Buffering capacity could be regarded as an additional measure of mitochondrial function, as explained in more detail in the discussion below. It is however difficult to explain why the rhod2 ΔF/Fo in NTG subjects was lower than in the control group, although ionomycin has been accused of inducing variable mitochondrial depolarisation in the acute phase in intact cells (Abramov et al 2003), thus causing unexpected changes to Ca^{+2}

kinetics. Perhaps, therefore, the changes described above (fluo3 ΔF/Fo and rhod2 ΔF/Fo) in the Ca^{+2} dynamics in the acute phase after ionomycin treatment may not be as representative as the changes during the more chronic phase (Δrhod2 chr / Δfluo3 chr), presented below.

Δrhod2 / Δfluo3 (chronic phase)

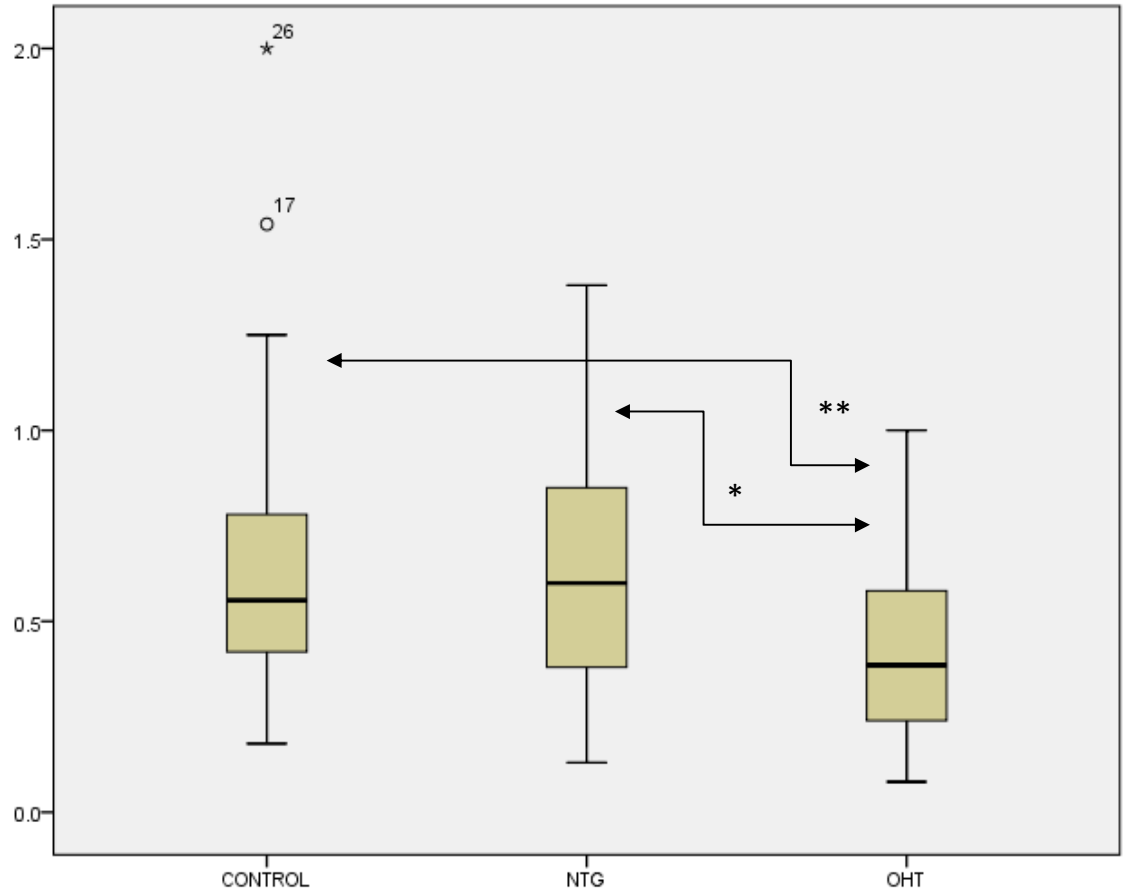

Fig 4.24: Graph showing the rate of increase in the rhod2 fluorescence during the chronic phase divided by the rate of increase in the fluo3 fluorescence during the same phase (Δrhod2 chr/ Δfluo3 chr) in the control, NTG and OHT lymphocytes.

The median (IQR) Δrhod2 chr/ Δfluo3 chr for the control, NTG and OHT groups, was 0.55 (0.41 to 0.79), 0.60 (0.37 to 0.88) and 0.39 (0.24 to 0.59),

respectively. A significant difference was noted between the OHT and the other two groups, while no difference was found between control and NTG (p=0.696). Similarly to the fluo3 ΔF/Fo and rhod2 ΔF/Fo above, the Δrhod2 chr/ Δfluo3 chr was lowest in the OHT group. In the absence of smokers, the Δrhod2 chr/ Δfluo3 chr in OHT [0.39 (0.28 to 0.58)] was again significantly lower, as compared to the control [0.55 (0.41 to 0.79)] and NTG [0.60 (0.37 to 0.88)] groups (Fig 4.25 below). The low Δrhod2 chr/ Δfluo3 chr in the OHT lymphocytes would suggest a relative reduction in free mitochondrial Ca^{+2} and relative increase in free cytosolic Ca^{+2} during the chronic phase of calcium mobilisation following ionomycin treatment. Again, this could potentially be interpreted as reflecting a better capacity of the OHT mitochondria to buffer free mitochondrial Ca^{+2}. Alternatively, this could also reflect a better function of the mitochondrial calcium uniporter (MCU) in the OHT lymphocytes, as explained in more detail in the discussion below.

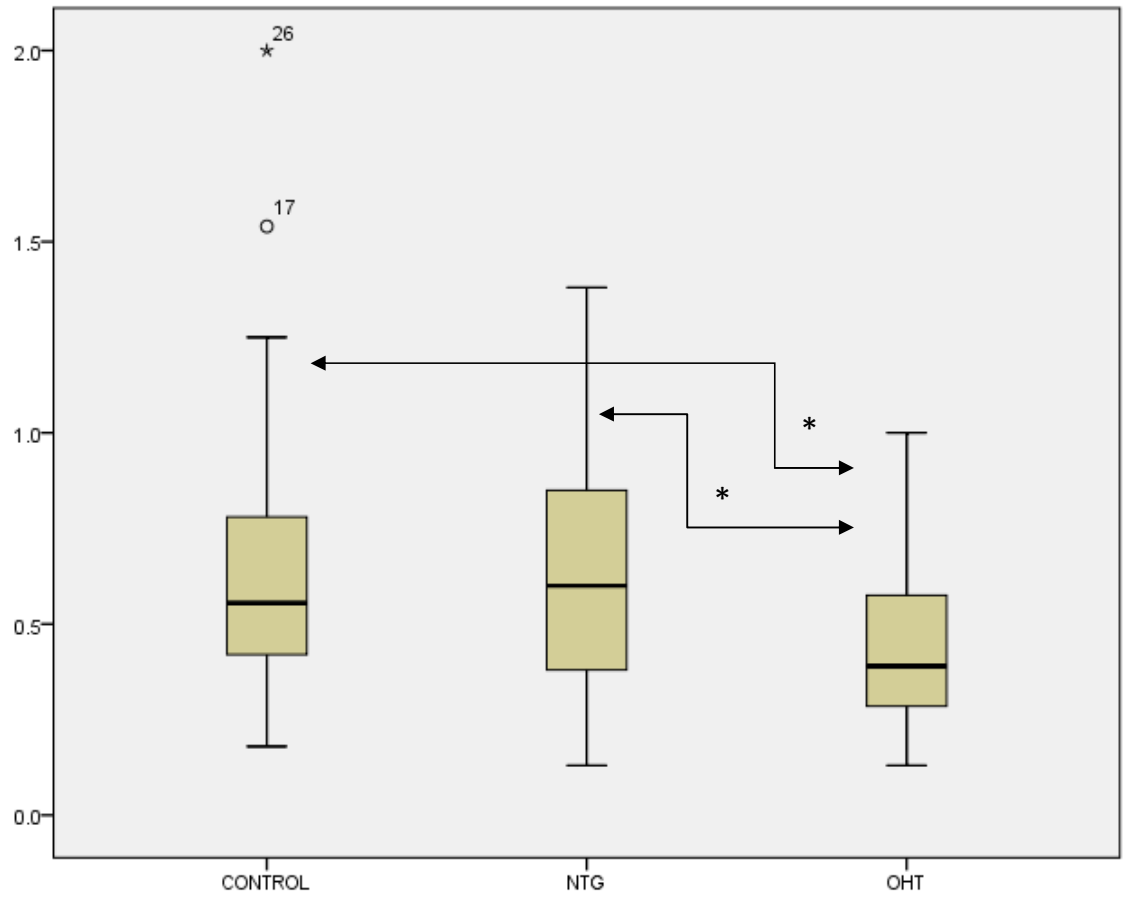

Fig 4.25: Graph showing the Δrhod2 chr/ Δfluo3 chr for the control, NTG and OHT lymphocytes, in non–smokers.

Discussion: In summary, these results highlight the enhanced capacity of the OHT mitochondria both to take up free Ca^{2+} (fluo3 ΔF/Fo), especially in non-smokers, and to buffer free Ca^{2+} (rhod2 ΔF/Fo and Δrhod2 chr/ Δfluo3 chr). The main transporter involved in the uptake of Ca^{2+} into the mitochondria is the MCU, an inner mitochondrial membrane (IMM)-located channel driven by the IMM electrochemical gradient (Kirichok et al 2004, De Stefani et al 2011, Bragadin et al 1979). Importantly, a biphasic effect of Ca^{2+} on the MCU has been reported: beyond a certain level, cytosolic Ca^{2+} inactivates the uniporter, preventing further Ca^{2+} uptake and this process might prevent an excessive accumulation of the cation in the mitochondria (Moreau et al 2006). Perhaps in

efficiently functioning mitochondria, such as in the OHT group, this compensatory mechanism remains intact after the ionomycin insult, thus protecting the OHT mitochondria from excessive influx of Ca^{2+}, while in less healthy mitochondria, such as in the Control and NTG groups, this mechanism is less efficient leading to overloading of the mitochondria with Ca^{2+} and increasing the Δrhod2 chr/ Δfluo3 chr. This overloading is known to lead to the opening of the mitochondrial permeability transition pore (mPTP) and cause cell death either by energetic collapse and ATP depletion or by initiating mitochondrial swelling (Giorgi et al 2008, Abramov et al 2003). Interestingly, a link between normal MCU function and intact mitochondrial metabolic activity has been suggested, and our ATP results would support this hypothesis. Evidence for this link can be obtained from a recent study from Perocchi et al, who demonstrated that silencing MICU1 (mitochondrial calcium uptake 1), a key regulator of MCU, abolishes Ca^{2+} entry in intact and permeabilised cells, and attenuates the metabolic coupling between cytosolic Ca^{2+} transients and activation of mitochondrial matrix dehydrogenases (Perocchi et al 2010).

Another explanation for finding that free mitochondrial Ca^{2+} was lower in the OHT lymphocytes, as compared to NTG and controls, is the capacity of the mitochondria under physiological conditions to buffer mitochondrial Ca^{2+} (Hoth et al 1997, Babcock et al 1997). This can be achieved either by interaction of mitochondrial Ca^{2+} with negatively charged intramitochondrial polyphosphates (PolyPs), strong chelators of divalent cations known to form complexes with Ca^{2+} and play an important role in cellular metabolism, or by efficient export of mitochondrial Ca^{2+} into the cytosol. The results presented here could imply that the healthy mitochondria in the OHT group are more capable of buffering mitochondrial Ca^{2+}, thus reducing the amount of free Ca^{2+} that can be detected by rhod2. PolyPs participate in the regulation of gene expression, protect cells

from the toxicity of heavy metals by forming complexes with them and participate in channel formation through assembly into complexes with polyhydroxybutyrate (PHB) and Ca^{2+} (polyP/Ca2+/PHB complex) (Reusch 1989). Importantly, the presence of abundant PolyPs in the OHT mitochondria would be in line with the better mitochondrial function noted in the OHT group, since PolyPs are known to directly bind to mitochondrial proteins and regulate their activities, and are required for normal function of the respiratory chain, especially Complex IV (Abramov et al 2007). Also, calcium export from the mitochondria into the cytosol is achieved via multiple mechanisms, including an electroneutral Na^{+}/Ca^{2+} exchanger (Crompton et al 1976, Gunter et al 1990) and our data could suggest that such mechanisms are more efficient in the healthier mitochondria of the OHT group, as compared to those from NTG patients and controls.

4.3.3.5 Mammalian Target of Rapamycin (mTOR) activity

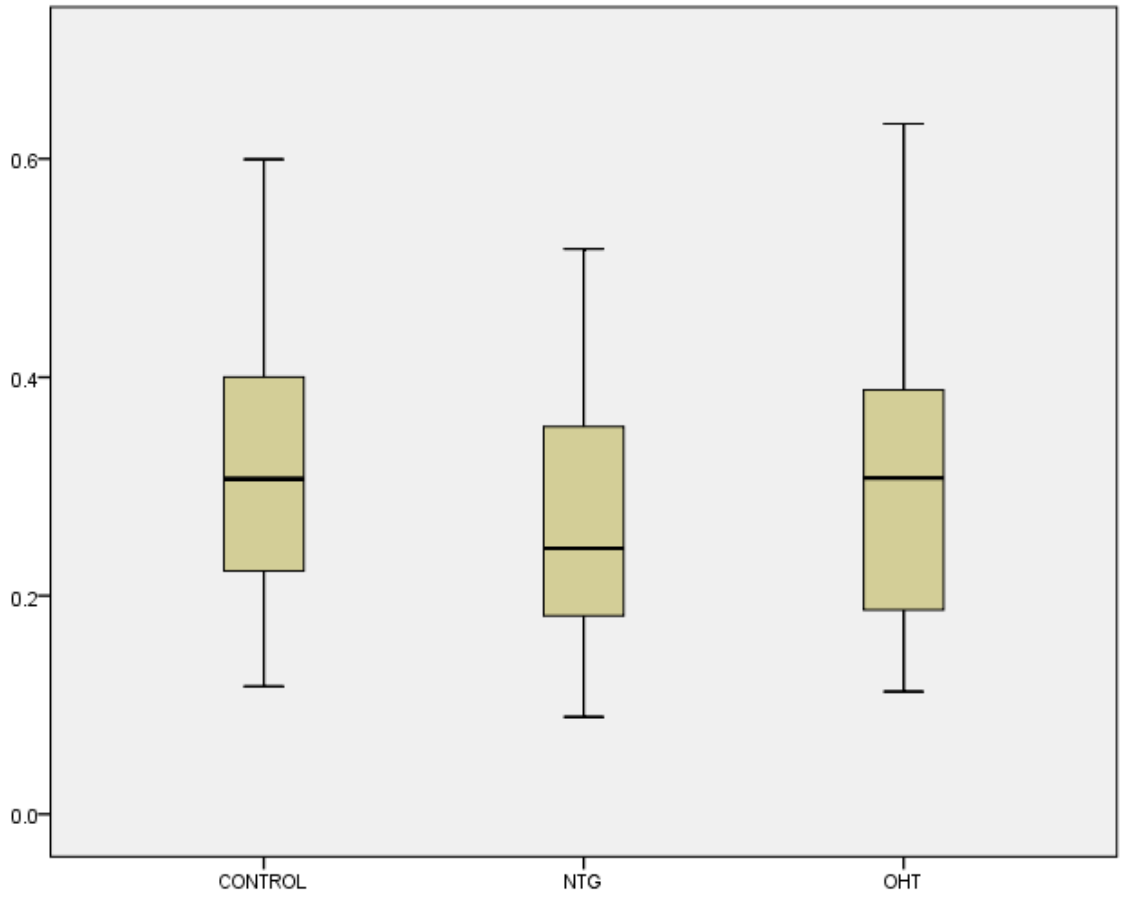

Fig 4.26: The mTOR activity, expressed as the ratio between phosphorylated (active) mTOR and total mTOR, in the control, NTG and OHT lymphocytes.

The median (IQR) mTOR activity in the control, NTG and OHT groups, was 0.307 (0.21 to 0.42), 0.243 (0.18 to 0.36) and 0.308 (0.19 to 0.40), respectively. There was a trend for the NTG cohort to have lower mTOR activity, as compared to the other two groups, although no statistically significant difference was noted between the three groups. Interestingly, activation of the mTOR pathway is known to mediate vasospastic phenomena (Zhang et al 2012) and in a *post hoc* analysis of a subgroup of patients without history of vasospasm/Raynaud's (all participants apart from 6 NTG subjects), a statistically significant reduction in the mTOR activity was noted in the NTG

subjects [0.229 (0.15 to 0.33)], as compared to the controls [0.307 (0.21 to 0.42)] (Fig 4.27 below). When the 3 OHT smokers were removed from the analysis, the median (IQR) in the OHT group increased from 0.308 (0.19 to 0.40) to 0.320 (0.21 to 0.40), further supporting the link between smoking, mTOR inhibition and lymphocytic mitochondrial dysfunction.

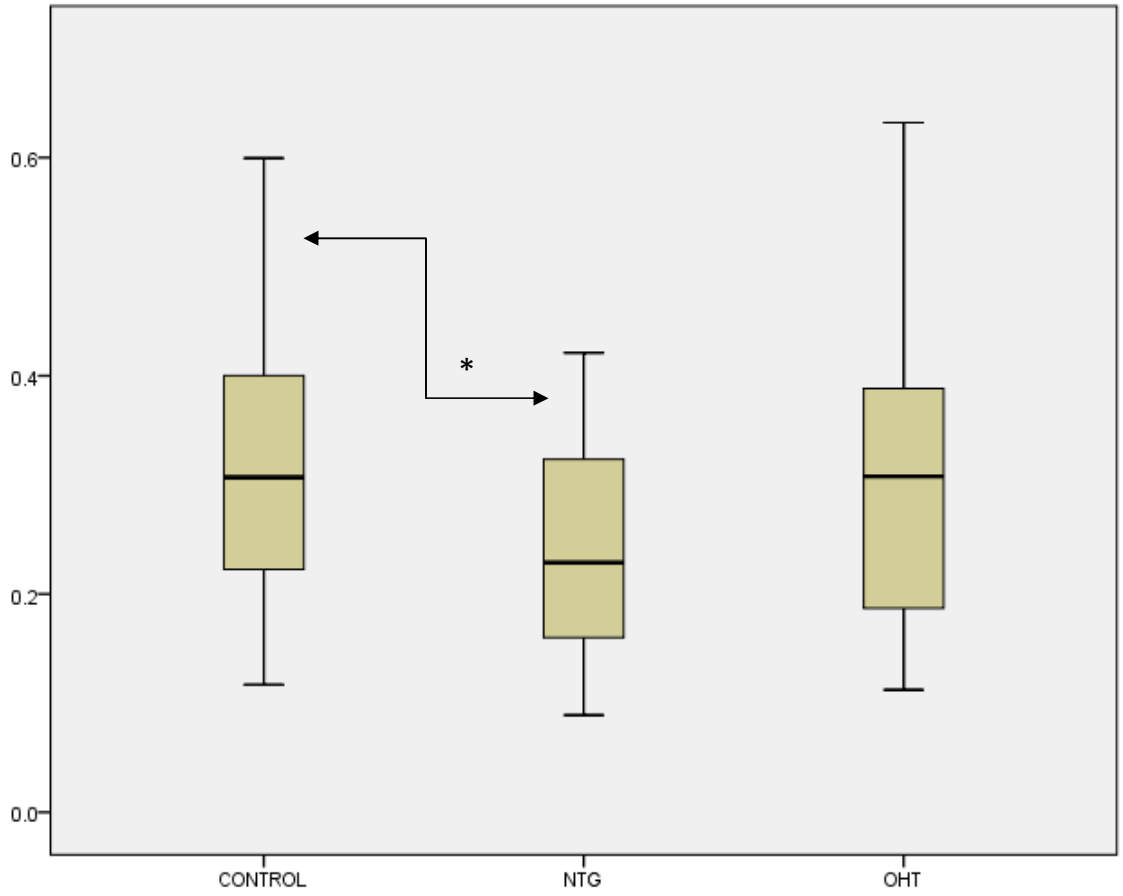

Fig 4.27: The mTOR activity in the control, NTG and OHT lymphocytes, in subjects without history of vasospasm-Raynaud's.

Discussion: As discussed in more detail in section 2.3.11, mTOR colocalises with the outer mitochondrial membrane (Desai et al 2002) and mTOR suppression has been found to result in increased autophagy, reduced mitochondrial function (Ramanathan et al 2009) and decreased mitochondrial respiration (Schieke et al 2006). Based on this relationship between mTOR activity and

mitochondrial function, the reduced mTOR activity in the lymphocytes of the NTG patients would suggest for the first time that mTOR dysfunction may be implicated in the pathogenesis of NTG and could shed some light to the link between mitochondrial dysfunction and glaucoma, at a cellular mechanistic level.

The link between mTOR and vasospasm is a very novel and interesting one. mTOR inhibitors have been shown to decrease hypoxia inducible factor 1α (HIF1α) levels (Carew et al 2011, Faivre et al 2006), while HIF1a inhibition is known to reduce the cerebral vasospasm following subarachnoid haemorrhage in rats and attenuate the expression of its downstream target vascular endothelial growth factor (VEGF) (Yan et al 2006). VEGF is a potent stimulant of angiogenesis and is involved in the pathogenesis of cerebral vasospasm (Bhardwaj 2003, Borel et al 2003, McGirt et al 2002). Also, in the recent study by Zhang et al (2012), treatment with the mTOR inhibitors rapamycin and AZD8055 led to the attenuation of angiographic vasospasm and improvement in clinical behavioral scores. The results presented in this thesis support the above link between mTOR and vasospasm, possibly mediated via HIF1a and VEGF, and highlight for the first time this link in humans with glaucoma.

4.3.3.6 Mitochondrial content

TOM20

TOM20 (Translocase of the Outer Membrane 20 or Mitochondrial import receptor subunit tom20) is a 20kDa outer mitochondrial membrane protein that forms a central component of the receptor complex responsible for the recognition and translocation of cytosolically synthesised mitochondrial

preproteins. Together with TOM22 it functions as the transit peptide receptor at the surface of the mitochondrial outer membrane and is a well known measure of mitochondrial content (Goping et al 1995, Likic et al 2005).

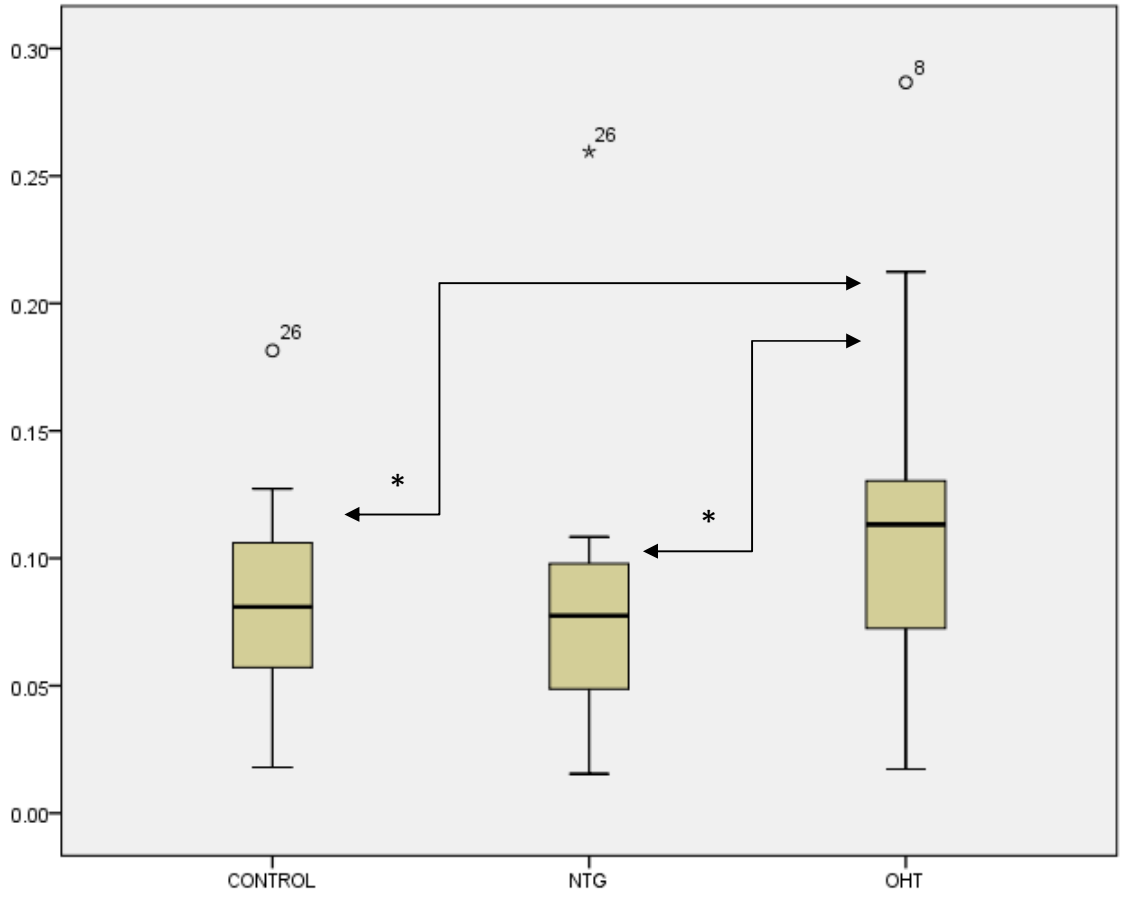

Fig 4.28: Graph showing the protein levels of TOM20 in the control, NTG and OHT lymphocytes. TOM20 is expressed as a percentage of Raji (100%, not shown here), which served as an internal control.

The median (IQR) TOM20 levels in the control, NTG and OHT groups, were 0.08 (0.57 to 0.11), 0.08 (0.04 to 0.10) and 0.11 (0.07 to 0.13). Interestingly, the levels of TOM20 were significantly higher in the OHT group, as compared to the other two groups, while no statistically significant difference was noted between the NTG and control (p=0.381) (Fig 4.29).

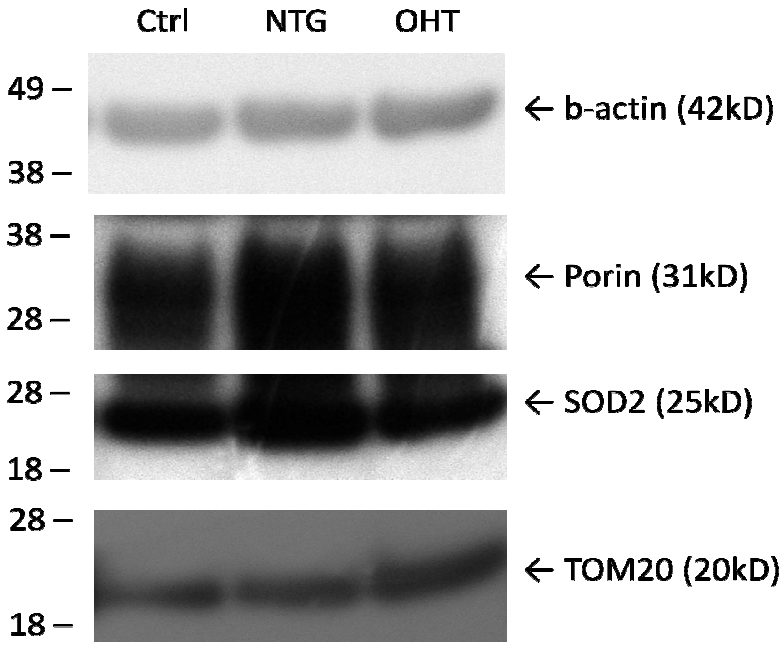

Fig 4.29: Representative western blot bands for TOM20, porin and SOD2, as well as for the loading control (b-actin).

Porin

Another established marker of mitochondrial content is porin, also known as voltage-dependent anion channel (VDAC), the most abundant protein in the mitochondrial outer membrane (Linden et al 1984). It has highly conserved structural and electrophysiological characteristics across plant, yeast, mouse and human species, with mammals having three VDAC isoforms encoded by separate autosomal genes (Sampson et al 1997). Mitochondrial porins play a significant role in diverse cellular processes, including diffusion of small hydrophilic molecules across the outer mitochondrial membrane, and regulation of mitochondrial ATP and calcium flux, and participate in the formation of the permeability transition pore complex (PTPC) responsible for the release of mitochondrial products that trigger apoptosis (Crompton et al 1998). Porins are also present in other cellular membranes, including in

caveolae and the plasma membrane, where they are involved in cell volume regulation and apoptosis (Bathori et al 1999).

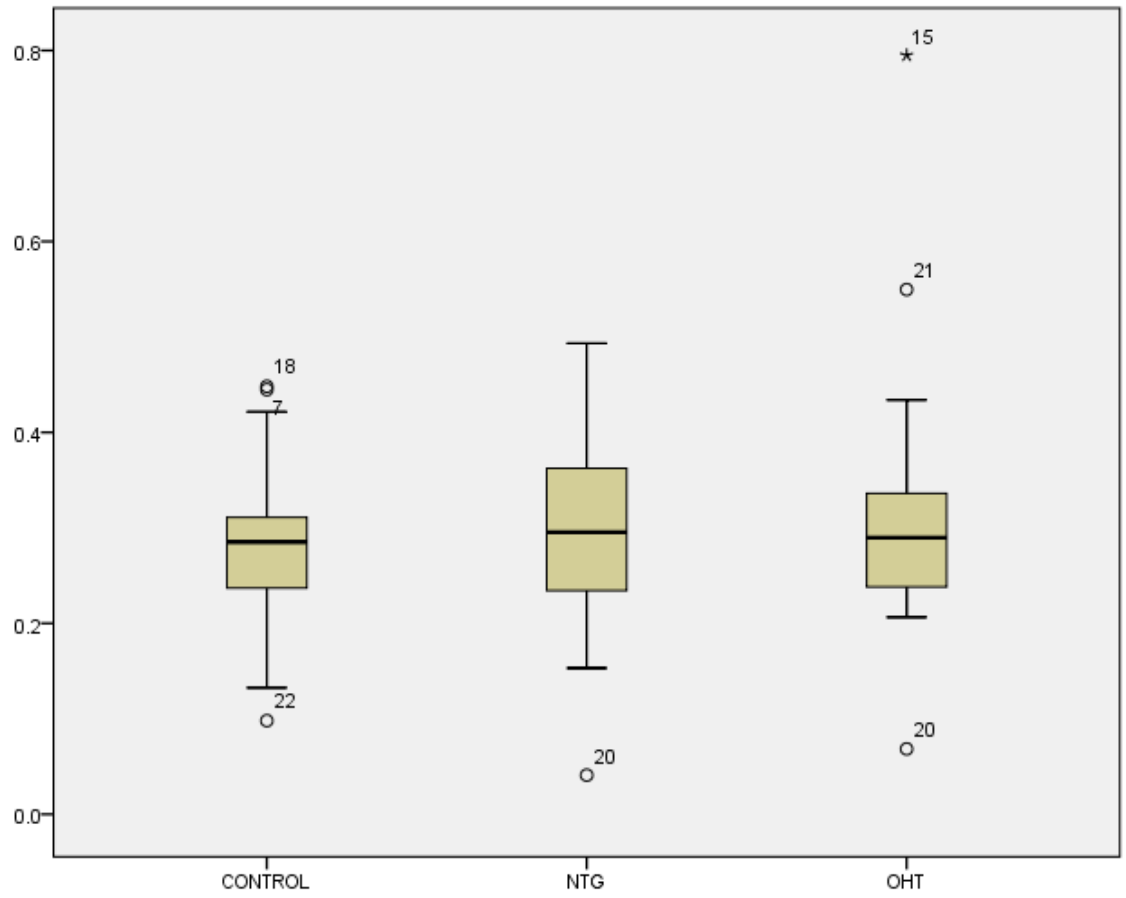

Fig 4.30: Graph showing the protein levels of porin in the control, NTG and OHT lymphocytes. Porin is expressed as a percentage of Raji (100%, not shown here), which served as an internal control.

The median (IQR) porin levels in the control, NTG and OHT groups, were 0.29 (0.24 to 0.32), 0.30 (0.23 to 0.37) and 0.29 (0.24 to 0.34). No statistically significant difference was noted in porin levels between the three groups (Fig 4.29).

Citrate synthase

As discussed in section 2.3.9, citrate synthase (CS), unlike TOM20 and porin, is localised in the mitochondrial matrix and is commonly used as a quantitative marker enzyme for the content of intact mitochondria (Holloszy et al 1970, Williams et al 1986). Due to its location in the mitochondria, it is thought to be less influenced by mitophagy and processes involved in mitochondrial damage, as compared to TOM20 and porin. CS is an integral enzyme in the Krebs cycle, where it catalyses the condensation of acetyl coenzyme A and oxaloacetate to form citrate (acetyl-CoA + oxaloacetate + H2O → citrate + CoA-SH), and thus its activity is considered to be less affected by changes in mitochondrial metabolism, including OXPHOS and glycolysis.

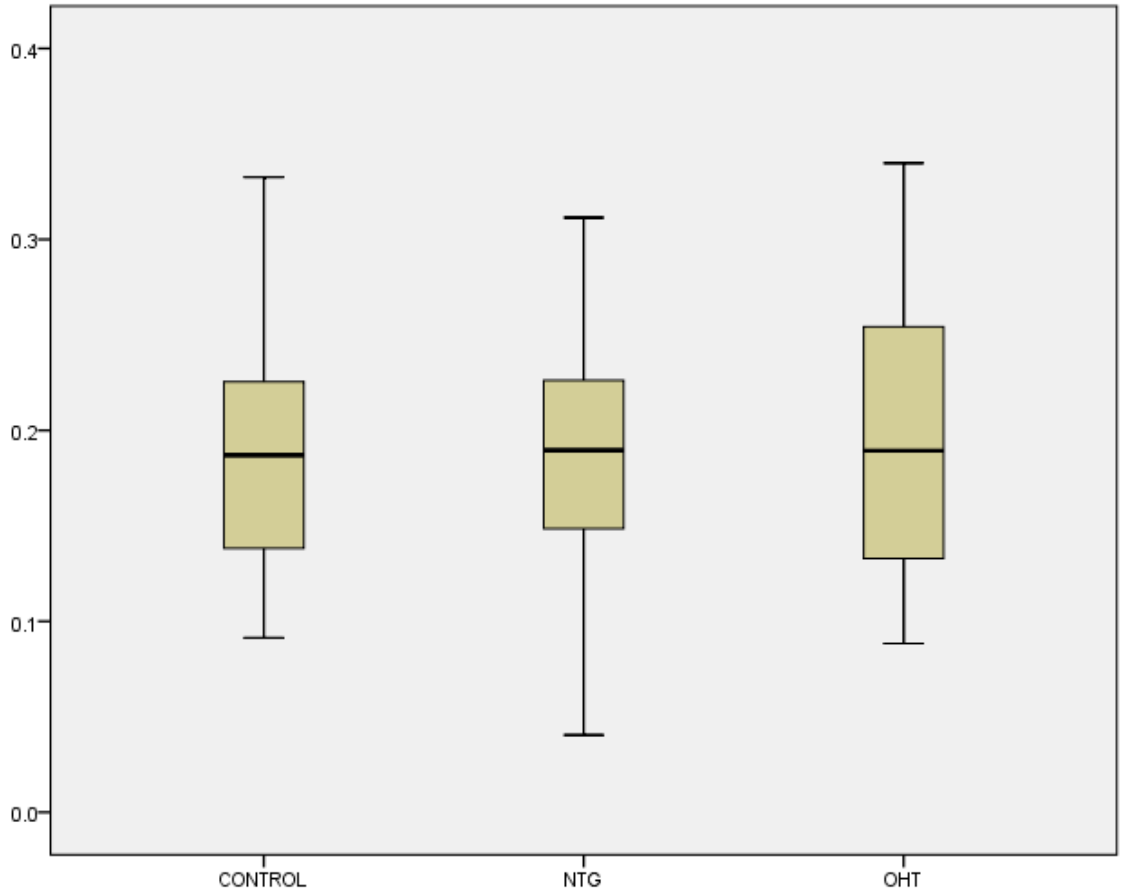

Fig 4.31: Graph showing the citrate synthase (CS) activity in the control, NTG and OHT lymphocytes. CS enzymatic activity is expressed in µmol/min/mg.

The median (IQR) CS activity in the control, NTG and OHT groups, were 0.19 (0.14 to 0.23), 0.19 (0.15 to 0.23) and 0.19 (0.13 to 0.26). Similarly to porin, no statistically significant difference was noted in the CS activity between the three groups.

Discussion: In summary, these results demonstrate no significant change in mitochondrial content, as demonstrated by porin levels and CS activity, thus suggesting that a functionally efficient mitochondrial electron transport chain may be a critical mechanism underlying the increased ATP synthesis and high ΔΨm noted in OHT, rather than any net increase in mitochondrial content *per se*. Interestingly, the TOM20 levels in OHT were increased, as compared to the other two groups. Since TOM20 is an important and specific component of an outer mitochondrial membrane receptor complex, this increase in OHT may reflect a selective increase in processes involving the outer mitochondrial membrane. Interestingly, increased density of theTOM20 clusters has recently been found to be associated with a higher mitochondrial activity and higher mitochondrial membrane potential (Wurm et al 2011), thus further supporting the finding of increased ATP and ΔΨm in OHT subjects. This correlation was demonstrated in cells of different species origin with distinct physiological activities (different respiratory rates, doubling times, and cytochrome c oxidase activities), as well as in cells grown to different densities. However, unlike CS, which is located in the matrix, TOM20 would be expected to be more influenced by mitophagy and other outer membrane processes involved in mitochondrial damage, as well as by changes in mitochondrial metabolism.

It is perhaps interesting to note that this lack of correlation between enhanced mitochondrial function and increased mitochondrial content noted in our OHT cohort has recently been confirmed in the context of diet restriction (DR)

(Hempenstall et al 2012). In this study, DR was able to induce PGC-1α, a marker of mitochondrial biogenesis, and increase mitochondrial respiration in mouse skeletal muscle, but without increasing mitochondrial content, as determined by CS activity (Hempenstall et al 2012), although other studies have shown an increase in CS activity following DR (Lopez-Lluch et al 2006). Interestingly, another study has been unable to demonstrate a change in CS activity in DR, while other markers of mitochondrial content and biogenesis were significantly increased (Civitarese et al 2007), with the authors suggesting that mtDNA level or other non-enzymatic structural markers of mitochondrial content (such as cardiolipin) may be better indicators of mitochondrial content than enzymatic CS activity. To provide a link with glaucoma, DR mice have recently been found to show greater recovery in inner retinal function following IOP challenge, as compared to age-matched *ad libitum* fed controls. DR was also associated with reduced oxidative stress levels (HO-1 and HNE) following injury and improved mitochondrial OXPHOS enzymatic activity (complex IV), as compared with *ad libitum* controls, with no significant change in CS activity (Kong et al 2012). DR is thought to promote mitochondrial biogenesis and extend life-span by inducing the expression of eNOS (Nisoli et al 2005) and the SIRT1 deacetylase (Cohen et al 2004) and it remains to be seen whether the same mechanisms that become activated in the mitochondria of DR mice operate in the mitochondria of OHT patients or whether DR is a more common lifestyle factor in OHT patients.

4.3.4 Measurements relating to oxidative stress and antioxidant defence

4.3.4.1 Dihydroethidium (DHE) staining

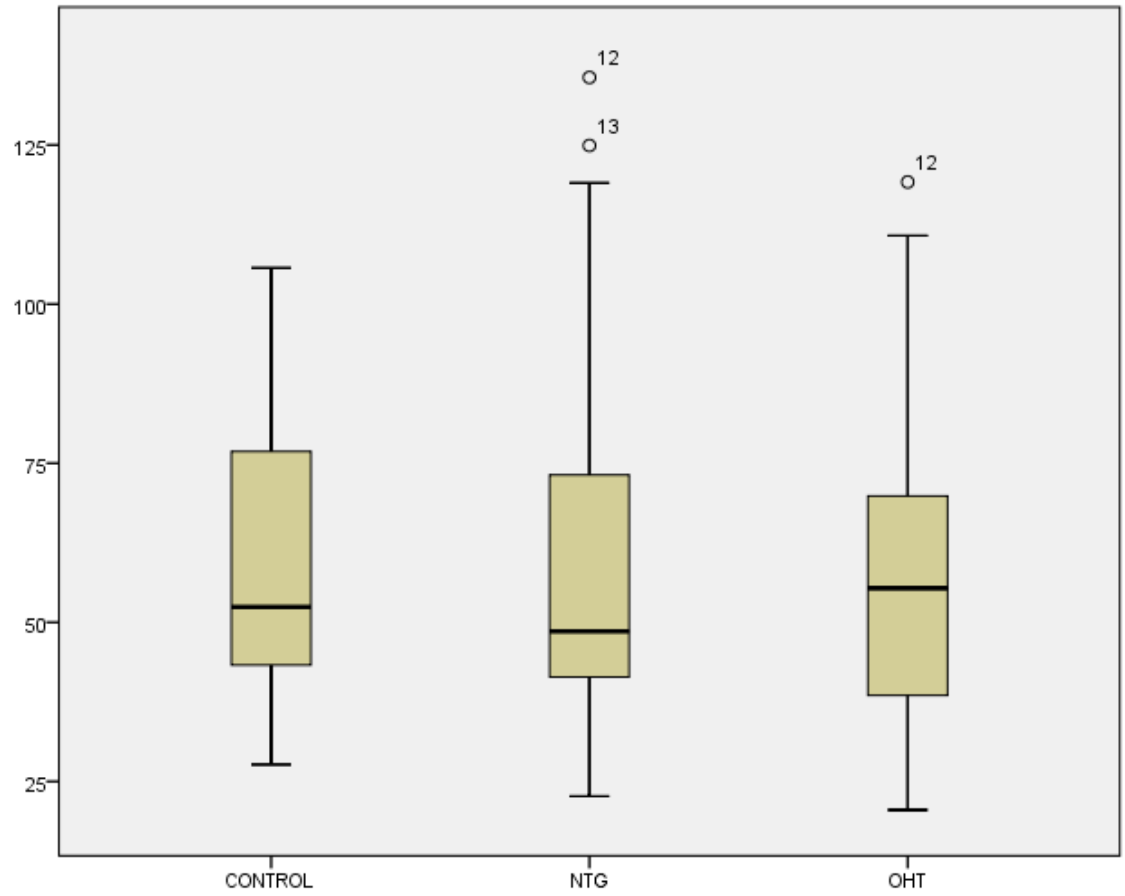

Fig 4.32: Graph showing the percentage change in the rate of DHE oxidation in the lymphocytes from control, NTG and OHT subjects at baseline (before treatment with 0.5µM rotenone for 24hrs). The results are expressed as the percentage change from Raji (100%, not shown), which served as an internal control.

The median (IQR) level of DHE staining in the control, NTG and OHT lymphocytes was 52.4% (42.3 to 77.1), 48.6% (41.3 to 74.6) and 55.4% (38.3 to 70.0), respectively. No statistically significant difference was noted between the three groups, suggesting similar baseline superoxide levels between control, NTG and OHT lymphocytes.

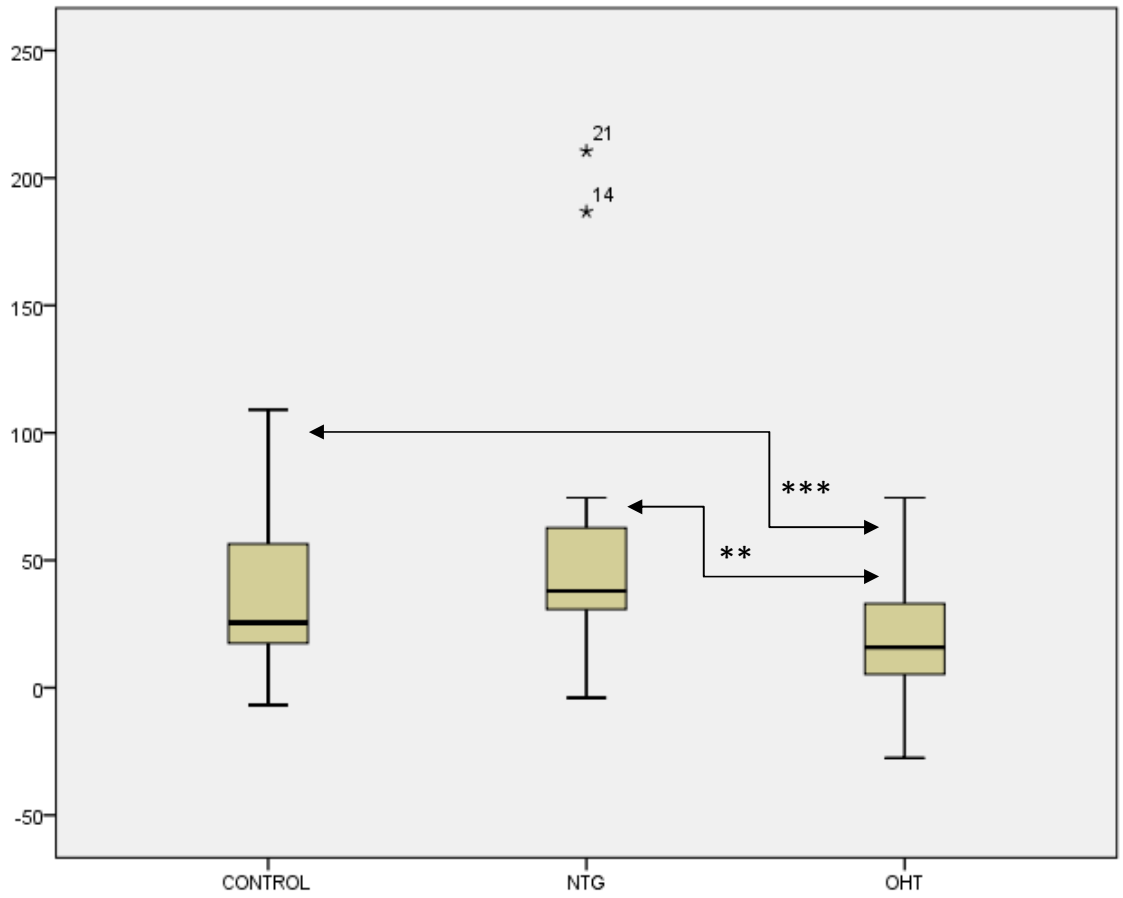

Fig 4.33: Graph showing the percentage increase in the rate of DHE oxidation in the lymphocytes from control, NTG and OHT subjects after treatment with 0.5µM rotenone for 24hrs. The results are expressed as the percentage increase from the level of DHE oxidation before rotenone exposure (100%, not shown) in the control, NTG and OHT lymphocytes.

The median (IQR) % increase in DHE staining in the control, NTG and OHT lymphocytes after rotenone treatment was 25.6% (16.7 to 57.9), 38.0% (30.6 to 62.9) and 15.9% (3.8 to 33.0), respectively. Although a statistically significant increase was noted upon rotenone treatment in all three groups, as expected given the strength and duration of the oxidative stress-inducing insult, this increase was significantly less in the OHT group, as compared to the other two groups. The percentage increase in the NTG and controls was similar, with the

NTG group showing the highest % increase in superoxide staining after exposure to rotenone.

Discussion: Superoxide anions, as measured by DHE staining, were present at similar levels in the lymphocytes from each group of participants. While high levels of ROS are considered to be toxic, causing cell damage and cell death, moderate amounts of ROS can be beneficial and serve in the function of a number of physiological cellular signalling pathways, in the defence against infectious agents, and in the induction of mitogenic responses (Valko et al 2007). Under physiological conditions, and although the mitochondrial electron transport chain is a very efficient system, the very nature of the alternating one-electron oxidation-reduction reactions it catalyses, predispose each electron carrier to side reactions with molecular oxygen to produce superoxide. Thus, it is commonly held that mitochondrial generation of superoxide represents the major intracellular source of oxygen radicals. With estimates of 1–2% of the total daily oxygen consumption going to mitochondrial superoxide generation, a 60 kg woman would produce some 160–320mmol of superoxide each day from mitochondrial respiration alone (based on an O2 consumption of 6.4 l/kg/day) and an 80 kg man would produce some 215–430mmol of superoxide per day (Cadenas et al 2000).

When cells were treated with rotenone to generate ROS within the mitochondria (Li et al 2003) and expose the lymphocytes to oxidative stress, the OHT lymphocytes were more capable of dealing with this insult, as compared to the control and NTG lymphocytes, thus further supporting the idea of the presence of more functionally efficient mitochondria in OHT.

4.3.4.2 Aconitase enzymatic assay

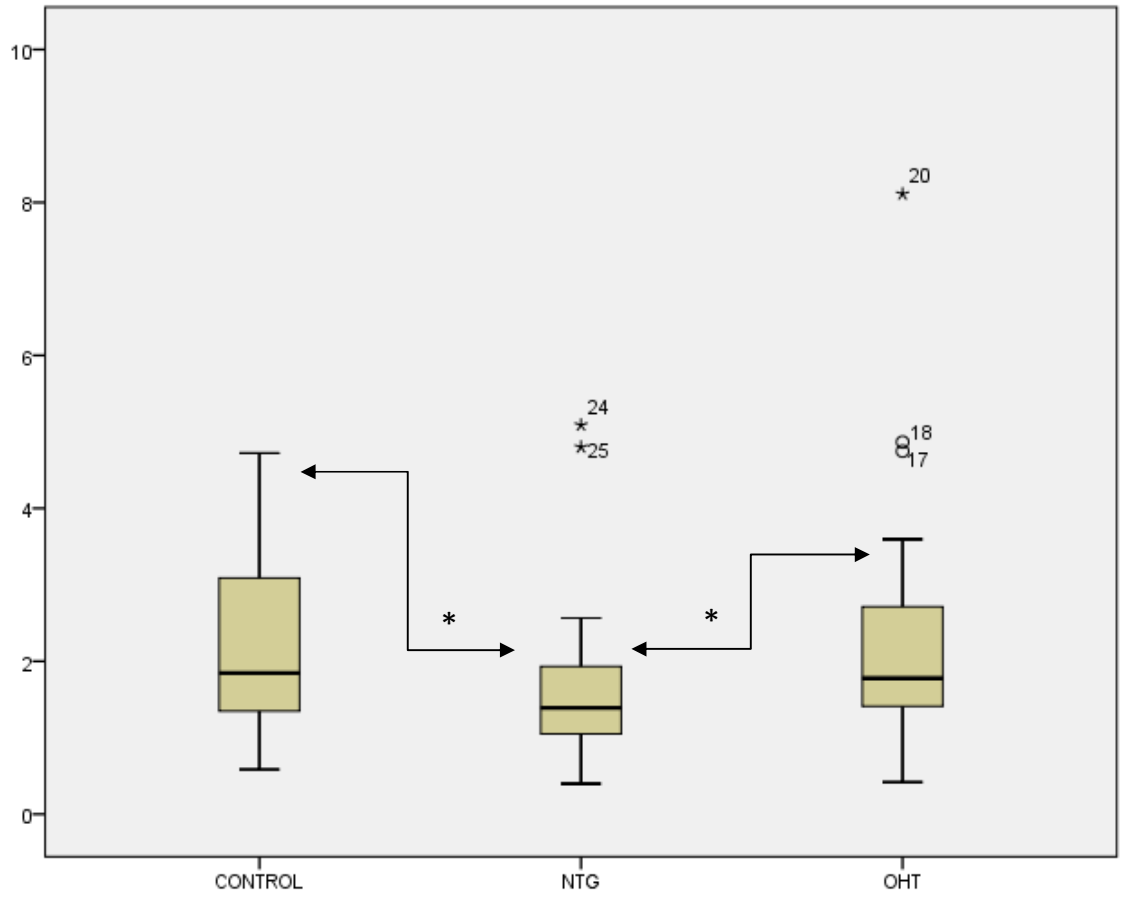

Fig 4.34: Graph showing the aconitase enzymatic activity in the control, NTG and OHT lymphocytes. In all measurements, the background (no cells with reaction buffer) has been subtracted and the aconitase activity is expressed in nmol/min/mg.

The median (IQR) aconitase activity in the control, NTG and OHT lymphocytes was 1.85 (1.35 to 3.10), 1.39 (1.03 to 2.01) and 1.78 (1.39 to 2.74), respectively. The aconitase activity in the NTG group was significantly lower, as compared to the control (p=0.015) and OHT (p=0.027) groups, thus suggesting increased systemic oxidative damage in NTG.

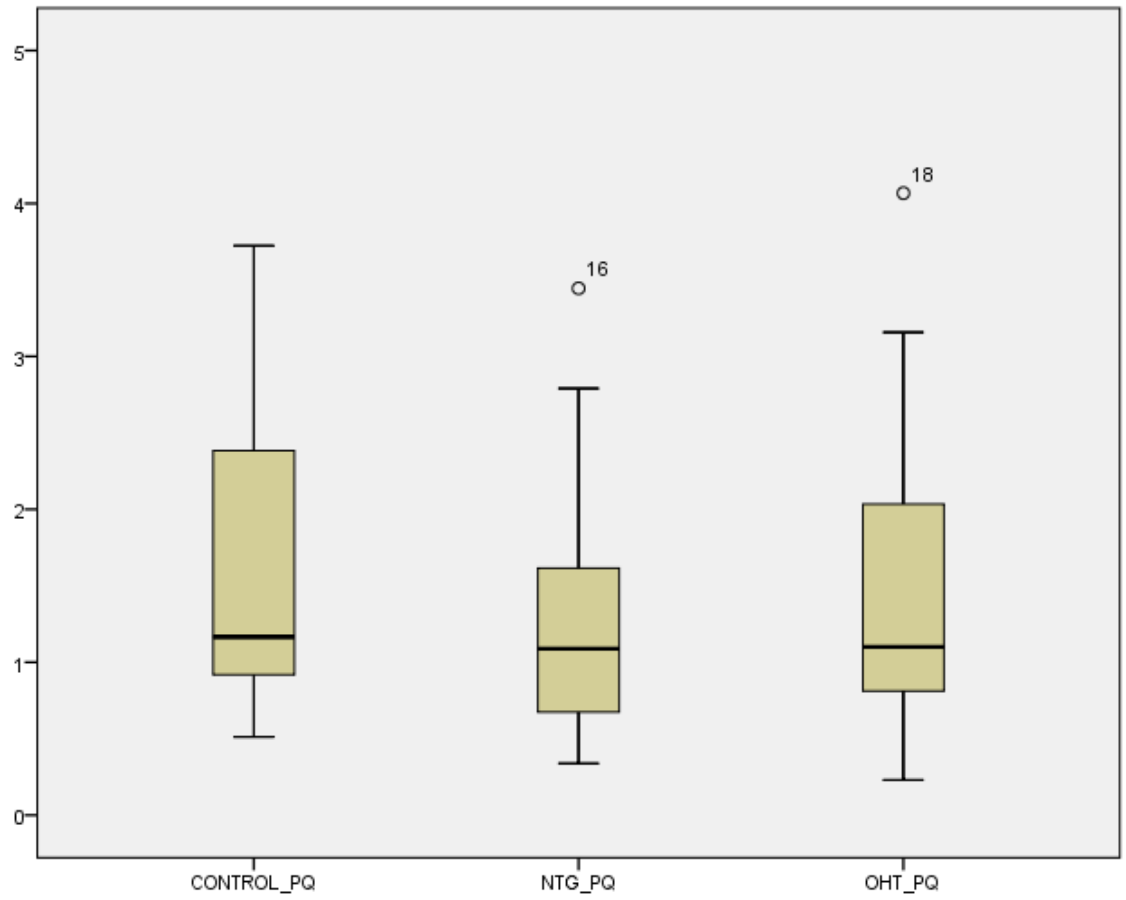

Fig 4.35: Graph showing the aconitase enzymatic activity in the control, NTG and OHT lymphocytes, after treatment with paraquat (PQ) 100µM for 24hrs. In all measurements, the background (no cells with reaction buffer) has been subtracted and the aconitase activity is expressed in nmol/min/mg.

The median (IQR) aconitase activity in the control, NTG and OHT lymphocytes after PQ treatment was, as expected, significantly reduced in all cases, as compared to the baseline (prior to PQ treatment), to 1.17 (0.92 to 2.42), 1.09 (0.65 to 1.69) and 1.10 (0.81 to 2.05), respectively. No significant difference was noted between the three groups after PQ treatment, suggesting that the PQ insult was sufficient to produce ROS and impact negatively on the aconitase activity in all cases, thus serving as a positive control in this experiment.

Discussion: As discussed in section 2.3.7, a reduction in aconitase enzymatic activity is a well known measure of cellular oxidative damage (Yan et al 1997), as aconitase is sensitive not only to free redicals, such as superoxide and hydrogen peroxide, but also to powerful oxidants, including peroxynitrite (Grune et al 1998). It therefore serves as a more generalised marker of oxidative damage in cells. Over 95% of all the oxygen we breathe undergoes a concerted tetravalent reduction to produce water in a reaction catalysed by complex IV in the mitochondrial electron transport chain (ETC) ($O_2 + 4e^- + 4H^+ \rightarrow 2H_2O$). Therefore, the cumulative oxidative damage noted in NTG may in part be attributed to a reduction in the ETC efficiency, as demonstrated by the reduced complex IV-linked ATP synthesis in NTG, thus extending the length of time that the electrons remain at complexes I and III, and increasing the potential for donation of electrons to oxygen (Kushnareva et al 2002). It is less likely that the opposite association is observed, in other words that the reduction in complex IV-linked ATP synthesis in NTG is caused by oxidative stress, especially since there is evidence to suggest that complex IV is remarkably resistant to oxidative inactivation (Zhang et al 1990). The same study, using bovine heart submitochondrial particles exposed radiolytically to various defined oxygen species, indicated that several different mitochondrial complexes (especially complex I and V, and less complex III) are mostly susceptible to inactivation by superoxide, but surprisingly rather resistant to the effects of other free radicals, such as H_2O_2. This could perhaps explain to some extent why the increased oxidative damage noted in NTG may not have impacted significantly on the complex I- and II/III-linked ATP synthesis in this group, as compared to the controls.

4.3.4.3 Superoxide dismutase 2 (SOD2)

SOD2 is a mitochondrial matrix protein, which transforms toxic superoxide, a byproduct of the mitochondrial ETC, into hydrogen peroxide and diatomic oxygen (Melov et al 1999). Thus, and similarly to glutathione peroxidase, SOD2 is considered one of the main cellular components of antioxidant defence (Macmillan-Crow et al 2001), thought to be upregulated as a response to oxidative stress. The relatively high rate of superoxide production in the inner mitochondrial membrane is in functional relationship to the localisation of SOD2 in the mitochondrial matrix (Mn-superoxide dismutase). The steady state concentration of superoxide in the mitochondrial matrix [$O_2^{\cdot-}$] may be calculated, based on the reaction below, considering the following aspects: a) the rate of superoxide production by the respiratory chain d[$O_2^{\cdot-}$]/dt; b) assuming that the main reaction of superoxide utilisation is the Mn-superoxide dismutase-catalysed disproportionation (k) and; c) the concentration of SOD2 in the mitochondrial matrix [SOD].

$$+d[O_2^{\bullet-}]/dt = k[SOD][O_2^{\bullet-}]$$

Thus, for the [superoxide] to remain the same, as shown between the three groups in our cohort, any increase in [SOD] would need to be accompanied by an equivalent increase in the rate of superoxide production by the respiratory chain d[superoxide]/dt.

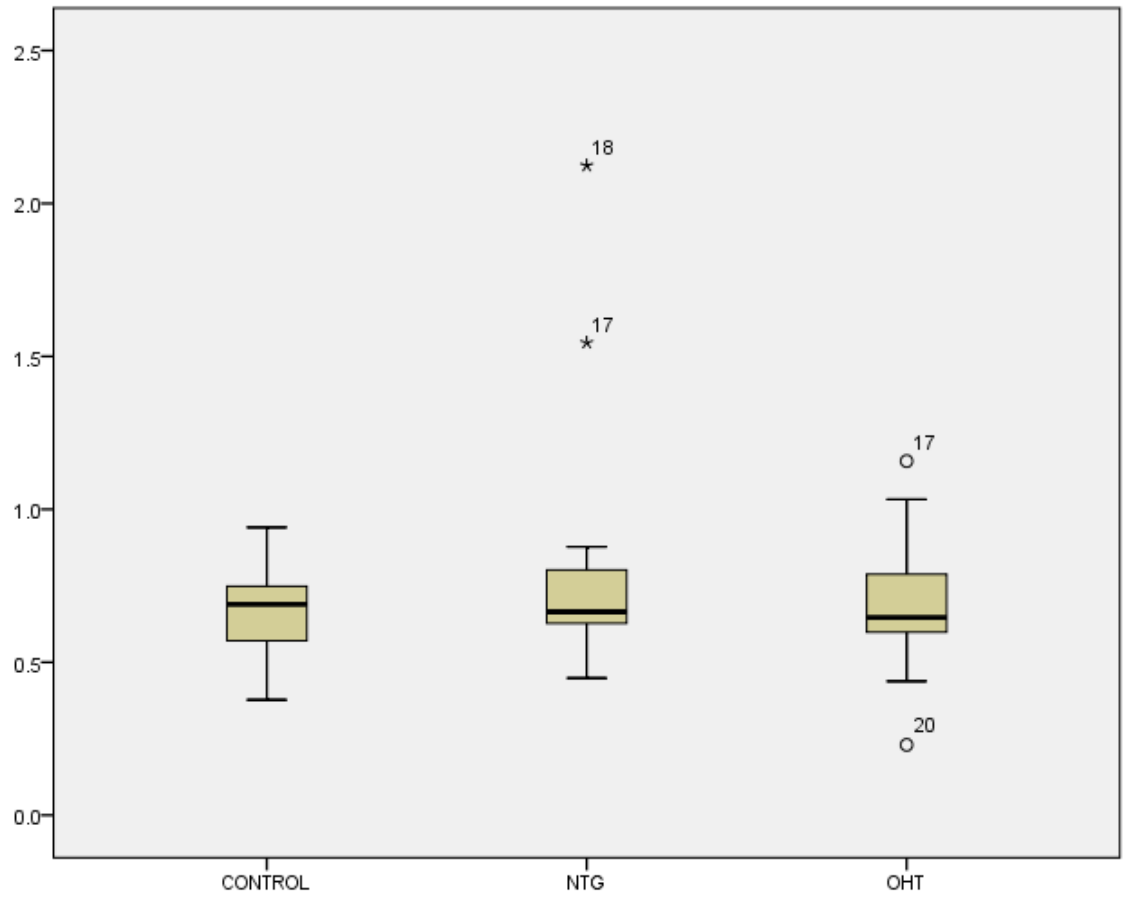

Fig 4.36: Graph showing the level of SOD2 in the control, NTG and OHT lymphocytes. SOD2 is expressed as a percentage of Raji (100%, not shown) that acted as an internal control.

The median (IQR) SOD2 level for the control, NTG and OHT lymphocytes, was 0.69 (0.57 to 0.75), 0.67 (0.63 to 0.83) and 0.69 (0.61 to 0.82), respectively. No difference was noted between the three groups (Fig 4.29), however when the level of SOD2 was corrected for mitochondrial content the SOD2 level in NTG [3.53 (3.03 to 4.57)] was significantly higher than that in OHT [3.28 (2.72 to 3.99] (p=0.046) (Fig 4.36 below). This result would suggest an increase in the antioxidant defences in NTG, potentially to compensate for the increased oxidative damage noted in this group of patients, as measured by the reduced aconitase activity.

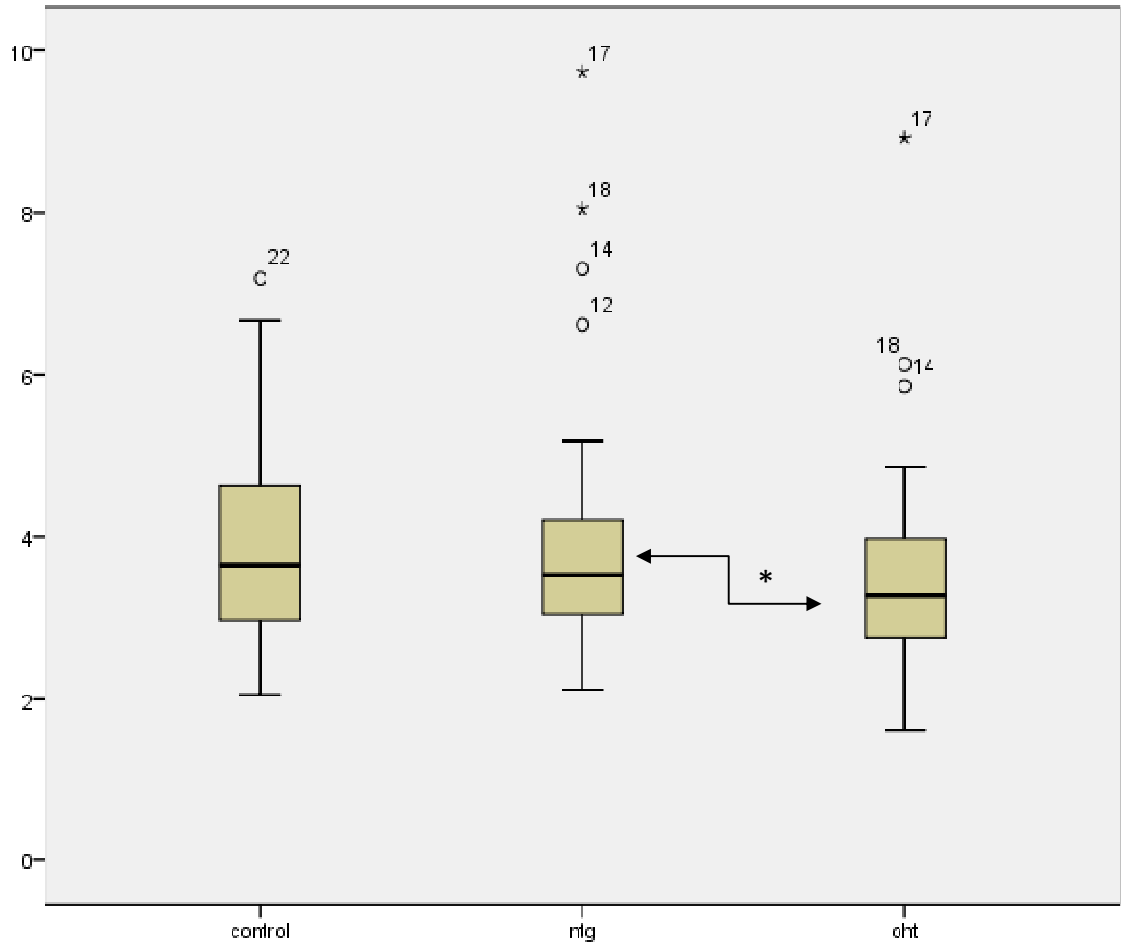

Fig 4.37: Graph showing the level of SOD2 in the control, NTG and OHT lymphocytes, after correction for mitochondrial content.

Discussion: Together these data suggest that at baseline the overall oxidative damage, as measured by aconitase, is increased in NTG. Although the baseline superoxide levels were not significantly increased in NTG, the overall rate of superoxide production is likely to be relatively higher in NTG, probably due to the protective masking effect of the relatively increased SOD2. The lower levels of SOD2 in OHT, with similar baseline superoxide levels to NTG, would suggest that the overall rate of superoxide production in OHT is lower than in NTG,

thus further supporting the idea of increased ETC efficiency in OHT. This efficiency is also highlighted by the fact that in OHT the mitochondria showed enhanced ETC function with increased energy production by the different mitochondrial complexes, higher $\Delta\Psi m$ and enhanced calcium buffering capacity, but without generating significantly more superoxide, as shown by the baseline DHE staining. Furthermore, under conditions of stress, the OHT lymphocytes showed superior antioxidant capacity to the NTG lymphocytes, as demonstrated by the smaller increase in DHE staining upon rotenone treatment, thus suggesting reduced susceptibility of the OHT cells to oxidative damage under these conditions.

Similarly to the present results of increased SOD2 in NTG, Ferreira et al (2004) have shown that the activity of two enzymes involved in antioxidant defence (SOD and glutathione peroxidase) in the aqueous humour of POAG patients was nearly 1.6 times greater, as compared to a control cataract group. Similarly, increased expression of the SOD2 gene has been observed in the aqueous humour of POAG patients (Ghanem et al 2010) and in the ciliary processes and iris tissue of subjects with pseudoexfoliation glaucoma (Zenkel et al 2007). However, in the study by Wolf et al (2009) no association was found between NTG and SOD2 sequence variants.

4.3.4.4 Urinary 8-hydroxydeoxyguanosine (8OHdG)

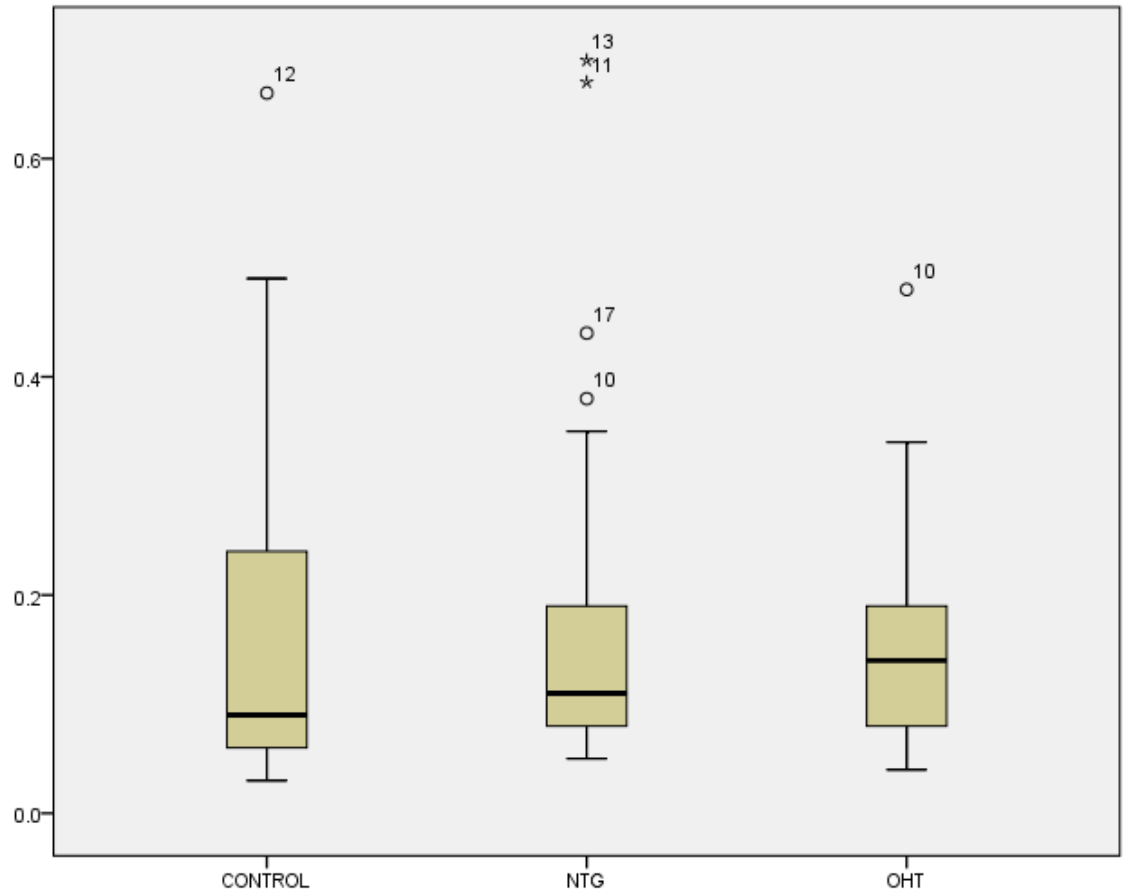

Fig 4.38: Graph showing the level of urinary 8OHdG in the control, NTG and OHT subjects. 8OHdG is corrected for the level of creatinine in the urine and expressed in ng/g creatinine.

The median (IQR) 8OHdG level in the urine of control, NTG and OHT subjects was 0.09 (0.06 to 0.24), 0.11 (0.075 to 0.20) and 0.14 (0.078 to 0.19), respectively. No statistically significant difference was noted between the three groups, in line with the finding of similar baseline systemic levels of superoxide in the lymphocytes amongst the three groups, as demonstrated by the DHE staining.

However, it is perhaps relevant to note that cancer and DM, conditions known to increase urinary 8OHdG (Wu et al 2004, Valavanidis et al 2009), were

relatively more common in the OHT group. In a *post hoc* analysis of a subgroup of subjects (28 controls, 24 NTGs and 22 OHTs) with no history of DM or active cancer, there was again no significant difference between the controls [0.09 (0.065 to 0.25)], NTG [0.11 (0.087 to 0.21)] and OHT subjects [0.14 (0.08 to 0.17)] (Fig 4.38 below), thus further supporting the above conclusion.

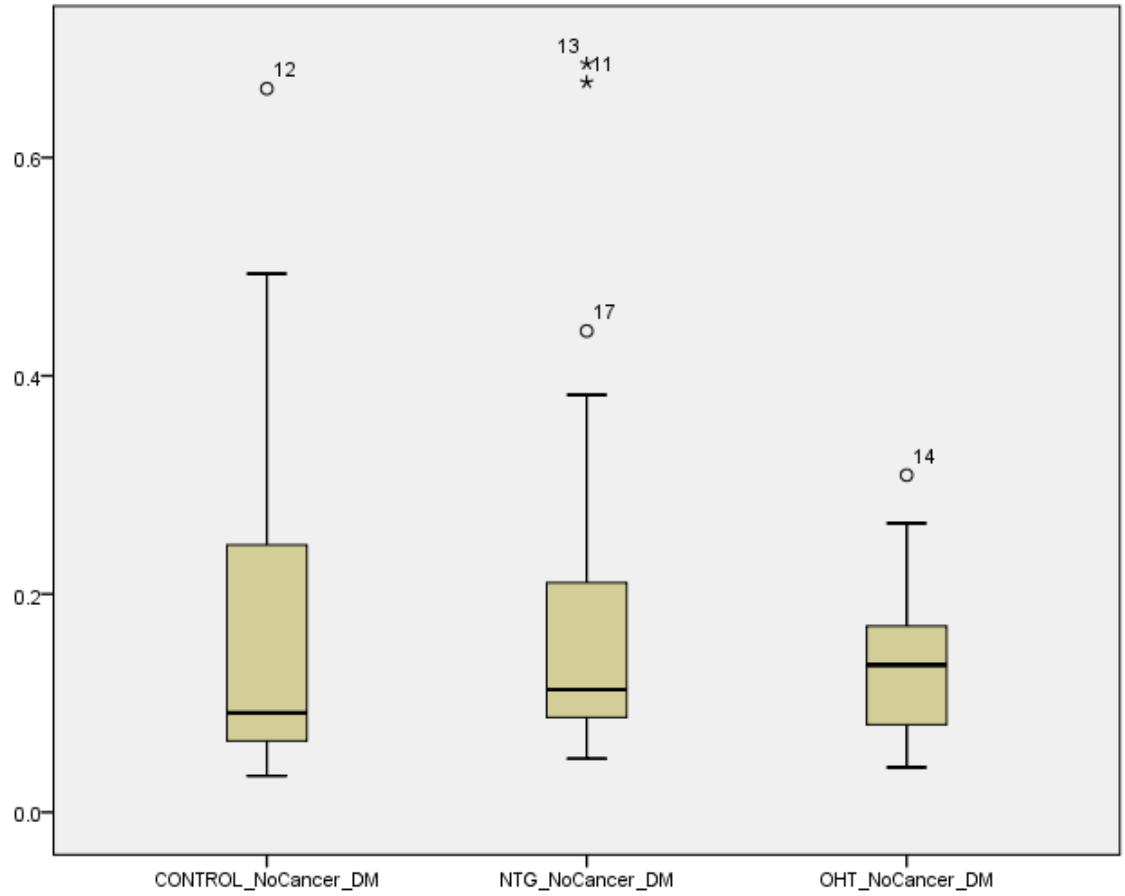

Fig 4.39: Graph showing the level of urinary 8OHdG in a subgroup of control, NTG and OHT subjects, with no history of DM or active cancer. 8OHdG is corrected for the level of creatinine in the urine and expressed in ng/g creatinine.

Discussion: The generation of superoxide and hydrogen peroxide by the respiratory chain, in close proximity to the active redox pools of Cu and Fe in

the mitochondrial membranes, provides the requisite conditions leading to hydroxyl radical (HO•) formation and, hence, the rather specific addition of HO• onto the desoxyguanosine base of DNA to yield 8OHdG (Giulivi et al 1995).

$$HO^{\bullet} + DNA\text{–}(dG) \rightarrow DNA\text{–}(8HodG)$$

The lack of any difference in the levels of superoxide at baseline between the three groups, as demonstrated by the DHE staining, may therefore explain the lack of any statistically significant difference in urinary 8-OHdG. Also, while ROS generation is thought to be qualitatively related to the amount of 8OHdG detected in the mtDNA (Cadenas et al 2000), the rates of ROS production are not supposed to be strictly correlated with 8-OHdG formation for various reasons: First, the actual sites of HO• formation in mitochondria are not known; second, the highly reactive HO• is able to diffuse several molecular diameters from its site of formation before it reacts; and third, formation of 8OHdG could result from site-specific damage, entailing cleavage by redox active metals (Cu, Fe) bound to the mtDNA. Thus, the stereo- and region-selectivity of HO• formation in the vicinity of the DNA determines the chemical structure of the products formed (Giulivi et al 1995).

Interestingly, urinary 8OHdG was reported to be reduced in 43 NTG patients as compared to 40 healthy controls, indicating, according to the authors, a compensatory response to increased systemic oxidative stress in glaucoma (Yuki et al 2010), while the presence of oxidative stress in several other diseases has been clearly linked with elevated, rather than reduced, urinary 8OHdG (Wu et al 2004, Kasai et al 1997). Another unexpected finding in the same study by Yuki et al was that the serum total antioxidant status (TAS) was significantly higher in NTG, as compared to controls, unlike previous studies

that have demonstrated reduced antioxidant capacity in glaucoma patients (Ferreira et al 2004, Sorkhabi et al 2011). To explain the lack of difference in urinary 8OHdG in our cohort, one would need to consider that oxidative stress may manifest differently in different tissues and at different disease stages, and that perhaps the Japanese NTG cohort in the study by Yuki et al (2010) is inherently different from our NTG cohort with fast VF progression. Unlike our cohort, the Japanese population in the study by Yuki et al was specially selected, with the authors excluding active or ex smokers, patients on vitamins or other forms of antioxidants and those with DM or any other systemic disease, except hypertension. Nevertheless, active cancer and DM were not associated with elevated urinary 8OHdG in our cohort.

In the study by Sorkhabi et al, where mainly the aqueous, and less so the serum, levels of 8OHdG were increased in glaucoma patients as compared to age-similar cataract patients, the authors proposed that in glaucoma the oxidative burden to the anterior chamber may be overwhelming, compromising the trabecular meshwork cells and their functions, and suggested that localised oxidative damage may play a more important role in the pathogenesis of glaucoma than systemic oxidative stress. This, as well as the intra-individual variability of the measurement (Pilger et al 2001) and the fact that measuring oxidative damage in a peripheral tissue, such as urine, may not be as sensitive or relevant to the pathogenesis of a disease like glaucoma, could perhaps explain the absence of any differences in the levels of 8OHdG between the three groups in our cohort. Also, 8OHdG is a specific marker of DNA oxidation and therefore the presence of oxidative damage in other macromolecules cannot be excluded, while the sensitivity of our measurement could have been influenced by the fact that DNA purification was not required

in our protocol, unlike previous studies that measured 8OHdG levels from purified trabecular meshwork DNA (Izzotti et al 2003).

4.3.4.5 Urate

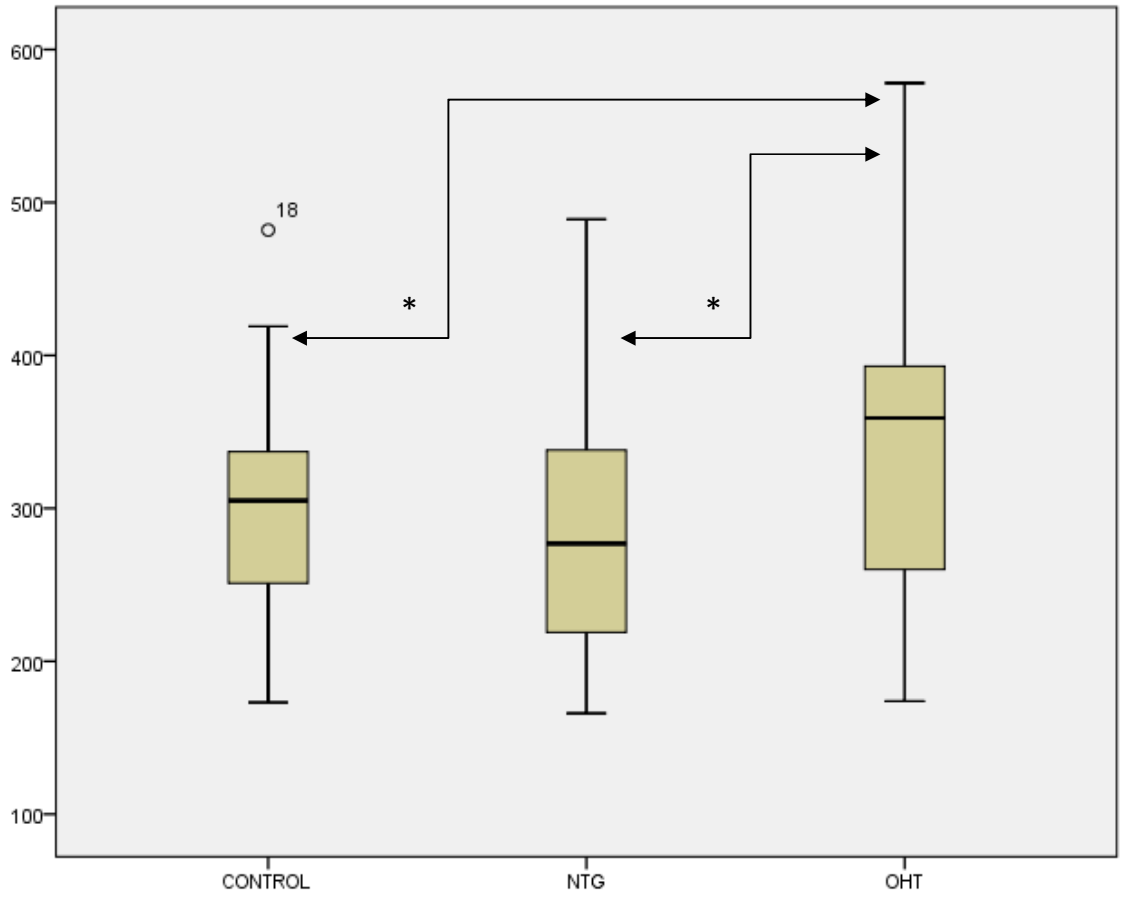

Fig 4.40: Graph showing the levels of urate in the serum of control, NTG and OHT subjects. Urate is expressed in µmol/lt (normal reference range 266-474 µmol/lt).

The median (IQR) urate levels in the control, NTG and OHT groups, were 305 µmol/lt (235 to 345) or 5.13mg/dl, 277 µmol/lt (217 to 343) or 4.66mg/dl and 359 µmol/lt (258 to 395) or 6.04mg/dl, respectively. The urate levels in the NTG group were significantly lower as compared to the OHT group (p=0.012),

while the urate levels in the OHT group were significantly higher to the controls (p=0.045), thus further supporting the idea of increased antioxidant capacity in OHT and relatively reduced antioxidant capacity in NTG.

Discussion: Whether or not urate functions physiologically as an antioxidant remains controversial (Glantzounis et al 2005), although there is some evidence in the literature to suggest that urate can act as an antioxidant *in vitro* (Becker 1993) and in humans (Ames et al 1981). Urate is the end product of purine metabolism in humans and serves as a primary antioxidant in the human blood, as it is known to remove singlet oxygen and radicals as effectively as vitamin C (Wayner et al 1987). Furthermore, a highly significant positive correlation between mammalian maximum life span and the concentration of serum urate has been reported (Cutler 1984). Urate has been shown to contribute up to two-thirds of the antioxidant capacity of human blood (Maxwell et al 1997) and intravenous infusion of urate has been found to increase the plasma total antioxidative status of healthy volunteers (Waring et al 2001). Thus, the observed association between OHT and higher urate levels may provide an alternative explanation for the enhanced capacity to deal with exogenous oxidative stress in this group, as demonstrated by DHE staining. At this stage it is not clear whether this association is merely an epiphenomenon or whether a causal relationship exists between higher urate levels and increased mitochondrial function, and this hypothesis will be tested in the UKGTS.

Also, there was a trend for urate levels to be lower in our NTG group, in line with multiple previous studies that have linked reduced antioxidant capacity with human glaucoma (Zanon-Moreno et al 2008, Gherghel et al 2005, Ren et

al 2006). However, unlike our study, Elisaf et al showed in 2001 that abnormalities of urate metabolism, such as hyperuricaemia and defective renal tubular transport of urate, were more common in 49 POAG patients with a known history of diabetes mellitus, as compared to 72 age and sex- matched controls (Elisaf et al 2001). The coexisting carbohydrate metabolism disturbances noted in the glaucoma group could not explain the urate metabolism abnormalities observed and the authors concluded that urate metabolism could independently play a role in glaucoma pathogenesis. Similarly, the study by Yuki et al (2010b) showed increased serum urate in NTG (P = 0.01; NTG 5.8 +/- 1.5 mg/dl vs control 4.9 +/- 1.4 mg/dl), although the same authors showed that serum levels of another antioxidant, vitamin C, were significantly lower in their NTG cohort, as compared to healthy controls. Aqueous urate levels have also been found to be higher at the time of surgery in eyes with unsuccessful outcomes after trabeculectomy, as compared to those with successful outcomes, and elevated aqueous urate has been proposed as a risk factor for trabeculectomy failure (Jampel et al 1998) by having a direct deleterious effect on trabecular tissues, retinal cells and wound healing.

4.3.4.10 Vitamins A and C

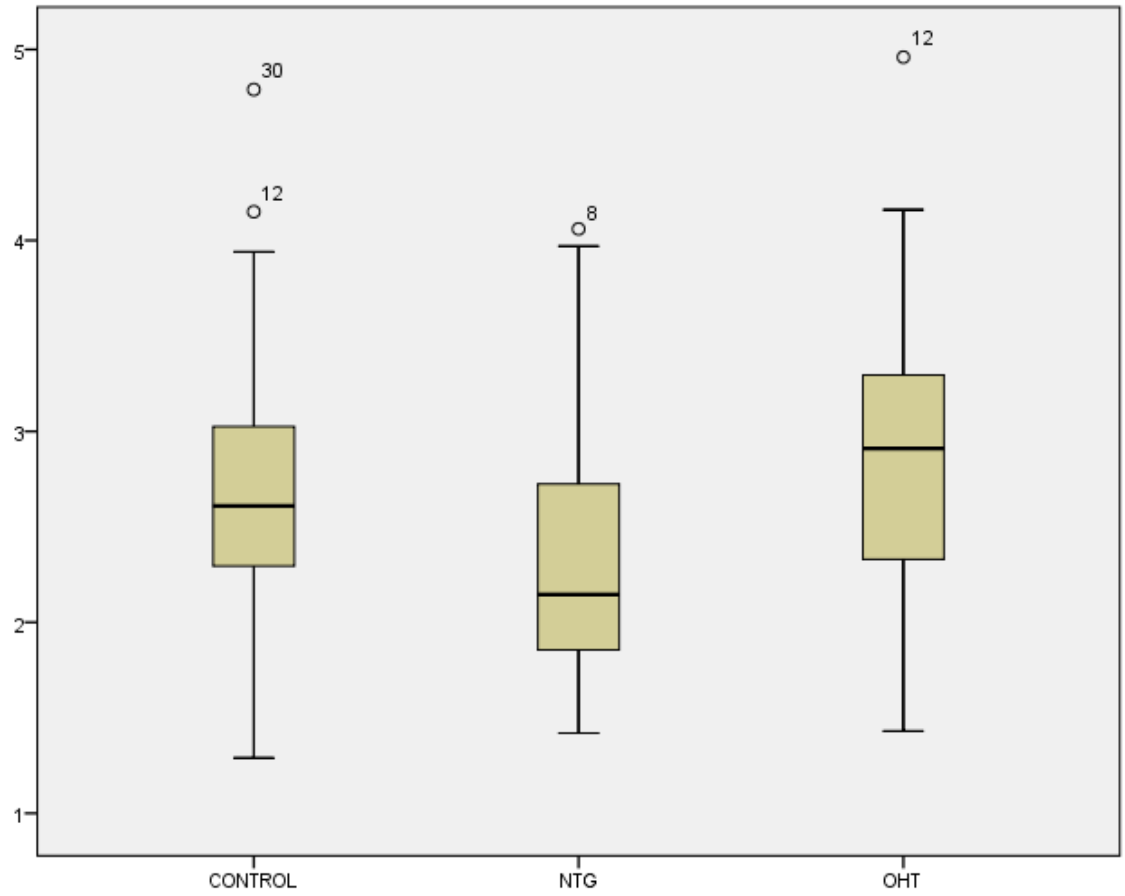

Fig 4.41: Graph showing the levels of vitamin A in the serum of control, NTG and OHT subjects. Vitamin A is expressed in µmol/lt (normal reference range 1.54-3.84 µmol/lt).

The median (IQR) vitamin A levels in the control, NTG and OHT groups, were 2.61 µmol/lt (2.28 to 3.03) or 74.8µg/dl, 2.15 µmol/lt (1.83 to 2.76) or 61.6µg/dl, and 2.91 µmol/lt (2.32 to 3.31) or 83.4µg/dl, respectively. There was a trend for the vitamin A levels in the NTG group to be lower as compared to the OHT (p=0.054) and control (p=0.077) groups, thus further supporting the idea of relatively reduced antioxidant capacity in NTG.

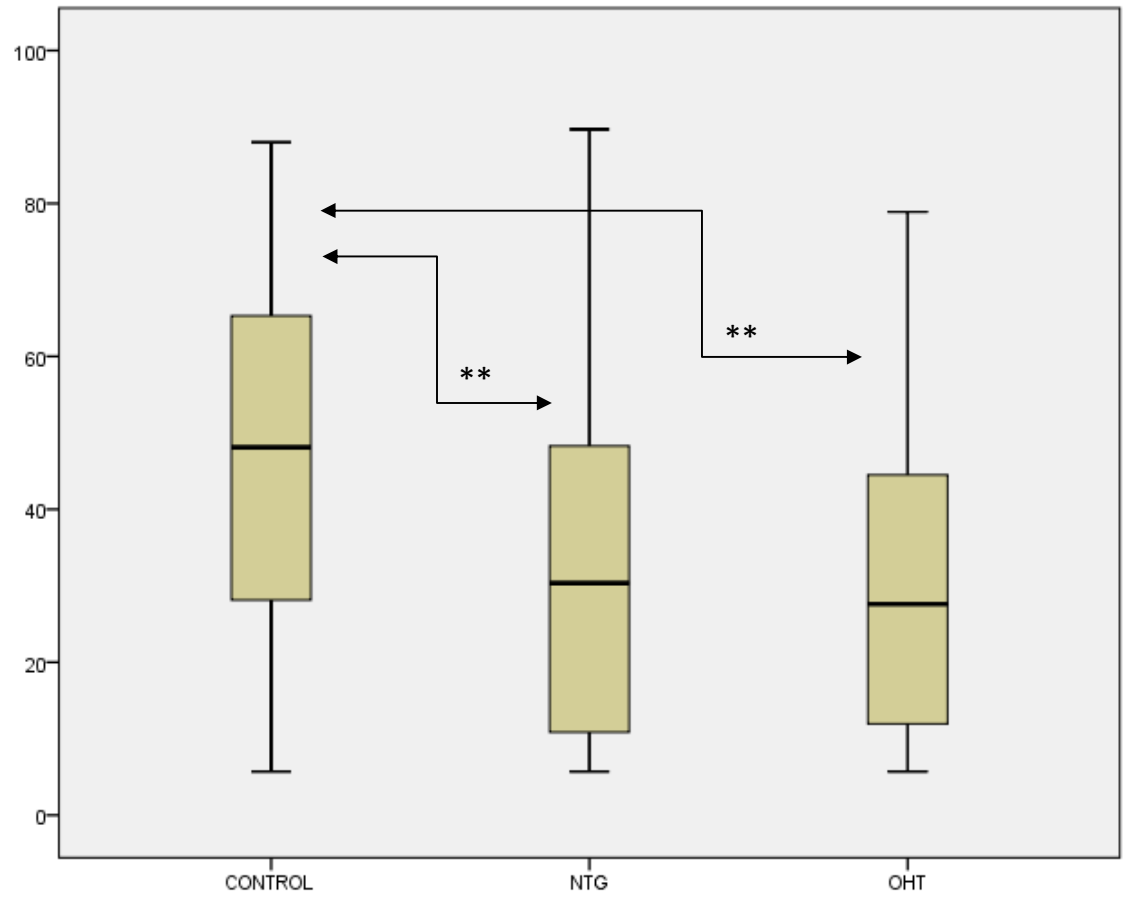

Fig 4.42: Graph showing the levels of vitamin C in the serum of control, NTG and OHT subjects. Vitamin C is expressed in µmol/lt (normal reference range >11.4µmol/lt).

The median (IQR) vitamin C levels in the control, NTG and OHT groups, were 48.1 µmol/lt (24.5 to 66.4) or 8.47µg/ml, 30.4 µmol/lt (10.4 to 50.4) or 5.35µg/ml and 27.6 µmol/lt (11.4 to 45.0) or 4.86µg/ml, respectively. The vitamin C levels in both the OHT (p=0.001) and NTG (p=0.002) groups were significantly lower, as compared to the control.

Discussion: Vitamin A (retinol) is an important antioxidant (Palace et al 1999) and an essential nutrient in maintaining ocular health. This vitamin plays a key role in the development of vision and the prevention of eye diseases (Luo et al

2006). Our study is the first to find a trend for reduced vitamin A levels in NTG patients, as compared to OHT and controls, thus further supporting the evidence that links reduced antioxidant capacity with glaucoma. In the study by Yuki et al, no statistically significant difference was seen in vitamin A (P = 0.41; normal-tension glaucoma; 82.1±26.7 μg/dl control; 77.1±30.1 μg/dl) between NTG and control groups (Yuki et al 2010b). Similarly, in the study by Zanon-Moreno et al (2011), although the plasma vitamin A concentrations tended to be lower in 150 POAG patients than in 150 controls, this difference was not statistically significant (519.3±47.1 ng/ml in POAG cases vs 527.7±58.9 ng/ml in controls; p=0.174) (Zanon-Moreno et al 2011).

With regards to vitamin C, the results presented here show significantly lower vitamin C levels in NTG, as compared to controls, thus further supporting the evidence that links reduced antioxidant capacity with glaucoma. Similarly, Yuki et al (2010b) reported lower vitamin C levels in their NTG cohort (P = 0.04; NTG 4.6±4.0 μg/ml vs control 6.3±3.9 μg/ml). Interestingly, the lower systemic vitamin C was associated with a mild IOP elevation that did not exceed 21 mmHg in these Japanese NTG patients (Yuki et al 2010b), with the authors speculating that reduction of vitamin C levels may cause IOP elevation and glaucomatous optic neuropathy, even in NTG patients. Moreover, in a recent study by Zanon-Moreno et al, POAG patients were found to have lower plasma vitamin C concentrations than control subjects (9.9±1.7 μg/ml vs 11.7±1.8 μg/ml, p<0.001) and the rs1279683 SNP in SLC23A2 (a gene encoding the Na^+-dependent L-ascorbic acid transporter 2) was significantly associated with lower vitamin C concentration and a higher risk of POAG (Zanon-Moreno et al 2011). An additional link between vitamin C and glaucoma has been proposed by Coleman et al (2008) in a relatively recent epidemiological study involving 1,155 women in the United States, who reported that a higher intake of kale,

known to be rich in vitamin C, was associated with a decreased risk of POAG (Coleman et al 2008). However, Kang et al did not find any significant associations between POAG and antioxidant consumption in the Nurses' Health Study (n = 76,200) and the Health Professionals Follow-up Study (n = 40,284), where participants were followed biennially from 1980 and 1986, respectively, to 1996 (Kang et al 2003).

The finding of lower serum vitamin C in OHT in this study appears to be conflicting to the elevated serum levels of another antioxidant, urate, found in the same group. Similarly conflicting results for vitamin C and urate were presented by Yuki et al (2010b) for NTG. It is, however, interesting to note that very few OHT subjects were on antioxidant supplements in our cohort, as compared to the other two groups, and this may have accounted for the relative reduction in vitamin C levels in the OHT group. Also, the aforementioned link between IOP elevation and reduced vitamin C levels reported by Yuki et al in 2010 for NTG, has been reinforced by studies reporting considerable reductions in IOP in glaucoma patients after administration of vitamin C (Fishbein et al 1972, Virno et al 1966). Vitamin C may reduce IOP by the depolymerisation of the trabecular meshwork`s hyaluronic acid component (Linner 1969) and it remains to be seen whether the significantly reduced vitamin C levels in OHT may have contributed to some extent to the significantly elevated IOP in this group. An alternative explanation for the high urate and low vitamin C in OHT could be based on *in vitro* studies indicating that interactions between urate and vitamin C can change the viscosity of some glycosaminoglycans (Liu et al 1984). More specifically, vitamin C reduces the viscosity of hyaluronic acid and increases outflow facility, while urate, used at concentrations within the range observed in the human aqueous, was found to inhibit the oxidative degradation of

rooster comb and umbilical cord hyaluronic acid by ascorbate *in vitro,* thus potentially reducing outflow facility and increasing IOP. Since the trabecular meshwork contains glycosaminoglycans as a portion of the extracellular matrix, it is tempting to suggest that increase in urate levels may have important implications in the trabecular meshwork physiology, decrease the outflow facility of aqueous humour and cause eventual IOP elevation in the OHT cohort.

4.3.4.7 Vitamin B6

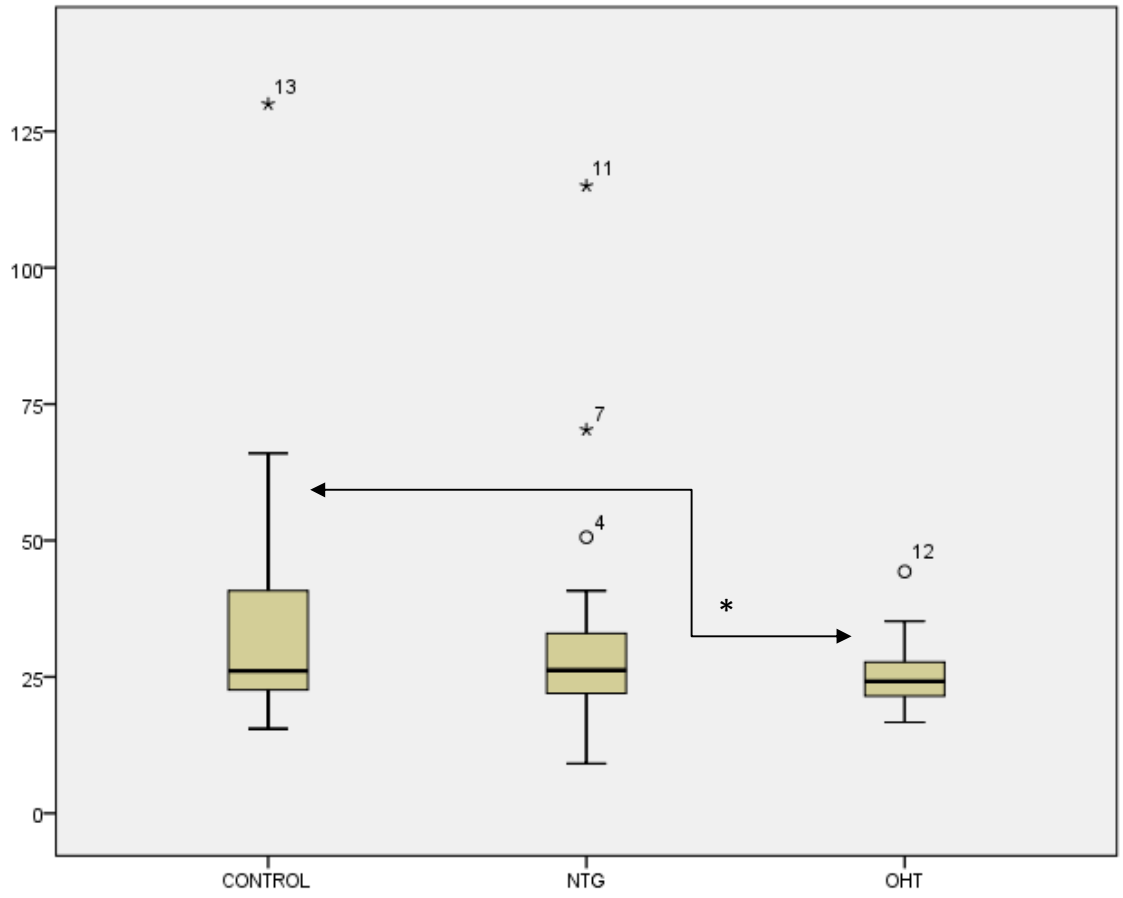

Fig 4.43: Graph showing the levels of vitamin B6 in the plasma of control, NTG and OHT subjects. Vitamin B6 is expressed in µg/lt (normal reference range 8.7-27.2 µg/lt).

The median (IQR) vitamin B6 levels in the control, NTG and OHT groups, were 26.1μg/lt (22.3 to 41.5), 26.2μg/lt (21.4 to 33.2) and 24.2μg/lt (21.5 to 27.9), respectively. The vitamin B6 plasma levels in OHT were lower as compared to the control group with the difference achieving marginal statistical significance (0.049). No difference was noted between the OHT and NTG groups (p=0.294) or between the NTG and control groups (p=0.761).

Discussion: In the case of Vitamin B6, no significant difference was noted between NTG and controls, unlike the study by Turgut et al where elevated serum B6 levels were noted in POAG (30.22±12.15μg/l) and NTG patients (30.50±11.29μg/l), as compared to controls (20.09±5.54μg/l) (Turgut et al 2010). It is interesting to note that the levels of vitamin B6 in our control group (median 26.1μg/lt) appear higher than those reported in the latter study, possibly due to the fact that 15 out of the 30 controls were on antioxidant supplements. Importantly, and unlike our study, the values presented by Turgut et al represent a more 'pure' population, since the authors included a whole list of patient exclusions ranging from any systemic disease (eg cardiomyopathy, diabetes mellitus, systemic hypertension, renal or hepatic dysfunction, gastrointestinal malabsorption, psychiatric illness) to any systemic medication or food supplement (Turgut et al 2010).

The levels of vitamin B6 have not been reported before in OHT. Similarly to vitamin C, the reduced vitamin B6 levels in OHT, as compared to controls, are likely to reflect the relatively small number of OHT patients that were on antioxidants, as compared to the other two groups. Also, the effect of antioxidant supplements on the vitamin B6 results is highlighted by the relatively high percentage of controls and NTG patients that exceed the physiological range of B6 (>27.2 μg/lt) and the higher IQR in these two groups,

as compared to the OHT group. The effect of antioxidant supplements on the vitamin C results is more difficult to detect, since there is no upper physiological limit for this vitamin.

4.3.4.8 Vitamins B12 and folate

Vitamin B12

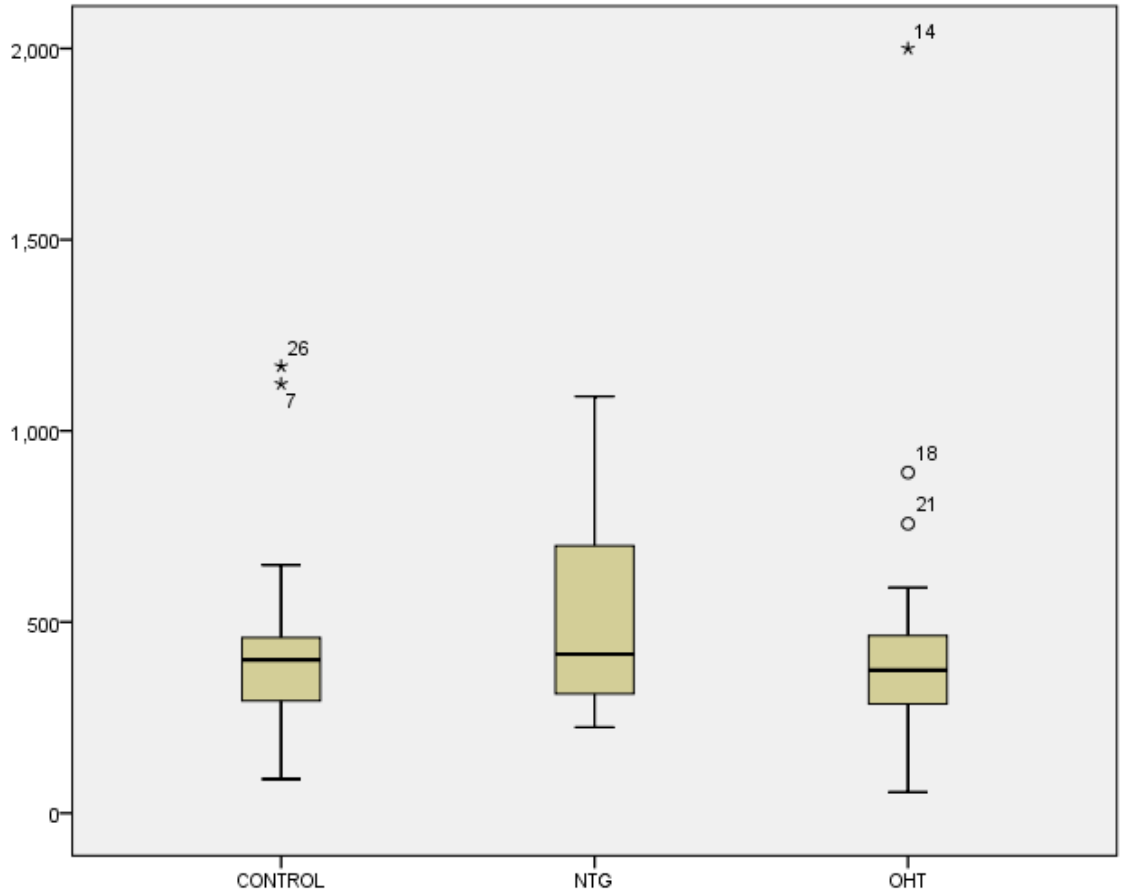

Fig 4.44: Graph showing the levels of vitamin B12 in the serum of control, NTG and OHT subjects. Vitamin B12 is expressed in pg/ml (normal reference range 191-663pg/ml).

The median (IQR) vitamin B12 levels in the control, NTG and OHT groups, were 401 pg/ml (289 to 471), 416 pg/ml (299 to 726) and 374pg/ml (282 to 470),

respectively. No difference was noted in the vitamin B12 levels between the three groups.

Serum folate

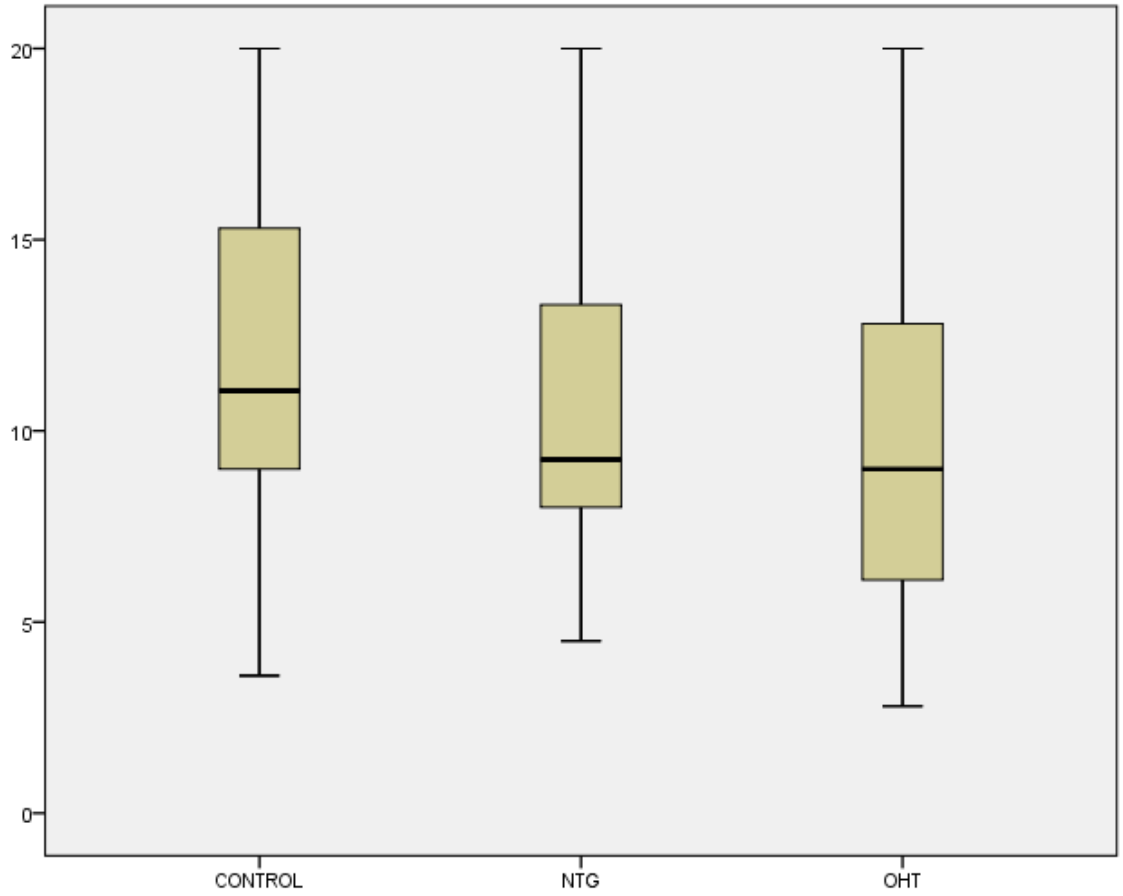

Fig 4.45: Graph showing the levels of serum folate in control, NTG and OHT subjects. Serum folate is expressed in µg/lt (normal reference range 4.6-18.7µg/lt).

The median (IQR) vitamin C levels in the control, NTG and OHT groups, were 11.1 µg/lt (8.8 to 15.5), 9.3 µg/lt (7.8 to 13.7) and 9.0 µg/lt (6.0 to 13.3), respectively. Similarly to B12, no difference was noted in the serum folate levels between the three groups.

RBC folate

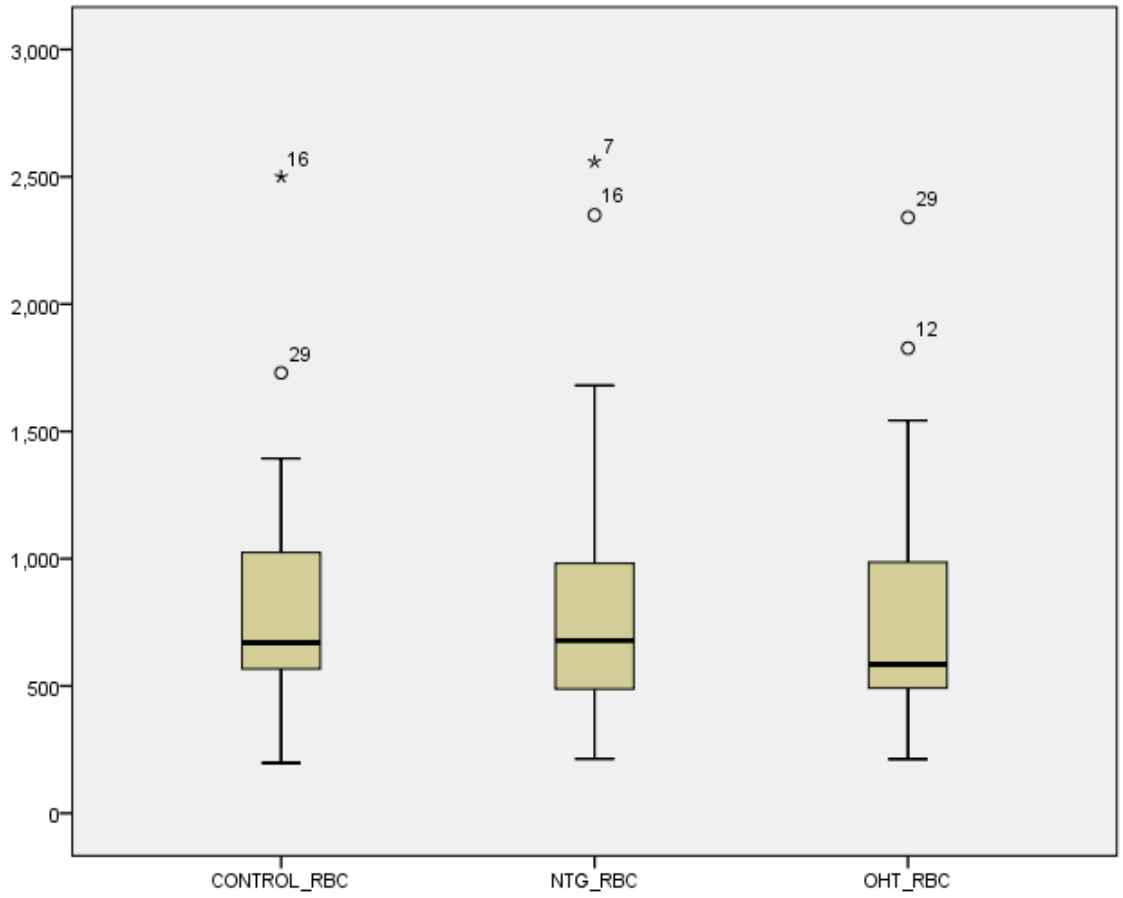

Fig 4.46: Graph showing the levels of red blood cell folate in control, NTG and OHT subjects. RBC folate is expressed in nmol/lt (normal reference range 158-1099 nmol/lt).

RBC folate was also measured, since it is thought to reflect long-term folate status, as compared to serum folate, which may be more influenced by recent dietary intake (Piyathilake et al 2007). The median (IQR) RBC folate levels in the control, NTG and OHT groups, were 671 nmol/lt (538 to 1048), 678 nmol/lt (467 to 1003) and 585 nmol/lt (478 to 1081), respectively. Similarly to B12 and serum folate, no difference was noted in the RBC folate levels between the three groups.

Discussion: Serum and RBC folate levels were similar between the three groups in our cohort, in line with the findings by Turgut et al that there was no difference in serum folate levels among control (9.00±6.39ng/ml), NTG (9.71±3.86ng/ml), PXG (10.82±4.92ng/ml) and POAG (11.59±9.40ng/ml) subjects (Turgut et al 2010). Also, the reported lack of statistically significant difference in B12 levels between the three groups in our cohort, is supported by the study by Turgut et al, who showed no difference in serum B12 levels among control subjects and NTG, PXG and POAG groups (Turgut et al 2010).

4.3.4.9 Homocysteine

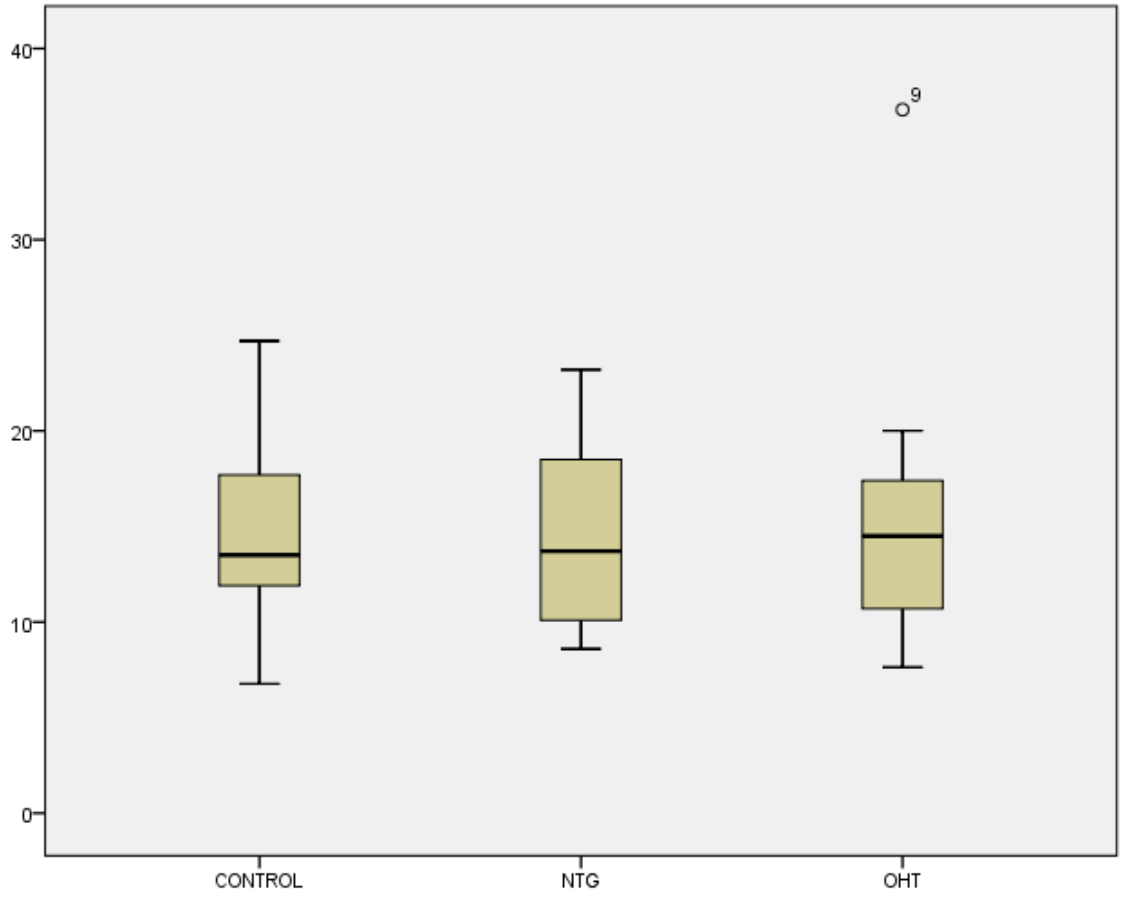

Fig 4.47: Graph showing the levels of plasma homocysteine in control, NTG and OHT subjects. Plasma homocysteine is expressed in µmol/lt (normal reference range <15µmol/lt).

The median (IQR) homocysteine levels in the control, NTG and OHT groups, were 13.5 µmol/lt (11.8 to 17.7), 13.7 µmol/lt (10.1 to 19.1) and 14.5 µmol/lt (10.6 to 17.5), respectively. Similarly to B12 and serum and RBC folate, no difference was noted in the homocysteine levels between the three groups.

Discussion: In view of the vascular theories in the aetiology of glaucoma (see sections 1.3.6 and 1.5.7), increased attention has been directed at studying the total plasma level of the amino acid homocysteine (tHcy), which has been identified as a possible risk factor for arteriosclerosis (McCully 1969) and symptomatic peripheral vascular (Clarke et al 1991), cerebrovascular (Perry et al 1995) and coronary heart disease (Nygard et al 1997). Hyperhomocysteinaemia has also been demonstrated to be a risk factor for retinal vascular disease, including central retinal vein and artery occlusion (Biousse et al 1997, Cahill et al 2000), as well as for non-arteritic ischemic optic neuropathy (Pianka et al 2000). A link has also been proposed between elevated tHcy (generally defined as tHcy ≥15µmol/l) and oxidative stress (Mujumdar et al 2001). In 2002, Bleich et al found for the first time a significantly higher mean tHcy level in 18 POAG patients (12.52µmol/l) compared with 19 control subjects (8.40µmol/l), while other studies have also shown increased Hcy levels in the tear fluid (Roedl et al 2008) and plasma (Roedl et al 2008, Clement et al 2009) of patients with OAG. A higher prevalence of the C677T single nucleotide polymorphism in the 5,10-methylentetrahydrofolate reductase (MTHFR) gene has also been noted in

POAG, leading to moderate hyperhomocysteinaemia (Junemann et al 2005). In addition, it has been suggested that elevated Hcy could impact on the microvascular circulation of the optic nerve head in glaucoma through its ability to cause endothelial injury (Stamler et al 1993), smooth muscle proliferation (Tsai et al 1994), platelet activation and thrombogenesis (Rodgers et al 1986), while Moore et al have demonstrated that homocysteine induces apoptotic cell death in mouse RGcs by NMDA receptor overstimulation and caspase-3 activation (Moore et al 2001).

However, the evidence on the role of homocysteine in glaucoma is conflicting and several studies (Wang et al 2004, Altintas et al 2005, Turgut et al 2010), including ours, have not shown any difference in tHcy levels between POAG, NTG and controls. In the study by Wang et al, for example, no difference was found in the mean tHcy level in 55 POAG patients (14.90µmol/l) as compared to 39 controls (14.30µmol/l). It is possible that the multifactorial nature of glaucoma in the different populations examined in different studies could mask the contribution of hyperhomocysteinaemia and account for the conflicting results. Another factor could be the different characteristics of the included populations, such as age, severity of glaucoma, nutritional status, presence of associated illnesses, use of medications and lifestyle determinants, including smoking, coffee consumption, alcoholism, and physical activity (Clarke et al 2001). Also, different methodologies used to assess plasma tHcy levels may explain at least in part the different results, since it has been suggested that measurements of tHcy with Enzyme Immunoassay (EIA) (such as in the study by Bleich et al above) have a higher inaccuracy and imprecision compared with High Performance Liquid Chromatography (HPLC) (Nexo et al 2000), which was used by Wang et al above. Also, data from the Centers for Disease Control and Prevention on 14 laboratories performing tHcy assays on

reference materials have indicated a high variation between laboratories, and for one reference material with a mean concentration of 11.1µmol/l, the reported values ranged from 8.3 to 14µmol/l (CDCP 1999). Finally, it is perhaps relevant to note that conflicting evidence also largely exists among the clinical studies evaluating tHcy as a risk factor for cardiovascular disease (Ford et al 2002), suggesting possibly that the role of elevate tHcy is not as clear and convincing as originally thought.

Interestingly, vitamins B6, B12 and folate are considered cofactors for the catabolism of homocysteine, and deficiencies in these vitamins have been associated with hyperhomocysteinaemia in PXG (Roedl et al 2007). For example, excess tHcy is converted to methionin by vitamin B12 and when vitamin B12 is deficient this can result in higher levels of Hcy. In our cohort, the levels of B6, B12 and folate in the NTG group were very similar to the other two groups, and these findings would certainly be in line with the lack of differences in the plasma tHcy levels between the three groups. If anything, the levels of B6 were slightly lower in the OHT group, potentially as a result of the high frequency of food supplementation in the other two groups, which may have masked the relative decrease in tHcy in the OHT cohort.

4.3.5 Perfusion pressure

Systolic perfusion pressure (day)

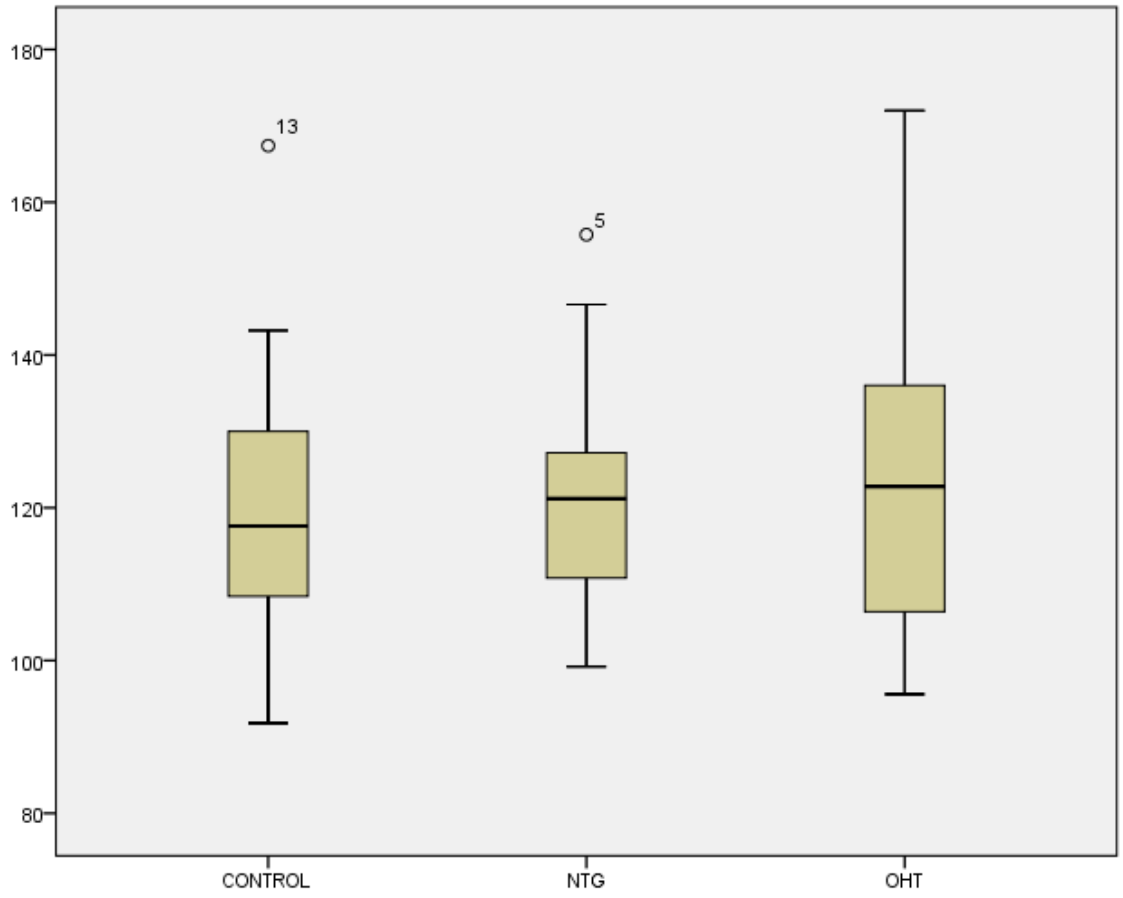

Fig 4.48: Graph showing the systolic perfusion pressure (SPP) during the day for the control, NTG and OHT subjects. The SPP was expressed in mmHg and calculated as follows: mean SBP during the day – mean GAT IOP.

The median (IQR) SPP for the control, NTG and OHT groups was 118mmHg (108 to 130), 121mmHg (110 to 127) and 123mmHg (106 to 136), respectively. No difference was noted in the SPP (day) between the three groups.

Diastolic perfusion pressure (day)

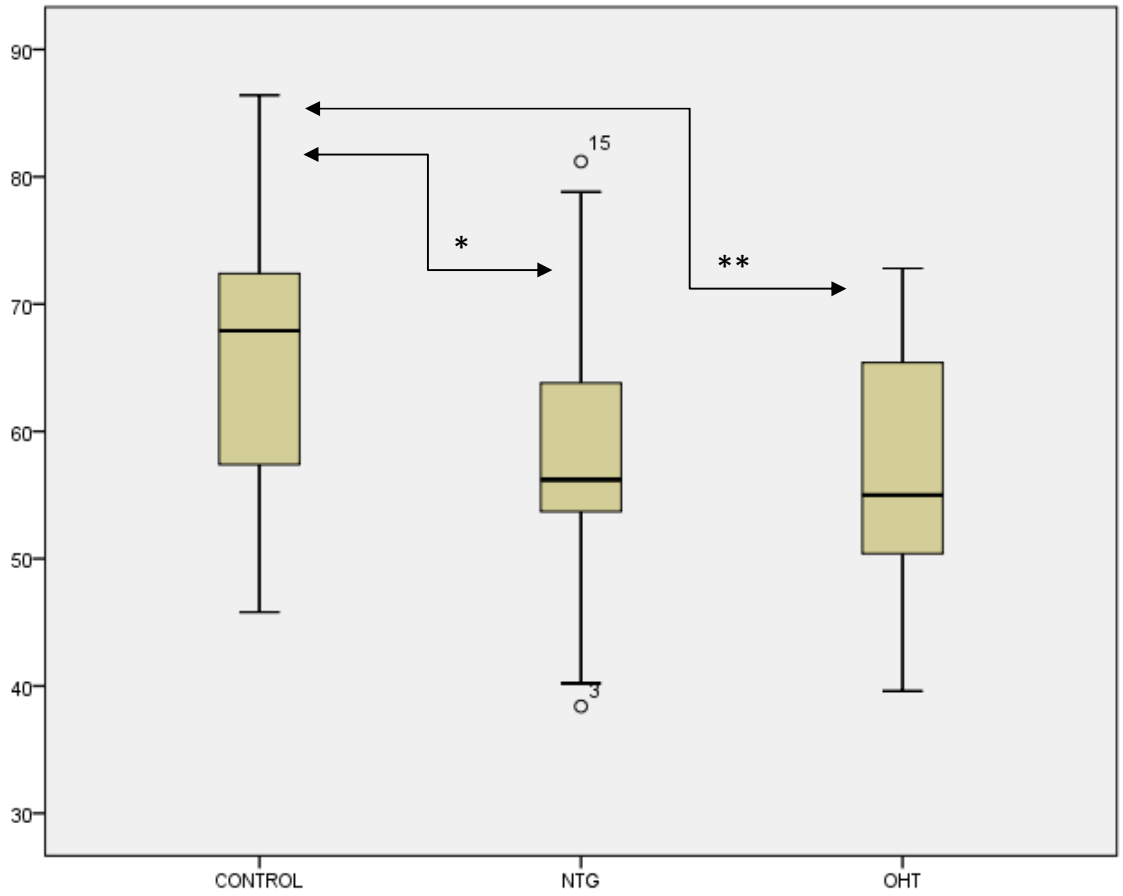

Fig 4.49: Graph showing the diastolic perfusion pressure (DPP) during the day for the control, NTG and OHT subjects. The DPP was expressed in mmHg and calculated as follows: mean DBP during the day – mean GAT IOP.

The median (IQR) DPP for the control, NTG and OHT groups was 68mmHg (57 to 73), 56mmHg (53 to 64) and 55mmHg (50 to 66), respectively. Interestingly, a statistically significant reduction was noted in the DPP of the NTG (p=0.11) and OHT (p=0.001) subjects, as compared to the control group.

Mean ocular perfusion pressure (day)

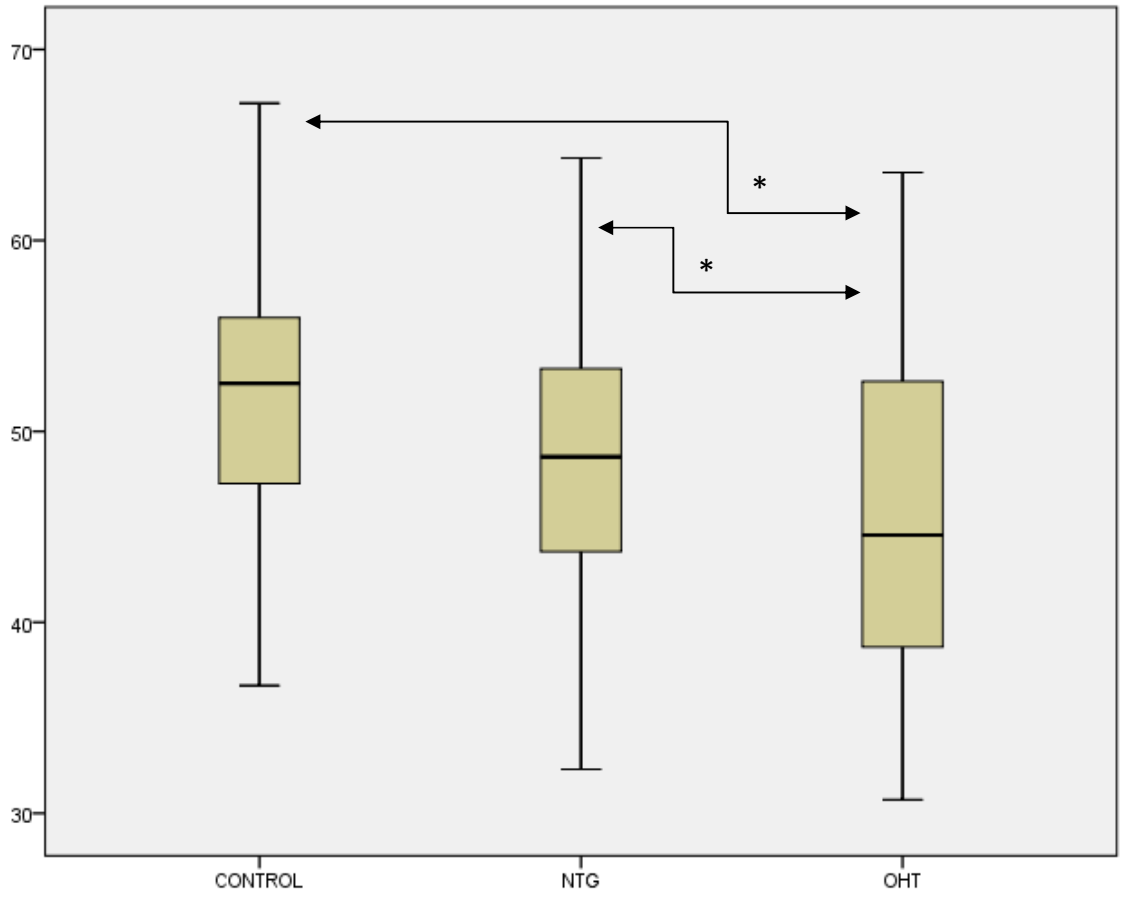

Fig 4.50: Graph showing the mean ocular perfusion pressure (MOPP) during the day for the control, NTG and OHT subjects. The MOPP (day) was expressed in mmHg and calculated as follows: 2/3 Mean arterial pressure (MAP) day – GAT IOP, where MAP day =2/3DBP (day) + 1/3SBP (day).

The median (IQR) MOPP (day) for the control, NTG and OHT groups was 53mmHg (47 to 56), 49mmHg (44 to 54) and 45mmHg (38 to 53), respectively. Similarly to DPP, a statistically significant reduction was noted in the MOPP (day) of the OHT subjects, as compared to the control group (p=0.026). Also, the MOPP (day) of the OHT patients was significantly lower, as compared to that of the NTG subjects (p=0.021). No difference was noted between the control and NTG groups (p=0.13).

SPP (night)

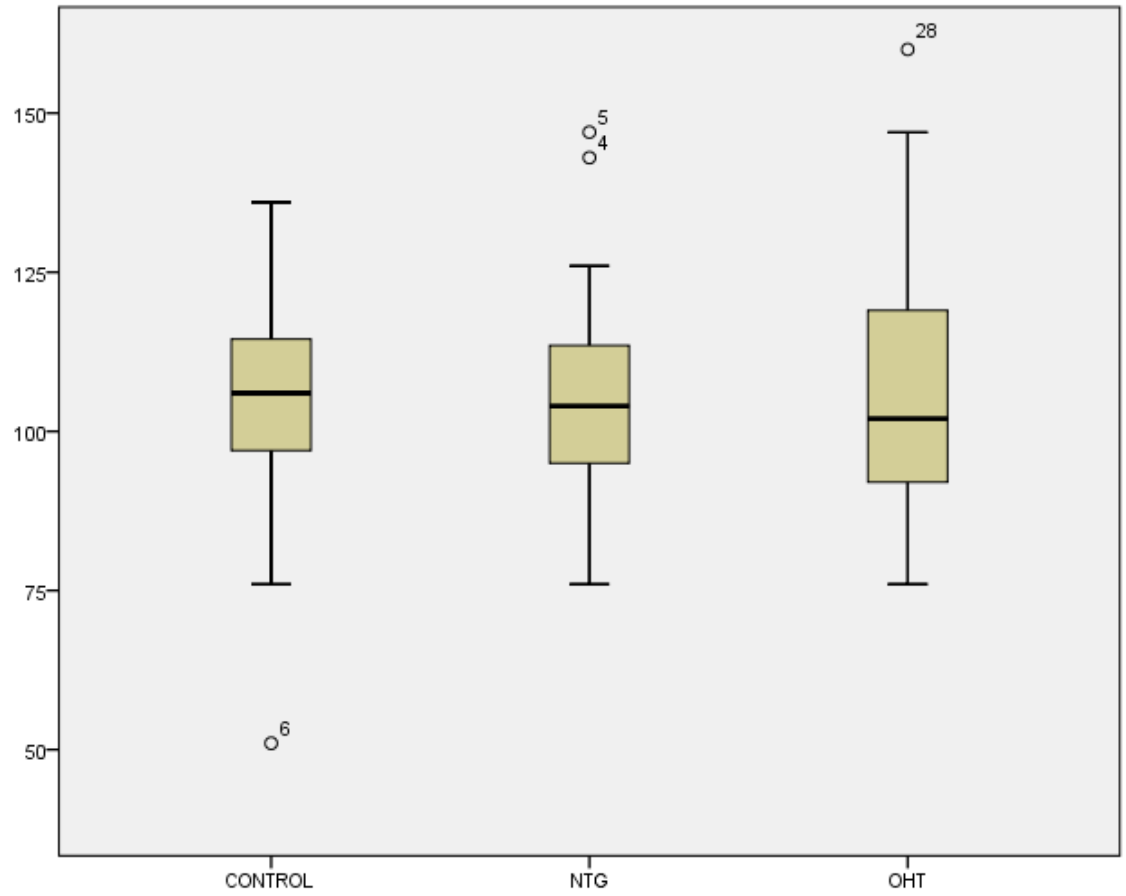

Fig 4.51: Graph showing the SPP at night for the control, NTG and OHT subjects. The SPP (night) was expressed in mmHg and calculated as follows: mean SBP at night – supine IOP.

The median (IQR) SPP 'at night' for the control, NTG and OHT groups was 106mmHg (97 to 115), 104mmHg (94 to 114) and 102mmHg (89 to 120), respectively. Similarly to the SPP (day), no difference was noted in the SPP (night) between the three groups.

DPP (night)

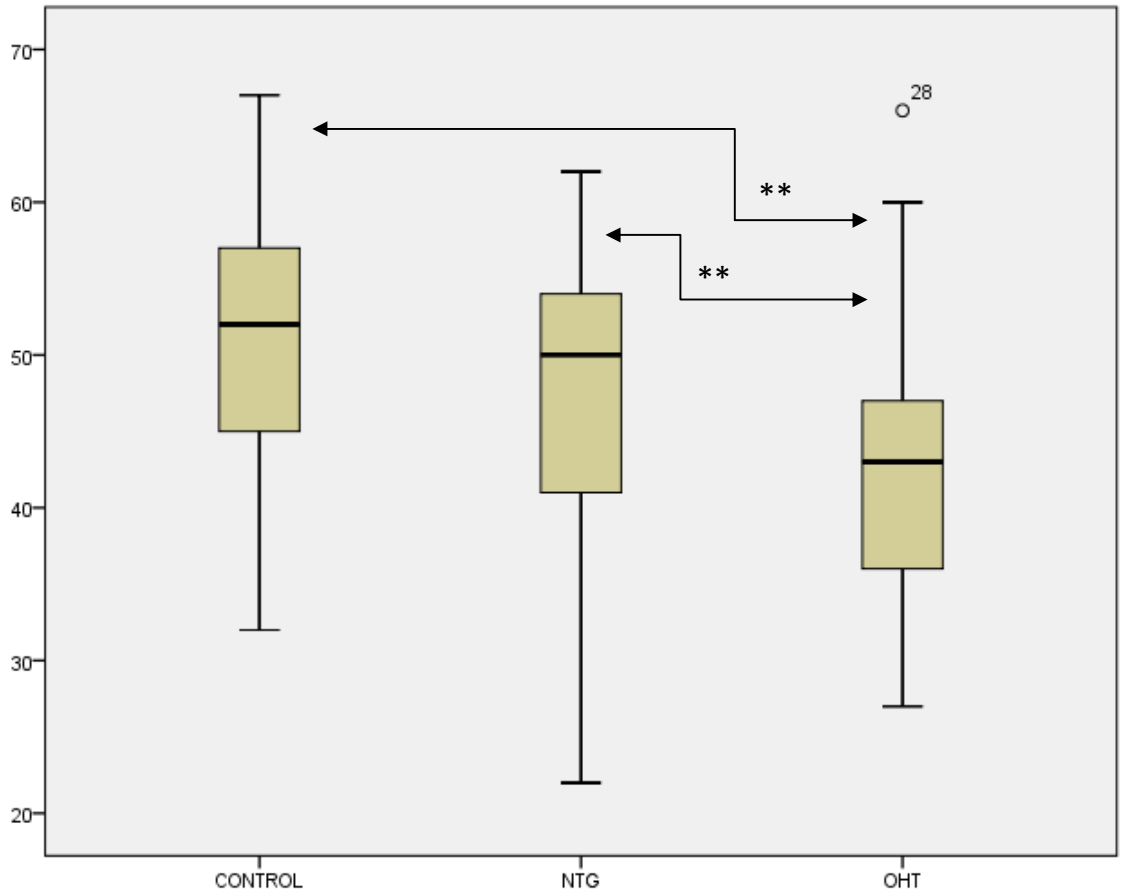

Fig 4.52: Graph showing the diastolic perfusion pressure (DPP) at night for the control, NTG and OHT subjects. The DPP (night) was expressed in mmHg and calculated as follows: mean DBP at night – supine IOP.

The median (IQR) DPP (night) for the control, NTG and OHT groups was 52mmHg (45 to 57), 50mmHg (41 to 54) and 43mmHg (34 to 47), respectively. Similarly to the MOPP (day), a statistically significant reduction was noted in the DPP (night) of the OHT subjects, as compared to the control (p=0.001) and NTG (p=0.006) groups. Unlike the DPP (day), the DPP (night) in the NTG cohort was not significantly lower as compared to the controls, probably reflecting the only slight reduction in DBP (night) in the NTG group, as compared to the significant reduction in DBP (day) noted in the same group.

Mean ocular perfusion pressure (night)

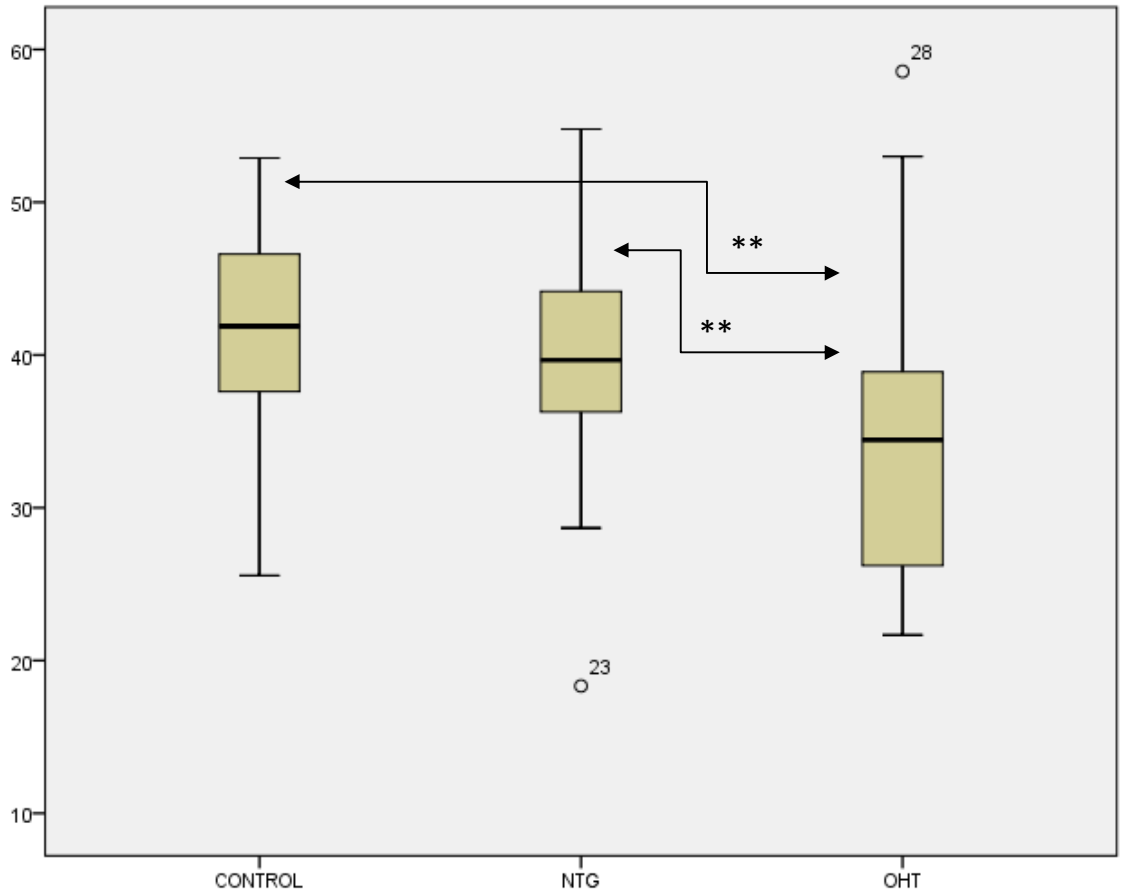

Fig 4.53: Graph showing the mean ocular perfusion pressure (MOPP) at night for the control, NTG and OHT subjects. The MOPP (night) was expressed in mmHg and calculated as follows: 2/3 Mean arterial pressure (MAP) night – supine IOP, where MAP night =2/3DBP (night) + 1/3SBP (night).

The median (IQR) MOPP (night) for the control, NTG and OHT groups was 42mmHg (37 to 47), 40mmHg (35 to 44) and 34mmHg (26 to 39), respectively. Similarly to the DPP (day and night) and the MOPP (day), a statistically significant reduction was noted in the MOPP (night) of the OHT subjects, as compared to the control group (p=0.009). Also, similarly to the MOPP (day) and DPP (night), the MOPP (night) of the OHT patients was significantly lower,

as compared to that of the NTG subjects (p=0.001). No difference was noted between the control and NTG groups (p=0.79).

Discussion: Based on Fig 4.48, it appears that the equally low DPP (day) in the NTG and OHT groups, as compared to the controls, reflects the relatively low DBP (day) in the case of the NTG patients and the relatively high mean GAT IOP (day) in the case of the OHT subjects. Similarly to our study, several studies, such as the LALES (Memarzadeh et al 2010), Barbados Eye Study (Leske et al 2008), EMGT (Leske et al 2007) and Egna-Neumarkt (Banomi et al 2000), have shown a link between low PPs and glaucoma, in line with the vascular hypothesis for the development of glaucomatous optic neuropathy. It is, however, interesting to note that in the LALES the association between low PPs and higher prevalence of OAG was not present in persons with low SBP and low DBP (Memarzadeh et al 2010), thus reflecting the influence of IOP on PP. This is evident in our NTG group by the low DBP (day), which might better reflect the potential vascular risks in this group than the PPs. An important strength of the analysis presented here is the use of 24-hr ABP monitoring, unlike many of the aforementioned epidemiological studies, such as the LALES and BES, which only performed 2 BP readings during the day. The pattern followed for the MOPP (day and night) is more similar to the DPP (day and night) than the SPP (day and night) pattern, as explained by the relatively higher contribution of DBP, as compared to SBP, to the calculation of MAP.

As discussed previously (see sections 1.3.6 and 1.5.7), vascular dysregulation has been associated with OAG (Flammer et al 2007, Grieshaber et al 2007). Apart from the role of chronically low perfusion in OAG, as supported in the present study by the reduced DPP (day) in NTG, vascular dysregulation could also manifest as unstable perfusion with either wide fluctuations or nocturnal

dips in perfusion pressure. In the present study, the median (IQR) % drop in the SPP from day to night for the control, NTG and OHT subjects was 13.4% (5.4 to 17.9), 14.2% (7.4 to 17.6) and 16.9% (8.1 to 19.6), respectively. No difference was noted in the % drop in the SPP between the three groups. However, the % drop in the DPP from day to night for the control, NTG and OHT subjects was 21.6% (11.5 to 28.4), 19.9% (13.2 to 26.1) and 29.0% (17.6 to 32.9), respectively, with the % drop in the DPP of the OHT subjects being significantly higher than the NTG patients (p=0.001) and showing a trend to be higher than the controls (p=0.097). Also, the % drop in the MOPP from day to night for the control, NTG and OHT subjects was 19.9% (8.6 to 26.3), 17.9% (8.6 to 23.1) and 26.6% (14.1 to 32.4), respectively. Similarly to the DPP, the % drop in the MOPP of the OHT subjects was significantly higher than the NTG patients (p=0.004) and showed a trend to be higher than the controls (p=0.076). In summary, in OHT, rather unexpectedly, the % drop in DPP and MOPP from day to night was more pronounced, despite starting from an already low DPP and MOPP during the day. Since mean GAT IOP during the day was overall similar to the supine IOP, the reported % drop in PPs is more likely to reflect changes in the SBP, DBP and MAP from day to night in these patients.

Chapter 5

General Discussion

Chapter 5: General discussion and future work

In this thesis, the methodology, baseline characteristics and results from the UKGTS, the first randomised, double-masked, placebo-controlled, multicentre treatment trial for OAG, are presented. As discussed in more detail in Chapter 3, the UKGTS confirms the importance of IOP in the pathogenesis of glaucoma and that IOPcc appears to predict progression behaviour better than the conventional measure (and the one used in all previous trials) of GAT. The survival analysis showed a statistically significant difference in the time from baseline to the event of confirmed VF progression in the medical treatment (latanoprost) group, as compared to placebo, over 24 months. Median IOP during follow-up, as measured by GAT, DCT, IOPcc and IOPg, was significantly, but weakly, correlated with VF progression. The IOPcc appeared the best predictor of progression across all the UKGTS sites, either because IOPcc provided a more accurate or consistent measure of IOP or because it may have better reflected ocular susceptibility to IOP, to the extent that susceptibility is influenced by the material properties of the eye and reflected in the corneal biomechanics. Also, IOPcc appeared to be less dependent on the operator, as shown by the relatively consistent relationship between IOP and progression rate across sites.

Interestingly, DCT IOP, despite being known to be the most accurate and precise IOP measurement, proved the best model to predict progression only at some UKGTS sites, when sites were considered individually, suggesting possible differences in calibration and/or operation across sites. Also, while the addition of CCT slightly improved the GAT IOP prediction model, CCT on its own was not a significant predictor of progression in the UKGTS. CH was superior to CCT in improving the GAT model prediction, suggesting that CH

better reflects the GAT IOP measurement error than CCT (see section 3.5.2). In summary, the UKGTS is the first randomised, double-masked, placebo-controlled, multicentre treatment trial for OAG, and the analysis presented here from this unique cohort provides a novel insight into the role of IOP, as a risk factor for progression. Future work will explore the association between additional covariates (CRF and AL) and both IOP and glaucoma progression. Also, the role of the diurnal IOP variation and of the DCT ocular pulse amplitude in glaucoma progression will be investigated.

In Chapter 4, the purpose of the mitochondrial pilot study was, for the first time, to explore the role, and measure the potential contribution, of systemic mitochondrial dysfunction- and oxidative stress- related risk factors as background susceptibility factors for glaucoma. A major strength of the mitochondrial exploratory study was its prospective and unique design, where patients at the extremes of IOP susceptibility (with progressing NTG and stable OHT) were compared to age-similar controls. NTG patients were carefully selected to have at least 5 years of follow-up demonstrating fast VF progression and a mean IOP<16mmHg. Similarly, OHT patients were required to have a mean IOP>24mmHg over at least 5 years of follow-up without VF progression. We carefully considered the possibility of including POAG patients in our analysis, although it was felt that, within a pilot study, focusing on patients with aggressive disease and normal IOP would be more likely to reveal and highlight the potential 'mitochondrial' or 'oxidative stress' component of the disease. Moreover, the clinical phenotyping of the participants was performed by one investigator (GL) and was detailed enough to include, amongst other things, phasing with GAT and DCT, analysis of corneal biomechanics with ORA, 24-hr BP monitoring and ocular biometry.

Studies on human samples, although in many ways closer to and more representative of human disease than studies on animals or cell cultures, tend to be associated with the variability that often characterises human beings. Being aware of this limitation, and to ensure the validity of our results, multiple experimental techniques were employed to evaluate mitochondrial function (ATP, TMRM, Calcium, mTOR), oxidative stress (DHE, aconitase, 8OHdG) and antioxidant reserve/defence (vitamins A, B6, B12, C, folate, urate, SOD2). Each of these techniques targeted a distinct and carefully selected component of cellular/mitochondrial function and, although this exploratory study was largely descriptive and has not exhaustively probed mechanisms, it has provided unique insight into potential mechanisms.

The utility of using lymphocyte-derived cells (lymphoblasts) to investigate systemic mitochondrial dysfunction in optic neuropathies has been demonstrated previously in studies that determined OXPHOS defects in LHON (Brown et al 2000, Brown et al 2001), ADOA (Van Bergen et al 2011) and POAG (Lee et al 2012). In this study, and in accordance to previous studies from our group (Schapira et al 1992) and other groups (Yoshino et al 1992, Barroso et al 1993, Shinde et al 2006) in Parkinson's disease, we chose to use fresh unstimulated peripheral blood cells. More specifically, and for the first time in the field of ophthalmology, we chose to use fresh unstimulated lymphocytes, as a more 'pure' human model that would minimise any potential effect of viral transformation on the measurements of mitochondrial function.

Glaucomatous optic neuropathy is increasingly considered a neurodegenerative disease, while recently the generalised neurodegenerative background of glaucoma was described by Rance et al, who reported vulnerability to widespread neurodegenerative disease in POAG patients,

including a temporal processing defect in the auditory pathways (Rance et al 2012). Interestingly, very few of our NTG patients had any co-existing neurological diseases, such as Parkinson's disease (n=1) or dementia (n=1). The lack of systemic phenotypic changes (eg neurological) in the NTG group, as one might anticipate in line with the reduced mitochondrial function reported for complex IV, may be explained by the relatively small contribution of complex IV, as compared to mitochondrial complexes I and II/III, to the total mitochondrial ATP production and by the diverse metabolic requirements of different tissues. To further illustrate the complexity of correlating phenotype with genotype and mitochondrial function, some patients with LHON do not appear to have primary LHON mutations (Lamminen et al 1997) or, in certain cases, any mtDNA changes at all (Fauser et al 2002).

LHON mutations have been described in patients with NTG (Opial et al 2001); however we did not screen for such mutations in our cohort. The VF loss found in our NTG group was atypical for hereditary optic neuropathies, and the vast majority of our patients were unusually old for LHON and other hereditary optic neuropathies. LHON is typically associated with subacute injury of the majority of optic nerve fibers (Howell et al 2003), often in a young adult male with a maternal family history of visual loss, and is a very different optic neuropathy from NTG, which causes the gradual loss of optic nerve fibres over a period of years in an older individual.

Glaucoma is clearly a multifactorial disease and it was therefore expected that mitochondrial dysfunction and oxidative stress might not be the dominant risk factors in all our NTG patients. In some patients other factors (such as vascular) may predominate and this could explain the lack of differences between the NTG and control groups, particularly in the ATP (Complex I and Complexes

II/III), TMRM, DHE and calcium measurements. The impact of co-existing systemic diseases could also not be ignored, as discussed in more detail in the results section, especially in the context of the mTOR and 8OHdG measurements.

The potential impact of topical medications on our measurements of oxidative stress and mitochondrial dysfunction was also considered, although no convincing evidence exists to date to suggest that drugs applied topically would have a major impact on human circulating lymphocytes. Moreover, it has been suggested that the two main types of glaucoma drops used nowadays, prostaglandin analogues and b-blockers, which were slightly more common in the NTG as compared to the OHT group, may have a protective, rather than damaging, effect. More specifically, in a relatively recent study by Izzotti at el, timolol was found to protect human endothelial cells in culture from oxidative stress and it was hypothesised that this antioxidant activity was involved in the therapeutic effect of this drug in glaucoma (Izzotti et al 2008). Moreover, prostaglandin E(2) has been shown to protect human lung fibroblasts from cigarette smoke extract-induced apoptosis (Sugiura et al 2007). Similar protective effects and improvement in the TAS in the aqueous of glaucoma patients have also been reported with topical dorzolamide (Zanon-Moreno et al 2009).

With regards to oxidative stress, the data presented here suggest that at baseline the overall oxidative damage, as measured by aconitase, is increased in NTG. Also, although the baseline superoxide levels were not significantly increased in NTG, the overall rate of superoxide production is likely to be relatively higher in NTG, probably due to the protective masking effect of the relatively higher SOD2. Importantly, the higher consumption of antioxidants in

the NTG cohort (14 out of 30), as compared to the OHT patients (7 out of 30) may have masked the lower antioxidant reserves noted in the NTG group and could explain the only marginally reduced levels of urate and vitamin A in this group. Also, the differences in antioxidant use between groups could explain the relatively reduced levels of vitamins C and B6 in the OHT group, where comparatively little antioxidant consumption was reported.

In OHT, the lower levels of SOD2 noted in this group with similar baseline superoxide levels to NTG, would suggest that the overall rate of superoxide production in OHT is lower than in NTG, thus further supporting the idea of increased ETC efficiency in OHT. This efficiency is also highlighted by the fact that in OHT the mitochondria showed enhanced ETC function with increased energy production by complexes I and II/III, higher $\Delta\Psi m$ and enhanced calcium buffering capacity, but without generating significantly more superoxide, as shown by the baseline DHE staining. Furthermore, under conditions of stress, the OHT lymphocytes showed superior antioxidant capacity to the NTG lymphocytes, as demonstrated by the smaller increase in DHE staining upon rotenone treatment, thus suggesting reduced susceptibility of the OHT cells to oxidative damage under these conditions.

In the study by Ferreira et al (2004), the level of water-soluble antioxidants (glutathione, vitamin C, tyrosine) was lower in the aqueous humour of POAG patients as compared to a control cataract group, while the activity of two enzymes involved in antioxidant defence (SOD and glutathione peroxidase) in the aqueous was nearly 1.6 times greater (Ferreira et al 2004). Such contradictory observations might be explained by the existence of compensatory mechanisms related to redox metabolism in glaucoma. It is also interesting to note that our results of increased SOD2 expression and lower

vitamin C in the NTG cohort would be in line with the results by Ferreira et al and would be supported by the above explanation.

A study is currently under way to better understand why patients with OHT have more efficient mitochondria by measuring for the first time the transcript levels of various genes that influence mitochondrial function/structure in the lymphocytes of OHT and NTG patients, and control subjects. Lymphocyte pellets from the 90 participants in the mitochondrial pilot study have been stored at -80^{o}C to assist with this genetic project and with other future analyses. Understanding the complex genetic influences that may lead to resistance to glaucoma damage and glaucoma progression in our OHT cohort is of paramount importance, in order to elucidate potentially important pathophysiological pathways amenable to therapeutic intervention. Apart from the stored lymphocyte pellets, stored serum and urine aliquots from the pilot mitochondrial study participants will be valuable for studies such as immunoproteomics (Grus et al 2008).

In the future, and in order to explore these mechanisms in more detail, a different model may be developed to characterise the mitochondria with the use of fibroblasts from NTG patients. Transforming fibroblasts into induced pluripotent stem cells (iPS) and from there to neurons or retinal ganglion cells (Chen et al 2010) would provide a model of human glaucoma, in which additional mechanistic pathways could be evaluated, potentially leading to new therapeutic approaches.

Furthermore, the unique UKGTS cohort, which includes OAG patients with detailed phenotyping and known rates of progression, would be ideally suited for an observational study looking at the relationship between systemic mitochondrial function, as measured in this thesis, and rate of progression.

This study would aim to explore whether the findings from the mitochondrial pilot study (with patients at the extreme of IOP susceptibility) operate as susceptibility factors in a wider unselected population of patients with glaucoma by associating mitochondrial function with progression rates. The identification of mitochondrial biomarkers associated most strongly with glaucoma progression, perhaps in certain subgroups of patients, may be used in glaucoma risk stratification, enabling closer monitoring and more intensive treatment of susceptible patients and, therefore, help prevent glaucoma blindness.

From a translational perspective, and should enhanced mitochondrial function be confirmed as protective for glaucoma development and progression, clinical trials aiming at improving systemic mitochondrial function might prove beneficial for delaying VF loss, especially in carefully selected subgroups of patients. Idebenone, as an example, has recently been shown to be safe and well tolerated, and also beneficial to LHON patients with discordant visual acuities, in other words to patients at the early stages of the disease (Klopstock et al 2011).

In summary, the mitochondrial pilot study suggests for the first time that OHT patients may have more efficient mitochondria at a systemic level, when compared to age-similar NTG subjects and non-glaucomatous controls. Overall, OHT lymphocytes produced higher levels of ATP (as demonstrated separately for Complex I and Complexes II/III), had higher mitochondrial membrane potential, enhanced capacity to deal with exogenous oxidative stress insults, higher serum levels of urate (a potent antioxidant), and were more capable of taking up and buffering cytosolic calcium, as compared to NTG and control lymphocytes. Lymphocytes from NTG patients, when compared to the OHT

and control groups, showed lower ATP synthesis from Complex IV, lower aconitase activity, lower serum levels of vitamin C, and enhanced antioxidant defence (SOD2), while there was a trend for the levels of another antioxidant (vitamin A) to be lower in the serum of NTG patients. No difference was noted in urinary 8OHdG levels between control, NTG and OHT subjects, in line with the presence of similar baseline superoxide levels in the lymphocytes of participants from each of the three groups. Also, the activity of mTOR, in a subgroup of patients with no history of vasospasm, was significantly lower in the NTG lymphocytes, as compared to the controls. In conclusion, this study implicates the role of a) systemic oxidative damage and complex IV-linked mitochondrial defects in the pathogenesis of NTG and b) healthy systemic mitochondria in resistance to glaucomatous optic neuropathy development and progression, particularly in the context of OHT.

References

Abitbol O, Bouden J, Doan S, et al. Corneal hysteresis measured with the Ocular Response Analyzer in normal and glaucomatous eyes. Acta Ophthalmol 2010; 88: 116-9.

Abramov AY and Duchen MR. Actions of ionomycin, 4-BrA23187 and a novel electrogenic Ca2+ ionophore on mitochondria in intact cells. Cell Calcium 2003; 33: 101-12.

Abramov AY, Fraley C, Diao CT, et al. Targeted polyphosphatase expression alters mitochondrial metabolism and inhibits calcium-dependent cell death. Proc Natl Acad Sci USA 2007; 104: 18091-6.

Abu-Amero KK, Cabrera VM, Larruga JM, et al. Eurasian and Sub-Saharan African mitochondrial DNA haplogroup influences pseudoexfoliation glaucoma development in Saudi patients. Mol Vis 2011; 17: 543–547.

Abu-Amero KK, Morales J, Bosley TM. Mitochondrial abnormalities in patients with primary open-angle glaucoma. Invest Ophthalmol Vis Sci 2006; 47: 2533–2541.

Abu-Amero KK, Morales J, Osman MN, et al. Nuclear and mitochondrial analysis of patients with primary angle-closure glaucoma. Invest Ophthalmol Vis Sci 2007; 48: 5591–5596.

Acehan D, Jiang X, Morgan DG, et al. Three-dimensional structure of the apoptosome: implications for assembly, procaspase-9 binding, and activation. Mol Cell 2002; 9: 423-32.

Advanced Glaucoma Intervention Study (AGIS): 2. Visual field test scoring and reliability. Ophthalmology 1994; 101: 1445–55.

Advanced Glaucoma Intervention Study (AGIS): 3. Baseline characteristics of black and white patients. Ophthalmology 1998; 105:1137-45.

Advanced Glaucoma Intervention Study (AGIS): 7. The relationship between control of intraocular pressure and visual field deterioration. The AGIS Investigators. Am J Ophthalmol 2000; 130: 429-40.

Advanced Glaucoma Intervention Study (AGIS): 8. Risk of cataract after trabeculectomy. Arch Ophthalmol 2001; 119: 1771–1780.

Advanced Glaucoma Intervention Study (AGIS): 12. Baseline risk factors for sustained loss of visual field and visual acuity in patients with advanced glaucoma. Am J Ophthalmol 2002; 134: 499-512.

Airaksinen PJ, Mustonen E, Alanko HI. Optic disc hemorrhages. Analysis of stereophotographs and clinical data of 112 patients. Arch Ophthalmol 1981; 99: 1795–1801.

Akaike H. A new look at the statistical model identification. IEEE Transactions on Automatic Control 1974; 19: 716–723.

Akiyama H, Nakazawa T, Shimura M, et al. Presence of mitogen-activated protein kinase in retinal Muller cells and its neuroprotective effect ischemia–reperfusion injury. Neuroreport 2002; 13: 2103–07.

Alexander C, Votruba M, Pesch UE, et al. OPA1, encoding a dynamin-related GTPase, is mutated in autosomal dominant optic atrophy linked to chromosome 3q28. Nat Genet 2000; 26: 211–5.

Altintaş O, Maral H, Yüksel N, et al. Homocysteine and nitric oxide levels in plasma of patients with pseudoexfoliation syndrome, pseudoexfoliation

glaucoma, and primary open-angle glaucoma. Graefes Arch Clin Exp Ophthalmol 2005; 243: 677-83.

Alvarado J, Murphy C, Polansky J, et al. Age-related changes in trabecular meshwork cellularity. Invest Ophthalmol Vis Sci 1981; 21: 714-27.

American Academy of Ophthalmology. Preferred practice pattern of primary open angle glaucoma. San Francisco: American Academy of Ophthalmology, 1996.

Ames BN, Cathcart R, Schwier E, et al. Uric acid provides an antioxidant defense in humans against oxidant- and radical caused aging and cancer: A hypothesis. Proc Natl Acad Sci USA 1981; 78: 6858-62.

Ames BN and Gold LS. Endogenous mutagens and the causes of aging and cancer. Mutat Res 1991; 250: 3-16.

Anand A, De Moraes CG, Teng CC, et al. Corneal hysteresis and visual field asymmetry in open angle glaucoma. Invest Ophthalmol Vis Sci 2010; 51: 6514-8.

Anderson DR and Quigley HA. The optic nerve. In: Hart Jr WM (ed.), Adler's Physiology of the Eye, 9th edn, Mosby, St. Louis, 1992, pp 616-639.

Andrews RM, Griffiths PG, Johnson MA, et al. Histochemical localisation of mitochondrial enzyme activity in human optic nerve and retina. Br J Ophthalmol 1999; 83: 231–5.

Andrews R, Ressiniotis T, Turnbull DM, et al. The role of mitochondrial haplogroups in primary open angle glaucoma. Br J Ophthalmol 2006; 90: 488–90.

Ang GS, Bochmann F, Townend J, et al. Corneal biomechanical properties in primary open angle glaucoma and normal tension glaucoma. J Glaucoma 2008; 17: 259–62.

Araie M, Sekine M, Suzuki Y, et al. Factors contributing to the progression of visual field damage in eyes with normal-tension glaucoma. Ophthalmology 1994; 101: 1440–44.

Artes PH, Chauhan BC. Longitudinal changes in the visual field and optic disc in glaucoma. Prog Retin Eye Res 2005; 24: 333–54.

Asrani S, Zeimer R, Wilensky J, et al. Large diurnal fluctuations in intraocular pressure are an independent risk factor in patients with glaucoma. J Glaucoma 2000; 9: 134-42.

Avisar R, Avisar E, Weinberger D. Effect of coffee consumption on intraocular pressure. Ann Pharmacother 2002; 36: 992–5.

Babcock DF, Herrington J, Goodwin PC, et al. Mitochondrial participation in the intracellular Ca2+ network. J Cell Biol 1997; 136: 833-44.

Bagnis A, Izzotti A, Centofanti M, et al. Aqueous humor oxidative stress proteomic levels in primary open angle glaucoma. Exp Eye Res 2012; 103: 55-62.

Baltan S, Inman DM, Danilov CA, et al. Metabolic vulnerability disposes retinal ganglion cell axons to dysfunction in a model of glaucomatous degeneration. J Neurosci 2010; 30: 5644–52.

Barnett NL and Pow DV. Antisense knockdown of GLAST, a glial glutamate transporter, compromises retinal function. Invest Ophthalmol Vis Sci 2000; 41: 585-91.

Barron MJ, Griffiths P, Turnbull DM, et al. The distributions of mitochondria and sodium channels reflect the specific energy requirements and conduction properties of the human optic nerve head. Br J Ophthalmol 2004; 88: 286-90.

Barroso N, Campos Y, Huertas R, et al. Respiratory chain enzyme activities in lymphocytes from untreated patients with Parkinson disease. Clin Chem 1993; 39: 667-9.

Bartz-Schmidt KU, Thumann G, Jonescu-Cuypers CP, et al. Quantitative morphologic and functional evaluation of the optic nerve head in chronic open-angle glaucoma. Surv Ophthalmol 1999; 44: S41–53.

Bàthori G, Parolini I, Tombola F, et al. Porin is present in the plasma membrane where it is concentrated in caveolae and caveolae-related domains. J Biol Chem 1999; 274: 29607-12.

Becker B. Towards the physiological function of uric acid. Free Radic Biol Med 1993; 14: 615–31.

Becker B, Kolker AE, Ballin N. Thyroid function and glaucoma. Am J Ophthalmol 1966; 61: 997–9.

Belenky MA, Smeraski CA, Provencio I, et al. Melanopsin retinal ganglion cells receive bipolar and amacrine cell synapses. J Comp Neurol 2003; 460: 380-93.

Bellezza AJ, Hart RT, Burgoyne CF. The optic nerve head as a biomechanical structure: initial finite element modeling. Invest Ophthalmol Vis Sci 2000; 41: 2991–3000.

Bengtsson B, Holmin C, Krakau CE. Disc haemorrhage and glaucoma. Acta Ophthamol (Copenh) 1981; 59: 1–14.

Bengtsson B, Leske MC, Hyman L, et al. Fluctuation of intraocular pressure and glaucoma progression in the early manifest glaucoma trial. Ophthalmology 2007; 114: 205-9.

Bergea B, Bodin L, Svedbergh B. Impact of intraocular pressure regulation on visual fields in open-angle glaucoma. Ophthalmology 1999; 106: 997-1004, discussion 1004-5.

Betarbet R, Sherer TB, MacKenzie G, et al. Chronic systemic pesticide exposure reproduces features of Parkinson's disease. Nat Neurosci 2000; 3: 1301–6.

Bhardwaj A. SAH-induced cerebral vasospasm: unraveling molecular mechanisms of a complex disease. Stroke 2003; 34: 427–33.

Bindokas VP, Jordan J, Lee CC et al. Superoxide production in rat hippocampal neurons: selective imaging with hydroethidine. J Neurosci 1996; 168: 1324-36.

Biousse V, Newman NJ, Sternberg P Jr. Retinal vein occlusion and transient monocular visual loss associated with hyperhomocystinemia. Am J Ophthalmol 1997; 124: 257–60.

Black JA, Waxman SG, Hildebrand C. Membrane specialization and axo-glial association in the rat retinal nerve fibre layer: freeze-fracture observations. J Neurocytol 1984; 13: 417-30.

Bochmann F, Ang GS, Azuara-Blanco A. Lower corneal hysteresis in glaucoma patients with acquired pit of the optic nerve (APON). Graefes Arch Clin Exp Ophthalmol 2008; 246: 735–8.

Boehm AG, Weber A, Pillunat LE, et al. Dynamic contour tonometry in comparison to intracameral IOP measurements. Invest Ophthalmol Vis Sci 2008; 49: 2472-7.

Bogacka I, Xie H, Bray GA, et al. Pioglitazone induces mitochondrial biogenesis in human subcutaneous adipose tissue *in vivo*. Diabetes 2005; 54: 1392-9.

Bonne C and Muller A. The glaucoma excitotoxicity theory. In: Haefliger IO and Flammer J (eds.), Nitric Oxide and Endothelin in the Pathogenesis of Glaucoma, Lippincott-Raven Publishers, New York, 1997, pp 205-12.

Bonomi L, Marchini G, Marraffa M, et al. Vascular risk factors for primary open angle glaucoma: the Egna-Neumarkt Study. Ophthalmology 2000; 107: 1287-93.

Borel CO, McKee A, Parra A, et al. Possible role for vascular cell proliferation in cerebral vasospasm after subarachnoid hemorrhage. Stroke 2003; 34: 427–33.

Bose S, Piltz JR, Breton ME. Nimodipine, a centrally active calcium antagonist, exerts a beneficial effect on contrast sensitivity in patients with normal-tension glaucoma and in control subjects. Ophthalmology 1995; 102: 1236–41.

Bosley TM, Abu-Amero KK, Ozand PT. Mitochondrial DNA nucleotide changes in non-arteritic ischemic optic neuropathy. Neurology 2004; 63: 1305–8.

Bouitbir J, Charles AL, Echaniz-Laguna A, et al. Opposite effects of statins on mitochondria of cardiac and skeletal muscles: a 'mitohormesis' mechanism involving reactive oxygen species and PGC-1. Eur Heart J 2012; 33: 1397-407.

Boulton M, Rozanowska M, Rozanowski B. Retinal photodamage. J Photochem Photobiol B 2001; 64: 144-61.

Bouvier M, Szatkowski M, Amato A, et al. The glial cell glutamate uptake carrier counter transports pH-changing anions. Nature 1992; 360: 471-4.

Boycott BB and Hopkins JM. Microglia in the retina of monkey and other mammals; its distinction from other types of glia and horizontal cells. Neurosci 1981; 6: 679-88.

Bragadin M, Pozzan T, Azzone GF. Kinetics of Ca^{2+} carrier in rat liver mitochondria. Biochemistry 1979; 18: 5972-8.

Brandon MC, Lott M, Nguyen KC, et al. MITOMAP. A human mitochondrial genome database–2004 update. Nucl Acids Res 2005; 33: D611–D613.

Brandstatter JH, Hartveit E, Sassoe Pognetto M, eta l. Expression of NMDA and high-affinity kainate receptor subunit mRNAs in the adult rat retina. Eur J Neurosci 1994; 6: 1100–12.

Brandt JD. Central corneal thickness-tonometry artifact, or something more? Ophthalmology 2007; 114: 1963–4.

Bray GM, Villegas-Pérez MP, Vidal-Sanz M, et al. Neuronal and nonneuronal influences of retinal ganglion cell survival, axonal regrowth, and connectivity after axotomy. Ann NY Acad Sci 1991; 633: 214–28.

Bristow EA, Griffiths PG, Andrews RM, et al. The distribution of mitochondrial activity in relation to optic nerve structure. Arch Ophthalmol 2002; 120: 791–6.

Broman AT, Congdon NG, Bandeen-Roche K, et al. Influence of corneal structure, corneal responsiveness, and other ocular parameters on tonometric measurement of intraocular pressure. J Glaucoma 2007; 16: 581–8.

Broman AT, Quigley HA, West SK, et al. Estimating the Rate of Progressive Visual Field Damage in Those with Open-Angle Glaucoma, from Cross-Sectional Data. Invest Ophthalmol Vis Sci 2008; 49: 66–76.

Brooks DE, Garcia GA, Dreyer EB, et al. Vitreous body glutamate concentration in dogs with glaucoma. Am J Vet Res 1997; 58: 864–7.

Brown MD, Trounce IA, Jun AS, et al. Functional analysis of lymphoblast and cybrid mitochondria containing the 3460, 11778, or 14484 Leber's hereditary optic neuropathy mitochondrial DNA mutation. J Biol Chem 2000; 275: 39831–6.

Brown MD, Allen JC, Van Stavern GP, et al. Clinical, genetic, and biochemical characterization of a Leber hereditary optic neuropathy family containing both the 11778 and 14484 primary mutations. Am J Med Genet 2001; 104: 331–8.

Browne GS, Nelson C, Nguyen T, et al. Stereoselective and substrate-dependent inhibition of hepatic mitochondria beta-oxidation and oxidative phosphorylation by the non-steroidal anti-inflammatory drugs ibuprofen, flurbiprofen, and ketorolac. Biochem Pharmacol 1999; 57: 837-44.

Bunce C, Xing W, Wormald R. Causes of blind and partial sight certifications in England and Wales: April 2007–March 2008. Eye (Lond) 2010; 24: 1692–9.

Burdon KP, Macgregor S, Hewitt AW, et al. Genome-wide association study identifies susceptibility loci for open angle glaucoma at TMCO1 and CDKN2B-AS1. Nat Genet 2011; 43: 574-8.

Bus JS and Gibson JE. Paraquat: model for oxidant-initiated toxicity. Environ Health Perspect 1984; 55: 37–46.

Cadenas E and Davies KJ. Mitochondrial free radical generation, oxidative stress, and aging. Free Radic Biol Med 2000; 29: 222-30.

Cadet J, Bourdat GD, Ham C, et al. Oxidative base damage to DNA: specificity of base excision repair enzymes. Mutat Res 2000; 462: 121- 128.

Cahill M, Karabatzaki M, Meleady R, et al. Raised plasma homocysteine as a risk factor for retinal vascular occlusive disease. Br J Ophthalmol 2000; 84: 154–7.

Caprioli J. Neuroprotection of the optic nerve in glaucoma. Acta Ophthalmologica 1997; 75: 364–7.

Caprioli J and Coleman AL. Intraocular pressure fluctuation: A risk factor for visual field progression at low intraocular pressures in the Advanced Glaucoma Intervention Study. Ophthalmology 2008; 115: 1123-9.

Cardellach F, Alonso JR, López S, et al. Effect of smoking cessation on mitochondrial respiratory chain function. J Toxicol Clin Toxicol 2003; 41: 223-8.

Carelli V, Ross-Cisneros FN, Sadun AA. Mitochondrial dysfunction as a cause of optic neuropathies. Prog Retin Eye Res 2004; 23: 53-89.

Carew JS, Kelly KR, Nawrocki ST. Mechanisms of mTOR inhibitor resistance in cancer therapy. Target Oncol 2011; 6: 17–27.

Carmignoto G, Maffei L, Candeo P, et al. Effect of NGF on the survival of rat retinal ganglion cells following optic nerve section. J Neurosci 1989; 9: 1763–72.

Carter-Dawson L, Crawford ML, Harwerth RS, et al. Vitreal glutamate concentration in monkeys with experimental glaucoma. Invest Ophthalmol Vis Sci 2002; 43: 2633–7.

Centers for Disease Control and Prevention. Assessment of laboratory tests for plasma homocysteine—selected laboratories, July–September 1998. MMWR 1999; 48: 1013–5.

Cellerino A, Carroll P, Thoenen H, et al. Reduced size of retinal ganglion cell axons and hypomyelination in mice lacking brain derived neurotrophic factor. Mol Cell Neurosci 1997; 9: 397–408.

Chan DC. Mitochondria: dynamic organelles in disease, aging, and development. Cell 2006; 125: 1241–52.

Chandrasekaran S, Rochtchina E, Mitchell P. Effects of caffeine on intraocular pressure: the Blue Mountains Eye Study. J Glaucoma 2005; 14: 504–7.

Charliat G, Jolly D, Blanchard F. Genetic risk factor in primary open-angle glaucoma: a case–control study. Ophthalmic Epidemiol 1994; 1: 131–8.

Chauhan BC, Garway-Heath DF, Goñi FJ, et al. Practical recommendations for measuring rates of visual fi eld change in glaucoma. Br J Ophthalmol 2008a; 92: 569–73.

Chauhan BC, Hutchison DM, LeBlanc RP, et al. Central corneal thickness and progression of the visual field and optic disc in glaucoma. Br J Ophthalmol 2005; 89: 1008-12.

Chauhan BC, Mikelberg FS, Balaszi AG, et al. Canadian Glaucoma Study: 2. risk factors for the progression of open-angle glaucoma. Arch Ophthalmol 2008b; 126: 1030-6.

Chaves RS, Melo TQ, Martins SA, et al. Protein aggregation containing beta-amyloid, alpha-synuclein and hyperphosphorylated tau in cultured cells of hippocampus, substantia nigra and locus coeruleus after rotenone exposure. BMC Neurosci 2010; 11: 144.

Cheah BC, Vucic S, Krishnan AV, et al. Neurophysiological index as a biomarker for ALS progression: validity of mixed effects models. Amyotroph Lateral Scler 2011; 12: 33–8.

Chen LB. Mitochondrial membrane potential in living cells. Annu Rev Cell Biol 1988; 4: 155–81.

Chen M, Chen Q, Sun X, et al. Generation of retinal ganglion-like cells from reprogrammed mouse fibroblasts. Invest Ophthalmol Vis Sci 2010; 51: 5970-8.

Chidlow G and Osborne NN. Rat retinal ganglion cell loss caused by kainate, NMDA and ischemia correlates with a reduction in mRNA and protein of Thy-1 and neurofilament light. Brain Res 2003; 963: 298–306.

Chihara E, Liu X, Dong J, et al. Severe myopia as a risk factor for progressive visual field loss in primary open-angle glaucoma. Ophthalmologica 1997; 211: 66–71.

Chiou CC, Chang PY, Chan EC, et al. Urinary 8-hydroxydeoxyguanosine and its analogs as DNA marker of oxidative stress: development of an ELISA and measurement in both bladder and prostate cancers. Clin Chim Acta 2003; 334: 87-94.

Choi WS, Palmiter RD, Xia Z. Loss of mitochondrial complex I activity potentiates dopamine neuron death induced by microtubule dysfunction in a Parkinson's disease model. J Cell Biol 2011; 192: 873–82.

Choo HJ, Kim JH, Kwon OB, et al. Mitochondria are impaired in the adipocytes of type 2 diabetic mice. Diabetologia 2006; 49: 784-91.

Chrysostomou V, Rezania F, Trounce IA, et al. Oxidative stress and mitochondrial dysfunction in glaucoma. Curr Opin Pharmacol 2013; 13: 12-5.

Chung HS, Harris A, Evans DW, et al. Vascular aspects in the pathophysiology of glaucomatous optic neuropathy. Surv Ophthalmol 1999a; 43: 43-50.

Chung HS, Harris A, Kagemann L, et al. Peripapillary retinal blood flow in normal tension glaucoma. Br J Ophthalmol 1999b; 83: 466-9.

Civitarese AE, Carling S, Heilbronn LK, et al. Calorie restriction increases muscle mitochondrial biogenesis in healthy humans. PLoS Med 200; 4: e76.

Clarke R, Daly L, Robinson K, et al. Hyperhomocysteinemia: an independent risk factor for vascular disease. N Engl J Med 1991; 324: 1149–355.

Clarke R and Stansbie D. Assessment of homocysteine as a cardiovascular risk factor in clinical practice. Ann Clin Biochem 2001; 38: 624–32.

Cleeter MW, Cooper JM, Schapira AH. Nitric oxide enhances MPP(+) inhibition of complex I. FEBS Lett 2001; 504: 50–2.

Cleeter MW, Chau KY, Gluck C, et al. Glucocerebrosidase inhibition causes mitochondrial dysfunction and free radical damage. Neurochem Int 2013; 62: 1-7.

Clement CI, Goldberg I, Healey PR, et al. Plasma homocysteine, MTHFR gene mutation, and open-angle glaucoma. J Glaucoma 2009; 18: 73-8.

Cohen HY, Miller C, Bitterman KJ, et al. Calorie restriction promotes mammalian cell survival by inducing the SIRT1 deacetylase. Science 2004; 305: 390–2.

Coleman AL. Glaucoma. Lancet 1999; 354: 1803-10.

Coleman AL and Miglior S. Risk factors for glaucoma onset and progression. Surv Ophthalmol 2008; 53: S3-10.

Collaborative Normal-Tension Glaucoma Study Group. Comparison of glaucomatous progression between untreated patients with normal-tension glaucoma and patients with therapeutically reduced intraocular pressures. Am J Ophthalmol 1998; 126: 487–97.

Congdon NG, Broman AT, Bandeen-Roche K, et al. Central corneal thickness and corneal hysteresis associated with glaucoma damage. Am J Ophthalmol 2006; 141: 868–75.

Corral-Debrinski M, Horton T, Lott MT, et al. Mitochondrial DNA deletions in human brain: regional variability and increase with advanced age. Nat Genet 1992; 2: 324–9.

CNTGS Study Group. The effectiveness of intraocular pressure reduction in the treatment of normal-tension glaucoma. Am J Ophthalmol 1998; 126: 498-505.

CNTGS Study Group. Comparison of glaucomatous progression between untreated patients with normal tension glaucoma and patients with therapeutically reduced intraocular pressures. Am J Ophthalmol 1998; 126: 487-97.

Crabb DP, Garway-Heath DF. Wait and see: varying the interval between visits to get better estimates of the rate of visual field progression in glaucoma. Invest Ophthalmol Vis Sci 2009; 50: 1669.

Crompton M, Capano M, Carafoli E. The sodium-induced efflux of calcium from heart mitochondria. Eur J Biochem 1976; 69: 453–62.

Crompton M, Virji S, Ward JM. Cyclophilin-D binds strongly to complexes of the voltage-dependent anion channel and the adenine nucleotide translocase to form the permeability transition pore. Eur J Biochem 1998; 258: 729-35.

Cunningham JT, Rodgers JT, Arlow DH, et al. mTOR controls mitochondrial oxidative function through a YY1-PGC-1alpha transcriptional complex. Nature 2007; 450: 736-40.

Curcio CA and Hendrickson AE. Organization and development of the primate photoreceptor mosaic. Prog Ret Eye Res 1991; 10: 89-120.

Cursiefen C, Wisse M, Cursiefen S, et al. Migraine and tension headache in high-pressure and normal-pressure glaucoma. Am J Ophthalmol 2000; 129: 102-4.

Cutler RG. Urate and ascorbate: their possible roles as antioxidants in determining longevity of mammalian species. Arch Gerontol Geriatr 1984; 3: 321–48.

Danesh-Meyer HV, Boland MV, Savino PJ, et al. Optic disc morphology in open-angle glaucoma compared with anterior ischemic optic neuropathies. Invest Ophthalmol Vis Sci 2010; 51: 2003–10.

De Flora S, Izzotti A, Randerath K, et al. DNA adducts and chronic degenerative disease. Pathogenetic relevance and implications in preventive medicine. Mutat Res 1996; 366: 197-238.

De Moraes CV, Hill V, Tello C, et al. Lower corneal hysteresis is associated with more rapid glaucomatous visual field progression. J Glaucoma 2012; 21: 209-13.

De Moraes CG, Liebmann JM, Greenfield DS, et al; Low-pressure Glaucoma Treatment Study Group. Risk factors for visual field progression in the low-pressure glaucoma treatment study. Am J Ophthalmol 2012; 154: 702-11.

De Stefani D, Raffaello A, Teardo E, et al. A forty-kilodalton protein of the inner membrane is the mitochondrial calcium uniporter. Nature 2011; 476: 336-40.

De Voogd S, Ikram MK, Wolfs RC, et al. Is diabetes mellitus a risk factor for open-angle glaucoma? The Rotterdam Study. Ophthalmology 2006; 113: 1827-31.

Delettre C, Lenaers G, Griffoin J, et al. Nuclear gene OPA1, encoding a mitochondrial dynamin-related protein, is mutated in dominant optic atrophy. Nat Genet 2000; 26: 207–10.

Desai BN, Myers BR, Schreiber SL. FKBP12-rapamycin-associated protein associates with mitochondria and senses osmotic stress via mitochondrial dysfunction. Proc Natl Acad Sci USA 2002; 99: 4319-24.

Detry-Morel M, Jamart J, Detry MB, et al. Clinical evaluation of the Pascal dynamic contour tonometer. J Fr Ophtalmol 2007; 30: 260-70.

Di Stefano PS, Friedman B, Radziejewski C, et al. The neurotrophins BDNF, NT-3 and NGF display distinct patterns of retrograde axonal transport in peripheral and central neurons. Neuron 1992; 8: 943–93.

Doughty MJ and Zaman ML. Human corneal thickness and its impact on intraocular pressure measures: a review and meta-analysis approach. Surv Ophthalmol 2000; 44: 367-408.

Douglas GR. Pathogenetic mechanisms of glaucoma not related to intraocular pressure. Curr Opin Ophthalmol 1998; 9: 34-8.

Drahota Z, Milerová M, Stieglerová A, et al. Developmental changes of cytochrome c oxidase and citrate synthase in rat heart homogenate. Physiol Res 2004; 53: 119-22.

Drance SM. Disc hemorrhages in the glaucomas. Surv Ophthalmol 1989; 33: 331–7.

Drance SM, Anderson DR, Schulzer M, et al. Risk factors for progression of visual field abnormalities in normal-tension glaucoma. Am J Ophthalmol 2001; 131: 699-708.

Drance SM, Douglas GR, Wijsman K, et al. Response of blood flow to warm and cold in normal and low-tension glaucoma patients. Am J Ophthalmol 1988; 105: 35-9.

Dreisbach AW, Greif RL, Lorenzo BJ, et al. Lipophilic beta-blockers inhibit rat skeletal muscle mitochondrial respiration. Pharmacology 1993; 47: 295-9.

Druzhyna NM, Wilson GL, Ledoux SP. Mitochondrial DNA repair in aging and disease. Mech Ageing Dev 2008; 129: 383–90.

Duval C, Negre-Salvayre A, Dogilo A, et al. Increased reactive oxygen species production with antisense oligonucleotides directed against uncoupling protein 2 in murine endothelial cells. Biochem Cell Biol 2002; 80: 757–64.

Ederer F, Gaasterland DA, Dally LG, et al. The Advanced Glaucoma Intervention Study (AGIS): 13. Comparison of treatment outcomes within race: 10-year results. Ophthalmology 2004; 111: 651–64.

Edwards R. Biosynthesis of retinoic acid by Muller glial cells: A model for the central nervous system? Prog Ret Eye Res 1994; 13: 231-42.

Edwards R, Thornton J, Ajit R, et al. Cigarette smoking and primary open angle glaucoma: a systematic review. J Glaucoma 2008; 17: 558-66.

Egorov SY, Krasnovsky AA Jr, Bashtanov MY, et al. Photosensitization of singlet oxygen formation by pterins and flavins. Time-resolved studies of oxygen

phosphorescence under laser excitation. Biochemistry (Mosc) 1999; 64: 1117-21.

Elisaf M, Kitsos G, Bairaktari E, et al. Metabolic abnormalities in patients with primary open-angle glaucoma. Acta Ophthalmol Scand 2001; 79: 129-32.

European Glaucoma Society. Terminology and guidelines for European Glaucoma Society, Savona, Italy, Dogma Srl, 1998.

Fain GL, Matthews HR, Cornwall MC, et al. Adaptation in vertebrate photoreceptors. Physiol Rev 2001; 81: 117-51.

Faivre S, Kroemer G, Raymond E. Current development of mTOR inhibitors as anticancer agents. Nat Rev Drug Discov 2006; 5: 671–88.

Fan BJ, Leung YF, Wang N, et al. Genetic and environmental risk factors for primary open-angle glaucoma. Chin Med J (Engl) 2004; 117: 706–10.

Fan BJ, Wang DY, Lam DS, et al. Gene mapping for primary open angle glaucoma. Clin Biochem 2006; 39: 249-58.

Fauser S, Luberichs J, Besch D, et al. Sequence analysis of the complete mitochondrial genome in patients with Leber's hereditary optic neuropathy lacking the three most common pathogenic DNA mutations. Biochem Biophys Res Commun 2002; 295: 342–7.

Fautsch MP, Bahler CK, Jewison DJ, et al. Recombinant TIGR/MYOC increases outflow resistance in the human anterior segment. Invest Ophthalmol Vis Sci 2000; 41: 4163-8.

Ferrarini AM, Sivieri S, Bulian P, et al. Time-course of interleukin-2 receptor expression in interferon beta-treated multiple sclerosis patients. J Neuroimmunol 1998; 84: 213–7.

Ferreira SM, Lerner SF, Brunzini R, et al. Oxidative stress markers in aqueous humor of glaucoma patients. Am J Ophthalmol 2004; 137: 62-9.

Ferreira SM, Lerner SF, Brunzini R, et al. Time course changes of oxidative stress markers in a rat experimental glaucoma model. Invest Ophthalmol Vis Sci 2010; 51: 4635-40.

Fingert JH, Stone EM, Sheffield VC, et al. Myocilin glaucoma. Surv Ophthalmol 2002; 47: 547–61.

Fink BD, Reszka KJ, Herlein JA, et al. Respiratory uncoupling by UCP1 and UCP2 and superoxide generation in endothelial cell mitochondria. Am J Physiol Endocrinol Metab 2005; 288: E71–9.

Fishbein SL and Goodstein S. The pressure lowering effect of ascorbic acid. Ann Ophthalmol 1972; 4: 487–91.

Fiskum G. Mitochondrial participation in ischemic and traumatic neural cell death. J Neurotrauma 2000; 17: 843-55.

FitzgibbonT and Taylor SF. Retinotopy of the human retinal nerve fibre layer and optic nerve head. J Comp Neurol 1996; 375: 238–251.

Flammer J, Haefliger IO, Orgul S, et al. Vascular dysregulation: a principal risk factor for glaucomatous damage? J Glaucoma 1999; 8: 212-9.

Flammer J and Mozaffarieh M. What is the present pathogenetic concept of glaucomatous optic neuropathy? Surv Ophthalmol 2007; 52: 162–73.

Flammer J and Orgul S. Optic nerve blood flow abnormalities in glaucoma. Prog Retinal Eye Res 1998; 17: 267-89.

Flammer J, Orgul S, Costa VP, et al. The impact of ocular blood flow in glaucoma. Prog Retin Eye Res 2002; 21: 359–93.

Flammer J, Pache M, Resink T. Vasospasm, its role in the pathogenesis of diseases with particular reference to the eye. Prog Retin Eye Res 2001; 20: 319-49.

Floyd RA. The role of 8-hydroxyguanine in carcinogenesis. Carcinogenesis 1990; 11: 1447- 50.

Forchheimer I, de Moraes CG, Teng CC, et al. Baseline mean deviation and rates of visual field change in treated glaucoma patients. Eye (Lond) 2011; 25: 626-32.

Ford ES, Smith SJ, Stroup DF, et al. Homocysteine and cardiovascular disease: a systematic review of the evidence with special emphasis on case-control studies and nested case-control studies. Int J Epidemiol 2002; 31: 59–70.

Foster PJ, Baasanhu J, Alsbirk PH, et al. Central corneal thickness and intraocular pressure in a Mongolian population. Ophthalmology 1998; 105: 969–73.

Foster PJ, Broadway DC, Hayat S, et al. Refractive error, axial length and anterior chamber depth of the eye in British adults: the EPIC-Norfolk Eye Study. Br J Ophthalmol 2010; 94: 827-30.

Foster PJ, Buhrmann R, Quigley HA, et al. The definition and classification of glaucoma in prevalence surveys. Br J Ophthalmol 2002; 86: 238–42.

Franco-Bourland RE, Guizar-Sahagun G, Garcia GA. Retinal vulnerability to glutamate excitotoxicity in canine glaucoma: induction of neuronal nitric oxide synthase in retinal ganglion cells. Proc West Pharmacol Soc 1998; 41: 201–4.

Gallego A. Comparative studies on horizontal cells and a note on microglial cells. Prog Ret Eye Res 1986; 5: 165-206.

Gardner PR, Nguyen DD, White CW. Aconitase is a sensitive and critical target of oxygen poisoning in cultured mammalian cells and in rat lungs. Proc Natl Acad Sci USA 1994; 91: 12248–52.

Garway-Heath DF, Lascaratos G, Bunce C, et al; on behalf of the UKGTS Investigators. The United Kingdom Glaucoma Treatment Study: a multicentre, randomized, placebo-controlled clinical trial. Design and methodology. Ophthalmology 2013; 120: 68-76.

Gasser P and Flammer J. Blood-cell velocity in the nailfold capillaries of patients with normal-tension and high-tension glaucoma. Am J Ophthalmol 1991; 111: 585-8.

Gasser P, Flammer J, Guthauser U, et al. Do vasospasms provoke ocular diseases? Angiology 1990; 41: 213-20.

Gasser P, Stumpfig D, Schotzau A, et al. Body mass index in glaucoma. J Glaucoma 1999; 8: 8–11.

Ghanem AA, Arafa LF, El-Baz A. Oxidative stress markers in patients with primary open-angle glaucoma. Curr Eye Res 2010; 35: 295-301.

Gherghel D, Griffiths HR, Hilton EJ, et al. Systemic reduction in glutathione levels occurs in patients with primary openangle glaucoma. Invest Ophthalmol Vis Sci 2005; 46: 877–83.

Gillespie BW, Musch DC, Guire KE, et al. The collaborative initial glaucoma treatment study: baseline visual field and test-retest variability. Invest Ophthalmol Vis Sci 2003; 44: 2613-20.

Giorgi C, De Stefani D, Bononi A, et al. Structural and functional link between the mitochondrial network and the endoplasmic reticulum. Int J Biochem Cell Biol 2009; 41: 1817-27.

Giorgi C, Romagnoli A, Pinton P, et al. Ca^{2+} signaling, mitochondria and cell death. Curr Mol Med 2008; 8: 119-30.

Girkin CA, McGwin G Jr, McNeal SF, et al. Hypothyroidism and the development of open-angle glaucoma in a male population. Ophthalmology 2004; 111: 1649-52.

Giulivi C, Boveris A, Cadenas E. Hydroxyl radical generation during mitochondrial electron transfer and the formation of 8-hydroxy-desoxyguanosine in mitochondrial DNA. Arch Biochem Biophys 1995; 316: 909–16.

Glantzounis GK, Tsimoyiannis EC, Kappas AM, et al. Uric acid and oxidative stress. Curr Pharm Des 2005; 11: 4145–51.

Glaucoma Laser Trial Research Group. The Glaucoma Laser Trial (GLT) and glaucoma laser trial follow-up study: 7. Results. Am J Ophthalmol 1995; 120: 718–31.

Glynn RJ, Seddon JM, Krug JH, et al. Falls in elderly patients with glaucoma. Arch Ophthalmol 1991; 109: 205.

Godley BF, Shamsi FA, Liang FQ, et al. Blue light induces mitochondrial DNA damage and free radical production in epithelial cells. J Biol Chem 2005; 280: 21061-6.

Goping IS, Millar DG, Shore GC. Identification of the human mitochondrial protein import receptor, huMas20p. Complementation of delta mas20 in yeast. FEBS Lett 1995; 373: 45–50.

Goto W, Ota T, Morikawa N, et al. Protective effects of timolol against the neuronal damage induced by glutamate and ischemia in the rat retina. Brain Res 2002; 958: 10–19.

Greaney MJ, Hoffman DC, Garway-Heath DF, et al. Comparison of optic nerve imaging methods to distinguish normal eyes from those with glaucoma. Invest Ophthalmol Vis Sci 2002; 43: 140–5.

Greenfield DS, Liebmann JM, Ritch R, et al. Visual field and intraocular pressure asymmetry in the low-pressure glaucoma treatment study. Ophthalmology 2007; 114: 460-5.

Grieshaber MC, Mozaffarieh M, Flammer J. What is the link between vascular dysregulation and glaucoma? Surv Ophthalmol 2007; 52: S144–54.

Grune T, Blasig IE, Sitte N, et al. Peroxynitrite increases the degradation of aconitase and other cellular proteins by proteasome. J Biol Chem 1998; 273: 10857–62.

Grunwald JE, Piltz J, Hariprasad SM, et al. Optic nerve and choroidal circulation in glaucoma. Invest Ophthalmol Vis Sci 1998; 39: 2329-36.

Grus FH, Joachim SC, Bruns K, et al. Serum autoantibodies to alpha-fodrin are present in glaucoma patients from Germany and the United States. Invest Ophthalmol Vis Sci 2006; 47: 968-76.

Grus FH, Joachim SC, Hoffmann EM, et al. Complex autoantibody repertoires in patients with glaucoma. Mol Vis 2004; 10: 132–7.

Grus FH, Joachim SC, Wuenschig D, et al. Autoimmunity and glaucoma. J Glaucoma 2008; 17: 79-84.

Grus F and Sun D. Immunological mechanisms in glaucoma. Semin Immunopathol 2008; 11: 11.

Gunter TE and Pfeiffer DR. Review Mechanisms by which mitochondria transport calcium. Am J Physiol 1990; 258: C755-86.

Halliwell B and Gutteridge JM. Free Radicals in Biology and Medicine. Oxford University Press, New York, 1999.

Hamilton ML, Van Remmen H, Drake JA, et al. Does oxidative damage to DNA increase with age? Proc Natl Acad Sci USA 2001; 98: 10469– 74.

Hannibal J, Hindersson P, Ostergaard J, et al. Melanopsin is expressed in PACAP-containing retinal ganglion cells of the human retinohypothalamic tract. Invest Ophthalmol Vis Sci 2004; 45: 4202-9.

Hargrave PA and McDowell JH. Rhodopsin and phototransduction: a model system for G protein-linked receptors. FASEB J 1992; 6: 2323-31.

Harman D. The biologic clock: the mitochondria? J Am Geriatr Soc 1972; 20: 145–7.

Harvey DJ, Beckett LA, Mungas DM. Multivariate modelling of two associated cognitive outcomes in a longitudinal study. J Alzheimers Dis 2003; 5: 357–65.

Hatefi Y. The mitochondrial electron transport and oxidative phosphorylation system. Annu Rev Biochem 1985; 54: 1015-69.

Hayreh SS. Inter-individual variation in blood supply of the optic nerve head. Its importance in various ischemic disorders of the optic nerve head, and

glaucoma, low-tension glaucoma and allied disorders. Doc Ophthalmol 1985; 59: 217-46.

Hayreh SS. The blood supply of the optic nerve head and the evaluation of it - myth and reality. Prog Retin Eye Res 2001; 20: 563–93.

Hayreh SS. The optic nerve head circulation in health and disease. The 1994 Von Sallman Lecture. Exp Eye Res 1995; 61: 259–272.

Hayreh SS. Posterior ciliary artery circulation in health and disease: the Weisenfeld lecture. Invest Ophthalmol Vis Sci 2004; 45: 749-57.

Heijl A. Frequent disc photography and computerized perimetry in eyes with optic disc hemorrhage. A pilot study. Acta Ophthalmol 1986; 64: 274 –81.

Heijl A, Bengtsson B, Hyman L, et al. Early Manifest Glaucoma Trial Group. Natural history of open-angle glaucoma. Ophthalmology 2009; 116: 2271–6.

Heijl A, Bengtsson B, Chauhan BC, et al. A comparison of visual field progression criteria of three major glaucoma trials in Early Manifest Glaucoma Trial patients. Ophthalmology 2008; 115: 1557-65.

Heijl A, Leske MC, Bengtsson B, et al. Reduction of intraocular pressure and glaucoma progression: results from the Early Manifest Glaucoma Trial. Arch Ophthalmol 2002; 120: 1268-79.

Hennis A, Wu SY, Nemesure B, et al; Barbados Eye Studies Group. Hypertension, diabetes and longitudinal changes in intraocular pressure. Ophthalmology 2003; 110: 908–14.

Herrmann W, Obeid R. Homocysteine: a biomarker in neurodegenerative diseases. Clin Chem Lab Med 2011; 49: 435–41.

Hewitt AW, Craig JE, Mackey DA. Complex genetics of complex traits: the case of primary open-angle glaucoma. Clin Experiment Ophthalmol 2006; 34: 472-84.

Higginbotham EJ, Kilimanjaro HA, Wilensky JT, et al. The effect of caffeine on intraocular pressure in glaucoma patients. Ophthalmology 1989; 96: 624–6.

Hildebrand C, Remahl S, Waxman SG. Axo-glial relations in the retina-optic nerve junction of the adult rat: electron-microscopic observations. J Neurocytol 1985; 14: 597-617.

Hiller R, Sperduto RD, Ederer F. Emidemiologic associations with nuclear, cortical, and posterior subcapsular cataracts. Am J Epidemiol 1986; 134: 916–25.

Hinokio Y, Suzuki S, Hirai M, et al. Urinary excretion of 8-oxo-7,8-dihydro-2-deoxyguanosine as a predictor of the development of diabetic nephropathy. Diabetologia 2002; 45: 877–82.

Hockberger PE, Skimina TA, Centonze VE, et al. Activation of flavin-containing oxidases underlies light-induced production of H_2O_2 in mammalian cells. Proc Natl Acad Sci USA 1999; 96: 6255-60.

Hollander H, Makarov F, Dreher Z, et al. Structure of the macroglia of the retina: sharing and division of labour between astrocytes and Muller cells. J Comp Neurol 1991; 313: 587-603.

Hollander H, Makarov F, Stefani FH, et al. Evidence of constriction of optic nerve axons at the lamina cribrosa in the normotensive eye in humans and other mammals. Ophthalmic Res 1995; 27: 296–309.

Holloszy J, Oscai LB, Don IJ, et al. Mitochondrial citric acid cycle and related enzymes: Adaptive response to exercise. Biochem Biophys Res Comm 1970; 40: 1368-73.

Holmin C, Thorburn W, Krakau CE. Treatment versus no treatment in chronic open angle glaucoma. Acta Ophthalmol (Copenh) 1988; 66: 170-3.

Hong S, Kim CY, Seong GJ, et al. Central corneal thickness and visual field progression in patients with chronic primary angle-closure glaucoma with low intraocular pressure. Am J Ophthalmol 2007a; 143: 362-3.

Hong S, Seong GJ, Hong YJ. Long-term intraocular pressure fluctuation and progressive visual field deterioration in patients with glaucoma and low intraocular pressures after a triple procedure. Arch Ophthalmol 2007b; 125: 1010-3.

Hoth M, Fanger CM, Lewis RS. Mitochondrial regulation of store-operated calcium signaling in T lymphocytes. J Cell Biol 1997; 137: 633-48.

Houle RE and Grant WM. Alcohol, vasopressin, and intraocular pressure. Invest Ophthalmol 1967; 6: 145–54.

Howard DJ, Ota RB, Briggs LA, et al. Environmental tobacco smoke in the workplace induces oxidative stress in employees, including increased production of 8-hydroxy-2-deoxyguanosine. Cancer Epidemiol Biomarkers Prev 1998; 7: 141– 6.

Howell N. LHON and other optic nerve atrophies: the mitochondrial connection. Dev Ophthalmol 2003; 37: 94–108.

Hoyng PFJ, de Jong N, Oosting H, et al. Platelet aggregation, disc hemorrhage and progressive loss of visual fields in glaucoma. Int Ophthalmol 1992; 16: 65–73.

Hudson G, Carelli V, Spruijt L, et al. Clinical expression of Leber hereditary optic neuropathy is affected by the mitochondrial DNA–haplogroup background. Am J Hum Genet 2007; 81: 228–33.

Hügel S, Horn M, de Groot M, et al. Effects of ACE inhibition and beta-receptor blockade on energy metabolism in rats postmyocardial infarction. Am J Physiol 1999; 277: H2167-75.

Hugkulstone CE, Smith LF, Vernon SA. Trabeculectomy in diabetic patients with glaucoma. Eye 1993; 7: 502–6.

IHS headache classification committee. Classification and diagnostic criteria for headache disorders, cranial neuralgias and facial pain. Cephalalgia 1988 8: 1-96.

Inagaki Y, Mashima Y, Fuse N, et al. Glaucoma Gene Research Group. Mitochondrial DNA mutations with Leber's hereditary optic neuropathy in Japanese patients with open-angle glaucoma. Jpn J Ophthalmol 2006; 50: 128-34.

Inden M, Kitamura Y, Abe M, et al. Parkinsonian rotenone mouse model: reevaluation of long-term administration of rotenone in C57BL/6 mice. Biol Pharm Bull 2011; 34: 92–6.

Inoue-Matsuhisa E, Sogo S, Mizota A, et al. Effect of MCI-9042, a 5-HT2 receptor antagonist, on retinal ganglion cell death and retinal ischemia. Exp Eye Res 2003; 76: 445–52.

Ishida K, Yamamoto T, Kitazawa Y. Clinical factors associated with progression of normal-tension glaucoma. J Glaucoma 1998; 7: 372–7.

Ishida K, Yamamoto T, Sugiyama K, et al. Disc haemorrhage is a significantly negative prognostic factor in normal-tension glaucoma. American Journal of Ophthalmology 2000; 129: 707-14.

Ishii K, Mori M, Oshika T. An evaluation of the effects of eyeball structure on ocular pulse amplitude in healthy subjects. Int Ophthalmol 2012; 32: 553-7.

Izzotti A, Bagnis A, Sacca SC. The role of oxidative stress in glaucoma. Mutat Res 2006; 612: 105-14.

Izzotti A, Saccà SC, Cartiglia C, et al. Oxidative deoxyribonucleic acid damage in the eyes of glaucoma patients. Am J Med 2003; 114: 638-46.

Izzotti A, Saccà SC, Di Marco B, et al. Antioxidant activity of timolol on endothelial cells and its relevance for glaucoma course. Eye (Lond) 2008; 22: 445-53.

Izzotti A, Sacca SC, Longobardi M, et al. Sensitivity of ocular anterior chamber tissues to oxidative damage and its relevance to the pathogenesis of glaucoma. Invest Ophthalmol Vis Sci 2009; 50: 5251-8.

Izzotti A, Sacca SC, Longobardi M, et al. Mitochondrial damage in the trabecular meshwork of patients with glaucoma. Arch Ophthalmol 2010; 128: 724–30.

Jampel HD. Target pressure in glaucoma therapy. J Glaucoma 1997; 6: 133–8.

Jampel HD, Moon JI, Quigley HA, et al. Aqueous humor uric acid and ascorbic acid concentrations and outcome of trabeculectomy. Arch Ophthalmol 1998; 116: 281-5.

Jämsén K. Thyroid disease, a risk factor for optic neuropathy mimicking normal-tension glaucoma. Acta Ophthalmol Scand 1996; 74: 456-60.

Ji JZ, Elyaman W, Yip HK, et al. CNTF promotes survival of retinal ganglion cells after induction of ocular hypertension in rats: the possible involvement of STAT3 pathway. Eur J Neurosci 2004; 19: 265–72.

Johnson EC, Deppmeier LM, Wentzien SK, et al. Chronology of optic nerve head and retinal responses to elevated intraocular pressure. Invest Ophthalmol Vis Sci 2000; 41: 431–42.

Jonas JB, Berenshtein E, Holbach L. Lamina cribrosa thickness and spatial relationships between intraocular space and cerebrospinal fluid space in highly myopic eyes. Invest Ophthalmol Vis Sci 2004; 45: 2660–5.

Jonas JB, Martus P, Budde WM. Anisometropia and degree of optic nerve damage in chronic open-angle glaucoma. Am J Ophthalmol 2002; 134: 547-51.

Jonas JB, Martus P, Horn FK, et al. Predictive factors of the optic nerve head for development or progression of glaucomatous visual field loss. Invest Ophthalmol Vis Sci 2004; 45: 2613-8.

Jonas JB, Stroux A, Velten I, et al. Central corneal thickness correlated with glaucoma damage and rate of progression. Invest Ophthalmol Vis Sci 2005; 46: 1269-74.

Jones SP, Teshima Y, Akao M, et al. Simvastatin attenuates oxidant-induced mitochondrial dysfunction in cardiac myocytes. Circ Res 2003; 93: 697-9.

Jou MJ, Jou SB, Guo MJ, et al. Mitochondrial reactive oxygen species generation and calcium increase induced by visible light in astrocytes. Ann N Y Acad Sci 2004; 1011: 45-56.

Ju WK, Liu Q, Kim KY, et al. Elevated hydrostatic pressure triggers mitochondrial fission and decreases cellular ATP in differentiated RGC-5 cells. Invest Ophthalmol Vis Sci 2007; 48: 2145–51.

Ju WK, Kim KY, Lindsey JD, et al. Intraocular pressure elevation induces mitochondrial fission and triggers OPA1 release in glaucomatous optic nerve. Invest Ophthalmol Vis Sci 2008; 49: 4903-11.

Jünemann AG, von Ahsen N, Reulbach U, et al. C677T variant in the methylentetrahydrofolate reductase gene is a genetic risk factor for primary open-angle glaucoma. Am J Ophthalmol 2005; 139: 721-3.

Jung JS, Kim HJ, Cho M. Action spectra for the generation of singlet oxygen from mitochondrial membranes from soybean (Glycine max) hypocotyls. Photochem Photobiol 1990; 51: 561-6.

Kahn HA, Leibowitz HM, Ganley JP, et al. The Framingham Eye Study. II. Association of ophthalmic pathology with single variables previously measured in the Framingham Heart Study. Am J Epidemiol 1977; 106: 33–41.

Kahn HA, Milton RC. Alternative definitions of open-angle glaucoma. Effect on prevalence and associations in the Framingham eye study. Arch Ophthalmol 1980; 98: 2172–7.

Kalloniatis M. Amino acids in neurotransmission and disease. J Am Optom Assoc 1995; 66: 750–7.

Kamei S, Chen-Kuo-Chang M, Cazevieille C, et al. Expression of the Opa1 mitochondrial protein in retinal ganglion cells: Its downregulation causes aggregation of the mitochondrial network. Invest Ophthalmol Vis Sci 2005; 46: 4288–94.

Kamal D, Garway-Heath D, Ruben S, et al. Results of the betaxolol versus placebo treatment trial in ocular hypertension. Graefes Arch Clin Exp Ophthalmol 2003; 241: 196–203.

Kandel ER and Squire LR. Neuroscience: breaking down scientific barriers to the study of brain and mind. Science 2000; 290: 1113-20.

Kang JH, Pasquale LR, Rosner BA, et al. Prospective study of cigarette smoking and the risk of primary open-angle glaucoma. Arch Ophthalmol 2003; 121: 1762-8.

Kang JH, Pasquale LR, Willett W, et al. Antioxidant intake and primary open-angle glaucoma: a prospective study. Am J Epidemiol 2003; 158: 337-46.

Kang JH, Willett WC, Rosner BA, et al. Prospective study of alcohol consumption and the risk of primary open-angle glaucoma. Ophthalmic Epidemiol 2007; 14: 141-7.

Kang JH, Willett WC, Rosner BA, et al. Caffeine consumption and the risk of primary open-angle glaucoma: a prospective cohort study. Invest Ophthalmol Vis Sci 2008; 49: 1924-31.

Kanngiesser HE, Kniestedt C, Robert YC. Dynamic contour tonometry: presenting a new tonometer. J Glaucoma 2005; 14: 344–50.

Kanski JJ, Nischal KK. The optic disc. In: Kanski JJ and Nischal KK (eds.), Ophthalmology, Clinical Signs and Differential Diagnosis, Mosby, St Louis, 1999, pp 247–285.

Kao JP, Harootunian AT, Tsien RY. Photochemically generated cytosolic calcium pulses and their detection by fluo-3. J Biol Chem 1989; 264: 8179-84.

Kapasi AA, Patel G, Goenka A, et al. Ethanol promotes T cell apoptosis through the mitochondrial pathway. Immunology 2003; 108: 313-20.

Karadimas P, Bouzas EA, Topouzis F, et al. Hypothyroidism and glaucoma. A study of 100 hypothyroid patients. Am J Ophthalmol 2001; 131: 126-8.

Karpova MB, Schoumans J, Ernberg I, et al. Raji revisited: cytogenetics of the original Burkitt's lymphoma cell line. Leukemia 2005; 19: 159-61.

Kasai H. Analysis of a form of oxidative DNA damage, 8-hydroxy-2-deoxyguanosine, as a marker of cellular oxidative stress during carcinogenesis. Mutat Res 1997; 387: 147-63.

Kass MA, Heuer DK, Higginbotham EJ, et al. Ocular Hypertension Treatment Study Group. The Ocular Hypertension Treatment Study: a randomized trial determines that topical ocular hypotensive medication delays or prevents the onset of primary open-angle glaucoma. Arch Ophthalmol 2002; 120: 701–13.

Katz J, Gilbert D, Quigley HA, et al. Estimating progression of visual field loss in glaucoma. Ophthalmology 1997; 104: 1017–25.

Katz LJ, Myers JS. Smoothing the intraocular pressure roller coaster: a new goal? Am J Ophthalmol 2009; 148: 177–8.

Kaufmann C, Bachmann LM, Robert YC, et al. Ocular pulse amplitude in healthy subjects as measured by dynamic contour tonometry. Arch Ophthalmol 2006; 124: 1104–8.

Kelley DE, He J, Menshikova EV, et al. Dysfunction of mitochondria in human skeletal muscle in type 2 diabetes. Diabetes 2002; 51: 2944-50.

Kerr J, Nelson P, O'Brien C. A comparison of ocular blood flow in untreated primary open angle glaucoma and ocular hypertension. Am J Ophthalmol 1998; 126: 42-51.

Kerrigan LA, Zack DJ, Quigley HA, et al. TUNEL-positive ganglion cells in human primary open-angle glaucoma. Arch Ophthalmol 1997; 115: 1031–5.

Khalil M and Gout I. Overexpression or downregulation of mTOR in mammalian cells. Methods Mol Biol 2012; 821: 87-103.

Kim JW and Chen PP. Central corneal pachymetry and visual field progression in patients with open-angle glaucoma. Ophthalmology 2004; 111: 2126–32.

Kirichok Y, Krapivinsky G, Clapham DE. The mitochondrial calcium uniporter is a highly selective ion channel. Nature 2004; 427: 360-4.

Kitazawa Y, Shirai H, Go FJ. The effect of Ca^{2+}-antagonist on visual field in low-tension glaucoma. Graefes Arch Clin Exp Ophthalmol 1989; 227: 408–12.

Klein BE, Klein R, Knudtson MD. Intraocular pressure and systemic blood pressure: longitudinal perspective: The Beaver Dam Eye Study. Br J Ophthalmol 2005; 89: 284–7.

Klein BE, Klein R, Linton KL. Intraocular pressure in an American community. The Beaver Dam Eye Study. Invest Ophthalmol Vis Sci 1992b; 33: 2224–8.

Klein BE, Klein R, Ritter LL. Relationship of drinking alcohol and smoking to prevalence of open-angle glaucoma. The Beaver Dam Eye Study. Ophthalmology 1993; 100: 1609–1.

Klein BE, Klein R, Sponsel WE, et al. Prevalence of glaucoma. The Beaver Dam Eye Study. Ophthalmology 1992a; 99: 1499-504.

Klopstock T, Yu-Wai-Man P, Dimitriadis K, et al. A randomized placebo-controlled trial of idebenone in Leber's hereditary optic neuropathy. Brain 2011; 134: 2677-86.

Knowles JR. Enzyme-catalyzed phosphoryl transfer reactions. Annu Rev Biochem 1980; 49: 877–919.

Ko ML, Peng PH, Ma MC, et al. Dynamic changes in reactive oxygen species and antioxidant levels in retinas in experimental glaucoma. Free Radic Biol Med 2005; 39: 365-73.

Kolb H. The neural organization of the human retina. In: Heckenlively JR and Arden GB (eds.), Principles and Practices of Clinical Electrophysiology of Vision, Mosby, St Louis, 1991, pp 25-52.

Kolb H, Linberg KA, Fisher SK. Neurons of the human retina: a Golgi study. J Comp Neurol 1992; 318: 147-87.

Kong YX, Van Bergen N, Bui BV, et al. Impact of aging and diet restriction on retinal function during and after acute intraocular pressure injury. Neurobiol Aging 2012; 33: 1126.

Kong YX, Van Bergen N, Trounce IA, et al. Increase in mitochondrial DNA mutations impairs retinal function and renders the retina vulnerable to injury. Aging Cell 2011; 10: 572–83.

Kong GY, Van Bergen NJ, Trounce IA, et al. Mitochondrial dysfunction and glaucoma. J Glaucoma 2009; 18: 93–100.

Kopsidas G, Kovalenko SA, Kelso JM, et al. An age-associated correlation between cellular bioenergy decline and mtDNA rearrangements in human skeletal muscle. Mutat Res 1998; 421: 27-36.

Kotecha A, Crabb DP, Spratt A, et al. The relationship between diurnal variations in intraocular pressure measurements and central corneal thickness and corneal hysteresis. Invest Ophthalmol Vis Sci 2009; 50: 4229-36.

Kotecha A, Elsheikh A, Roberts CR, et al. Corneal thickness and age-related biomechanical properties of the cornea measured with the ocular response analyzer. Invest Ophthalmol Vis Sci 2006; 47: 5337–47.

Kotecha A, White E, Schlottmann PG, et al. Intraocular pressure measurement precision with the Goldmann applanation, dynamic contour, and ocular response analyzer tonometers. Ophthalmology 2010; 117: 730-7.

Kotecha A, White ET, Shewry JM, et al. The relative effects of corneal thickness and age on Goldmann applanation tonometry and dynamic contour tonometry. Br J Ophthalmol 2005; 89: 1572–5.

Kowaltowski AJ and Vercesi AE. Mitochondrial damage induced by conditions of oxidative stress. Free Radical Biology and Medicine 1999; 26: 463-71.

Kowaltowski AJ, Castilho RF, Vercesi AE. Mitochondrial permeability transition and oxidative stress. FEBS 2001; 495: 12-15.

Kramer RH and Molokanova E. Modulation of cyclic-nucleotide-gated channels and regulation of vertebrate phototransduction. The Journal of Experimental Biology 2001; 204: 2921–31.

Kremmer S, Kreuzfelder E, Klein R, et al. Antiphosphatidylserine antibodies are elevated in normal tension glaucoma. Clin Exp Immunol 2001; 125: 211–5.

Kroemer G, Petit P, Zamzami N, et al. The biochemistry of programmed cell death. Faseb J 1995; 9: 1277–87.

Kroemer G, Reed JC. Mitochondrial control of cell death. Nat Med 2000; 6: 513–9.

Kruman I, Guo Q, Mattson MP. Calcium and reactive oxygen species mediate staurosporine-induced mitochondrial dysfunction and apoptosis in PC12 cells. J Neurosci Res 1998; 51: 293-308.

Krupin T, Liebmann JM, Greenfield DS, et al. Low-Pressure Glaucoma Study Group. The Low-pressure Glaucoma Treatment Study (LoGTS): study design and baseline characteristics of enrolled patients. Ophthalmology 2005; 112: 376–85.

Krupin T, Liebmann JM, Greenfield DS, et al. A randomized trial of brimonidine versus timolol in preserving visual function: results from the Low-pressure Glaucoma Treatment Study. Am J Ophthalmol 2011; 151: 671–81.

Kuehn MH, Fingert JH, Kwon YH. Retinal ganglion cell death in glaucoma: mechanisms and neuroprotective strategies. Ophthalmol Clin North Am 2005; 18: 383-95.

Kushnareva Y, Murphy AN, Andreyev A. Complex I-mediated reactive oxygen species generation: modulation by cytochrome c and NAD(P)+ oxidation-reduction state. Biochem J 2002; 368: 545-53.

Kynigopoulos M, Tzamalis A, Ntampos K, et al. Decreased ocular pulse amplitude associated with functional and structural damage in open-angle glaucoma. Eur J Ophthalmol 2012; 22: 111-6.

Lafuente MP, Villegas-Perez MP, Sells-Navarro I, et al. Retinal ganglion cell death after acute retinal ischemia is an ongoing process whose severity and

duration depends on the duration of the insult. Neuroscience 2002; 109: 157–168.

Lamminen T, Huoponen K, Sistonen P, et al. mtDNA haplotype analysis in Finnish families with leber hereditary optic neuroretinopathy. Eur J Hum Genet 1997; 5: 271–9.

Lamontagne J, Pepin E, Peyot ML, et al. Pioglitazone acutely reduces insulin secretion and causes metabolic deceleration of the pancreatic beta-cell at submaximal glucose concentrations. Endocrinology 2009; 150: 3465-74.

Lascaratos G, Garway-Heath DF, Willoughby C, et al. Mitochondrial dysfunction in glaucoma: understanding genetic influences. Mitochondrion 2012; 12: 202-12.

Lascaratos G, Ji D, Wood J, et al. Light (400-760nm) affects mitochondrial function and induces neuronal death in retinal cell cultures. Vision Research 2007; 47: 1191-201.

Lascaratos G, Shah A, Garway-Heath DF. The Genetics of Pigment Dispersion Syndrome and Pigmentary Glaucoma. Surv Ophthalmol 2013; 58: 164-75.

Le A, Mukesh BN, McCarty CA, et al. Risk factors associated with the incidence of open-angle glaucoma: the visual impairment project. Invest Ophthalmol Vis Sci 2003; 44: 3783-9.

Lean ME, Han TS, Morrison CE. Waist circumference as a measure for indicating need for weight management. BMJ 1995; 311: 158-61.

Lee M, Cho EH, Lew HM, et al. Relationship between ocular pulse amplitude and glaucomatous central visual field defect in normal-tension glaucoma. J Glaucoma 2012; 21: 596-600.

Lee PC, Bordelon Y, Bronstein J, et al. Traumatic brain injury, paraquat exposure, and their relationship to Parkinson disease. Neurology 2012; 79: 2061-6.

Lee PP, Walt JW, Rosenblatt LC, et al. Association between intraocular pressure variation and glaucoma progression: data from a United States chart review. Am J Ophthalmol 2007; 144: 901-7.

Lee S, Sheck L, Crowston JG, et al. Impaired complex-I-linked respiration and ATP synthesis in primary open-angle glaucoma patient lymphoblasts. Invest Ophthalmol Vis Sci 2012; 53: 2431-7.

Lee YA, Shih YF, Lin LL, et al. Association between high myopia and progression of visual field loss in primary open-angle glaucoma. J Formos Med Assoc 2008; 107: 952-7.

Lemasters JJ. Selective mitochondrial autophagy, or mitophagy, as a targeted defense against oxidative stress, mitochondrial dysfunction, and aging. Rejuvenation Res 2005; 8: 3-5.

Leite MT, Alencar LM, Gore C, et al. Comparison of corneal biomechanical properties between healthy blacks and whites using the Ocular Response Analyzer. Am J Ophthalmol 2010; 150: 163-8.

Leske MC. Ocular perfusion pressure and glaucoma: clinical trial and epidemiologic findings. Curr Opin Ophthalmol 2009; 20: 73–8.

Leske MC, Chylack LT Jr, Wu SY. The Lens Opacities Case-Control Study. Risk factors for cataract. Arch Ophthalmol 1991; 109: 244–51.

Leske MC, Connell AMS, Schachat AP, et al. The Barbados Eye Study: prevalence of open angle glaucoma. Arch Ophthalmol 1994; 112: 821–9.

Leske MC, Connell AMS, Wu SY, et al. Risk factors for open-angle glaucoma: the Barbados Eye Study. Arch Ophthalmol 1995; 113: 918–24.

Leske MC, Heijl A, Hussein M, et al. Early Manifest Glaucoma Trial Group. Factors for glaucoma progression and the effect of treatment: the Early Manifest Glaucoma Trial. Arch Ophthalmol 2003; 121: 48–56.

Leske MC, Heijl A, Hyman L, et al. Early Manifest Glaucoma Trial Group. Early Manifest Glaucoma Trial: design and baseline data. Ophthalmology 1999; 106: 2144–53.

Leske MC, Heijl A, Hyman L, et al. Predictors of long-term progression in the early manifest glaucoma trial. Ophthalmology 2007; 114: 1965-72.

Leske MC, Nemesure B, He Q, et al. Patterns of open-angle glaucoma in the Barbados Family Study. Ophthalmology 2001; 108: 1015–22.

Leske MC, Warheit-Roberts L, Wu SY. Open-angle glaucoma and ocular hypertension: the Long Island Glaucoma Case-control Study. Ophthalmic Epidemiol 1996; 3: 85–96.

Leske MC, Wu SY, Hennis A, et al. Risk factors for incident open-angle glaucoma. The Barbados Eye Studies. Ophthalmology 2008; 115: 85-93.

Levin LA. Optic nerve. In: Kaufman PL and Alm A (eds.), Adler's Physiology of the Eye, 10th edn, Mosby, St Louis, 2003, pp 603–638.

Levin LA. Retinal Ganglion Cells and Neuroprotection for Glaucoma. Survey of Ophthalmology 2003; 48: S21-S24.

Li GY, Osborne NN. Oxidative-induced apoptosis to an immortalized ganglion cell line is caspase independent but involves the activation of poly (ADP-ribose) polymerase and apoptosis-inducing factor. Brain Res 2008; 1188: 35-43.

Li H, Kumar Sharma L, Li Y, et al. Comparative bioenergetic study of neuronal and muscle mitochondria during aging. Free Radic Biol Med 2013; 63: 30-40.

Li N, Ragheb K, Lawler G, et al. Mitochondrial complex I inhibitor rotenone induces apoptosis through enhancing mitochondrial reactive oxygen species production. J Biol Chem 2003; 278: 8516-25.

Liang FQ and Godley BF. Oxidative stress-induced mitochondrial DNA damage in human retinal pigment epithelial cells: a possible mechanism for RPE aging and age-related macular degeneration. Exp Eye Res 2003; 76: 397–403.

Lichter PR, Musch DC, Gillespie BW, et al. Interim clinical outcomes in the Collaborative Initial Glaucoma Treatment Study comparing initial treatment randomized to medications or surgery. Ophthalmology 2001; 108: 1943-53.

Lightowlers RN, Chinnery PF, Turnbull DM, et al. Mammalian mitochondrial genetics: heredity, heteroplasmy and disease. Trends Genet 1997; 13: 450–5.

Likic VA, Perry A, Hulett J, et al. Patterns that define the four domains conserved in known and novel isoforms of the protein import receptor Tom20. J Mol Biol 2005; 347: 81–93.

Lin HY, Hsu WM, Chou P, et al. Intraocular pressure measured with a noncontact tonometer in an elderly Chinese population: the Shihpai Eye Study. Arch Ophthalmol 2005; 123: 381–6.

Lin MT and Beal MF. Mitochondrial dysfunction and oxidative stress in neurodegenerative diseases. Nature 2006; 443: 787–95.

Lin MT, Simon DK, Ahn CH, et al. High aggregate burden of somatic mtDNA point mutations in aging and Alzheimer's disease brain. Hum Mol Genet 2002b; 11: 133–45.

Linden M, Andersson G, Gellerfors P, et al. Subcellular distribution of rat liver porin. Biochim Biophys Acta 1984; 770: 93–6.

Lindholm LH, Carlberg B, Samuelsson O. Should beta blockers remain first choice in the treatment of primary hypertension? A meta-analysis. Lancet 2005; 366: 1545–53.

Linner E. The pressure lowering effect of ascorbic acid in ocular hypertension. Acta Ophthalmol (Copenh) 1969; 47: 685–9.

Lipton SA and Rosenberg PA. Excitatory amino acids as a final common pathway for neurologic disorders. N Engl J Med 1994; 330: 613-22.

Liu B and Neufeld AH. Activation of epidermal growth factor receptor signals induction of nitric oxide synthase-2 in human optic nerve head astrocytes in glaucomatous optic neuropathy. Neurobiol Dis 2003; 13: 109–23.

Liu B and Neufeld AH. Expression of nitric oxide synthase-2 (NOS-2) in reactive astrocytes of the human glaucomatous optic nerve head. Glia 2000; 30: 178–86.

Liu KM, Swann D, Lee P, et al. Inhibition of oxidative degradation of hyaluronic acid by uric acid. Curr Eye Res 1984; 3: 1049-53.

Loft S, Vistisen K, Ewertz M, et al. Oxidative DNA damage estimated by 8-hydroxydeoxyguanosine excretion in humans: influence of smoking, gender and body mass index. Carcinogenesis 1992; 13: 2241–7.

López-Lluch G, Hunt N, Jones B, et al. Calorie restriction induces mitochondrial biogenesis and bioenergetic efficiency. Proc Natl Acad Sci USA 2006; 103: 1768–73.

Loukil I, Korchène N, Hachicha F, et al. Ocular risk factors for progression of primary open angle glaucoma in the Tunisian population. J Fr Ophtalmol 2012 Dec 4 [Epub ahead of print] PMID: 23218598.

Louzada-Junior P, Dias JJ, Santos WF, et al. Glutamate release in experimental ischaemia of the retina: an approach using microdialysis. J Neurochem 1992; 59: 358–63.

Luo X, Budihardjo I, Zou H, et al. Bid, a Bcl2 interacting protein, mediates cytochrome c release from mitochondria in response to activation of cell surface death receptors. Cell 1998; 94: 481-90.

Luo X, Heidinger V, Picaud S, et al. Selective excitotoxic degeneration of adult pig retinal ganglion cells *in vitro*. Invest Ophthalmol Vis Sci 2001; 42: 1096–106.

Luo T, Sakai Y, Wagner E, et al. Retinoids, eye development, and maturation of visual function. J Neurobiol 2006; 66: 677-86.

Ma Y-T, Hsieh T, Forbes ME, et al. BDNF injected into the superior colliculus reduces development retinal ganglion cell death. J Neurosci 1998; 18: 2097–107.

MacDonald BK, Cockerell OC, Sander JW, et al. The incidence and lifetime prevalence of neurological disorders in a prospective community-based study in the UK. Brain 2000; 123: 665-76.

Mackey DA, Oostra RJ, Rosenberg T, et al. Primary pathogenic mtDNA mutations in multigeneration pedigrees with Leber hereditary optic neuropathy. Am J Hum Genet 1996; 59: 481–5.

Macmillan-Crow LA and Cruthirds DL. Invited review: manganese superoxide dismutase in disease. Free Radic Res 2001; 34: 325–36.

Madigan MC, Sadun AA, Rao NS, et al. Tumor necrosis factor-alpha (TNF-alpha)-induced optic neuropathy in rabbits. Neurol Res 1996; 18: 176-84.

Mangouritsas G, Morphis G, Mourtzoukos S, et al. Association between corneal hysteresis and central corneal thickness in glaucomatous and non-glaucomatous eyes. Acta Ophthalmol 2009; 87: 901-5.

Mansour-Robaey S, Clarke DB, Wang Y-C, et al. Effects of ocular injury and administration of brain-derived neurotrophic factor on survival and regrowth of axotomized retinal ganglion cells. Proc Natl Acad Sci USA 1994; 91: 1632–6.

Marin-Garcia J, Ananthakrishnan R, Goldenthal MJ. Human mitochondrial function during cardiac growth and development. Molec Cell Biochem 1998; 179: 21-6.

Mariotti S, Caturegli P, Barbesino G, et al. Thyroid function and thyroid autoimmunity independently modulate serum concentration of soluble interleukin 2 (IL-2) receptor (sIL-2R) in thyroid diseases. Clin Endocrinol 1992; 37: 415–22.

Martin KRG, Levkovitch-Verbin H, Valenta D, et al. Retinal glutamate transporter changes in experimental glaucoma and after optic nerve transection in the rat. Invest Ophthalmol Vis Sci 2002; 43: 2236-43.

Martin KR, Quigley HA, Zack DJ, et al. Gene therapy with brain-derived neurotrophic factor as a protection: retinal ganglion cells in a rat glaucoma model. Invest Ophthalmol Vis Sci 2003; 44: 4357–65.

Martinez-Bello C, Chauhan BC, Nicolela MT, et al. Intraocular pressure and progression of glaucomatous visual field loss. Am J Ophthalmol 2000; 129: 302–8.

Maruyama I, Ohguro H, Ikeda Y. Retinal ganglion cells recognized by serum autoantibody against gamma-enolase found in glaucoma subjects. Invest Ophthalmol Vis Sci 2000; 41: 1657-65.

Mason RP, Kosoko O, Wilson MR, et al. National survey of the prevalence and risk factors of glaucoma in St Lucia, West Indies: part I, prevalence findings. Ophthalmology 1989; 96: 1363–8.

Masland RH. The neuronal organization of the retina. Neuron 2012 18; 76: 266-80.

Maxwell SR, Thomason H, Sandler D, et al. Antioxidant status in patients with uncomplicated insulin-dependent and non-insulin-dependent diabetes mellitus. Eur J Clin Invest 1997; 27: 484–90.

McCully KS. Vascular pathology of homocysteinemia: Implications for the pathogenesis of arteriosclerosis. Am J Pathol 1969; 56: 111–28.

McGirt MJ, Lynch JR, Blessing R, et al. Serum von Willebrand factor, matrix metalloproteinase-9, and vascular endothelial growth factor levels predict the onset of cerebral vasospasm after aneurysmal subarachnoid hemorrhage. Neurosurgery 2002; 51: 1128–34.

Meguro A, Inoko H, Ota M, et al. Genome-wide association study of normal tension glaucoma: common variants in SRBD1 and ELOVL5 contribute to disease susceptibility. Ophthalmology 2010; 117: 1331-8.

Melov S, Coskun P, Patel M, et al. Mitochondrial disease in superoxide dismutase 2 mutant mice. Proc Natl Acad Sci USA 1999; 96: 846–51.

Memarzadeh F, Ying-Lai M, Chung J, et al. Blood Pressure, Perfusion Pressure, and Open-Angle Glaucoma: The Los Angeles Latino Eye Study. Invest Ophthalmol Vis Sci 2010; 51: 2872–7.

Mey J and Thanos S. Intravitreal injections of neurotrophic factors support the survival of axotomized retinal ganglion cells in adult rats *in vivo*. Brain Res 1993; 602: 304–17.

Minckler DS, Bunt AH, Johanson GW. Orthograde and retrograde axoplasmic transport during acute ocular hypertension in the monkey. Invest Ophthalmol Vis Sci 1977; 16: 426–41.

Minta A, Kao JP, Tsien RY. Fluorescent indicators for cytosolic calcium based on rhodamine and fluorescein chromophores. J Biol Chem 1989; 264: 8171-8.

Miró O, Alonso JR, Jarreta D, et al. Smoking disturbs mitochondrial respiratory chain function and enhances lipid peroxidation on human circulating lymphocytes. Carcinogenesis 1999; 20: 1331-6.

Mitchell P, Rochtchina E, Lee AJ, et al. Bias in self-reported family history and relationship to glaucoma: the Blue Mountains Eye Study. Ophthalmic Epidemiol 2002; 9: 333–45.

Mitchell P, Smith W, Attebo K, et al. Prevalence of open-angle glaucoma in Australia. The Blue Mountains Eye Study. Ophthalmology 1996; 103: 1661–9.

Mittag TW, Danias J, Pohorenec G, et al. Retinal damage after 3 to 4 months of elevated intraocular pressure in a rat glaucomamodel. Invest Ophthalmol Vis Sci 2000; 41: 3451–9.

Monemi S, Spaeth G, DaSilva A, et al. Identification of a novel adult-onset primary open-angle glaucoma (POAG) gene on 5q22.1. Hum Mol Genet 2005; 14: 725-33.

Moore P, El-sherbeny A, Roon P, et al. Apoptotic cell death in the mouse retinal ganglion cell layer is induced *in vivo* by the excitatory amino acid homocysteine. Exp Eye Res 2001; 73: 45–57.

Moosmann B and Behl C. Mitochondrially encoded cysteine predicts animal lifespan. Ageing Cell 2008; 7: 32–46.

Moreau B, Nelson C, Parekh AB. Biphasic regulation of mitochondrial Ca2+ uptake by cytosolic Ca2+ concentration. Curr Biol 2006; 16: 1672-7.

Moreira PI, Custodio J, Moreno A, et al. Tamoxifen and estradiol interact with the flavin mononucleotide site of complex I leading to mitochondrial failure. J Biol Chem 2006; 281: 10143–52.

Moreno MC, Campanelli J, Sande P, et al. Retinal oxidative stress induced by high intraocular pressure. Free Radic Biol Med 2004; 37: 803-12.

Morgan J, Caprioli J, Koseki Y. Nitric oxide mediates excitotoxic and anoxic damage in rat retinal ganglion cells cocultured with astroglia. Arch Ophthalmol 1999; 117: 1524– 9.

Morgan AJ and Jacob R. Ionomycin enhances Ca2+ influx by stimulating store-regulated cation entry and not by a direct action at the plasma membrane. Biochem J 1994; 300: 665–72.

Mori K, Ando F, Nomura H, et al. Relationship between intraocular pressure and obesity in Japan. Int J Epidemiol 2000; 29: 661–6.

Morita T, Shoji N, Kamiya K, et al. Intraocular pressure measured by dynamic contour tonometer and ocular response analyzer in normal tension glaucoma. Graefes Arch Clin Exp Ophthalmol 2010; 248: 73-7.

Morrison JC, Johnson EC, Cepurna W, et al. Understanding mechanisms of pressure-induced optic nerve damage. Prog Retin Eye Res 2005; 24: 217–40.

Mosinger JL, Price MT, Bai HY, et al. Blockade of both NMDA and non-NMDA receptors is required for optimal protection against ischemic neuronal degeneration in the *in vivo* adult mammalian retina. Exp Neurol 1991; 113: 10-7.

Motsko SP, Jones JK. Is there an association between hypothyroidism and open-angle glaucoma in an elderly population? An epidemiologic study. Ophthalmology 2008; 115: 1581-4.

Mujumdar VS, Aru GM, Tyagi SC. Induction of oxidative stress by homocysteine impairs endothelial function. J Cell Biochem 2001; 82: 491–500.

Muñoz-Negrete FJ, Rebolleda G, Almodóvar F, et al. Hypothyroidism and primary open-angle glaucoma. Ophthalmologica 2000; 214: 347-9.

Musarrat J, Arezina-Wilson J, Wani AA. Prognostic and aetiological relevance of 8-hydroxyguanosine in human breast carcinogenesis. Eur J Cancer 1996; 32A: 1209–14.

Musch DC, Gillespie BW, Lichter PR, et al. Visual field progression in the Collaborative Initial Glaucoma Treatment Study: the impact of treatment and other baseline factors. Ophthalmology 2009; 116: 200-7.

Musch DC, Gillespie BW, Niziol LM, et al. Intraocular pressure control and long-term visual field loss in the Collaborative Initial Glaucoma Treatment Study. Ophthalmology 2011; 118: 1766-73.

Musch DC, Lichter PR, Guire KE, et al. CIGTS Study Group. The Collaborative Initial Glaucoma Treatment Study: study design, methods, and baseline characteristics of enrolled patients. Ophthalmology 1999; 106: 653– 62.

Muskens RP, de Voogd S, Wolfs RC, et al. Systemic antihypertensive medication and incident open-angle glaucoma. Ophthalmology 2007; 114: 2221-6.

Myung IJ, Forster MR and Browne MW. Model selection (special issue). Journal of Mathematical Psychology 2000; 44: 1-2.

Nakano M, Ikeda Y, Taniguchi T, et al. Three susceptible loci associated with primary open-angle glaucoma identified by genome-wide association study in a Japanese population. Proc Natl Acad Sci USA 2009; 106: 12838-42.

Nakano M, Ikeda Y, Tokuda Y, et al. Common variants in CDKN2B-AS1 associated with optic-nerve vulnerability of glaucoma identified by genome-wide association studies in Japanese. PLoS One 2012; 7: e33389.

Naoi M, Maruyama W, Yi H, et al. Mitochondria in neurodegenerative disorders: regulation of the redox state and death signalling leading to neuronal death and survival. J Neural Transm 2009; 116: 1371–81.

Navé BT, Ouwens M, Withers DJ, et al. Mammalian target of rapamycin is a direct target for protein kinase B: identification of a convergence point for opposing effects of insulin and amino-acid deficiency on protein translation. Biochem J 1999; 344: 427-31.

Neal MJ, Cunningham JR, Hutson PH, et al. Effects of ischaemia on neurotransmitter release from the isolated retina. J Neurochem 1994; 62: 1025–33.

Negishi H, Ikeda K, Kuga S, et al. The relation of oxidative DNA damage to hypertension and other cardiovascular risk factors in Tanzania. J Hypertens 2001; 19: 529-33.

Nemesure B, Leske MC, He Q, et al. Analyses of reported family history of glaucoma: a preliminary investigation. The Barbados Eye Study Group. Ophthalmic Epidemiol 1996; 3: 135–41.

Nessim M, Mollan SP, Wolffsohn JS, et al. The relationship between measurement method and corneal structure on apparent intraocular pressure in glaucoma and ocular hypertension. Cont Lens Anterior Eye 2013; 36: 57-61.

Netland PA, Chaturvedi N, Dreyer EB. Calcium channel blockers in the management of low-tension and open-angle glaucoma. Am J Ophthalmol 1993; 115: 608-13.

Neufeld AH. Nitric oxide: a potential mediator of retinal ganglion cell damage in glaucoma. Surv Ophthalmol 1999; 43: 129-135.

Neufeld AH, Das S, Vora S, et al. A prodrug of a selective inhibitor of inducible nitric oxide synthase is neuroprotective in the rat model of glaucoma. J Glaucoma 2002; 11: 221–5.

Neufeld A, Hernández M, Gonzalez M, et al. Cyclooxygenase-1 and cyclooxygenase-2 in the human optic nerve head. Exp Eye Res 1997; 65: 739-45.

Neufeld AH, Hernandez MR, Gonzalez M. Nitric oxide synthase in the human glaucomatous optic nerve head. Arch Ophthalmol 1997; 115: 497–503.

Neufeld AH, Sawada A, Becker B. Inhibition of nitric-oxide synthase 2 by aminoguanidine provides neuroprotection of retinal ganglion cells in a rat model of chronic glaucoma. Proc Natl Acad Sci USA 1999; 96: 9944–8.

Newhouse K, Hsuan SH, Chang SH, et al. Rotenone-induced apoptosis is mediated by p38 and JNK MAP kinases in human dopaminergic SH-SY5Y cells. Toxicol Sci 2004; 79: 137–46.

Newman LA, Walker MT, Brown RL, et al. Melanopsin forms a functional short-wavelength photopigment. Biochemistry 2003; 42: 12734-8.

Nexo E, Engbaek F, Ueland PM, et al. Evaluation of novel assays in clinical chemistry: quantification of plasma total homocysteine. Clin Chem 2000; 46: 1150-6.

NICE clinical guideline 85. Glaucoma: diagnosis and management of chronic open angle glaucoma and ocular hypertension. http://www.nice.org.uk/CG85, 2009.

Nickells RW. Apoptosis of retinal ganglion cells in glaucoma: an update of the molecular pathways involved in cell death. Surv Ophthalmol 1999; 43: S151–61.

Nisoli E, Tonello C, Cardile A, et al. Calorie restriction promotes mitochondrial biogenesis by inducing the expression of eNOS. Science 2005; 310: 314–7.

Nouri-Mahdavi K, Hoffman D, Coleman AL, et al. Predictive factors for glaucomatous visual field progression in the Advanced Glaucoma Intervention Study. Ophthalmology 2004; 111: 1627-35.

Nygard O, Nordrehaug JE, Refsum H, et al. Plasma homocysteine levels and mortality in patients with coronary artery disease. N Engl J Med 1997; 337: 230–6.

O'Brien C, Schwartz B, Takamoto T, et al. Intraocular pressure and the rate of visual field loss in chronic open-angle glaucoma. Am J Ophthalmol 1991; 111: 491-500.

O'Neill EC, Danesh-Meyer HV, Kong GX, et al. Optic disc evaluation in optic neuropathies. The optic disc assessment project. Ophthalmology 2011; 118: 964–70.

Okisaka S, Murakami A, Mizukawa A, et al. Apoptosis in retinal ganglion cells increase in human glaucomatous eyes. Jpn J Ophthalmol 1997; 41: 84–8.

Opial D, Boehnke M, Tadesse S, et al. Leber's hereditary optic neuropathy mitochondrial DNA mutations in normal-tension glaucoma. Graefes Arch Clin Exp Ophthalmol 2001; 239: 437–40.

Orgül S and Flammer J. Headache in normal-tension glaucoma patients. J Glaucoma 1994a; 3: 292-5.

Orgül S and Flammer J. Interocular visual-field and intraocular-pressure asymmetries in normal-tension-glaucoma. Eur J Ophthalmol 1994b; 4: 199-201.

Osborne NN. Pathogenesis of ganglion "cell death" in glaucoma and neuroprotection: focus on ganglion cell axonal mitochondria. Prog Brain Res 2008; 173: 339–52.

Osborne NN. Mitochondria: their role in ganglion cell death and survival in primary open angle glaucoma. Exp Eye Res 2010; 90: 750–7.

Osborne NN, Casson RJ, Wood JP, et al. Retinal ischemia: mechanisms of damage and potential therapeutic strategies. Prog Retinal Eye Res 2004; 23: 91-147.

Osborne N, Lascaratos G, Bron A, et al. A hypothesis to suggest that light is a risk factor in glaucoma and the mitochondrial optic neuropathies. British Journal of Ophthalmology 2006; 90: 237-41.

Osborne NN, Melena J, Chidlow G, et al. A hypothesis to explain ganglion cell death caused by vascular insults at the optic nerve head: possible implication for the treatment of glaucoma. Br J Ophthalmol 2001; 85: 1252-9.

Osborne NN, Ugarte M, Chao M, et al. Neuroprotection in relation to retinal ischemia and relevance to glaucoma. Surv Ophthalmol 1999b; 43: 102–28.

Osborne NN, Wood JP, Chidlow G, et al. Ganglion cell death in glaucoma: what do we really know? Br J Ophthalmol 1999a; 83: 980–6.

Owsley C, McGwin G, Ball K. Vision impairment, eye disease, and injurious motor vehicle crashes in the elderly. Ophthalmic Epidemiol 1998; 5: 101–13.

Palace VP, Khaper N, Qin Q, et al. Antioxidant potentials of vitamin A and carotenoids and their relevance to heart disease. Free Radic Biol Med 1999; 26: 746–61.

Pallikaris IG, Kymionis GD, Ginis HS, et al. Ocular rigidity in living human eyes. Invest Ophthalmol Vis Sci 2005; 46: 409–14.

Pang IH, Johnson EC, Jia L, et al. Evaluation of inducible nitric oxide synthase in glaucomatous optic neuropathy and pressure-induced optic nerve damage. Invest Ophthalmol Vis Sci 2005; 46: 1313–21.

Patel PR, Bevan RJ, Mistry N, et al. Evidence of oligonucleotides containing 8-hydroxy-2'-deoxyguanosine in human urine. Free Radic Biol Med 2007; 42: 552-8.

Patergnani S, Suski JM, Agnoletto C, et al. Calcium signaling around Mitochondria Associated Membranes (MAMs). Cell Commun Signal 2011; 9: 19.

Pease ME, McKinnon SJ, Quigley HA, et al. Obstructed axonal transport of BDNF and its receptor TRKB in experimental glaucoma. Invest Ophthalmol Vis Sci 2000; 41: 764–74.

Peczon J and Grant W. Glaucoma, Alcohol, and Intraocular Pressure. Arch Ophthalmol 1965; 73: 495–501.

Peirson S and Foster RG. Melanopsin: another way of signaling light. Neuron 2006; 49: 331-9.

Pello R, Martin MA, Carelli V, et al. Mitochondrial DNA background modulates the assembly kinetics of OXPHOS complexes in a cellularmodel of mitochondrial disease. Hum Mol Genet 2008; 17: 4001–11.

Pepose JS, Feigenbaum SK, Qazi MA, et al. Changes in corneal biomechanics and intraocular pressure following LASIK using static, dynamic, and noncontact tonometry. Am J Ophthalmol 2007; 143: 39-47.

Perocchi F, Gohil VM, Girgis HS, et al. MICU1 encodes a mitochondrial EF hand protein required for Ca2+ uptake. Nature 2010; 467: 291-6.

Perry IJ, Refsum H, Morris RW, et al. Prospective study of serum total homocysteine concentration and risk of stroke in middle-aged British men. Lancet 1995; 346: 1395–8.

Phelps CD and Corbett JJ. Migraine and low-tension glaucoma. A case-control study. Invest Ophthalmol Vis Sci 1985; 26: 1105-8.

Pianka P, Almog Y, Man O, et al. Hyperhomocystinemia in patients with nonarteritic anterior ischemic optic neuropathy, central retinal artery occlusion, and central retinal vein occlusion. Ophthalmology 2000; 107: 1588–92.

Pilger A, Germadnik D, Riedel K, et al. Longitudinal study of urinary 8-hydroxy-2Vdeoxyguanosine excretion in healthy adults. Free Radic Res 2001; 35: 273–80.

Piyathilake CJ, Robinson CB, Cornwell P. A practical approach to red blood cell folate analysis. Anal Chem Insights 2007; 2: 107-10.

Poinoosawmy D, Fontana L, Wu JX, et al. Frequency of asymmetric visual field defects in normal-tension and high-tension glaucoma. Ophthalmology 1998; 105: 988-91.

Polyak SL. The Retina. University of Chicago Press, Chicago, 1941.

Pozzan T and Rizzuto R. High tide of calcium in mitochondria. Nat Cell Biol 2000; 2: E25–7.

Pourcelot S, Faure H, Firoozi F, et al. Urinary 8-oxo-7,8-dihydro-2-deoxyguanosine and 5-(hydroxymethyl) uracil in smokers. Free Radic Res 1999; 30: 173–80.

Price GM, Uauy R, Breeze E, et al. Weight, shape, and mortality risk in older persons: elevated waist-hip ratio, not high body mass index, is associated with a greater risk of death. Am J Clin Nutr 2006; 84: 449–60.

Provencio I, Rodriguez IR, Jiang G, et al. A novel human opsin in the inner retina. J Neurosci 2000; 20: 600-5.

Quigley HA. Number of people with glaucoma worldwide. Br J Ophthalmol 1996; 80: 389–93.

Quigley HA. Glaucoma. The Lancet 2011; 377: 1367-7.

Quigley HA. Neuronal death in glaucoma. Prog Retin Eye Res 1999; 18: 39-57.

Quigley H and Anderson DR. The dynamics and location of axonal transport blockade by acute intraocular pressure elevation in primate optic nerve. Invest Ophthalmol 1976; 15: 606–16.

Quigley HA, McKinnon SJ, Zack DJ, et al. Retrograde axonal transport of bdnf in retinal ganglion cells is blocked by acute iop elevation in rats. Invest Ophthalmol Vis Sci 2000; 41: 3460–6.

Quigley HA, Sanchez RM, Dunkelberger GR, et al. Chronic glaucoma selectively damages large optic nerve fibers. Invest Ophthalmol Vis Sci 1987; 28: 913–20.

Raffray M and Cohen GM. Apoptosis and necrosis in toxicology: a continuum or distinct modes of death? Pharmacol Ther 1997; 75: 153–77.

Raichle ME and Gusnard DA. Appraising the brain's energy budget. Proc Natl Acad Sci USA 2002; 99: 10237–9.

Ramanathan A and Schreiber SL. Direct control of mitochondrial function by mTOR. Proc Natl Acad Sci USA 2009; 106: 22229-32.

Ramdas WD, Wolfs RC, Hofman A, et al. Ocular perfusion pressure and the incidence of glaucoma: real effect or artifact? The Rotterdam Study. Invest Ophthalmol Vis Sci 2011a; 52: 6875–81.

Ramdas WD, Wolfs RC, Hofman A, et al. Lifestyle and risk of developing open-angle glaucoma: the Rotterdam study. Arch Ophthalmol 2011b; 129: 767-72.

Rance G, O'Hare F, O'Leary S, et al. Auditory processing deficits in individuals with primary open-angle glaucoma. Int J Audiol 2012; 51: 10–5.

Rao KN, Kaur I, Chakrabarti S. Lack of association of three primary open-angle glaucoma-susceptible loci with primary glaucomas in an Indian population. Proc Natl Acad Sci USA 2009; 106: E125-6.

Rasker MT, Van den Enden A, Bakker D, et al. Rate of visual field loss in progressive glaucoma. Arch Ophthalmol 2000; 118: 481–8.

Rasker MT, Enden A, Bakker DB, et al. Deterioration of visual fields in patients with glaucoma with and without optic disc hemorrhages. Arch Ophthalmol 1997; 115: 1257–63.

Rauen T, Taylor WR, Kuhlbrodt K, et al. High affinity glutamate transporters in the rat retina: a major role of the glial glutamate transporter GLAST-1 in transmitter clearance. Cell Tissue Res 1998; 291: 19-31.

Read RM and Spaeth GL. The practical clinical appraisal of the optic disc in glaucoma: the natural history of cup progression and some specific disc-field correlations. Trans Am Acad Ophthalmol Otolaryngol 1974; 78: 255–74.

Reichelt J, Joachim SC, Pfeiffer N, et al. Analysis of autoantibodies against human retinal antigens in sera of patients with glaucoma and ocular hypertension. Curr Eye Res 2008; 33: 253-61.

Reichenbach A and Robinson SR. The involvement of Muller cells in the outer retina. In: Djamgoz MBA, Archer SN and Vallerga S (eds.), Neurobiology and

clinical aspects of the outer retina, Chapman and Hall, London, 1995, pp 395-416.

Reichenbach A, Schippel K, Schumann R, et al. Ultrastructure of rabbit retinal nerve fibre layer-neuro-glial relationships, myelination, and nerve fibre spectrum. J Hirnforsch 1988; 29: 481-91.

Reimertz C, Kogel D, Lankiewicz S, et al. Ca2+ induced inhibition of apoptosis in human SH-SY5Y neuroblastoma cells: degradation of apoptotic protease activating factor 1 (APAF-1). J Neurochem 2001; 78: 1256–66.

Ren H, Magulike N, Ghebremeskel K, et al. Primary open-angle glaucoma patients have reduced levels of blood docosahexaenoic and eicosapentaenoic acids. Prostaglandins Leukot Essent Fatty Acids 2006; 74: 157–63.

Reusch RN. Poly-beta-hydroxybutyrate/calcium polyphosphate complexes in eukaryotic membranes. Proc Soc Exp Biol Med 1989; 191: 377-81.

Rezaie T, Child A, Hitchings R, et al. Adult-onset primary open angle glaucoma caused by mutations in optineurin. Science 2002; 295: 1077–9.

Riesbeck K, Bredberg A, Forsgren A. Ciprofloxacin does not inhibit mitochondrial functions but other antibiotics (tetracyclins and chloramphenicol) do. Antimicrob Agents Chemother 1990; 34: 167–9.

Robb-Gaspers LD, Rutter GA, Burnett P, et al. Coupling between cytosolic and mitochondrial calcium oscillations: role in the regulation of hepatic metabolism. Biochim Biophys Acta 1998; 1366: 17-32.

Rodgers GM and Kane WH. Activation of endogenous factor V by a homocysteine-induced vascular endothelial cell activator. J Clin Invest 1986; 77: 1909–16.

Rodieck RW. The vertebrate retina: principles of structure and function, WH Freeman and Company, San Francisco, 1973.

Roedl JB, Bleich S, Schlötzer-Schrehardt U, et al. Increased homocysteine levels in tear fluid of patients with primary open-angle glaucoma. Ophthalmic Res 2008; 40: 249–56.

Roedl JB, Bleich S, Reulbach U, et al. Vitamin deficiency and hyperhomocysteinemia in pseudoexfoliation glaucoma. J Neural Transm 2007; 114: 571-5.

Romano C, Barrett DA, Li Z, et al. Anti-rhodopsin antibodies in sera from subjects with normal-pressure glaucoma. Invest Ophthalmol Vis Sci 1995; 36: 1968-75.

Rose G, McCartney P, Reid DD. Self-administration of a questionnaire on chest pain and intermittent claudication. Br J Prev Soc Med 1977; 31: 42–8.

Rossetti L, Marchetti I, Orzalesi N, et al. Randomized clinical trials on medical treatment of glaucoma: are they appropriate to guide clinical practice? Arch Ophthalmol 1993; 111: 96–103.

Russell RA, Malik R, Chauhan BC, et al. Improved estimates of visual field progression using Bayesian linear regression to integrate structural information in patients with ocular hypertension. Invest Ophthalmol Vis Sci 2012; 53: 2760-9.

Sacca SC and Izzotti A. Oxidative stress and glaucoma: injury in the anterior segment of the eye. Progress in Brain Research 2008; 173: 385-407.

Sacca SC, Izzotti A, Rossi P, et al. Glaucomatous outflow pathway and oxidative stress. Exp Eye Res 2007; 84: 389-99.

Sacca SC, Pascotto A, Camicione P, et al. Oxidative DNA damage in the human trabecular meshwork: clinical correlation in patients with primary open-angle glaucoma. Arch Ophthalmol 2005; 123: 458–63.

Sampson MJ, Lovell RS, Craigen WJ. The murine voltage-dependent anion channel gene family. Conserved structure and function. J Biol Che 1997; 272: 18966-73.

Sarfarazi M, Child A, Stoilova D, et al. Localization of the fourth locus (GLC1E) for adult-onset primary open angle glaucoma to the 10p15-p14 region. Am J Hum Genet 1998; 62: 641–52.

Sawada A, Kitazawa Y, Yamamoto T, et al. Prevention of visual field defect progression with brovincamine in eyes with normal-tension glaucoma. Ophthalmology 1996; 103: 283–8.

Scaduto RC Jr and Grotyohann LW. Measurement of mitochondrial membrane potential using fluorescent rhodamine derivatives. Biophys J 1999; 76: 469-77.

Schapira AH. Mitochondrial disease. Lancet 2006; 368: 70–82.

Schapira AH. Oxidative stress and mitochondrial dysfunction in neurodegeneration. Curr Opin Neurol 1996; 9: 260-4.

Schapira AH, Mann VM, Cooper JM, et al. Mitochondrial function in Parkinson's disease. The Royal Kings and Queens Parkinson's Disease Research Group. Ann Neurol 1992; 32: S116-24.

Shapiro AL, Viñuela E, Maizel JV Jr. Molecular weight estimation of polypeptide chains by electrophoresis in SDS-polyacrylamide gels. Biochem Biophys Res Commun 1967; 28: 815–20.

Schieke SM, Phillips D, McCoy JP Jr, et al. The mammalian target of rapamycin (mTOR) pathway regulates mitochondrial oxygen consumption and oxidative capacity. J Biol Chem 2006; 281: 27643-52.

Schlottmann PG, De Cilla S, Greenfield DS, et al. Relationship between visual field sensitivity and retinal nerve fiber layer thickness as measured by scanning laser polarimetry. Invest Ophthalmol Vis Sci 2004; 45: 1823–9.

Schneider U, Schwenk H, Bornkamm G. Characterization of EBV-genome negative "null" and "T" cell lines derived from children with acute lymphoblastic leukemia and leukemic transformed non-Hodgkin lymphoma. Int J Cancer 1977; 19: 621–6.

Schnitzer J. Astrocytes in mammalian retina. Prog Ret Eye Res 1988; 7: 209-32.

Schultz JS, Werner EB, Krupin T, et al. Intraocular pressure and visual field defects after argon laser trabeculoplasty in chronic open-angle glaucoma. Ophthalmology 1987: 94: 553–7.

Schwenn O, Troost R, Vogel A, et al. Ocular pulse amplitude in patients with open angle glaucoma, normal tension glaucoma, and ocular hypertension. Br J Ophthalmol 2002; 86: 981-4.

Scofield RH. Autoantibodies as predictors of disease. Lancet 2004; 363: 1544-6.

Sekiguchi M and Tsuzuki T. Oxidative nucleotide damage: consequences and prevention. Oncogene 2002; 21: 8895–904.

Shah H, Kniestedt C, Bostrom A, et al. Role of central corneal thickness on baseline parameters and progression of visual fields in open angle glaucoma. Eur J Ophthalmol 2007; 17: 545-9.

Shah S, Laiquzzaman M, Bhojwani R, Mantry S, Cunliffe I. Assessment of the biomechanical properties of the cornea with the ocular response analyzer in normal and keratoconic eyes. Investigative Ophthalmology & Visual Science 2007; 48: 3026–31.

Shah S, Laiquzzaman M, Yeung I, et al. The use of the Ocular Response Analyser to determine corneal hysteresis in eyes before and after excimer laser refractive surgery. Cont Lens Anterior Eye 2009; 32: 123-8.

Shamoto-Nagai M, Maruyama W, Kato Y, et al. An inhibitor of mitochondrial complex I, rotenone, inactivates proteasome by oxidative modification and induces aggregation of oxidized proteins in SH-SY5Y cells. J Neurosci Res 2003; 74: 589–97.

Shapley R and Victor J. Hyperacuity in cat retinal ganglion cells. Science 1986; 231: 999-1002.

Shareef S, Sawada A, Neufeld AH. Isoforms of nitric oxide synthase in the optic nerves of rat eyes with chronic moderately elevated intraocular pressure. Invest Ophthalmol Vis Sci 1999; 40: 2884–91.

Shields WB. Textbook of Glaucoma, 4th ed, Williams and Wilkins, Baltimore, 1997.

Shin DH, Becker B, Kolker AE. Family history in primary open-angle glaucoma. Arch Ophthalmol 1977; 95: 598–600.

Shinde S and Pasupathy K. Respiratory-chain enzyme activities in isolated mitochondria of lymphocytes from patients with Parkinson's disease: preliminary study. Neurol India 2006; 54: 390-3.

Siegner SW and Netland PA. Optic disc haemorrhages and progression of glaucoma. Ophthalmology 1996; 103: 1014–24.

Sievers J, Hausmann B, Unsicker K, et al. Fibroblast growth factors promote survival of rat retinal ganglion cells after transection of the optic nerve. Neurosci Lett 1987; 76: 157–62.

Silveira LCL, Russelakis-Carneiro M, Perry VH. The ganglion cell response to optic nerve injury in the cat: differential responses revealed by neurofibrillar staining. J Neurocytol 1994; 23: 75–86.

Sivitz WI and Yorek MA. Mitochondrial dysfunction in diabetes: from molecular mechanisms to functional significance and therapeutic opportunities. Antioxid Redox Signal 2010; 12: 537-77.

Smeitink J, van den Heuvel L, DiMauro S. The genetics and pathology of oxidative phosphorylation. Nat Rev Genet 2001; 2: 342–52.

Smith BT, Belani S, Ho AC. Ultraviolet and near-blue light effects on the eye. Int Ophthalmol Clin 2005; 45: 107-15.

Smith PK, Krohn RI, Hermanson GT, et al. Measurement of protein using bicinchoninic acid. Anal Biochem 1985; 150: 76-85.

Solfrizzi V, D'Introno A, Colacicco AM, et al. Circulating biomarkers of cognitive decline and dementia. Clin Chim Acta 2006; 364: 91–112.

Somasundaram S, Sigthorsson G, Simpson RJ, et al. Uncoupling of intestinal mitochondrial oxidative phosphorylation and inhibition of cyclooxygenase are required for the development of NSAID-enteropathy in the rat. Aliment Pharmacol Ther 2000; 14: 639–50.

Sommer A, Tielsch JM, Katz J, et al. Relationship between intraocular pressure and primary open angle glaucoma among white and black Americans: The Baltimore Eye Survey. Arch Ophthalmol 1991; 109: 1090–5.

Sorkhabi R, Ghorbanihaghjo A, Javadzadeh A, et al. Oxidative DNA damage and total antioxidant status in glaucoma patients. Mol Vis 2011; 17: 41-6.

Stalmans I, Harris A, Vanbellinghen V, et al. Ocular pulse amplitude in normal tension and primary open angle glaucoma. J Glaucoma 2008; 17: 403-7.

Stamler JS, Osborne JA, Jaraki O, et al. Adverse vascular effects of homocysteine are modulated by endotheliumderived relaxing factor and related oxides of nitrogen. J Clin Invest 1993; 91: 308–18.

Stennicke HR, Jurgensmeier JM, Shin H, et al. Pro-caspase-3 is a major physiologic target of caspase-8. J Biol Chem 1998; 273: 27084-90.

Stewart WC, Chorak RP, Hunt HH, et al. Factors associated with visual loss in patients with advanced glaucomatous changes in the optic nerve head. Am J Ophthalmol 1993; 116: 176-81.

Stewart WC, Kolker AE, Sharpe ED, et al. Factors associated with long-term progression or stability in primary open-angle glaucoma. Am J Ophthalmol 2000; 130: 274-9.

Stoilova D, Child A, Trivan OC, et al. Localization of a locus (GLC1B) for adult-onset primary open angle glaucoma to the 2 cen-q13 region. Genomics 1996; 36: 142–50.

Stone J and Dreher Z. Relationship between astrocytes, ganglion cells and vasculature of the retina. J Comp Neurol 1987; 255: 35-49.

Stone EM, Fingert JH, Alward WLM, et al. Identification of a gene that causes primary open angle glaucoma. Science 1997; 275: 668–70.

Strouthidis NG, Scott A, Peter NM, et al. Optic disc and visual field progression in ocular hypertensive subjects: detection rates, specificity, and agreement. Invest Ophthalmol Vis Sci 2006; 47: 2904–10.

Subash P, Gurumurthy P, Sarasabharathi A, et al. Urinary 8-OHdG: A marker of oxidative stress to DNA and total antioxidant status in essential hypertension with South Indian population. Indian J Clin Biochem 2010; 25: 127-32.

Sucher NJ, Lipton SA, Dreyer EB. Molecular basis of glutamate toxicity in retinal ganglion cells. Vision Res 1997; 37: 3483–93.

Sugiura H, Liu X, Togo S, et aI. Prostaglandin E(2) protects human lung fibroblasts from cigarette smoke extract-induced apoptosis via EP(2) receptor activation. J Cell Physiol 2007; 210: 99-110.

Sugiyama K, Tomita G, Kitazawa Y, et al. The association of optic disc hemorrhage with retinal nerve fiber layer defect and peripapillary atrophy in normal-tension glaucoma. Ophthalmology 1997; 104: 1926–33.

Sullivan-Mee M, Lewis SE, Pensyl D, et al. Factors influencing intermethod agreement between Goldmann applanation, Pascal Dynamic Contour, and Ocular Response Analyzer tonometry. J Glaucoma 2012 Mar 7 [Epub ahead of print] PMID: 22407388.

Surgucheva I, McMahan B, Ahmed F, et al. Synucleins in glaucoma: implication of gamma-synuclein in glaucomatous alterations in the optic nerve. J Neurosci Res 2002; 68: 97-106.

Susin SA, Zamzami N, Castedo M, et al. Bcl-2 inhibits the mitochondrial release of an apoptogenic protease. Journal of Experimental Medicine 1996; 184: 1331-41.

Suzuki Y, Shirato S, Adachi M, et al. Risk factors for the progression of treated primary open-angle glaucoma: a multivariate life-table analysis. Graefes Arch Clin Exp Ophthalmol 1999; 237: 463–7.

Tamm ER. Myocilin and glaucoma: facts and ideas. Prog Retin Eye Res 2002; 21: 395-428.

Tanwar M, Dada T, Sihota R, et al. Mitochondrial DNA analysis in primary congenital glaucoma. Mol Vis 2010; 16: 518–33.

Tao W, Wen R, Goddard MB, et al. Encapsulated cell-based delivery of CNTF reduces photoreceptor degeneration in animal models of retinitis pigmentosa. Invest Ophthalmol Vis Sci 2002; 43: 3292–8.

Tatton WG, Chalmers-Redman RM, Sud A, et al. Maintaining mitochondrial membrane impermeability: an opportunity for new therapy in glaucoma? Surv Ophthalmol 2001; 45: S277–S283.

Taylor D. Optic nerve axons: life and death before birth. The Bowman lecture. Eye 2005; 19: 499–527.

Teng CC, De Moraes CG, Prata TS, et al. The region of largest β-zone parapapillary atrophy area predicts the location of most rapid visual field progression. Ophthalmology 2011; 118: 2409-13.

Terman A. The effect of age on formation and elimination of autophagic vacuoles in mouse hepatocytes. Gerontology 1995; 41: 319–26.

Tezel G. The role of glia, mitochondria, and the immune system in glaucoma. Invest Ophthalmol Vis Sci 2009; 50: 1001-12.

Tezel G, Edward DP, Wax MB. Serum autoantibodies to optic nerve head glycosaminoglycans in subjects with glaucoma. Arch Ophthalmol 1999; 117: 917-24.

Tezel G, Li LY, Patil RV, et al. TNF-alpha and TNFalpha receptor-1 in the retina of normal and glaucomatous eyes. Invest Ophthalmol Vis Sci 2001; 42: 1787–94.

Tezel G, Seigel GM, Wax MB. Autoantibodies to small heat shock proteins in glaucoma. Invest Ophthalmol Vis Sci 1998; 39: 2277-87.

Tezel G and Wax MB. The immune system and glaucoma. Curr Opin Ophthalmol 2004; 15: 80-4.

Tezel G and Wax MB. Increased production of tumor necrosis factor alpha by glial cells exposed to simulated ischemia or elevated hydrostatic pressure induces apoptosis in cocultured retinal ganglion cells. J Neurosci 2000; 20: 8693-700.

Tezel G and Wax MB. The mechanisms of hsp27 antibody-mediated apoptosis in retinal neuronal cells. J Neurosci 2000; 20: 3552-62.

Tezel G and Yang X. Caspase-independent component of retinal ganglion cell death, *in vitro*. Invest Ophthalmol Vis Sci 2004; 45: 4049-59.

Tezel G, Yang X, Cai J. Proteomic identification of oxidatively modified retinal proteins in a chronic pressure-induced rat model of glaucoma. Invest Ophthalmol Vis Sci 2005; 46: 3177-87.

Tezel G, Yang X, Luo C, et al. Mechanisms of immune system activation in glaucoma: oxidative stress-stimulated antigen presentation by the retina and optic nerve head glia. Invest Ophthalmol Vis Sci 2007; 48: 705-14.

Thanos S, Bähr M, Barde Y-A, et al. Survival and axonal elongation of adult rat retinal ganglion cells. Eur J Neurosci 1989; 1: 19–24.

Thorleifsson G, Walters GB, Hewitt AW, et al. Common variants near CAV1 and CAV2 are associated with primary open-angle glaucoma. Nat Genet 2010; 42: 906-9.

Thorsby E and Bratlie A. A rapid method for preparation of pure lymphocyte suspensions. In: Terasaki PI (ed), Histocompatibility Testing, Munksgaard, Copenhagen, 1970, p 655.

Tielsch JM, Katz J, Sommer A, et al. Family history and risk of primary open angle glaucoma. The Baltimore Eye Survey. Arch Ophthalmol 1994; 112: 69–73.

Tielsch JM, Katz J, Sommer A, et al. Hypertension, perfusion pressure, and primary open-angle glaucoma: a population based assessment. Arch Ophthalmol 1995; 113: 216–21.

Tielsch JM, Sommer A, Katz J, et al. Racial variations in the prevalence of primary open angle glaucoma. The Baltimore Eye Survey. JAMA 1991; 266: 369-74.

Thoreson WB and Mangel SC. Lateral interactions in the outer retina. Prog Retin Eye Res 2012; 31: 407-41.

Tolomeo M, Mancuso S, Todaro M, et al. Mitochondrial disruption and apoptosis in lymphocytes of an HIV infected patient affected by lactic acidosis

after treatment with highly active antiretroviral therapy. J Clin Pathol 2003; 56: 147-51.

Topouzis F, Coleman AL, Harris A, et al. Association of blood pressure status with the optic disk structure in non-glaucoma subjects: the Thessaloniki eye study. Am J Ophthalmol 2006; 142: 60-7.

Trifan OC, Traboulsi EI, Stoilova D, et al. The third locus (GLC1D) for adult-onset primary open angle glaucoma maps to the 8q23 region. Am J Ophthalmol 1998; 126: 17-28.

Trivino A, Ramirez JM, Salazar JJ, et al. Immunohistochemical study of human optic nerve head astroglia. Vision Res 1996; 36: 2015-28.

Tsai JC, Perrella MA, Yoshizumi M, et al. Promotion of vascular smooth muscle cell growth by homocysteine: a link to atherosclerosis. Proc Natl Acad Sci USA 1994; 91: 6369–73.

Turgut B, Kaya M, Arslan S, et al. Levels of circulating homocysteine, vitamin B6, vitamin B12, and folate in different types of open-angle glaucoma. Clin Interv Aging 2010; 5: 133-9.

Uchida H, Ugurlu S, Caprioli J. Increasing peripapillary atrophy is associated with progressive glaucoma. Ophthalmology 1998; 105: 1541–5.

Ugurlu S, Weitzman M, Nduaguba C, et al. Acquired pit of the optic nerve: a risk factor for progression of glaucoma. Am J Ophthalmol 1998; 125: 457-64.

Usui T, Iwata K, Shirakashi M, et al. Prevalence of migraine in low-tension glaucoma and primary open-angle glaucoma in Japanese. Br J Ophthalmol 1991; 75: 224-6.

Vajaranant TS, Nayak S, Wilensky JT, et al. Gender and glaucoma: what we know and what we need to know. Curr Opin Ophthalmol 2010; 21: 91-9.

Valavanidis A, Vlachogianni T, Fiotakis C. 8-hydroxy-2' -deoxyguanosine (8-OHdG): A critical biomarker of oxidative stress and carcinogenesis. J Environ Sci Health C Environ Carcinog Ecotoxicol Rev 2009; 27: 120-39.

Valko M, Leibfritz D, Moncol J, et al. Free radicals and antioxidants in normal physiological functions and human disease. Int J Biochem Cell Biol 2007; 39: 44-84.

Van Adel BA, Kostic C, Deglon N, et al. Delivery of ciliary neurotrophic factor via lentiviral-mediated transfer protects axotomized retinal ganglion cells for an extended period of time. Hum Gene Ther 2003; 14: 103–15.

Van Bergen N, Crowston J, Kearns L, et al. Mitochondrial oxidative phosphorylation compensation may preserve vision in patients with OPA1-linked autosomal dominant optic atrophy. PLoS One 2011; 6: e21347.

Varma R, Hwang LJ, Grunden JW, et al. Assessing the efficacy of latanoprost vs timolol using an alternate efficacy parameter: the intervisit intraocular pressure range. Am J Ophthalmol 2009; 148: 221-6.

Varma R, Hwang LJ, Grunden JW, et al. Inter-visit intraocular pressure range: an alternative parameter for assessing intraocular pressure control in clinical trials. Am J Ophthalmol 2008; 145: 336-42.

Varma R, Ying-Lai M, Francis BA, et al. Los Angeles Latino Eye Study Group. Prevalence of open angle glaucoma and ocular hypertension in Latinos: the Los Angeles Latino Eye Study. Ophthalmology 2004; 111: 1439–48.

Vass C, Hirn C, Sycha T, et al. Medical interventions for primary open angle glaucoma and ocular hypertension. Cochrane Database Syst Rev 2007; 4: CD003167.

Vester JW and Stadie WC. Studies of oxidative phosphorylation by hepatic mitochondria from the diabetic cat. J Biol Chem 1957; 227: 669-76.

Villegas-Pérez MP, Vidal-Sanz M, Bray GM, et al. Influences of peripheral nerve graft on the survival and regrowth of axotomized retinal ganglion cells in adult rats. J Neurosci 1988; 8: 265–80.

Virno M, Bucci MG, Pecori-Giraldi J, et al. Intravenous glycerol-vitamin C (sodium salt) as osmotic agents to reduce intraocular pressure. Am J Ophthalmol 1966; 62: 824-33.

Viswanathan AC, Fitzke FW, Hitchings RA. Early Detection of Visual Field Progression in Glaucoma: A Comparison of PROGRESSOR and Statpac 2. Br J Ophthalmol 1997; 81: 1037-42.

Wagenmakers EJ and Farrell S. AIC model selection using Akaike weights. Psychonomic bulletin & review 2004; 11: 192-6.

Wamsley S, Gabelt BT, Dahl DB, et al. Vitreous glutamate concentration and axon loss in monkeys with experimental glaucoma. Arch Ophthalmol 2005; 123: 64–70.

Wang AS, Alencar LM, Weinreb RN, et al. Repeatability and reproducibility of Goldmann applanation, Dynamic Contour, and Ocular Response Analyzer tonometry. J Glaucoma 2013; 22: 127-32.

Wang JJ, Mitchell P, Smith W. Is there an association between migraine headache and open-angle glaucoma? Findings from the Blue Mountains Eye Study. Ophthalmology 1997; 104: 1714-9.

Wang L, Dong J, Cull G, et al. Varicosities of intraretinal ganglion cell axons in human and nonhuman primates. Invest Ophthalmol Vis Sci 2003; 44: 2-9.

Wang X, Harmon J, Zabrieskie N, et al. Using the Utah Population Database to assess familial risk of primary open angle glaucoma. Vis Res 2010; 50: 2391-5.

Wang X, Niwa M, Hara A, et al. Neuronal degradation in mouse retina after a transient ischemia and protective effect of hypothermia. Neurol Res 2002; 24: 730–5.

Wang X, Tay SS, Ng YK. An immunohistochemical study of neuronal and glial cell reactions in retinae of rats with experimental glaucoma. Exp Brain Res 2000; 132: 476–84.

Waring WS, Webb DJ, Maxwell SR. Systemic uric acid administration increases serum antioxidant capacity in healthy volunteers. J Cardiovasc Pharmacol 2001; 38: 365–71.

Wax MB, Tezel G, Saito I, et al. Anti-Ro/SS-A positivity and heat shock protein antibodies in patients with normal-pressure glaucoma. Am J Ophthalmol 1998; 125: 145–57.

Wax MB, Yang J, Tezel G. Serum autoantibodies in patients with glaucoma. J Glaucoma 2001; 10: S22–4.

Wayner DD, Burton GW, Ingold KU, et al. The relative contributions of vitamin E, urate, ascorbate and proteins to the total peroxyl radical-trapping

antioxidant activity of human blood plasma. Biochim Biophys Acta 1987; 22: 408-19.

Weber K and Osborn M. The reliability of molecular weight determinations by dodecyl sulfate-polyacrylamide gel electrophoresis. J Biol Chem 1969; 244: 4406–12.

Weber TA and Reichert AS. Impaired quality control of mitochondria: aging from a new perspective. Exp Gerontol 2010; 45: 503–11.

Wei YH. Mitochondrial DNA alterations as ageing-associated molecular events. Mutat Res 1992; 275: 145–55.

Wei YH. Mitochondrial DNA mutations and oxidative damage in aging and diseases: an emerging paradigm of gerontology and medicine. Proc Natl Sci Counc Repub China B 1998; 22: 55–67.

Weinreb RN and Khaw PT. Primary open-angle glaucoma. Lancet 2004; 363: 1711-20.

Weizer JS, Asrani S, Stinnett SS, et al. The clinical utility of dynamic contour tonometry and ocular pulse amplitude. J Glaucoma 2007; 16: 700-3.

Wells AP, Garway-Heath DF, Poostchi A, et al. Corneal hysteresis but not corneal thickness correlates with optic nerve surface compliance in glaucoma patients. Invest Ophthalmol Vis Sci 2008; 49: 3262–8.

Whitmore AV, Libby RT, John SW. Glaucoma: thinking in new ways-a role for autonomous axonal self-destruction and other compartmentalised processes? Prog Retin Eye Res 2005; 24: 639-62.

Wiechelman K, Braun RD, Fitzpatrick JD. Investigation of the bicinchoninic acid protein assay: Identification of the groups responsible for color formation. Anal Biochem 1988; 175: 231-7.

Wiggs JL, Kang JH, Yaspan BL, et al; GENEVA Consortium. Common variants near CAV1 and CAV2 are associated with primary open-angle glaucoma in Caucasians from the USA. Hum Mol Genet 2011; 20: 4707-13.

Williams RS, Salmons S, Newsholme E, et al. Regulation of nuclear and mitochondrial gene expression by contractile activity in skeletal muscle. J Biol Chem 1986; 261: 376-80.

Wilson MR, Hertzmark E, Walker AM, et al. A case-control study of risk factors in open angle glaucoma. Arch Ophthalmol 1987; 105: 1066–71.

Wilson R, Bennett DA, Gilley DW, et al. Progression of parkinsonism and loss of cognitive function in Alzheimer disease. Arch Neurol 2000; 57: 855–60.

Wilson R, Richardson TM, Hertzmark E, et al. Race as a risk factor for progressive glaucomatous damage. Ann Ophthalmol 1985; 17: 653–9.

Wilson R, Walker AM, Dueker DK, et al. Risk factors for rate of progression of glaucomatous visual field loss: a computer-based analysis. Arch Ophthalmol 1982; 100: 737–41.

Wirtz MK, Samples JR, Kramer PL, et al. Mapping a gene for adult onset primary open angle glaucoma to chromosome 3q. Am J Hum Genet 1997; 60: 296–304.

Wirtz MK, Samples JR, Rust K, et al. GLC1F, a new primary open angle glaucoma locus, maps to 7q35-q36. Arch Ophthalmol 1999; 117: 237–41.

Woldemussie E, Wijono M, Ruiz G. Muller cell response to laser-induced increase in intraocular pressure in rats. Glia 2004; 47: 109–19.

Wolf C, Gramer E, Müller-Myhsok B, et al. Mitochondrial haplogroup U is associated with a reduced risk to develop exfoliation glaucoma in the German population. BMC Genet 2010; 11: 8.

Wolf C, Gramer E, Müller-Myhsok B, et al. Evaluation of nine candidate genes in patients with normal tension glaucoma: a case control study. BMC Med Genet 2009; 10: 91.

Wolfs RCW, Klaver CCW, Ramrattan RS, et al. Genetic risk of primary open glaucoma. Arch Ophthalmol 1998; 116: 1640–5.

Wolfs RCW, Klaver CCW, Vingerling JR, Grobbe DE, Hofman A, de Jong PTVM. Distribution of central corneal thickness and its association with intraocular pressure. The Rotterdam Study. Am J Ophthalmol 1997; 123: 767-72.

Wood J, Lascaratos G, Bron A, et al. The influence of light exposure on cultured retinal ganglion cells. Molecular Vision 2008; 14: 334-44.

World Health Organisation, Waist circumference and waist–hip ratio: report of a WHO expert consultation, Geneva, 2008.

Wu LL, Chiou CC, Chang PY, et al. Urinary 8-OHdG: a marker of oxidative stress to DNA and a risk factor for cancer, atherosclerosis and diabetics. Clin Chim Acta 2004; 339: 1-9.

Wu SY and Leske MC. Associations with intraocular pressure in the Barbados Eye Study. Arch Ophthalmol 1997; 115: 1572–6.

Wurm CA, Neumann D, Lauterbach MA, et al. Nanoscale distribution of mitochondrial import receptor Tom20 is adjusted to cellular conditions and exhibits an inner-cellular gradient. Proc Natl Acad Sci USA 2011; 108: 13546-51.

Wyllie AH, Beattie GJ, Hargreaves AD. Chromatin changes in apoptosis. Histochem J 1981; 13: 681–92.

Wyllie AH, Kerr JF, Currie AR. Cell death: the significance of apoptosis. Int Rev Cytol 1980; 68: 251–306.

Yamamoto T and Kitazawa Y. Vascular pathogenesis of normal-tension glaucoma: a possible pathogenetic factor, other than intraocular pressure, of glaucomatous optic neuropathy. Prog Retin Eye Res 1998; 17: 127-43.

Yamazaki S, Inoue Y, Yoshikawa K. Peripapillary fluorescein angiographic findings in primary open angle glaucoma. Br J Ophthalmol 1996; 80: 812-7.

Yan LJ, Levine RL, Sohal RS. Oxidative damage during aging targets mitochondrial aconitase. Proc Natl Acad Sci USA 1997; 94: 11168-72.

Yan J, Chen C, Lei J, et al. 2-Methoxyestradiol reduces cerebral vasospasm after 48 hours of experimental subarachnoid hemorrhage in rats. Exp Neurol 2006; 202: 348–56.

Yang J, Patil RV, Yu H, et al. T cell subsets and sIL-2R/IL-2 levels in patients with glaucoma. Am J Ophthalmol 2001; 131: 421–6.

Yang J, Tezel G, Patil RV, et al. Serum autoantibody against glutathione S-transferase in subjects with glaucoma. Invest Ophthalmol Vis Sci 2001; 42: 1273-6.

Yasuda SU, Sausville EA, Hutchins JB, et al. Amiodarone-induced lymphocyte toxicity and mitochondrial function. J Cardiovasc Pharmacol 1996; 28: 94-100.

Yoshida M, Ishikawa M, Kokaze A, et al. Association of life-style with intraocular pressure in middle-aged and older Japanese residents. Jpn J Ophthalmol 2003; 47: 191–8.

Yoshino H, Nakagawa-Hattori Y, Kondo T, et al. Mitochondrial complex I and II activities of lymphocytes and platelets in Parkinson's disease. J Neural Transm Park Dis Dement Sect 1992; 4: 27-34.

Yu DY and Cringle SJ. Oxygen distribution and consumption within the retina in vascularised and avascular retinas and in animal models of retinal disease. Prog Retin Eye Res 2001; 20: 175-208.

Yuki K, Murat D, Kimura I, et al. Increased serum total antioxidant status and decreased urinary 8-hydroxy-2-deoxyguanosine levels in patients with normal-tension glaucoma. Acta Ophthalmol Copenh 2010; 88: e259-64.

Yuki K, Murat D, Kimura I, et al. Reduced-serum vitamin C and increased uric acid levels in normal-tension glaucoma. Graefes Arch Clin Exp Ophthalmol 2010b; 248: 243-8.

Yu-Wai-Man P. Mitochondrial dysfunction in glaucoma: closing the loop. Invest Ophthalmol Vis Sci 2012; 53: 2438.

Yu-Wai-Man CY, Chinnery PF, Griffiths PG. Optic neuropathies — importance of spatial distribution of mitochondria as well as function. Medical Hypotheses 2005; 65: 1038–42.

Yu-Wai-Man CY, Griffiths PG, Hudson G, et al. Inherited mitochondrial optic neuropathies. J Med Genet 2009; 46: 145–58.

Yu-Wai-Man P, Stewart JD, Hudson G, et al. OPA1 increases the risk of normal but not high tension glaucoma. J Med Genet 2010; 47: 120–5.

Yucel YH, Zhang Q, Weinreb RN, et al. Effects of retinal ganglion cell loss on magno-, parvo-, koniocellular pathways in the lateral geniculate nucleus and visual cortex in glaucoma. Prog Retin Eye Res 2003; 22: 465-81.

Zanon-Moreno V, Garcia-Medina JJ, Gallego-Pinazo R, et al. Antioxidant status modifications by topical administration of dorzolamide in primary open-angle glaucoma. Eur J Ophthalmol 2009; 19: 565-71.

Zanon-Moreno V, Ciancotti-Olivares L, Asencio J, et al. Association between a SLC23A2 gene variation, plasma vitamin C levels, and risk of glaucoma in a Mediterranean population. Mol Vis 2011; 17: 2997-3004.

Zanon-Moreno V, Marco-Ventura P, Lleo-Perez A, et al. Oxidative stress in primary open-angle glaucoma. J Glaucoma 2008; 17: 263–268.

Zenkel M, Kruse FE, Naumann GO, et al. Impaired cytoprotective mechanisms in eyes with pseudoexfoliation syndrome/glaucoma. Invest Ophthalmol Vis Sci 2007; 48: 5558–66.

Zhang DX and Gutterman DD. Mitochondrial reactive oxygen species-mediated signaling in endothelial cells. Am J Physiol Heart Circ Physiol 2007; 292: 2023-31.

Zhang W, Khatibi NH, Yamaguchi-Okada M, et al. Mammalian target of rapamycin (mTOR) inhibition reduces cerebral vasospasm following a subarachnoid hemorrhage injury in canines. Exp Neurol 2012; 233: 799-806.

Zhang Y, Marcillat O, Giulivi C, et al. The oxidative inactivation of mitochondrial electron transport chain components and ATPase. J Biol Chem 1990; 265: 16330–6.

PhD-related publications and published abstracts to date

Lascaratos G, Garway-Heath DF, Burton R, Bunce C, Xing W, Crabb DP, Russell RA, Shah A, on behalf of the UKGTS Investigators. The United Kingdom Glaucoma Treatment Study: a multicenter, randomized, double-masked, placebo-controlled clinical trial. Baseline characteristics. Ophthalmology 2013; 120: 2540-5.

Garway-Heath DF, **Lascaratos G**, Bunce C, Crabb D, Russell R, Shah A, on behalf of the UKGTS Investigators. The United Kingdom Glaucoma Treatment Study: a multicentre, randomized, placebo-controlled clinical trial. Design and methodology. Ophthalmology 2013; 120: 68-76.

Lascaratos G, Garway-Heath DF, Willoughby C, Chau KY, Schapira AHV. Mitochondrial dysfunction in glaucoma: understanding genetic influences. Mitochondrion 2012; 12: 202-12.

Lascaratos G, Shah A, Garway-Heath DF. The genetics of pigment dispersion syndrome and pigmentary glaucoma. Survey of Ophthalmology 2013; 58: 164-75.

Lascaratos G, Chau D, Schapira AHV, Garway-Heath DF. ATP synthesis, as a measure of mitochondrial function, in patients with normal tension glaucoma vs ocular hypertension – preliminary findings. ARVO Optic Nerve Degeneration and Ageing Conference, Obergurgl, Austria, 5-7 December 2012.

Lascaratos G, Chau D, Schapira AH, Garway-Heath DF. Aconitase activity as a measure of oxidative stress in patients with normal tension glaucoma vs ocular hypertension – preliminary findings. Invest Ophthalmol Vis Sci 2012 53: E-Abstract 3843. 2012 ARVO Annual Meeting, Fort Lauderdale, Florida, 8 May 2012 **(awarded AFER/NIHR BRC for Ophthalmology ARVO Travel Grant 2012)**

Lascaratos G, Chau D, Zhu H, Schapira AHV, Gout I, Garway-Heath DF. Systemic mTOR activity, as a regulator of mitochondrial function, in patients with normal tension glaucoma vs ocular hypertension. Biochemical Society Focused Meeting, Talks about TORCs: recent advances in target of rapamycin signaling, London, 14-15 March 2013.

DF Garway-Heath, **G Lascaratos**, C Bunce, D Crabb, R Russell, A Shah, K Suzuki, E White, F Amalfitano, on behalf of the UKGTS Investigators. The United Kingdom Glaucoma Treatment Study (UKGTS): baseline characteristics and main outcomes. 2013 ARVO Annual Meeting, Seattle, Washington, 7 May 2013 (accepted).

Lascaratos G, Chau D, Zhu H, Schapira AHV, Garway-Heath DF. Mitochondrial membrane potential, as a measure of mitochondrial function, in patients with normal tension glaucoma vs ocular hypertension. 2013 ARVO Annual Meeting, Seattle, Washington, 6 May 2013 (accepted) and UCL Faculty of Brain Sciences PG Poster Symposium 2013, London, 31 January 2013.

Other publications relevant to and referenced in PhD thesis

Wood J, **Lascaratos G**, Bron A and Osborne N. The influence of light exposure on cultured retinal ganglion cells. Molecular Vision 2008; 14:334-344.

Lascaratos G, Ji D, Wood J and Osborne N. Light (400-760nm) affects mitochondrial function and induces neuronal death in retinal cell cultures. Vision Research 2007; 47: 1191-1201.

Osborne N, **Lascaratos G**, Bron A, Chidlow G and Wood J. A hypothesis to suggest that light is a risk factor in glaucoma and the mitochondrial optic neuropathies. British Journal of Ophthalmology 2006; 90: 237-241.